科技部補助專題研究計畫成果報告
期末報告

鎳在台灣不抽菸肺癌之角色(第3年)

計 畫 類 別 ： 整合型計畫
計 畫 編 號 ： NSC 101-2632-B-040-001-MY3
執 行 期 間 ： 103年08月01日至104年07月31日
執 行 單 位 ： 中山醫學大學醫學系

計 畫 主 持 人： 吳子卿
共 同 主 持 人： 柯俊良、葉姝蘭、王耀震、張元衍
計畫參與人員： 碩士級-專任助理人員：張致寧
碩士級-專任助理人員：邱秉松
碩士級-專任助理人員：陳怡帆
碩士級-專任助理人員：錢鵬如
碩士班研究生-兼任助理人員：陳琮閔
碩士班研究生-兼任助理人員：林峰益
碩士班研究生-兼任助理人員：侯婷譯
碩士班研究生-兼任助理人員：許人婕
碩士班研究生-兼任助理人員：許芷婷
碩士班研究生-兼任助理人員：張惠怡
碩士班研究生-兼任助理人員：趙佩岑
博士班研究生-兼任助理人員：詹淑婷
博士班研究生-兼任助理人員：陳博銘
博士班研究生-兼任助理人員：蔡隆宏
博士班研究生-兼任助理人員：邱育瑚
博士班研究生-兼任助理人員：吳芝嫻
博士後研究：吳德威

報 告 附 件 ： 出席國際會議研究心得報告及發表論文

處 理 方 式 ：
1.公開資訊：本計畫涉及專利或其他智慧財產權，2年後可公開查詢
2.「本研究」是否已有嚴重損及公共利益之發現：否
3.「本報告」是否建議提供政府單位施政參考：否

中　華　民　國　104　年　10　月　30　日

中 文 摘 要 ： 關於鎳暴露誘發肺癌發展的機制目前所知不多。因此本計畫將探討:(1)鎳累積在肺組織中，是否會增加肺癌細胞EGFR的突變，鎳是否會藉由誘發miR-21的表現而抑制RECK及SPRY2蛋白的表現增加腫瘤侵犯的情形，及IL-10在腫瘤的侵犯過程中所扮演的腳色。(2)氯化鎳誘發上皮-間質型態轉換(EMT)過程與癌化的機制。(3)鎳暴露是否會藉由抑制DNA的修復而增加p53的突變。(4)氯化鎳是否會影響RAW264.7表面抗原及其功能的表現。(5)植化素抑制鎳誘發肺癌細胞轉移的效率及其可能的機制。我們主要的發現包括:(1)在未抽菸的病人中，鎳累積在肺組織與EGFR的突變，miR21表現及較差的預後較差是有相關性的。在EGFR突變的肺癌細胞中，miR21增加癌細胞的侵犯，是藉由降低RECK及SPRY2蛋白的表現。此外，在肺腺癌HPV-16/18 E6呈陽性的腫瘤當中，IL-10調控CIP2A表現增加可能在增加癌細胞的侵犯上扮演重要角色。(2)氯化鎳藉由增加miR-4471與抑制其標靶基因TAB2表現，進而誘發細胞的纖維化。(3) 鎳藉由損壞DNA修復，而增加p53突變的風險，特別在未抽菸的女性當中。而突變的p53，可能藉由向上調控Nrf2的表現，而造成非小細胞肺癌對順鉑治療的阻抗性。(4)鎳會向下調控巨噬細胞表現抗原的表現，長時間暴露在氯化鎳下亦會損害巨噬細胞在LPS刺激下的基本功能。(5)數種植化素能夠抑制鎳誘發肺癌細胞A549細胞及H1299細胞侵犯的情形，特別是槲皮酮及白楊素。其機制是藉由向下調控TLR4/NFκB訊號路徑。在異腫瘤移植裸鼠中，槲皮酮能顯著的抑制肺癌細胞的轉移。縱合以上，這些研究結果提供鎳造成肺癌發展更多的訊息及其可能的治療策略。

中 文 關 鍵 詞 ： 肺癌、鎳、IL-10、上皮-間質型態轉換、纖維化、 Nrf2、巨噬細胞、槲皮酮、白楊素

英 文 摘 要 ： Few of the mechanisms by which nickel (Ni) induce tumor development are known. Thus, this team project investigated: 1, Whether Ni in lung tissues could promote the risk of EGFR mutation, whether miR-21 induced by Ni promotes tumor invasion and the role of IL-10 in lung tumor invasion. 2, The mechanisms by which Ni induce the EMT process and carcinogenesis. 3, Whether Ni increases the occurrence of p53 mutations due to inhibition of DNA repair. 4, The effect of Ni on the expression of functionally distinct surface antigens in macrophages. 5, The phytochemicals which efficiently inhibit Ni-induced metastasis in lung cancer cells and the possible mechanisms. The major findings were: 1, Ni accumulation in lung tissues was associated with EGFR mutations, miR-21 expression, and a poor outcome in lung cancer patients who never smoked. The expression of miR-21 promoted invasiveness by decreasing the expression of RECK and SPRY2 in EGFR-mutated lung cancer cells. In addition, IL-10-mediated CIP2A might play a crucial role in the tumor aggressiveness. 2, NiCl2 induced the expression of fibronectin via the induction of miR-4417 and down-

regulated the target gene of miR-4417, TAB2. 3, Ni increased the risk of p53 mutation due to defective DNA repair, especially in female lifetime non-smokers. Mutant p53 conferred cisplatin resistance via upregulation of Nrf2 expression. 4, Ni downregulated the surface antigen expression in macrophages. Ni exposure for a long time also impaired essential functions of macrophages stimulated by LPS. 5, Several phytochemicals inhibited Ni-induced invasion and migration in A549 and H1299 cells, especially quercetin and chrysin. The mechanisms were associated with the downregulation of TLR4/NF-κB signaling. Quercetin inhibited the metastasis of lung cancer cells in tumor-bearing nude mice. In summary, these results provide more information about the mechanisms by which Ni contributes to the development of lung cancer and the possible therapeutic strategies.

英文關鍵詞：lung cancer, nickel, IL-10,epithelial-mesenchymal transition, fibrogenesis, Nrf2, macrophages, quercetin

科技部補助專題研究計畫成果報告

（□期中進度報告/v 期末報告）

鎳在台灣不抽菸肺癌形成之角色

計畫類別：□個別型計畫　v 整合型計畫

計畫編號：MOST 101-2632-B-040-001-MY3

執行期間： 2012 年 8 月 1 日至 2015 年 7 月 31 日

執行機構及系所：中山醫學大學

計畫主持人：吳子卿

共同主持人：柯俊良、李輝、王耀震、張元衍、葉姝蘭

計畫參與人員：鄭雅文、阮婷、吳德威、陳柏銘、蔡隆宏、邱育瑚、林伯霖、吳芝嫻、湯曉君、詹淑婷、張致寧、余佩璇

本計畫除繳交成果報告外，另含下列出國報告，共 2 份：

□執行國際合作與移地研究心得報告

v 出席國際學術會議心得報告

期末報告處理方式：

1. 公開方式：

   □非列管計畫亦不具下列情形，立即公開查詢

   v 涉及專利或其他智慧財產權，□一年 v 二年後可公開查詢

2.「本研究」是否已有嚴重損及公共利益之發現：v 否 □是

3.「本報告」是否建議提供政府單位施政參考 V 否 □是，____（請列舉提供之單位；本部不經審議，依勾選逕予轉送）

中　華　民　國　104 年 10　月 30　日

中文摘要：
關於鎳暴露誘發肺癌發展的機制目前所知不多。因此本整合型計畫將探討:(1)鎳累積在肺組織中，是否會增加肺癌細胞 EGFR 的突變，鎳是否會藉由誘發 miR-21 的表現而抑制 RECK 及 SPRY2 蛋白的表現增加腫瘤侵犯的情形，及 IL-10 在腫瘤的侵犯過程中所扮演的腳色。(2)氯化鎳誘發上皮-間質型態轉換(EMT)過程與癌化的機制。(3)鎳暴露是否會藉由抑制 DNA 的修復而增加 p53 的突變。(4)氯化鎳是否會影響 RAW264.7 表面抗原及其功能的表現。(5)植化素抑制鎳誘發肺癌細胞轉移的效率及其可能的機制。我們主要的發現包括:(1)在未抽菸的病人中，鎳累積在肺組織與 EGFR 的突變，miR21 表現及較差的預後較差是有相關性的。在 EGFR 突變的肺癌細胞中，miR21 增加癌細胞的侵犯，是藉由降低 RECK 及 SPRY2 蛋白的表現。此外，在肺腺癌 HPV-16/18 E6 呈陽性的腫瘤當中，IL-10 調控 CIP2A 表現增加可能在增加癌細胞的侵犯上扮演重要角色。(2)氯化鎳藉由增加 miR-4471 與抑制其標靶基因 TAB2 表現，進而誘發細胞的纖維化。(3) 鎳藉由損壞 DNA 修復，而增加 p53 突變的風險，特別在未抽菸的女性當中。而突變的 p53，可能藉由向上調控 Nrf2 的表現，而造成非小細胞肺癌對順鉑治療的阻抗性。(4)鎳會向下調控巨噬細胞表現抗原的表現，長時間暴露在氯化鎳下亦會損害巨噬細胞在 LPS 刺激下的基本功能。(5)數種植化素能夠抑制鎳誘發肺癌細胞 A549 細胞及 H1299 細胞侵犯的情形，特別是槲皮酮及白楊素。其機制是藉由向下調控 TLR4/NFκB 訊號路徑。在異腫瘤移植裸鼠中，槲皮酮能顯著的抑制肺癌細胞的轉移。縱合以上，這些研究結果提供鎳造成肺癌發展更多的訊息及其可能的治療策略。
中文關鍵詞： 鎳、肺癌、EGFR、miR21、IL-10、miR-4471、p53、槲皮酮、白楊素
英文摘要：
Few of the mechanisms by which nickel (Ni) induce tumor development are known. Thus, this team project investigated: 1, Whether Ni in lung tissues could promote the risk of EGFR mutation, whether miR-21 induced by Ni promotes tumor invasion and the role of IL-10 in lung tumor invasion. 2, The mechanisms by which Ni induce the EMT process and carcinogenesis. 3, Whether Ni increases the occurrence of p53 mutations due to inhibition of DNA repair. 4, The effect of Ni on the expression of functionally distinct surface antigens in macrophages. 5, The phytochemicals which efficiently inhibit Ni-induced metastasis in lung cancer cells and the possible mechanisms. The major findings were: 1, Ni accumulation in lung tissues was associated with EGFR mutations, miR-21 expression, and a poor outcome in lung cancer patients who never smoked. The expression of miR-21 promoted invasiveness by decreasing the expression of RECK and SPRY2 in EGFR-mutated lung cancer cells. In addition, IL-10-mediated CIP2A might play a crucial role in the tumor aggressiveness. 2, $NiCl_2$ induced the expression of fibronectin via the induction of miR-4417 and down-regulated the target gene of miR-4417, TAB2. 3, Ni increased the risk of p53 mutation due to defective DNA repair, especially in female lifetime non-smokers. Mutant p53 conferred cisplatin resistance via upregulation of Nrf2 expression. 4, Ni downregulated the surface antigen expression in macrophages. Ni exposure for a long time also impaired essential functions of macrophages stimulated by LPS. 5, Several phytochemicals inhibited Ni-induced invasion and migration in A549 and H1299 cells, especially quercetin and chrysin. The mechanisms were associated with the downregulation of TLR4/NF-κB signaling. Quercetin inhibited the metastasis of lung cancer cells in tumor-bearing nude mice. In summary, these results provide more information about the mechanisms by which Ni contributes to the development of lung cancer and the possible therapeutic strategies.
英文關鍵詞：nickel, lung cancer, EGFR, miR-21, IL-10, miR-4471, p53, quercetin, chrysin

科技部補助「私立大學校院發展研發特色專案計畫」成果報告

（□期中進度報告/v 期末報告）

鎳在台灣不抽菸肺癌形成之角色

計畫類別：整合型計畫

計畫編號：MOST 101-2632-B-040-001-MY3

執行期間： 2012 年 8 月 1 日至 2015 年 7 月 31 日

執行機構及系所：中山醫學大學
計畫主持人：吳子卿
共同主持人：柯俊良、李輝、王耀震、張元衍、葉姝蘭
計畫參與人員：鄭雅文、阮婷、吳德威、陳柏銘、蔡隆宏、邱育瑚、林伯霖、吳芝嫻、湯曉君、詹淑婷、張致寧、余佩璇

本計畫除繳交成果報告外，另含下列出國報告，共 2 份：
□執行國際合作與移地研究心得報告
v 出席國際學術會議心得報告

期末報告處理方式：

2. 公開方式：

□非列管計畫亦不具下列情形，立即公開查詢

v 涉及專利或其他智慧財產權，□一年 v 二年後可公開查詢

2.「本研究」是否已有嚴重損及公共利益之發現：v 否 □是

3.「本報告」是否建議提供政府單位施政參考 v 否 □是，____（請列舉提供之單位；本部不經審議，依勾選逕予轉送）

中　華　民　國 104　年 10　月 30　日

成果報告內容

一、計畫方面：

(一)計畫目前執行進度及是否達到預定目標

1. 本計畫共有 5 個子計畫，**均按進度完成，三年期的計畫每年均如期繳交期中報告，**完成的研究主要之成果包括:

(1)瞭解鎳與肺癌形成之相關機制:

A. 在未抽菸的病人中，鎳累積在肺組織與 EGFR 的突變，miR21 表現及較差的預後較差是有相關性的。在 EGFR 突變的肺癌細胞中，miR21 增加癌細胞的侵犯，是藉由降低 RECK 及 SPRY2 蛋白的表現。此外，在肺腺癌 HPV-16/18 E6 呈陽性的腫瘤當中，IL-10 調控 CIP2A 表現增加可能在增加癌細胞的侵犯上扮演重要角色。

B.氯化鎳藉由增加 miR-4471 與抑制其標靶基因 TAB2 表現,進而誘發細胞的纖維化。

C. 鎳藉由損壞 DNA 修復，而增加 p53 突變的風險，特別在未抽菸的女性當中。而突變的 p53，可能藉由向上調控 Nrf2 的表現，而造成非小細胞肺癌對順鉑治療的阻抗性。另外鎳會向下調控巨噬細胞表現抗原的表現，長時間暴露在氯化鎳下亦會損害巨噬細胞在 LPS 刺激下的基本功能。

(2)瞭解植化素對鎳誘發肺癌細胞轉移宜的抑制作用及機制

數種植化素能夠抑制鎳誘發肺癌細胞 A549 細胞及 H1299 細胞侵犯的情形，特別是槲皮酮及白楊素。其機制是藉由向下調控 TLR4/NFκB 訊號路徑。在異腫瘤移植裸鼠中，槲皮酮能顯著的抑制肺癌細胞的轉移。

2.詳細結案內容按子計畫報告如下:

目錄

子計畫一

鎳誘發 IL-10 表現在肺腫瘤化之角色

Abstract

We explored that nickel accumulation in lung tissues could contribute to EGFR mutations in never-smokers with lung cancer. We enrolled 76 never-smoking patients to evaluate nickel level in adjacent normal lung tissues by ICP-MS. The prevalence of EGFR mutations was significantly higher in the high-nickel subgroup than in the low-nickel subgroup. Intriguingly, the OR for the occurrence of EGFR mutations in female, adenocarcinoma, and female adenocarcinoma patients was higher than that of all patients. Mechanistically, SPRY2 and RECK expressions were decreased by nickel-induced miR-21 via activation of the EGFR/NF-κB signaling pathway, which promoted invasiveness in lung cancer cells, and particularly in the cells with EGFR L858R expression vector transfection. The patients' nickel levels were associated with miR-21 expression levels. Kaplan-Meier analysis revealed poorer overall survival (OS) and shorter relapse free survival (RFS) in the high-nickel subgroup than in low-nickel subgroup. The high-nickel/high-miR-21 subgroup had shorter OS and RFS periods when compared to the low-nickel/low-miR-21 subgroup. Our findings indicated that nickel exposure may not only contribute to cancer incidence but also promote tumor invasion in lung cancer. A positive association of EGFR mutation with HPV16/18 infection has been shown in our previous report and nickel exposure was also associated with HPV infection in lung cancer. We therefore examined whether IL-10 production could be increased by HPV infection due to nickel exposure and in turn reduce virus clearance capability due to immune suppression by IL-10. We found that IL-10 protein and mRNA expression was decreased in E6-knockdown TL1 cells and increased in E6-overexpressing TL4 cells. In addition, IL-10 transcription was predominantly regulated by E6-mediated phosphorylation of CREB and C/EBPβ via PI3K signaling pathway. IL-10-mediated tumor aggressiveness *in vitro* and *in vivo* occurs through increased CIP2A expression via PI3K signaling pathway. Among patients, IL-10 mRNA expression in lung tumors was positively correlated with CIP2A mRNA expression. Cox-regression analysis showed that IL-10 and CIP2A mRNA levels may independently predict survival in patients with lung adenocarcinoma, especially in patients with E6-positive tumors. IL-10 production from lung tumors and immune cells promotes lung adenocarcinoma aggressiveness and patients with poor survival. We thus suggest that an EGFR or PI3K inhibitor combined with chemotherapy may potentially enhance tumor regression and improve patients' outcome and life quality.

Introduction

Epidemiological studies have indicated that nickel exposure may contribute to respiratory cancer incidence in workers (Beveridge et al, 2010; De Matteis et al, 2012; Grimsrud et al, 2002); thus, nickel is considered a group 1 human carcinogen by the International Agency Research in Cancer (IARC) of the World Health Organization (WHO). Nickel is frequently used in the semi-conductor industry, which is a vital contributor to economic development in Taiwan. A positive association has been reported between soil nickel contamination and lung cancer incidence in Taiwan (Huang et al, 2013) and a Taiwanese case-control study indicated that nickel accumulation in lung tumors was associated with an increased risk of lung cancer incidence (Kao et al, 2006). In the present study, we first examined whether nickel exposure could promote tumor invasion in lung cancer.

The carcinogenic action of nickel compounds is thought to involve oxidative stress, genomic DNA damage, epigenetic effects, and the regulation of gene expression by activation of certain transcription factors related to corresponding signal transduction pathways (Ding et al, 2006; Ding et al, 2009). For example, hypoxia and nickel exposure inhibit the Jmjc-domain-containing histone demethylase (JMJD1A) and repress Sprouty2 (SPRY2) expression to promote anchorage -independent growth in human bronchial epithelial BEAS-2B cells (Chen et al, 2010a). Nickel exposure also induces the epithelial-mesenchymal transition via reactive oxygen species (ROS)-mediated E-cadherin promoter methylation (Wu et al, 2012). A recent report indicated that nickel accumulation was associated with an increased risk of p53 mutation in lung cancer via a decreased in DNA repair capability for removing ROS-induced 8-oxoguanosine (Chiou et al, 2014). However, the underlying mechanism by which nickel exposure leads to lung tumorigenesis is still largely unidentified.

The activation of NF-κB plays a crucial role in human tumorigenesis, including lung cancer, and nickel activation of the NF-κB signaling pathway has been demonstrated by various groups (Ding et al, 2006; Kasprzak et al, 2003). A previous report indicated that the genotoxic agents, camptothecin and doxorubicin, induced NF-κB-dependent microRNA (miR)-21 upregulation, which in turn promoted invasiveness in breast cancer cells (Niu et al, 2012). Tumor malignancy in gliomas is promoted by miR-21 via targeting of SPRY2 and tumor suppressor reversion-inducing cysteine-rich protein with Kazal motifs (RECK) (Gabriely et al, 2008; Kwak et al, 2011). We therefore hypothesized that NF-κB activation in response to nickel

exposure might promote cell invasiveness via induction of miR-21, and decrease of SPRY2 and RECK expression. We expected that this would be especially apparent in lung cancer cells harbored epidermal growth factor receptor (EGFR) mutations, since miR-21 is an EGFR-regulated anti-apoptotic factor in lung cancer of never-smokers (Seike et al, 2009).

IL-10 belongs to Th2 cytokine for anti-inflammation and it also inhibits T cell immunity to block tumor immune surveillance (Brooks et al, 2006; Moore et al, 2001; Sharma et al, 1999). Most studies have indicated that IL-10 expression in immune cells, including macrophages, infiltrating T lymphocytes, and NK cells, promotes progression of tumors in kinds of cancer types including lung cancer (Kim et al, 2006; Shih et al, 2005). In lung cancer cases, some reports have indicated that loss of IL-10 in lung tumors may promote tumor progression and result in poor clinical outcomes in patients; however, an opposite effect has been reported in other studies (De Vita et al, 2000; Lu et al, 2004; Soria et al, 2003). Interestingly, the absence of IL-10 expression has been associated with poor outcome in stage I lung cancer, whereas in late-stage lung cancer, the presence of IL-10-positive macrophages at the tumor margins can be an indicator of poor prognosis (De Vita et al, 2000; Lu et al, 2004; Soria et al, 2003). In addition, shorter survival times have been reported in advanced lung cancer patients who had high serum IL-10 levels, when compared with similar patients who had low serum IL-10 levels (De Vita et al, 2000) . Therefore, the role of IL-10 in lung tumorigenesis remains elusive.

The infection of human papillomavirus (HPV) 16/18 has been documented to associate with cancers of squamous epithelia. However, in Taiwan, HPV 16/18 infection rate was significantly higher in lung adenocarcinoma than in lung squamous cell carcinoma (Cheng et al, 2001; Cheng et al, 2007). A high HPV infection rate in Taiwanese lung cancer reflects the possibility that imbalanced immune function might play an important role in cancer development, especially in Taiwanese women who never smoked (never-smokers) (Cheng et al, 2001). IL-10 has been shown to determine virus clearance and infection persistence (Brooks et al, 2006). HPV infection is a major etiological factor in cervical carcinogenesis. IL-10 mRNA levels in cervical intraepithelial neoplasia (CIN) were significantly higher than in normal cervical tissues (Azar et al, 2004; Bais et al, 2005; Sharma et al, 2007). The up-regulated secretion of IL-10 may inhibit immune response against HPV infection in early cervical lesions. Reports have shown that higher IL-10 could be detected in plasma of patients with CIN III and with carcinoma than in patients with CIN I and CIN II (Azar et al, 2004; Bais et al, 2005; Sharma et al, 2007). Moreover, patients suffering from cervical cancer show higher IL-10 expression in

HPV16 positive tumors than in HPV16 negative tumors, which again indicates an association between IL-10 and the carcinogenesis of HPV-associated cancer (Fernandes et al, 2005). Conceivably, HPV persistent infection might cause integration of HPV DNA into host chromosomes, leading to expression of E6 and E7 oncoproteins, and consequently to promotion of tumor progression via inactivation of the p53 and Rb pathways (zur Hausen, 2000; zur Hausen, 2002). Previous reports have indicated that patients with HPV-associated advanced stage cervical and oropharyngeal cancer who had high IL-10 expression in serum or plasma also had poorer survival when compared with patients with low IL-10 expression (Bais et al, 2005; El-Sherif et al, 2001). We expected that IL-10 detected in blood circulation might represent IL-10 expressed not only in immune cells but also IL-10 that derived from tumor cells.

In the present study, we first examined the possibility that nickel accumulation in lung tissues could promote the risk of EGFR mutation in lung cancer, especially in female never-smokers. We next examined whether miR-21 induced by nickel exposure could promote tumor invasion via suppressing SPRY2 and RECK expression, and consequently resulting in poor outcome in lung cancer patients. In addition, IL-10 expression in lung tumors could be elevated by E6 oncoprotein and IL-10 induced by E6 in lung tumors could be responsible for *in vitro* and *in vivo* tumor invasion.

Results

Part I: Nickel may contribute to EGFR mutation and synergistically promotes tumor invasion in EGFR-mutated lung cancer via nickel-induced miR-21 expression

The association between nickel levels and EGFR mutations in lung cancer patients

Nickel exposure has been associated with increased p53 mutation in lung cancer due to decreased DNA repair capability (Chiou et al., 2014). Based on this rationale, we hypothesized that nickel exposure could be associated with the occurrence of EGFR mutations in lung cancer of never-smokers. Seventy six adjacent normal lung tissues from never-smoking lung cancer patients showed the median value for nickel levels of 0.38 μg/g dry weight of lung tissue and this value was used as a cutoff point to divide patients into high-nickel and low-nickel subgroups. After adjusting for possible confounding factors including gender and tumor histology, EGFR-mutated patients were more prevalent in the high-nickel subgroup than in the low-nickel subgroup. (36.8% vs. 13.2%, OR, 4.36, 95% CI, 1.29-14.74, P = 0.018; Table 1). The higher OR value was more significantly revealed in female, ADC, and female ADC patients when compared with all patients (12.7; P = 0.005 for female; 5.62, P = 0.012 for ADC; 11.71, P = 0.007 for female ADC; Table 1). However, the nickel level was not associated with EGFR mutation in male, SCC, and male ADC patients (Table 1). The results revealing that the contribution of nickel exposure on the occurrence of EGFR mutation was more important in female, ADC, and female ADC patients compared with their counterparts. These results suggest that nickel accumulation in lung tissues may be more contributive to EGFR mutation occurrence in never-smoking lung cancer patients, especially in female ADC patients.

A decrease in SPRY2 and RECK expression by nickel-induced miR-21 may promote invasiveness in lung cancer cells

MiR-21 is evidently upregulated by the NF-κB signaling pathway (Ling et al., 2012; Niu et al., 2012). We therefore examined the possibility that nickel might activate the NF-κB signaling pathway to induce miR-21 expression in lung cancer cells. MTT assay was performed to obtain the optimal concentration of nickel chloride used for lung cancer cell experiments. Lower 25% cytotoxicity of these three cell types was induced by 0.5 mM nickel chloride and thus 0.25 and 0.5 mM of nickel chloride were used for cell experiments (Supplementary Figure 1). Consistent with previous studies (Pulido and Parrish, 2003; Lu et al., 2005),

N-acetyl-L-cysteine (NAC) reduced nickel chloride-induced ROS generation and NF-κB reporter activity in H1355 and H23 cells (Supplementary Figure 2). We thus expected that NF-κB activation by nickel chloride-induced ROS could promote miR-21 expression. As shown in Figure 1A, the levels of miR-21 were increased by nickel chloride in a dose-dependent manner. Western blotting analysis showed that SPRY 2 and RECK, the miR-21 target genes, were dose-dependently decreased by nickel chloride treatment (Figure 1A). We further treated both cell types with miR-21 inhibitor to determine whether nickel-induced miR-21 could down-regulate SPRY 2 and RECK expression. As expected, miR-21 levels were decreased by the miR-21 inhibitor in both cell types treated with 0.5 mM nickel chloride. Moreover, the expression of SPRY2 and RECK was reversed by miR-21 inhibitor transfection, but a more significant restoration of expression by the miR-21 inhibitor was seen for RECK than for SPRY2 in both cell types (Figure 1B). The Boyden chamber invasion assay indicated that the invasion capability was increased by nickel chloride treatment in a dose- dependent manner. However, the invasion capability induced by nickel chloride was decreased by miR-21 inhibitor transfection in both cell types (Figure 1C). These results suggest that the decrease in SPRY2 and RECK expression by nickel-induced miR-21 expression might promote invasiveness in lung cancer cells.

Nickel induces miR-21 expression via activation of the EGFR/NF-κB signaling pathway

We examined the possibility that the elevation of miR-21 expression by nickel chloride could occur by activation of the EGFR/NF-κB signaling pathway. Western blotting analysis showed that the expression of EGFR and nuclear p65 in H1355 and H23 cells was concomitantly increased by nickel chloride treatment in a dose-dependent manner; however, cytoplasmic p65 expression was unchanged by nickel chloride treatment (Figure 2A). The expression of C23 and α-tubulin were used as nuclear and cytoplasmic protein controls, respectively. Luciferase reporter assay further confirmed that the DNA binding to the NF-κB promoter was increased by nickel chloride-induced nuclear NF-κB expression. We used NF-κB inhibitor BAY11-7082 or EGFR inhibitor PD153035 to determine whether miR-21 induction by nickel chloride occurred through the EGFR/NF-κB pathway. As shown in Figure 2B, the expression of miR-21 was markedly decreased and the expression of SPRY2 and RECK was reversed by NF-κB or EGFR inhibitors in both cell types.

We next examined the possibility that nickel chloride exposure could elevate miR-21 expression in EGFR-mutated lung cancer cells to synergistically reduce SPRY 2 and RECK

expression. H1355 and H23 cells were treated with nickel chloride and/or transfection of EGFR L858R expression vector. The expression of miR-21 levels in both cell types was increased by nickel chloride or EGFR L858R transfection compared with parental control cells (Figure 2C). Interestingly, the greatest increase in miR-21 level was observed in both cell types with nickel chloride treatment plus EGFR L858R transfection. Western blotting analysis further confirmed that the expressions of SPRY2 and RECK were most significantly decreased in both cell types by combining nickel chloride with EGFR L858R compared with parental control cells or both cell types treated with nickel chloride or transfected EGFR L858R expression vector alone (Figure 2C). Consequently, the expressions of miR-21, EGFR, SPRY2, and RECK in EGFR-mutated H1975 cells were changed by nickel chloride treatment and/or shEGFR transfection (Figure 2D). These results suggest that nickel chloride-induced miR-21 functions via the EGFR/NF-κB signaling pathway, resulting in a synergistic decrease in SPRY2 and RECK expression in EGFR-mutated cells when compared with EGFR-wild-type cells.

RECK overexpression may reverse nickel-mediated invasiveness in lung cancer cells

We tested whether RECK overexpression could reverse nickel-mediated cell invasiveness, H1355 and H23 cells were treated with 0.5 mM nickel chloride and then transfected with two doses of RECK expression vector. RECK expression in H1355 and H23 cells was significantly decreased by nickel chloride when compared to both cell types transfected with empty vector (VC) and RECK expression in both cell types was expectedly elevated by transfecting RECK expression vector. EGFR expression was elevated by nickel chloride treatment, but the increased in EGFR expression can be reversed by RECK overexpression in both cell types (Figure 3 upper panel). Nevertheless, the increase of invasion capability by nickel chloride treatment can be reversed by RECK overexpression in both cell types (Figure 3 lower panel). These results suggest that RECK might play a role in nickel-mediated invasiveness in lung cancer cells.

Association of miR-21 expression levels with nickel levels and EGFR mutations in lung cancer patients

In the study population (n = 76), the association of nickel levels, EGFR mutations, and miR-21 levels with various clinico-pathological parameters including age, genders, tumor histology, tumor stage, tumor size and nodal micrometastasis were not observed, except EGFR mutations and gender factors (P = 0.017, Supplementary Table 1). The association of miR-21 expression

levels with nickel levels and EGFR mutations are presented in Table 2. The miR-21 expression levels were significantly higher in the high-nickel subgroup than in the low-nickel subgroup (odd ratio, OR, 2.73, P = 0.035). However, miR-21 expression levels was not associated with EGFR mutations in this study population. Intriguingly, the combined effect of nickel exposure plus EGFR mutation was only apparent in the high-nickel/wild-type EGFR subgroup, and not in the high-nickel/mutated-EGFR subgroup when the low-nickel/wild-type EGFR subgroup was used as a reference (OR, 4.61 for high-nickel/wild-type EGFR subgroup, P = 0.010; Table 2). These results suggest that nickel levels may play a more important role than EGFR mutational status in miR-21 expression in lung cancer patients.

Association of nickel level, miR-21 level, and RECK expression with OS and RFS in lung cancer patients

We examined whether nickel, miR-21, and RECK levels might be associated with OS and RFS in lung cancer patients with or without EGFR mutations. The median follow-up time after surgery was 813 days (range 141-1825 days). Over the course of this study, 40 patients died. Follow-up data indicated that 24 patients had tumor relapse (4 patients had local recurrence, 13 patients had distant metastasis, and 7 patients had both local recurrence and distant metastasis). Kaplan-Meier analysis indicated that the high-nickel subgroup had a shorter OS and RFS periods than the low-nickel subgroup (P = 0.007 for OS, P = 0.008 for RFS; Figure 4A). However, the prognostic value of miR-21 level and RECK mRNA expression on OS and RFS was not observed in the study population (data not shown). Intriguingly, the high-nickel/low-miR-21, low-nickel/high-miR-21, and high-nickel /high-miR-21 subgroups exhibited poorer OS and RFS when compared to the low-nickel/low-miR-21 subgroup (P = 0.001 for OS, P = 0.002 for RFS, Figure 4B). The prognostic value of nickel levels combined with RECK mRNA levels on OS and RFS was not shown in this study population (P = 0.051 for OS, P = 0.069 for RFS, Figure 4C). These patient results seemed to support the finding of the cell model.

Part II: IL-10 promotes tumor aggressiveness via upregulation of CIP2A transcription in lung adenocarcinoma

IL-10 expression was higher in E6-positive lung cancer cells than in E6-negative lung cancer cells

We explored whether IL-10 expressed from lung tumors could promote tumor progression by enrolling a panel of lung cancer cells to evaluate IL-10 protein and mRNA expression. IL-10 protein and mRNA expression was higher in HPV16 E6-positive TL1 and TL2 than in E6-negative lung cancer cells (Figure 51A). Higher expression was also found in E6-positive SiHa and HeLa cervical cancer cells than in E6-negative C33A cervical cancer cells (Figure 5A). Therefore, E6 appeared to promote IL-10 expression.

Knockdown and overexpression of E6, by shRNA and a cDNA plasmid, respectively, were then used to examine whether IL-10 expression could be modulated by E6 in TL1 and TL4 cells. E6 expression was decreased and p53 expression was increased by E6-knockdown in TL1 cells. Conversely, E6 expression was increased and p53 expression was decreased by E6-overexpression in TL4 cells (Figure 5B). In addition, IL-10 protein expression was modulated by E6-knockdown or overexpression in a pattern consistent with the IL-10 mRNA levels found in TL1 or TL4 cells (Figure 5B). Therefore, IL-10 induction due to E6 oncoprotein expression in lung cancer cells might occur through transcriptional activation.

Upregulation of IL-10 by E6 is mediated through PI3K/AKT signaling pathway

We verified which signaling pathway might be linked with E6-induced IL-10 transcription by using different specific inhibitors. Western blotting data showed that IL-10 expression was significantly reduced in a dose-dependent manner in TL1 cells treated with wortmannin or LY294002 (PI3K inhibitors), and was slightly decreased by treatment with PD153035 (an EGFR inhibitor); however, IL-10 expression was not changed by treatment with PD98059 or U0126 (MEK inhibitors) or BAY11-7082 (a NFkB inhibitor) (Figure 6A, upper panel). We further tested whether IL-10 production in E6-positive cells was mediated through PI3K/AKT pathway by treating TL1 and E6-overexpressing TL4 cells with LY294002 and wortmannin. IL-10 expression was reduced in a dose-dependent manner in both cell types by LY294002 and wortmannin (Figure 6A, lower panel).

We then explored which transcriptional factor(s) might be responsible for IL-10 transcription by using software analysis to predict the putative binding sites of transcription factors (http://www.genome.jp/tools/motif/). As shown in Figure 6B, the IL-10 promoter (-858~+1) had putative binding sites of C/EBPα, C/EBPβ, CREB, and MZF-1 (Figure 6B, upper panel). Three promoter regions for the IL-10 gene (-855~+1, -458~+1, and -349~+1) were constructed for evaluation of luciferase reporter activity. Separately transfected each of these three

promoters into TL1 cells resulted in activities of the -458~+1 and -349~+1 promoters that were 95% and 38%, respectively, of the reporter activity of -855~+1 promoter. This finding suggests that C/EBPβ and CREB, located at -458~-349 promoter region, might play an important role in IL-10 transcription. The luciferase reporter activity of the -458~+1 promoter in TL1 cells was markedly reduced by E6-knockdown and by the inhibitors of PI3K, but to a lesser extent by inhibitors of the EGFR signaling pathway (Figure 6B, lower panel). This suggested a crucial role for phosphorylation of CREB and C/EBPβ, via the PI3K/AKT signaling pathway, in IL-10 transcription.

Phosphorylation of CREB and C/EBPβ by E6 via PI3K/AKT signaling pathway plays a crucial role in IL-10 transcription

We next questioned whether phosphorylation of CREB and C/EBPβ by E6, via the PI3K/AKT pathway, could play an important role in E6-mediated IL-10 transcription. Western blotting data showed that levels of phosphorylated CREB and C/EBPβ protein were markedly reduced by PI3K inhibitors (LY294002 and wortmannin), but the total protein levels of CREB and C/EBPβ were not changed by these inhibitors. As expected, the phosphorylation of both proteins was decreased by treatment with an EGFR inhibitor (PD98059) (Figure 6C, left panel). ChIP analysis further indicated that the DNA binding activities of CREB and C/EBPβ were diminished by PI3K inhibitors, but not by the EGFR inhibitor (Figure 6C, right panel). Therefore, phosphorylation of CREB and C/EBPβ via PI3K/AKT signaling pathway appeared to play a crucial role in E6-mediated IL-10 transcription in lung cancer cells.

IL-10 induced by E6 is responsible for soft-agar growth, invasion, and xenograft tumor nodule formation

We used soft-agar colony formation and Boyden chamber assays to explore whether IL-10 induced by E6 could promote anchorage independent soft-agar growth and invasiveness, respectively. As expected, IL-10 expression was reduced in IL-10-knockdown TL1 cells and elevated in IL-10-overexpressing TL4 cells (Figure 7A). The doubling time was significantly elevated in IL-10-knockdown TL1 cells and reduced in IL-10-overexpressing TL4 cells (23.4 ± 0.2, 26.1 ± 0.5, and 35.1 ± 1.0 for IL-10-knockdown TL1; 30.1 ± 0.3, 25.8 ± 0.3, and 20.6 ± 1.5 for IL-10-overexpressing TL4, Supplementary Figure 3). The representative soft-agar growth colony sizes decreased markedly in IL-10-knockdown TL1 cells and increased in IL-10 overexpression TL4 cells when compared with non-specific shRNA control (NC) and vector

control (VC) cells (Figure 7B). The capability for soft-agar growth and invasiveness was significantly reduced in IL-10-knockdown TL1 and elevated in IL-10-overexpressing TL4 cells in a dose-dependent manner when compared with NC and VC cells (Figure 7B). We further established a stable clone of IL-10-knockdown TL1 cells, in which IL-10 expression had almost disappeared (Figure 7C). We then injected nude mice with these clonal cells via the tail vein to determine whether a lower number of lung tumor nodules would form after 4 months, compared to injection with NC cells. The number of tumor nodules was significantly lower in nude mice injected with the IL-10-knockdown stable clone than in mice injected with NC cells (10.5 ± 7.6 vs. 26.5 ± 6.7, $P = 0.003$, Figure 7C). Therefore, IL-10 expression induced by E6 oncoprotein may be responsible for soft-agar growth, invasion, and xenograft tumor nodule formation.

IL-10 promotes tumor aggressiveness via upregulation of CIP2A

We explored the underlying mechanism of tumor aggressiveness induced by IL-10, using a PCR-array to examine which molecule might involve in IL-10-induced tumor progression. PCR-array analysis showed a marked decrease in c-Myc expression in IL-10 knockdown TL1 cells compared to expression in NC cells among the 94 gene examined. c-Myc expression has been shown to be regulated by a CIP2A-PP2A axis (Junttila et al, 2007). Therefore, we expected that the IL-10 induced by E6 might upregulate CIP2A, thereby contributing to c-Myc expression and consequently promoting tumor aggressiveness. Western blotting analysis showed that c-Myc and CIP2A expressions were concomitantly decreased in IL-10 knockdown TL1 cells and increased in E6-overexpressing TL4 cells (Figure 8A). The elevated expression of c-Myc and CIP2A by E6 was restored by IL-10 knockdown in E6-transfected TL4 cells (Figure 8A). Interestingly, CIP2A mRNA expression was consistent in its protein expression in IL-10 knockdown TL1, E6-transfected TL4, and IL-10-knockdown E6-transfected TL4 cells, suggesting that IL-10 could transactivate CIP2A transcription in E6-positive lung cancer cells (Figure 8A).

Phosphorylation of CREB via PI3K/AKT pathway is responsible for IL-10-mediated CIP2A transcription

We next examined which signaling pathway might be linked with the upregulation of CIP2A transcription induced by IL-10. Three promoters of the CIP2A gene (-972~+1, -452~+1, and -162~+1) were constructed: the putative transcriptional factors on these promoter regions are

shown in Figure 8B (upper panel). These promoters were transfected into TL1 cells to verify which promoter region might be more important for CIP2A transcription. The luciferase reporter activity assays indicated that the -452~+1 promoter had 71% of the reporter activity of the -972~+1 promoter, whereas the -162~+1 promoter had only 11% of the reporter activity of -972~+1 promoter (Figure 8B, middle panel). This finding suggests that CREB, NF-kB, and AP-1 might be involved in CIP2A transcription.

The reporter activity of the -452~+1 promoter in TL1 cells was markedly suppressed by E6-knockdown, LY294002, and wortmannin, but not by PD153035. Therefore, we expected that the PI3K/AKT pathway might be involved in IL-10 mediated CIP2A transcription via phosphorylation of CREB. Western blotting analysis indicated that the total CREB protein expression was not changed by E6-knockdown or by treatment of different inhibitors, but expression of phosphorylated CREB protein almost disappeared after treatment with LY294002 and wortmannin followed by E6- and IL-10-knockdown, and PD980509. ChIP analysis further confirmed that phosphorylated CREB was bound to the CIP2A promoter (Figure 8C). Phosphorylation of CREB therefore clearly played a crucial role in IL-10 mediated CIP2A transcription. We further verified whether IL-10-mediated CIP2A could be responsible for IL-10-induced cell invasion. TL4 cells were transfected with two doses of IL-10. Western blotting showed that CIP2A and c-Myc expression was concomitantly increased by IL-10 transfection in a dose-dependent manner (Fig. 8D upper panel). The invasion capability of TL4 cells was significantly elevated by IL-10 transfection (Fig. 8D lower panel). However, the invasion capability of IL-10-transfected TL4 cells was restored by CIP2A-knockdown (Fig. 8D lower panel). This result clearly indicates that CIP2A is responsible for IL-10-mediated cell invasion.

IL-10 mRNA expression levels are positively correlated with HPV16/18 E6 oncoprotein and CIP2A mRNA expression in tumors of lung adenocarcinoma patients

We verified whether IL-10 expression could be associated with HPV16/18 E6 oncoprotein expression by evaluating IL-10 mRNA expression levels and E6 oncoprotein levels in lung tumors from 98 lung adenocarcinoma patients using real-time RT-PCR and immunohistochemistry. The distribution and prognostic value of parameters of patients were summarized in Supplementary Table 2. Univariate analysis showed that patients with advanced stage (II, III), higher T value (T3, T4), and advanced nodel involvement (N1, N2) had shorter

overall survival periods than with early stage (I), lower T value (T1, T2) and non-nodal involvement (N0) (P = 0.004 for stage, P = 0.001 for T, P = 0.002 for N; Supplementary Table 2). As shown in Supplementary Table 3, IL-10 mRNA expression levels were higher in E6-positive tumors than in E6-negative tumors (168.1 ± 40.5 vs. 64.7 ± 24.5, P = 0.032; Supplementary Table 3). We next examined whether IL-10 expression could be related to CIP2A expression in lung tumors. Real-time RT-PCR analysis showed that CIP2A mRNA expression was significantly higher in tumors expressing high levels of IL-10 than in tumors expressing low levels (424.4 ± 85.5 vs. 188.5 ± 50.9, P = 0.020). These *in vivo* observations in lung tumors from lung adenocarcinoma patients were consistent with the earlier *in vitro* findings in lung cancer cell cultures.

IL-10 mRNA and CIP2A mRNA expression may independently predict survival in lung adenocarcinoma patients

Kaplan Meier analysis showed that patients with high IL-10 mRNA and CIP2A mRNA tumors had shorter overall survival than those with low IL-10 mRNA and CIP2A mRNA tumors (Supplementary Figure 4A). The prognostic significance of IL-10 and CIP2A mRNA levels was observed in patients with E6 positive tumors (Supplementary Figure 4B), not in patients with E6 negative tumors (Supplementary Figure 4C). Multivariate Cox regression analysis was used to estimate whether IL-10 and CIP2A mRNA expression level could independently predict survival in patients with lung adenocarcinoma. As expected, patients with stage II+III tumors had shorter median survival and lower 5-year survival percentage than did patients with stage I tumors (19.2 vs. 79.3 months, 18.3 vs. 57.4%; HR, 2.498, 95% CI, 1.373-4.546, P = 0.003; Table 1). Patients with high IL-10 mRNA levels had poorer survival than those with low IL-10 mRNA levels (HR, 2.083, 95% CI, 1.241-3.495, P = 0.005, Table 1, Supplementary Figure 4). In addition, poorer survival was found in patients with high CIP2A mRNA levels than in patients with low CIP2A mRNA levels (HR, 1.809, 95% CI, 1.063-3.079, P = 0.029, Table 1, Supplementary Figure 4). Therefore, shorter median survival and lower 5-year survival rate were observed in patients with high IL-10 and CIP2A mRNA levels in tumor than in those with low IL-10 and CIP2A mRNA levels in tumor. Moreover, the prognostic significance of IL-10 mRNA and CIP2A mRNA expression levels was seen only in patients with E6-positive tumors and not in patients with E6-negative tumors (Table 2, Supplementary Figure 4). We further confirm the finding by the presence or absence of HPV 16/18 DNA in this study population. The prognostic significance of IL-10 mRNA and CIP2A mRNA levels

were also observed in patients with HPV 16/18 DNA positive tumors and not in patients with HPV 16/18 DNA negative tumors (Supplementary Table 4). These clinical observations for lung adenocarcinoma patients were consistent with the findings from the mechanistic studies in cell models. Therefore, we suggest that IL-10 and CIP2A mRNA may independently predict survival in lung adenocarcinoma patients. Correctively, our findings indicated that nickel exposure may not only contribute to cancer incidence but also promote tumor invasion in lung cancer. We thus suggest that EGFR or PI3K inhibitor combined with chemotherapy may potentially enhance tumor regression and improve patients' outcome and life quality.

Discussion

Part I: Nickel may contribute to EGFR mutation and synergistically promotes tumor invasion in EGFR-mutated lung cancer via nickel-induced miR-21 expression

Most Taiwanese women (> 90%) and one-third of Taiwanese men (35%) suffering from lung cancer are lifetime never-smokers (Ministry of Health and Welfare, 2010). However, in Taiwan, lung cancer is the leading cause of cancer deaths in women and the second cause of cancer deaths in men (Ministry of Health and Welfare, 2010). These lung cancer statistics for Taiwan contrast with the general perception that cigarette smoking is the major etiological factor for lung cancer. Therefore, environmental exposure other than cigarette smoking may play an important role in lung cancer incidence in Taiwanese never-smokers.

This expectation can be supported by a recent report indicating that nickel soil contamination was associated with lung cancer incidence in Taiwan, particularly in lung ADC (Huang et al, 2013). Our recent report indicated that nickel accumulation in lung tissues may increase the risk of p53 mutation occurrence in lung cancer via reduced DNA repair capability (Chiou et al, 2014). The association between nickel exposure and p53 mutation occurrence was most evident in never-smoking female lung cancer patients (Chiou et al, 2014). In the present study, we further showed that nickel accumulation in lung tissues was associated with EGFR mutations in lung cancer of never-smokers, and particularly in female lung ADC patients. These results strongly support the epidemiological studies indicating that nickel exposure may contribute to lung cancer incidence in never-smokers at least partially via an increase in the occurrence of p53 and EGFR mutations.

RECK is a membrane glycoprotein that may inhibit tumor metastasis and angiogenesis by negatively regulating MMP activity (Noda et al, 2003; Oh et al, 2001). Therefore, RECK is down-regulated in several tumors including lung tumors and its down-regulation is a step in the pathway towards malignant conversion. RECK depletion promotes cell proliferation via an increased in phosphorylation of AKT and ERK, cyclin D1 expression, and down-regulation of p19, p53, and p21 (Kitajima et al, 2011). SPRY2 expression and EGFR activity are elevated by RECK depletion (Kitajima et al, 2011). We therefore expected to find that RECK, depleted by the induction of miR-21 by nickel exposure, was further depleted by activation of EGFR and in turn down-regulated the miR-21-induced expression of SPRY2. As shown in Figure 2, EGFR and nuclear p65 expression were concomitantly increased by nickel chloride exposure. Consistently, cells immortalized by nickel exposure have increased amounts of EGFR present on their cell membranes, suggesting that EGFR may participate in nickel-induced immortalization (Mollerup et al, 1996). Nickel also activates the PI3K/AKT, MAPK.ERK, p38, and JNK signaling pathways (Carpenter & Jiang, 2013; Ke et al, 2008; Mongan et al, 2008). Therefore, we expected that NF-κB activation by nickel would induce miR-21 expression through the EGFR/PI3K/ERK cascades. The invasion capability induced by nickel chloride in H1355 and H23 cells was nearly reversed by transfection with the RECK expression vector (Figure 3). These results seemed to support the possibility that RECK targeted by nickel-induced miR-21 might be partially responsible for invasiveness in lung cancer cells, particularly in EGFR-mutated cells.

A negative correlation between miR-21 levels and RECK and SPRY2 expression was also observed in a subset of the study population. This observation from lung cancer patients seemed to support the findings of the cell models ($P = 0.022$ for RECK, $P = 0.022$ for SPRY2; Supplementary Table 5). The prognostic analysis showed that the high-nickel/low-miR-21, high-nickel/high-miR-21, and low-nickel/high-miR-21 subgroups exhibited worse OS and RFS when compared with the low-nickel /low-miR-21 subgroup (Figure 4B). More surprisingly, nickel level showed a prognostic significance for OS and RFS in this study population (Figure 4A). Therefore, the nickel level may have a greater prognostic value for OS and RFS than did the miR-21 and RECK expression levels. These results suggest that nickel-induced miR-21 expression, via a decreased in

RECK expression, may only partially contribute to tumor invasion and poor outcome in lung cancer patients. These results reveal that the cell experiments using high concentrations of nickel chloride for a short term treatment seemed to be not completely reflected the observations from lung cancer patients. Further investigation is needed to investigate nickel-mediated lung tumor progression and invasion in animal model under low concentrations of nickel for a long term treatment.

Part II: IL-10 promotes tumor aggressiveness via upregulation of CIP2A transcription in lung adenocarcinoma

Early studies reported that IL-10 is commonly expressed in human lung tumors suggest that it may play an active immunoregulatory role in the lung tumor microenvironment (Hatanaka et al, 2001; Huang et al, 1995; Mocellin et al, 2005; Sharma et al, 1999; Smith et al, 1994; Yanagawa et al, 1999). IL-10 is considered to be an autocrine growth factor of immune cells, and it participates notably in increases of tumor cell proliferation of melanoma, gastric, and thyroid cancers (Sredni et al, 2004; Todaro et al, 2006). The majority of reports indicate that IL-10 produced from immune cells may promote lung cancer growth via suppressing immune surveillance (Wang et al, 2011; Zeni et al, 2007). This suppression is due to defected function of both T cells and antigen presenting cells (Sharma et al, 1999). No evidence has yet shown that IL-10 expressed in tumor cells could promote tumor progression. Therefore, the nature of IL-10-promoted tumor malignancy of lung cancer cells, i.e., whether it occurs via an autocrine or paracrine pathway, is still unclear. In the present study, we provided the molecular evidence to show that IL-10 is induced by HPV E6 oncoprotein and acts as an autocrine growth factor that not only promotes lung cancer growth, but also promotes anchorage-independent soft-agar growth and invasiveness (Figure 7). We also tested the the effect of exogenous IL-10 on migration capability of lung cancer cells. As expected, the capability was decreased by IL-10 neutralized antibody in TL1 cells, but the capability was increased by IL-10 recombinant protein in TL4 cells (Supplementary Figure 3). The autocrine regulation of cell growth by IL-10 is mediated through the IL-10 receptor (IL-10R). The results presented here for TL1 cells consistently showed that the capability for migration and invasion promoted by IL-10 could be diminished by IL-10R-knockdown (Supplementary Figure 4). This strongly suggests that IL-10 induced by E6 can directly promote lung cancer cell invasiveness and soft-agar growth via the autocrine loop of IL-10/IL-10R.

IL-10 may play a dual role in the development and progression of human cancers (Lin & Karin, 2007). A recent report demonstrated that IL-10 deficiency increases chemical-induced tumor incidence, growth, and foci formation in IL-10 knockout C57BL/6 mice compared with wild-type mice in a colitis-associated colon cancer model (Tanikawa et al, 2012). The authors further indicated that IL-10 deficiency increases the numbers of myeloid-derived suppressor cells in which high levels of IL-1β was expressed to block tumor growth (Tanikawa et al, 2012). In melanoma, IL-10 has been shown to suppress tumor growth and metastasis via inhibition of angiogenesis, indicating an anti-tumor action of IL-10 (Huang et al, 1996). However, in animal models and in human tumors, IL-10 was shown to promote metastatic potential in lung tumor cells *in vivo* by promoting angiogenesis and resistance to apoptosis (Hatanaka et al, 2001; Zeng et al, 2010). IL-10 is not only expressed by tumor cells but also expressed by different types of immune cells (Kim et al, 2006; Shih et al, 2005). The limitation of this study is to quantify the IL-10 expression from tumor cells, and to exclude IL-10 expression from the surrounding non-tumor and immune cells. In the present study, tumor tissues from lung cancer patients were obtained from the frozen section of surgically resected lung tumor parts according to the pathology examination. Therefore, we considered that IL-10 was largely expressed from tumor cells. Elevation of serum or tumor-expressed IL-10 may independently predict poor prognosis in advanced lung cancer patients (De Vita et al, 2000; Hatanaka et al, 2000). Moreover, after chemotherapy, patients whose serum IL-10 levels were stable or elevated showed a greater risk of tumor recurrence and distant metastasis, and of chemoresistance, when compared with patients with lower serum IL-10 expression (De Vita et al,

2000). Our results appear to support this observation as we found that tumor-derived and exogenous IL-10 may promote tumor aggressiveness and poor outcome in lung adenocarcinoma patients who had HPV 16/18 E6-positive tumors.

Upregulation of IL-10 production by phosphorylation of CREB via the PI3K/AKT pathway has been shown in immune cells such as monocytes and macrophages (Mosser & Zhang, 2008; Saraiva & O'Garra, 2010). Notably, HPV E6 upregulates cIAP2 via the EGFR/PI3K/AKT cascades, and in turn contributes to cisplatin resistance in HPV associated lung cancer. These results give the clue that HPV E6 might regulate IL-10 expression in lung cancer via the PI3K/AKT signaling pathway (Wu et al, 2010). In the present study, IL-10 production in E6-positive lung cancer cells was predominantly regulated by phosphorylation of CREB via the PI3K/AKT pathway (Figure 6). Unexpectedly, IL-10 was able to activate CIP2A transcription via the phosphorylation of CREB induced by the PI3K signaling pathway and also promoted tumor malignancy (Figure 8). CIP2A has been shown to have an oncogenic role in human malignancies, operating via inactivation of PP2A and stabilization of c-Myc protein (Junttila et al, 2007). CIP2A over-expression has been associated with poor prognosis in various human carcinomas, including lung cancer (Dong et al, 2011; Ma et al, 2011; Xu et al, 2011). A prognostic value of CIP2A and IL-10 mRNA levels was also indicated in the present study population (Table 3). Moreover, the correlation of CIP2A with IL-10 expression in lung tumors was also supported by our mechanistic studies from lung cancer cell models (Figure 8).

Recently, ectopic CIP2A expression in hepatocellular carcinoma and head and neck squamous cell carcinoma cells has been suggested to enhance PI3K/AKT activation (Chen et al, 2010b; Lin et al, 2012). Therefore, it is conceivable that a feedback loop of IL-10-CIP2A-phosphorylated-CREB may be involved in the progression of E6-mediated IL-10 lung adenocarcinoma. Previous studies indicated that a proteasome inhibitor, bortezomib, significantly reduced CIP2A expression and increased apoptosis in hepatocellular carcinoma and head and neck carcinoma cells (Chen et al, 2010b; Chen et al, 2011; Huang et al, 2012; Lin et al, 2012; Tseng et al, 2012). Therefore, we expected that bortezomib or a PI3K inhibitor could be used to suppress tumor invasiveness and to improve the outcome in HPV-associated lung adenocarcinoma patients who had high IL-10 expression. In summary, we provide evidence that IL-10-mediated CIP2A may play a crucial role in the tumor aggressiveness of lung adenocarcinoma, particularly in patients with HPV 16/18 E6-positive tumors.

Materials and Methods

Study subjects and specimen collection

For Nickel analysis**,** surgical specimens were obtained from 76 patients with primary non-small cell lung cancer (NSCLC) between 1993 and 2003 at Taichung Veterans General Hospital, Taichung, Taiwan. Lung tumors and adjacent normal lung tissues were surgically resected from lung cancer patients. These tissues were immediately snap-frozen and subsequently stored at –80 ^{o}C. None of the patients received neoadjuvant chemotherapy or radiotherapy before surgery. Lung tissues underwent a series of examinations of pathological stages by board-certified pathologists. The tumor histology and stage of each specimen were determined according to the WHO classification. Demographic data for each patients including age, gender, and smoking status were collected from patient interviews and review of hospital charts. As shown in Supplementary Table 1, all patients were lifetime never-smokers. The patients' ages ranged from 40 to 82 years (mean, 63.4 years). There were 38 male (50.0%) and 38 female (50.0%) patients. Patients with adenocarcinoma (ADC) histology were more prevalent than were those with squamous cell carcinoma (SCC) histology (67.1% vs. 32.9%). Overall survival (OS) and relapse free survival (RFS) was calculated from the day of surgery to the date of death or last follow-up. Patients were asked to sign written informed consent forms and was approved by the Institutional Review Board, Chung Shan Medical University Hospital (CS07159).

For IL-10 expression analysis, this study consisted of 98 lung cancer patients. All patients were unrelated ethnic Chinese and residents of central Taiwan. The inclusion criteria for patients were: primary diagnosed with lung adenocarcinoma; no metastatic disease at diagnosis; no previous diagnosis of carcinoma; no neoadjuvant treatment before primary surgery; no evidence of disease within one month of primary surgery. Lung tumor specimens were collected by surgical resection, and surgically resected tissues were stored at −80℃ at the Division of Thoracic Surgery, Taichung Veterans General Hospital. Patients were consecutively recruited between 1993 and 2004. This study was approved by the hospital's Institutional Review Board (Institutional Review Board, Chung Shan Medical University Hospital. CSMUH No: CS11177). The TNM stage, tumor type and stage of each collected specimen were histologically determined according to the WHO classification system. The age of all patients was between 26 and 84 years (mean ± SD = 64.2 ± 11.2). Clinical parameters and overall survival data were collected from chart review and the Taiwan Cancer Registry, Department of Health, Executive Yuan, ROC. The survival time was defined to be the period of time from the date of primary surgery to the date of death. The median follow-up time after surgery was 21.5 months and the median overall survival of all patients was 21.9 months. During this survey, 63 patients died. Based on follow-up data, 35 patients relapsed (15 had local recurrence, 35 had distant metastasis, and 11 had local and distant metastasis). Among these patients, tumors frequently relapsed in the lung (15 patients) and metastasized in the bone (13 patients), brain (10 patients), liver (5 patients), pleura (4 patients), chest wall (3 patients), and mediastinum (1 patient). In total, 11 patients had tumors that metastasized to more than one organ.

Inductively coupled plasma mass spectrometry (ICP-MS) analysis

Nickel content in adjacent normal lung tissue was analyzed by ICP-MS (Agilent Technologies, Model 7700X, Santa Clara, CA) after microwave-assisted closed vessel digestion. Initially, all frozen tissues were equilibrated for 0.5 h at room temperature and then heated for 4 h at 103 to 105 ^{o}C. Subsequently, the dry tissue samples were weighed into digestion vessels made of ultrapure quartz and were digested with 2 ml 65% nitric acid and 1 ml 30% hydrogen peroxide. After cooling, the solutions were diluted to 10 ml with ultrapure water, and stored at 4 ^{o}C until analysis. Specimens were analyzed alongside quality control (QC) materials (Standard reference material 1577a; bovine liver) to evaluate the accuracy of the instrumental methods and the

analytical procedure. During the actual sample analysis, QC analyses were performed including a calibration check (correlation coefficient above 0.995), blank sample analysis, duplicate sample analysis (relative percent difference below 15.4%), and spiked sample analysis (relative recovery percent difference below 5%). Nickel content was calculated as micrograms per gram dry weight of lung tissue. Nickel concentration determined by ICP-MS with less than 3-fold of the method detection limit (MDL) was considered as non-detection. In the present study, no nickel concentration was less than 3-fold of the MDL in any specimen. Tissue samples were analyzed for the presence of nickel while the analyst was blinded to the clinical status of the individual patients.

Direct sequencing

Direct sequencing was performed using polymerase chain reaction (PCR) products amplified from lung tumors of lung cancer patients to detect EGFR mutations in exons 19 and 21 (Tung et al., 2013). DNA was extracted from microdissected lung tumors. Target sequences were amplified in a 50 μl reaction mixture containing 20 pmol of each primer, 2.5 units tag polymerase (TAKARA Shuzo, Shiga, Japan), 0.5 mM deoxyribonucleotide triphosphates (dNTPs), 5 μl PCR reaction buffer, and 1μl genomic DNA (100 ng) as the template. Target sequences were amplified using the following primers: (5′-CCAGATCACTGGGCAGCATGTGGCACC-3′ and 5′-AGCAGGGTCTAGAGCAGAGCAGCTGCC-3′) for exon 19 and (5′ -TCAGAGCCTGGCATGAACATGACCCTG-3 ′ and 5′-GGTCCCTGGTG -TCAGGAAAATGCTGG-3′) for exon 21. The PCR products were sequenced with an automated sequencing system (3100 Avant Genetic Analyzer, Applied Biosystems, Hitachi, Japan), and the same primers used for PCR were used for DNA sequencing. The occurrence of EGFR mutations were confirmed by direct sequencing of both strands.

Real-time PCR

Total RNA was extracted by homogenization in 1 ml TRIzol reagent, followed by chloroform extraction and ethanol precipitation. A 3 μg sample of total RNA was reverse transcribed using SuperScript II Reverse Transcriptase (Invitrogen Life Technologies). The RECK and SPRY2 mRNA expressions of reverse transcribed products were analyzed by a Real-Time Thermocycler 7500 (Applied Biosystems, Foster City, CA) using the following primers: (5′-TGATGGCTGGGT -TGGCTTAG-3′ and 5′-TTTGAAGATGCCTGCTTGCA-3′) for RECK and (5′-GATCACGGAGTTCAGATGTGTTCT-3′ and 5′-GGCTCCCCACGCTGT -3′) for SPRY2. A 10 ng sample of DNase 1-treated total RNA was subjected to miR-21 real-time PCR analysis with the TaqMan miRNA Reverse Transcription Kit, miRNA assay, and a Real-Time Thermocycler 7500. RNU6B was used as the small RNA reference housekeeping gene.

Lung cancer cells and culture conditions

H1355, H23, H1975, SiHa, HeLa, C33A, A549 and H1299 cancer cell lines were obtained from The American Type Culture Collection (ATCC) (Wu et al, 2011). TL1, TL2, and TL4 cells were kindly provided by Dr. Cheng YW (Cheng et al, 2007). All of these three cell lines are p53 wild type. TL1 and TL2 cell lines are HPV 16 E6 positive and TL4 is HPV E6 negative. Cells were cultured and stored according to the suppliers' instructions.

Cytotoxicity assay

In vitro cytotoxicity of nickel chloride was studied using the 3-(4,5-dimethylthiazol-2-yl) -2,5-diphenyltetrazolium bromide (MTT; Sigma, St Louis, MO) assay was described previously (Chiou et al., 2014). The cell survival curves were used to calculate the concentration of nickel chloride that resulted in 75%

cell survival in three cell lines.

Western blotting

The detail procedures of western blotting analysis were described previously (Wu et al., 2014). The specific antibodies for detection of EGFR, RECK, SPRY2, α-tubulin, AKT, and p-AKT were purchased from GeneTex (GeneTex Inc., Irvine, CA), and p65 as well as C23 antibody were obtained from Santa Cruz Biotechnology (Santa Cruz Biotechnology, Santa Cruz, CA). β-actin antibody was purchased from Sigma (St Louis, MO).

Boyden chamber assay

A Boyden chamber with a pore size of 8 μm was used for the *in vitro* cell invasion assay. The inhibitor of miR-21 or RECK expression vector was transfected into H1355 and H23 cells. After 24 h incubation, both cell types were treated with nickel chloride (Sigma, St Louis, MO) for an additional 24 h and then 1×10^4 cells in 0.5% serum containing culture medium (HyClone, Ogden, UT) were plated in the upper chamber, and 10% fetal bovine serum was added to the culture medium in the lower chamber as a chemoattractant. The upper side of the filter was covered with 0.2% Matrigel (Collaborative Research, Boston, MI) and diluted in RPMI-1640. After 24 h, the cells on the upper side of the filter were removed, and cells that adhered to the underside of the filter were fixed in 95% ethanol and stained with 10% Giemsa dye. The number of invasive cells was counted by examining ten contiguous fields of each sample to obtain a representative number of the cells that invaded across the membrane. A detailed procedure was described previously (Wu et al., 2014).

Plasmid constructs and transfection

The shEGFR (TRCN0000121067) plasmid was purchased from National RNAi Core Facility, Academia Sinica, Taiwan. The expression vector of EGFR L858R (#11012) was purchased from Addgene (Cambridge, MA). The expression vector of RECK (RG212174) was purchased from OriGene (Rockville, MD). The CIP2A-Luc plasmid was constructed by inserting a 972, 452 or 162 bps XhoI/KpnI fragment into an XhoI/KpnI-treated pGL3 vector (Promega).The expression plasmids were transiently transfected into lung cancer cells (5×10^5) using the TurboFect reagent (Fermentas, Glen Burnie, MD) according to the manufacturer's protocols. After 48 h, cells were harvested and whole-cell extracts were used for subsequent experiments.

MiR-21 inhibitor transfection

The transfection of miR-21 inhibitor was described previously (Lin et al., 2014). In brief, the standard protocol for Lipofectamine 2000 transfection reagent (Invitrogen, Foster City, CA) was used to transfect the miR-21 inhibitor (40-80 nM per dish; Ambion, Foster City, CA) and non-specific miR controls (Ambion, Foster City, CA) into cells that were cultured in a 100-mm dish at a density of 5×10^5 cells/dish. The transfection efficiency was determined by real-time PCR.

Luciferase reporter assay

The NF-κB-luciferase construct was kindly provided by Dr. Tsui-Chun Tsou (Division of Environmental Health and Occupational Medicine, National Health Research Institutes, Zhunan, Miaoli, Taiwan). The NF-κB-luciferase reporter plasmid (3 μg) and the pSV-β-galactosidase plasmid (3 μg) were co-transfected into cells for 24 h. After transfection, the cells were incubated in fresh medium containing various concentrations of nickel chloride for an additional 24 h. Luciferase reporter activity and β-galactosidase activity were determined by using the Luciferase Assay System and β-galactosidase Enzyme Assay System (Promega, Madison, WI), respectively. The NF-κB-luciferase activity was normalized against the β-galactosidase

activity.

Immunohistochemical staining

Immunohistochemical (IHC) staining to evaluate HPV 16/18 E6 expression in tumor tissues was performed as described previously (Cheng et al, 2007). Briefly, formalin-fixed and paraffin-embedded specimens were sectioned at a thickness of 3 μm. Sections were deparaffinized in xylene, rehydrated through serial dilutions of alcohol, and washed in *phosphate-buffered saline*, the buffer which was used for all subsequent washes. Sections were heated in a microwave oven twice for 5 min in citrate buffer, and then incubated with polyclonal anti-HPV16 or HPV18 E6 antibody (Santa Cruz Biotechnology and Chemicon International, Inc.) for 90 min at 25℃. The conventional streptavidin peroxidase method (DAKO, LSAB Kit K675) was performed to develop signals and the cells were counterstained with hematoxylin. Negative E6 immunostaining was defined to be with 0% to 10% positive nuclei, and cases with >10% positive nuclei were decided to be positive for E6 immunostaining. Three observers independently evaluated the intensities of the signals.

Cell doubling time, Migration, invasion assay and anchorage-independent soft agar growth

The procedures and methods were as described previously (Wu et al, 2011). In anchorage-independent soft agar growth assay, the colonies larger than 150 μm in diameter were counted.

Animal model

BALB/cAnN.Cg-*Foxn1*^{nu}/CrlNarl mice were maintained in a standard mouse facility at Chung Shan Medical University. When these nude mice were 7 weeks of age, NC and IL-10 knockdown TL1 stable cells were injected via the tail vein ($1x10^6$). The mice were then sacrificed after four months. The tumor nodules (diameter > 1 mm) on the surface of lung were counted. Some tumor nodules were frozen at −80 °C for the determination of IL-10 expression by real-time RT-PCR. The remaining lung specimens were stained with hematoxylin and eosin (H&E) and the pathology was confirmed by pathologists.

Chemicals and antibodies

PD153035 was purchased from Calbiochem. All other chemicals were acquired from Sigma Aldrich. Anti-IL-10Ra (C-20), anti-CIP2A (HL1916), anti-p-CREB (Ser133), anti-CREB (Thr217) and anti-c-Myc (9E10) antibodies were purchased from Santa Cruz Biotechnology, Inc. Anti-Akt and anti-p-Akt (Ser 473) antibodies were purchased from Cell Signaling. Anti-human IL-10 antibody (MAB2171) was purchase from R & D Systems, Inc. The antibody for p53 (BP53-12), β-actin and secondary antibodies were purchased from Sigma Aldrich.

Statistical analysis

The median value of nickel content, mRNA expression level in lung cancer patients were used as a cutoff point to divide patients into high- and low- subgroups. The association of clinico-pathological parameters with nickel levels, EGFR mutation, IL-10 and miR-21 levels was determined by the χ^2 test. Survival curves were plotted by the Kaplan-Meier methods using a SPSS statistical software program (version 18.0; SPSS). The log-rank test was used to assess the prognostic significance of different parameters on OS and RFS in lung cancer patients. The P values were calculated using a two-tailed statistical test and $P < 0.05$ was considered statistically significant. SAS 9.1 for Windows (SAS, Cart, NC, USA) was used for the analyses.

References

Azar KK, Tani M, Yasuda H, Sakai A, Inoue M, Sasagawa T (2004) Increased secretion patterns of interleukin-10 and tumor necrosis factor-alpha in cervical squamous intraepithelial lesions. *Human pathology* **35:** 1376-1384

Bais AG, Beckmann I, Lindemans J, Ewing PC, Meijer CJ, Snijders PJ, Helmerhorst TJ (2005) A shift to a peripheral Th2-type cytokine pattern during the carcinogenesis of cervical cancer becomes manifest in CIN III lesions. *Journal of clinical pathology* **58:** 1096-1100

Beveridge R, Pintos J, Parent ME, Asselin J, Siemiatycki J (2010) Lung cancer risk associated with occupational exposure to nickel, chromium VI, and cadmium in two population-based case-control studies in Montreal. *American journal of industrial medicine* **53:** 476-485

Brooks DG, Trifilo MJ, Edelmann KH, Teyton L, McGavern DB, Oldstone MB (2006) Interleukin-10 determines viral clearance or persistence in vivo. *Nature medicine* **12:** 1301-1309

Carpenter RL, Jiang BH (2013) Roles of EGFR, PI3K, AKT, and mTOR in heavy metal-induced cancer. *Current cancer drug targets* **13:** 252-266

Chen H, Kluz T, Zhang R, Costa M (2010a) Hypoxia and nickel inhibit histone demethylase JMJD1A and repress Spry2 expression in human bronchial epithelial BEAS-2B cells. *Carcinogenesis* **31:** 2136-2144

Chen KF, Liu CY, Lin YC, Yu HC, Liu TH, Hou DR, Chen PJ, Cheng AL (2010b) CIP2A mediates effects of bortezomib on phospho-Akt and apoptosis in hepatocellular carcinoma cells. *Oncogene* **29:** 6257-6266

Chen KF, Yu HC, Liu CY, Chen HJ, Chen YC, Hou DR, Chen PJ, Cheng AL (2011) Bortezomib sensitizes HCC cells to CS-1008, an antihuman death receptor 5 antibody, through the inhibition of CIP2A. *Molecular cancer therapeutics* **10:** 892-901

Cheng YW, Chiou HL, Sheu GT, Hsieh LL, Chen JT, Chen CY, Su JM, Lee H (2001) The association of human papillomavirus 16/18 infection with lung cancer among nonsmoking Taiwanese women. *Cancer research* **61:** 2799-2803

Cheng YW, Wu MF, Wang J, Yeh KT, Goan YG, Chiou HL, Chen CY, Lee H (2007) Human papillomavirus 16/18 E6 oncoprotein is expressed in lung cancer and related with p53 inactivation. *Cancer Res* **67:** 10686-10693

Chiou YH, Wong RH, Chao MR, Chen CY, Liou SH, Lee H (2014) Nickel accumulation in lung tissues is associated with increased risk of p53 mutation in lung cancer patients. *Environmental and molecular mutagenesis* **55:** 624-632

De Matteis S, Consonni D, Lubin JH, Tucker M, Peters S, Vermeulen R, Kromhout H, Bertazzi PA, Caporaso NE, Pesatori AC, Wacholder S, Landi MT (2012) Impact of occupational carcinogens on lung cancer risk in a general population. *International journal of epidemiology* **41:** 711-721

De Vita F, Orditura M, Galizia G, Romano C, Roscigno A, Lieto E, Catalano G (2000) Serum interleukin-10 levels as a prognostic factor in advanced non-small cell lung cancer patients. *Chest* **117:** 365-373

Ding J, Miao ZH, Meng LH, Geng MY (2006) Emerging cancer therapeutic opportunities target DNA-repair systems. *Trends in pharmacological sciences* **27:** 338-344

Ding X, Mohd AB, Huang Z, Baba T, Bernardini MQ, Lyerly HK, Berchuck A, Murphy SK, Buermeyer AB, Devi GR (2009) MLH1 expression sensitises ovarian cancer cells to cell death mediated by XIAP inhibition.

British journal of cancer **101:** 269-277

Dong QZ, Wang Y, Dong XJ, Li ZX, Tang ZP, Cui QZ, Wang EH (2011) CIP2A is overexpressed in non-small cell lung cancer and correlates with poor prognosis. *Annals of surgical oncology* **18:** 857-865

El-Sherif AM, Seth R, Tighe PJ, Jenkins D (2001) Quantitative analysis of IL-10 and IFN-gamma mRNA levels in normal cervix and human papillomavirus type 16 associated cervical precancer. *The Journal of pathology* **195:** 179-185

Fernandes AP, Goncalves MA, Duarte G, Cunha FQ, Simoes RT, Donadi EA (2005) HPV16, HPV18, and HIV infection may influence cervical cytokine intralesional levels. *Virology* **334:** 294-298

Gabriely G, Wurdinger T, Kesari S, Esau CC, Burchard J, Linsley PS, Krichevsky AM (2008) MicroRNA 21 promotes glioma invasion by targeting matrix metalloproteinase regulators. *Molecular and cellular biology* **28:** 5369-5380

Grimsrud TK, Berge SR, Haldorsen T, Andersen A (2002) Exposure to different forms of nickel and risk of lung cancer. *American journal of epidemiology* **156:** 1123-1132

Hatanaka H, Abe Y, Kamiya T, Morino F, Nagata J, Tokunaga T, Oshika Y, Suemizu H, Kijima H, Tsuchida T, Yamazaki H, Inoue H, Nakamura M, Ueyama Y (2000) Clinical implications of interleukin (IL)-10 induced by non-small-cell lung cancer. *Annals of oncology : official journal of the European Society for Medical Oncology / ESMO* **11:** 815-819

Hatanaka H, Abe Y, Naruke M, Tokunaga T, Oshika Y, Kawakami T, Osada H, Nagata J, Kamochi J, Tsuchida T, Kijima H, Yamazaki H, Inoue H, Ueyama Y, Nakamura M (2001) Significant correlation between interleukin 10 expression and vascularization through angiopoietin/TIE2 networks in non-small cell lung cancer. *Clinical cancer research : an official journal of the American Association for Cancer Research* **7:** 1287-1292

Huang CY, Wei CC, Chen KC, Chen HJ, Cheng AL, Chen KF (2012) Bortezomib enhances radiation-induced apoptosis in solid tumors by inhibiting CIP2A. *Cancer letters* **317:** 9-15

Huang L, Chen D, Ding Y, Feng S, Wang ZL, Liu M (2013) Nickel-cobalt hydroxide nanosheets coated on NiCo2O4 nanowires grown on carbon fiber paper for high-performance pseudocapacitors. *Nano letters* **13:** 3135-3139

Huang M, Wang J, Lee P, Sharma S, Mao JT, Meissner H, Uyemura K, Modlin R, Wollman J, Dubinett SM (1995) Human non-small cell lung cancer cells express a type 2 cytokine pattern. *Cancer Res* **55:** 3847-3853

Huang S, Xie K, Bucana CD, Ullrich SE, Bar-Eli M (1996) Interleukin 10 suppresses tumor growth and metastasis of human melanoma cells: potential inhibition of angiogenesis. *Clinical cancer research : an official journal of the American Association for Cancer Research* **2:** 1969-1979

Junttila MR, Puustinen P, Niemela M, Ahola R, Arnold H, Bottzauw T, Ala-aho R, Nielsen C, Ivaska J, Taya Y, Lu SL, Lin S, Chan EK, Wang XJ, Grenman R, Kast J, Kallunki T, Sears R, Kahari VM, Westermarck J (2007) CIP2A inhibits PP2A in human malignancies. *Cell* **130:** 51-62

Kao CT, Ding SJ, Wang CK, He H, Chou MY, Huang TH (2006) Comparison of frictional resistance after immersion of metal brackets and orthodontic wires in a fluoride-containing prophylactic agent. *American journal of orthodontics and dentofacial orthopedics : official publication of the American Association of Orthodontists, its constituent societies, and the American Board of Orthodontics* **130:** 568 e561-569

Kasprzak KS, Bal W, Karaczyn AA (2003) The role of chromatin damage in nickel-induced carcinogenesis. A

review of recent developments. *Journal of environmental monitoring : JEM* **5:** 183-187

Ke Q, Li Q, Ellen TP, Sun H, Costa M (2008) Nickel compounds induce phosphorylation of histone H3 at serine 10 by activating JNK-MAPK pathway. *Carcinogenesis* **29:** 1276-1281

Kim R, Emi M, Tanabe K, Arihiro K (2006) Tumor-driven evolution of immunosuppressive networks during malignant progression. *Cancer Res* **66:** 5527-5536

Kitajima S, Miki T, Takegami Y, Kido Y, Noda M, Hara E, Shamma A, Takahashi C (2011) Reversion-inducing cysteine-rich protein with Kazal motifs interferes with epidermal growth factor receptor signaling. *Oncogene* **30:** 737-750

Kwak HJ, Kim YJ, Chun KR, Woo YM, Park SJ, Jeong JA, Jo SH, Kim TH, Min HS, Chae JS, Choi EJ, Kim G, Shin SH, Gwak HS, Kim SK, Hong EK, Lee GK, Choi KH, Kim JH, Yoo H, Park JB, Lee SH (2011) Downregulation of Spry2 by miR-21 triggers malignancy in human gliomas. *Oncogene* **30:** 2433-2442

Lin WW, Karin M (2007) A cytokine-mediated link between innate immunity, inflammation, and cancer. *The Journal of clinical investigation* **117:** 1175-1183

Lin YC, Chen KC, Chen CC, Cheng AL, Chen KF (2012) CIP2A-mediated Akt activation plays a role in bortezomib-induced apoptosis in head and neck squamous cell carcinoma cells. *Oral oncology*

Lu C, Soria JC, Tang X, Xu XC, Wang L, Mao L, Lotan R, Kemp B, Bekele BN, Feng L, Hong WK, Khuri FR (2004) Prognostic factors in resected stage I non-small-cell lung cancer: a multivariate analysis of six molecular markers. *Journal of clinical oncology : official journal of the American Society of Clinical Oncology* **22:** 4575-4583

Ma L, Wen ZS, Liu Z, Hu Z, Ma J, Chen XQ, Liu YQ, Pu JX, Xiao WL, Sun HD, Zhou GB (2011) Overexpression and small molecule-triggered downregulation of CIP2A in lung cancer. *PloS one* **6:** e20159

Mocellin S, Marincola FM, Young HA (2005) Interleukin-10 and the immune response against cancer: a counterpoint. *Journal of leukocyte biology* **78:** 1043-1051

Mollerup S, Rivedal E, Maehle L, Haugen A (1996) Nickel(II) induces alterations in EGF- and TGF-beta 1-mediated growth control during malignant transformation of human kidney epithelial cells. *Carcinogenesis* **17:** 361-367

Mongan M, Tan Z, Chen L, Peng Z, Dietsch M, Su B, Leikauf G, Xia Y (2008) Mitogen-activated protein kinase kinase kinase 1 protects against nickel-induced acute lung injury. *Toxicological sciences : an official journal of the Society of Toxicology* **104:** 405-411

Moore KW, de Waal Malefyt R, Coffman RL, O'Garra A (2001) Interleukin-10 and the interleukin-10 receptor. *Annual review of immunology* **19:** 683-765

Mosser DM, Zhang X (2008) Interleukin-10: new perspectives on an old cytokine. *Immunological reviews* **226:** 205-218

Niu J, Shi Y, Tan G, Yang CH, Fan M, Pfeffer LM, Wu ZH (2012) DNA damage induces NF-kappaB-dependent microRNA-21 up-regulation and promotes breast cancer cell invasion. *The Journal of biological chemistry* **287:** 21783-21795

Noda M, Oh J, Takahashi R, Kondo S, Kitayama H, Takahashi C (2003) RECK: a novel suppressor of malignancy linking oncogenic signaling to extracellular matrix remodeling. *Cancer metastasis reviews* **22:** 167-175

Oh J, Takahashi R, Kondo S, Mizoguchi A, Adachi E, Sasahara RM, Nishimura S, Imamura Y, Kitayama H, Alexander DB, Ide C, Horan TP, Arakawa T, Yoshida H, Nishikawa S, Itoh Y, Seiki M, Itohara S, Takahashi C, Noda M (2001) The membrane-anchored MMP inhibitor RECK is a key regulator of extracellular matrix integrity and angiogenesis. *Cell* **107:** 789-800

Saraiva M, O'Garra A (2010) The regulation of IL-10 production by immune cells. *Nature reviews Immunology* **10:** 170-181

Seike M, Goto A, Okano T, Bowman ED, Schetter AJ, Horikawa I, Mathe EA, Jen J, Yang P, Sugimura H, Gemma A, Kudoh S, Croce CM, Harris CC (2009) MiR-21 is an EGFR-regulated anti-apoptotic factor in lung cancer in never-smokers. *Proceedings of the National Academy of Sciences of the United States of America* **106:** 12085-12090

Sharma A, Rajappa M, Saxena A, Sharma M (2007) Cytokine profile in Indian women with cervical intraepithelial neoplasia and cancer cervix. *International journal of gynecological cancer : official journal of the International Gynecological Cancer Society* **17:** 879-885

Sharma S, Stolina M, Lin Y, Gardner B, Miller PW, Kronenberg M, Dubinett SM (1999) T cell-derived IL-10 promotes lung cancer growth by suppressing both T cell and APC function. *J Immunol* **163:** 5020-5028

Shih CM, Lee YL, Chiou HL, Hsu WF, Chen WE, Chou MC, Lin LY (2005) The involvement of genetic polymorphism of IL-10 promoter in non-small cell lung cancer. *Lung Cancer* **50:** 291-297

Smith DR, Kunkel SL, Burdick MD, Wilke CA, Orringer MB, Whyte RI, Strieter RM (1994) Production of interleukin-10 by human bronchogenic carcinoma. *Am J Pathol* **145:** 18-25

Soria JC, Moon C, Kemp BL, Liu DD, Feng L, Tang X, Chang YS, Mao L, Khuri FR (2003) Lack of interleukin-10 expression could predict poor outcome in patients with stage I non-small cell lung cancer. *Clinical cancer research : an official journal of the American Association for Cancer Research* **9:** 1785-1791

Sredni B, Weil M, Khomenok G, Lebenthal I, Teitz S, Mardor Y, Ram Z, Orenstein A, Kershenovich A, Michowiz S, Cohen YI, Rappaport ZH, Freidkin I, Albeck M, Longo DL, Kalechman Y (2004) Ammonium trichloro(dioxoethylene-o,o')tellurate (AS101) sensitizes tumors to chemotherapy by inhibiting the tumor interleukin 10 autocrine loop. *Cancer research* **64:** 1843-1852

Tanikawa T, Wilke CM, Kryczek I, Chen GY, Kao J, Nunez G, Zou W (2012) Interleukin-10 ablation promotes tumor development, growth, and metastasis. *Cancer research* **72:** 420-429

Todaro M, Zerilli M, Ricci-Vitiani L, Bini M, Perez Alea M, Maria Florena A, Miceli L, Condorelli G, Bonventre S, Di Gesu G, De Maria R, Stassi G (2006) Autocrine production of interleukin-4 and interleukin-10 is required for survival and growth of thyroid cancer cells. *Cancer research* **66:** 1491-1499

Tseng LM, Liu CY, Chang KC, Chu PY, Shiau CW, Chen KF (2012) CIP2A is a target of bortezomib in human triple negative breast cancer cells. *Breast cancer research : BCR* **14:** R68

Wang R, Lu M, Zhang J, Chen S, Luo X, Qin Y, Chen H (2011) Increased IL-10 mRNA expression in tumor-associated macrophage correlated with late stage of lung cancer. *Journal of experimental & clinical cancer research : CR* **30:** 62

Wu CH, Tang SC, Wang PH, Lee H, Ko JL (2012) Nickel-induced epithelial-mesenchymal transition by reactive oxygen species generation and E-cadherin promoter hypermethylation. *The Journal of biological chemistry* **287:** 25292-25302

Wu DW, Liu WS, Wang J, Chen CY, Cheng YW, Lee H (2011) Reduced p21(WAF1/CIP1) via alteration of p53-DDX3 pathway is associated with poor relapse-free survival in early-stage human papillomavirus-associated lung cancer. *Clinical cancer research : an official journal of the American Association for Cancer Research* **17:** 1895-1905

Wu HH, Wu JY, Cheng YW, Chen CY, Lee MC, Goan YG, Lee H (2010) cIAP2 upregulated by E6 oncoprotein via epidermal growth factor receptor/phosphatidylinositol 3-kinase/AKT pathway confers resistance to cisplatin in human papillomavirus 16/18-infected lung cancer. *Clin Cancer Res* **16:** 5200-5210

Xu P, Xu XL, Huang Q, Zhang ZH, Zhang YB (2011) CIP2A with survivin protein expressions in human non-small-cell lung cancer correlates with prognosis. *Med Oncol*

Yanagawa H, Takeuchi E, Suzuki Y, Ohmoto Y, Bando H, Sone S (1999) Presence and potent immunosuppressive role of interleukin-10 in malignant pleural effusion due to lung cancer. *Cancer letters* **136:** 27-32

Zeng L, O'Connor C, Zhang J, Kaplan AM, Cohen DA (2010) IL-10 promotes resistance to apoptosis and metastatic potential in lung tumor cell lines. *Cytokine* **49:** 294-302

Zeni E, Mazzetti L, Miotto D, Lo Cascio N, Maestrelli P, Querzoli P, Pedriali M, De Rosa E, Fabbri LM, Mapp CE, Boschetto P (2007) Macrophage expression of interleukin-10 is a prognostic factor in nonsmall cell lung cancer. *The European respiratory journal* **30:** 627-632

zur Hausen H (2000) Papillomaviruses causing cancer: evasion from host-cell control in early events in carcinogenesis. *Journal of the National Cancer Institute* **92:** 690-698

zur Hausen H (2002) Papillomaviruses and cancer: from basic studies to clinical application. *Nature reviews Cancer* **2:** 342-350

Figures and Tables

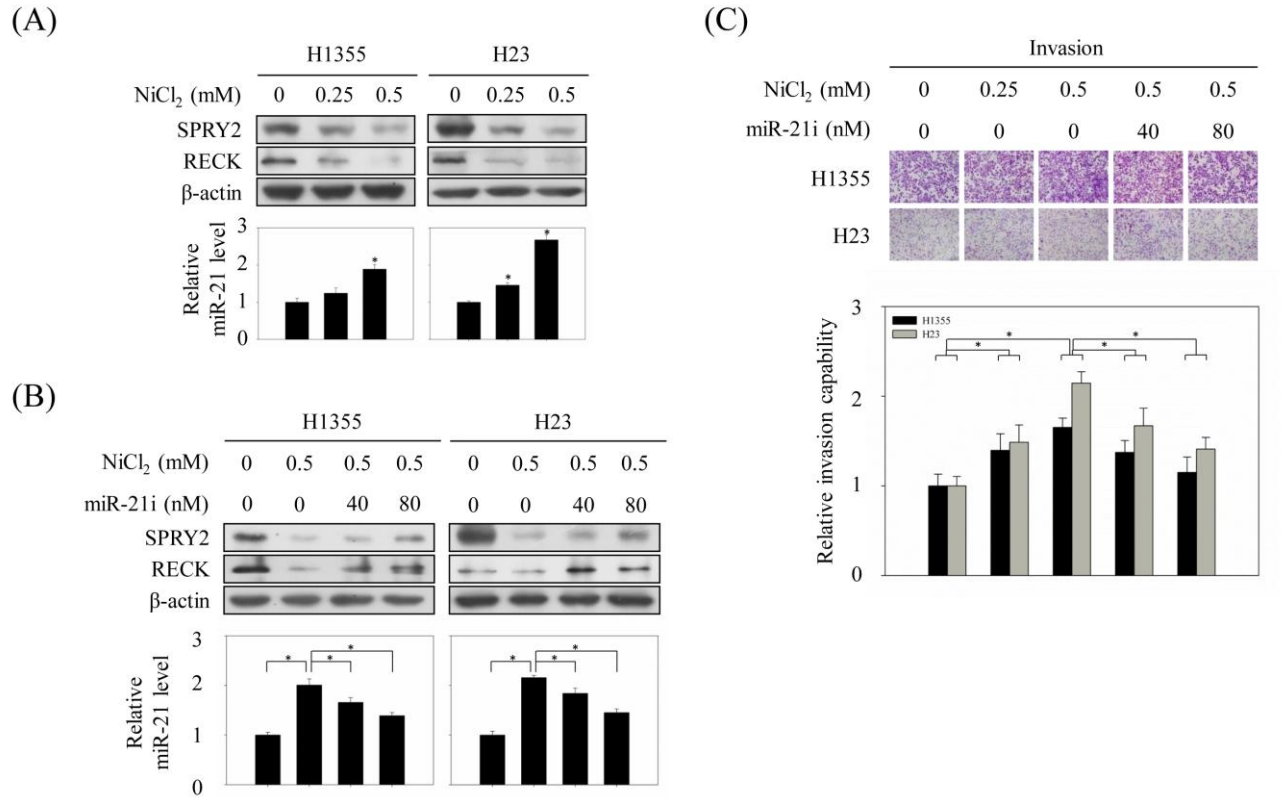

Figure 1. Nickel-induced miR-21 expression is responsible for invasion capability in lung cancer cells. H1355 and H23 cells were treated with different concentrations of nickel chloride for 24 h and then total proteins and RNAs were extracted from the cell pellets. (A) The expressions of SPRY2 and RECK were evaluated using western blot using the specific antibody. MiR-21 expression levels were determined by real-time PCR. (B) The inhibitor of miR-21 (miR-21 i) was transfected into H1355 and H23 cells for 24 h and then both cells were treated with 0.5 mM nickel chloride for an additional 24 h. Western blotting and real-time RT-PCR analysis was performed to evaluate the protein and mRNA expression, respectively, of RECK, SPRY2, and miR-21 in both cells with nickel chloride and/or combined with miR-21 inhibitor. (C) 1×10^4 cells were seeded into a Boyden chamber to evaluate invasion capability after both cell types were treated with nickel chloride and/or combined with miR-21 inhibitor. The invasion capability was normalized against untreated parental cells of both types. The data represent three independent experiments. P value was calculated by student t test. * $P < 0.05$.

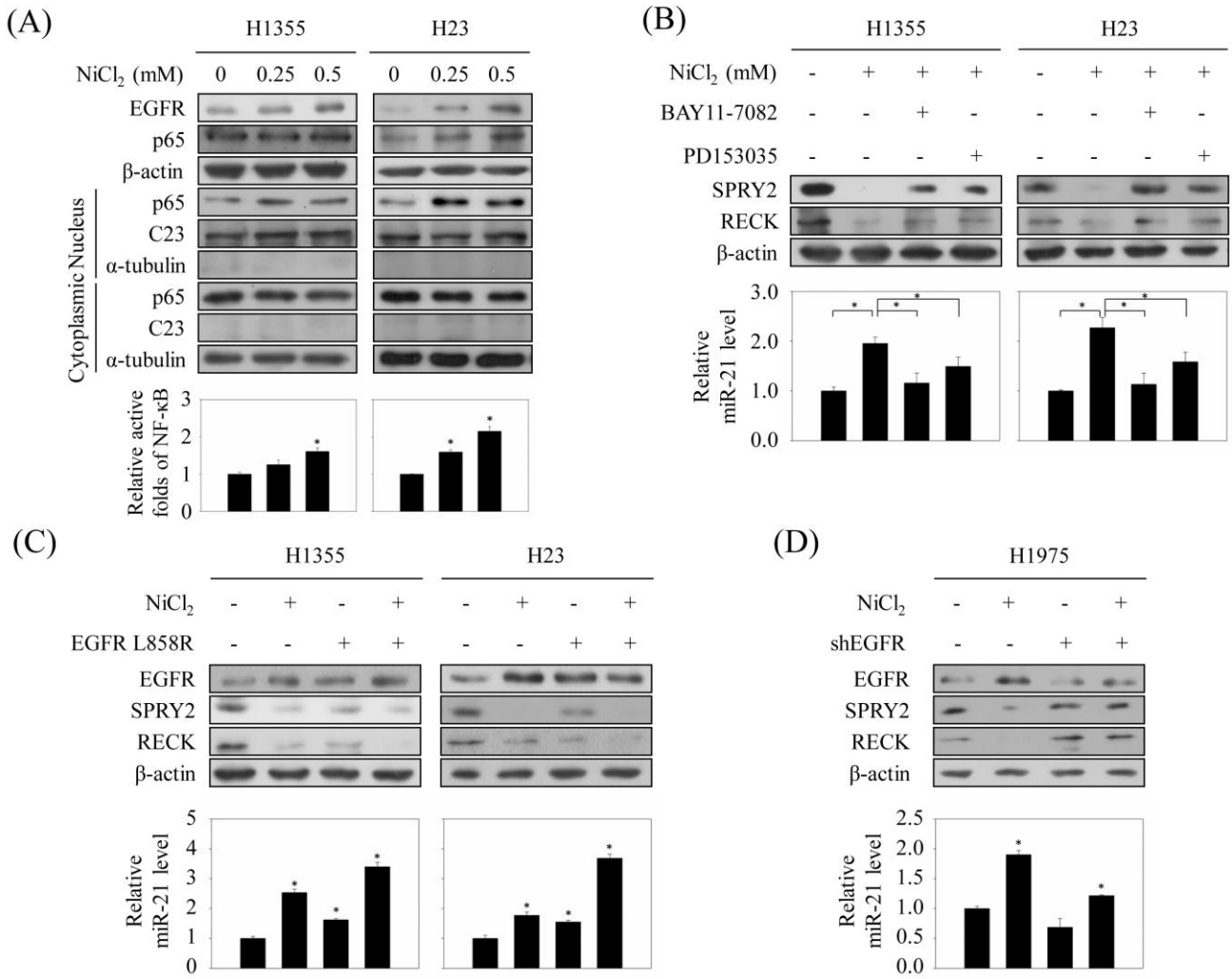

Figure 2. Nickel induces miR-21 expression via activating the EGFR/NF-κB signaling pathway. H1355 and H23 cells were treated with nickel chloride for 24 h and the total proteins and nuclear and cytoplasmic fractions were prepared for western blotting analysis. (A) The EGFR and p65 expression in total protein extracts and the expression of p65 in cytoplasmic and nuclear fractions were evaluated. The expressions of β-actin, C23, and α-tubulin were used as total, nuclear, and cytoplasmic protein control, respectively. The relative NF-κB-luciferase reporter activity in H1355 and H23 cells was evaluated by a luciferase reporter assay . (B) Both cell types were treated with 0.5 mM nickel chloride and/or combined with NF-κB inhibitor BAY11-7082 (20 μM) or EGFR inhibitor PD153035 (0.5μM) treatment. Western blotting and real-time PCR were performed to evaluate SPRY2, RECK, and miR-21 expression. (C) Both cell types were treated with 0.5 mM nickel chloride and/or combined with EGFR L858R expression vector transfection. The total proteins were extracted from cell pellets to evaluate the expressions of EGFR, SPRY2, and RECK using western blotting analysis. β-actin was used as protein a loading control. The expression levels of miR-21 were determined by real-time PCR. (D) EGFR mutant H1975 cells (L858R) were transfected with shEGFR to knock down EGFR expression and then treated with 0.5 mM nickel chloride for an additional 24 h. The expressions of EGFR and SPRY2 and RECK were evaluated by western blotting analysis. MiR-21 expression levels were evaluated by real-time PCR analysis. The data represent three independent experiments. P value was obtained by student t test. * $P < 0.05$.

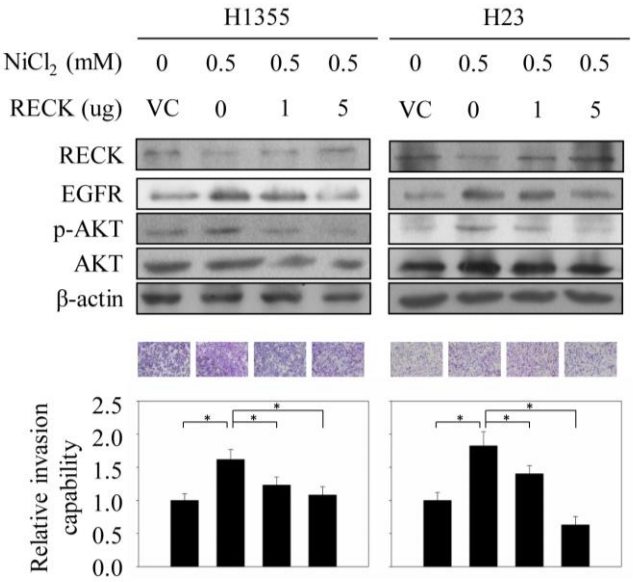

Figure 3. The decrease in RECK expression by nickel-mediated miR-21 is partially responsible for cell invasion. H1355 and H23 cells were treated with 0.5 mM nickel chloride and/or combined with RECK expression vector transfection. The changes in RECK, EGFR, p-AKT, and AKT protein expression in both cell types were evaluated by western blotting using specific antibodies. β-actin was used as a protein loading control. A sample of 1×10^4 of both treated cell types was seeded into Boyden chambers to evaluate invasion capability. The representative invasive cells are shown on Matrigel membranes (bottom panel). The relative invasion capability of both cell types with different treatments were normalized against untreated cells of both types (bottom panel). The data represent three independent experiments. P value was obtained by student t test. * $P < 0.05$. VC: vector control.

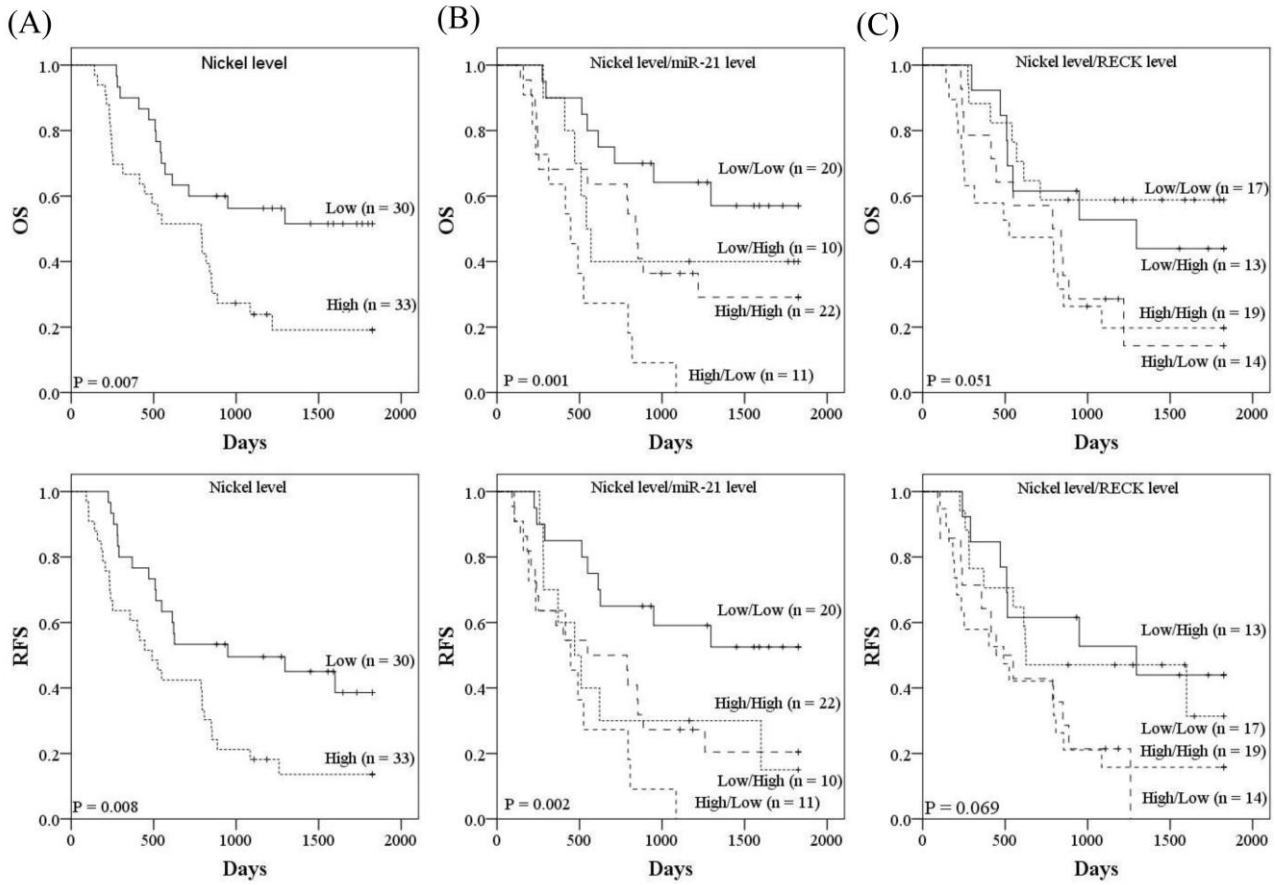

Figure 4. Kaplan-Meier survival curves of Nickel level, Nickel plus miR-21, and nickel plus RECK mRNA level for OS and RFS in lung cancer patients. (A) The survival curves for OS and RFS in high-nickel subgroup vs. low-nickel subgroup. (B) The combined effect of nickel level plus miR-21 level on OS and RFS. The prognostic value of high-nickel/low-miR-21 and high-nickel/high-miR-21 subgroups vs. low-nickel/low-miR-21 subgroup for OS and RFS (OS: $P < 0.001$ for high-nickel/low-miR-21 subgroup, $P = 0.05$ for high-nickel/high-miR-21 subgroup; RFS: $P < 0.001$ for high-nickel/low-miR-21 subgroup, $P = 0.02$ for high-nickel /high-miR-21 subgroup). (C) The combined effect of nickel level plus RECK expression level on OS and RFS (RFS: $P = 0.042$ for high-nickel/high-RECK subgroup, $P = 0.029$ for high-nickel/low-RECK subgroup; OS: $P = 0.077$, high-nickel /high-RECK subgroup vs. low-nickel/high-RECK subgroup). The P value was calculated by a log-rank test.

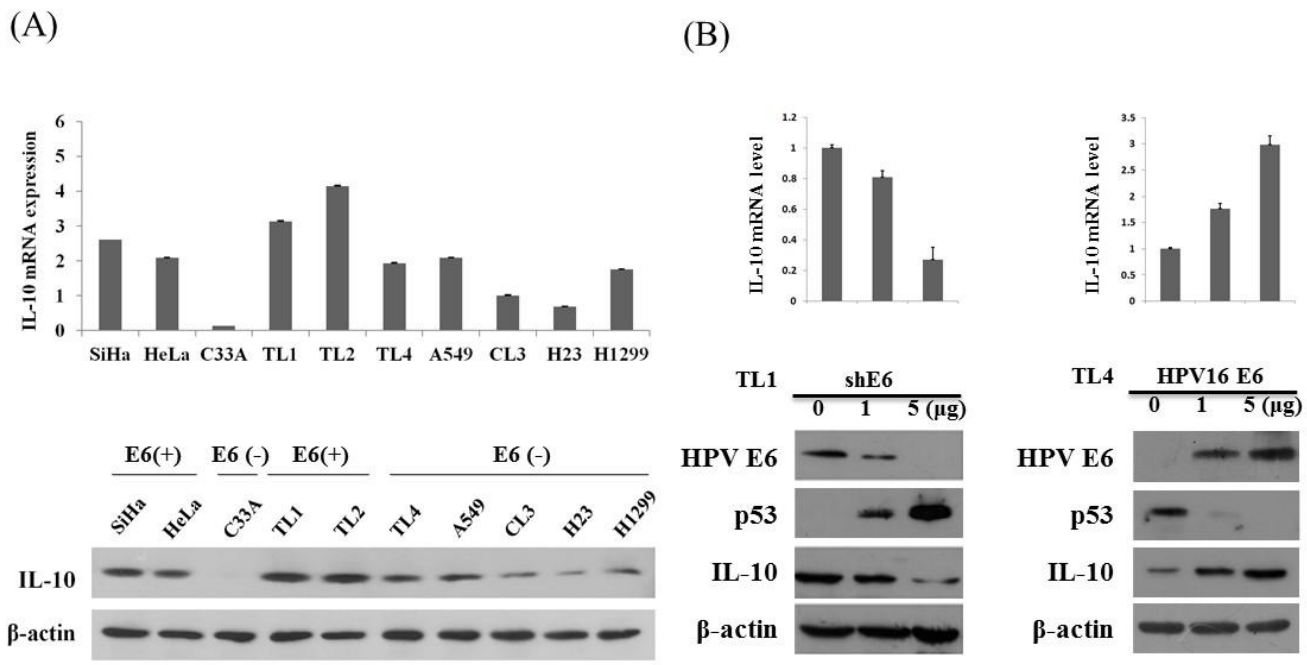

Figure 5. High IL-10 mRNA and protein expression in HPV16 E6-positive cell lines compared with HPV negative cell lines in a panel of lung and cervical cancer cell lines. (A) Relative IL-10 mRNA and protein expression levels of cancer cell lines were determined by real-time RT-PCR and western blot. The IL-10 mRNA expression of CL3 cell line was used as reference (mRNA expression level = 1). The E6(+) and E6(-) indicated the HPV E6 expression of cell lines. (B) TL1 cells were transfected with HPV16 E6 shRNA (left panel) and TL4 cells were transfected with HPV16 E6 cDNA plasmid (right panel) as indicated. HPV16 E6, p53, IL-10 protein expressions were determined by western blot. The changes of IL-10 mRNA expression levels were evaluated by real-time RT-PCR. Experiments in this figure were repeated at least three times and similar results were obtained.

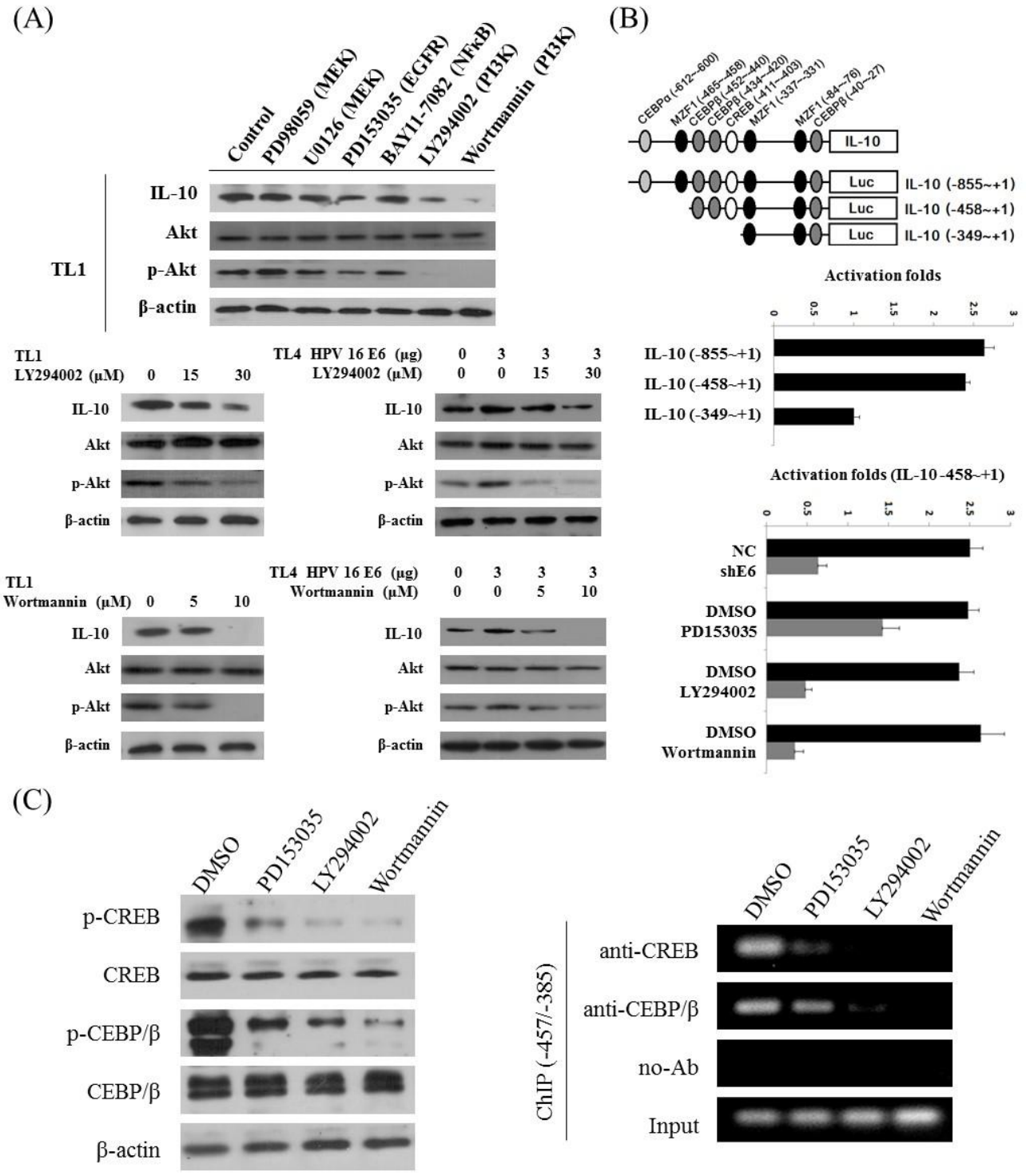

Figure 6. CREB and C/EBP β may be responsible for IL-10 transcription via PI3K pathway in TL1 and TL4 cell lines. (A) TL1 cells were treated with MEK (PD98059, 20μM and U0126, 10μM), EGFR (PD153035, 0.5μM), NF-κB (BAY11-7082, 20μM) and PI3K inhibitors (LY294002, 30μM and wortmannin, 10μM) and protein expression of IL-10, AKT, p-AKT and β-actin was measured by western blot. TL1 cells were treated with PI3K inhibitors at various concentrations as indicated. TL4 cells were transfected with 3 μg HPV16 E6 cDNA plasmid or vector control plasmid for 48 hr. The medium was renewed and then those cells were treated with PI3K inhibitors at various concentrations as indicated. Protein expression was measured by western blot. (B) Diagram summarized the positions of the putative binding sites of transcriptional factors on IL-10 promoter constructs (-855~+1) predicted by software analysis. Luciferase reporter assay was performed to evaluate the promoter activity of these three constructs including -855~+1, -458~+1, and -349~+1. TL1

cells were transfected with these three promoter constructs separately and β-gal was served as an internal control. The luciferase reporter activity of these three constructs was determined and the reporter activity of IL-10 (-349~+1) construct was served as control (activity = 1) for presentation. Luciferase reporter assay was performed to measure the promoter activity of IL-10 (-458~+1) construct in TL1 cells which were transfected with HPV E6 shRNA or treated with EGFR or PI3K inhibitors as indicated. TL1 cells were transfected with IL-10 (-458~+1) construct, TL1 cells transfected with IL-10 (-458~+1) construct were treated with E6 shRNA, EGFR (PD153035, 0.5μM) and PI3K inhibitors (LY294002, 30μM and wortmannin, 10μM) for 48 hr, and then to determine the reporter activity by luciferase reporter assay. β-gal was served as an internal control. (C) TL1 cells were treated with EGFR (PD153035, 0.5μM) and PI3K inhibitors (LY294002, 30μM and wortmannin, 10μM). Phosphorylated CREB (p-CREB), total CREB, p-CEBP/β, and total C/EBPβ expression levels were evaluated by western blot, and β-actin was used as a protein loading control. ChIP assay was performed to evaluate the DNA bonding ability of p-CREB and p-CEBP/β on the putative binding site of IL-10 promoter region. TL1 cells were treated with EGFR (PD153035, 0.5μM) and PI3K inhibitors (LY294002, 30μM and wortmannin, 10μM) and fixed for ChIP assay. The products were amplified by PCR and the result was presented by gel-electrophoresis. Experiments in this figure were repeated at least three times and similar results were obtained.

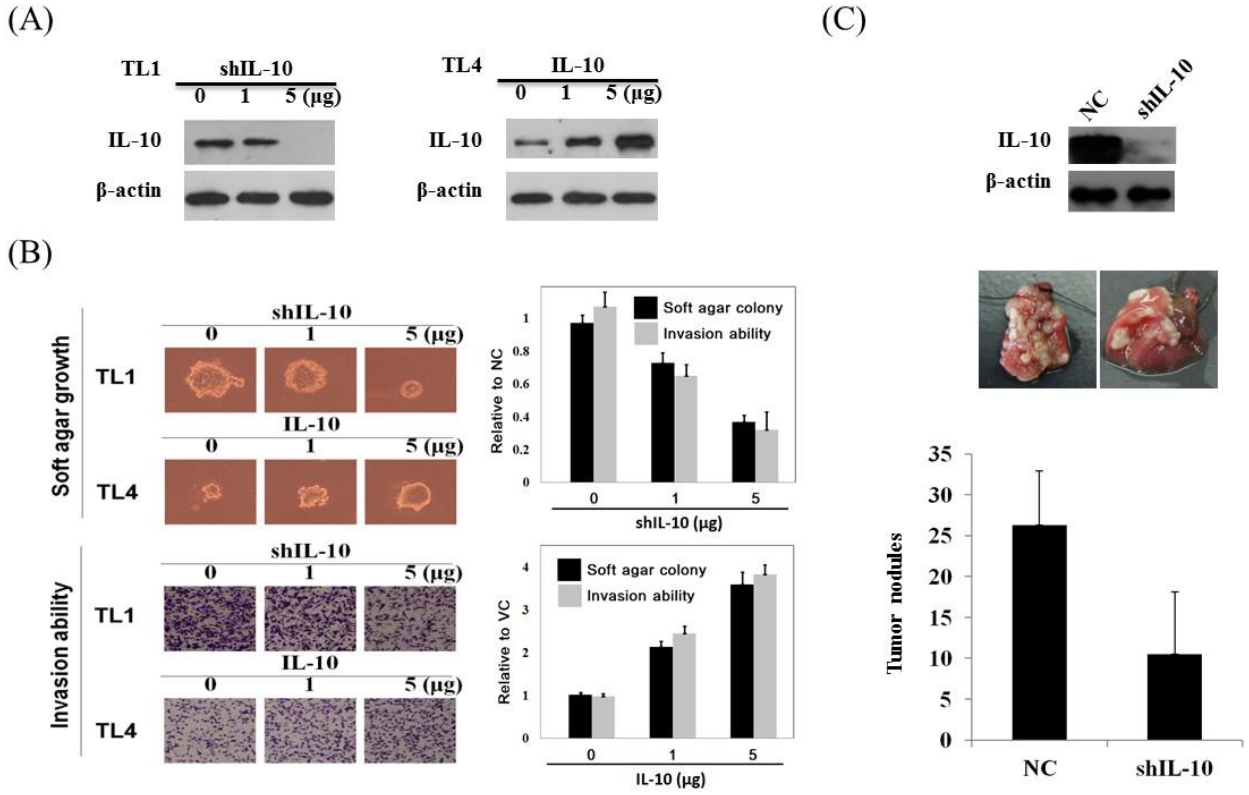

Figure 7. IL-10 promotes the capability of soft-agar growth, invasiveness and lung tumor nodule formation in nude mice in TL1 and TL4 cells. (A) shRNA and cDNA plasmid of IL-10 were respectively transfected into TL1 and TL4 cells, and then IL-10 protein expression was determined by western blot and β-actin was as a protein loading control. (B) Matrigel invasion and soft-agar colony formation assay were used to evaluate the invasiveness and soft-agar growth capability after TL1 cells transfected with IL-10 shRNA and TL4 cells transfected with IL-10 cDNA plasmid as compared with their control cells. The results were show as representative pictures in left panel and the quantitative graph in the right panel. (C) IL-10 and β-actin protein expression of stable clones was shown as upper panel. NC and IL-10 knockdown TL1 stable cells were injected into nude mice via tail vein ($1*10^6$). The mice were sacrificed after four months (N = 5 for each

group). The gross pictures of the tumor nodules formed in mice lung shown in right panel and the quantitative graph shown in left panel (p = 0.003). Experiments of figure 2A and 2B were repeated at least three times and similar results were obtained.

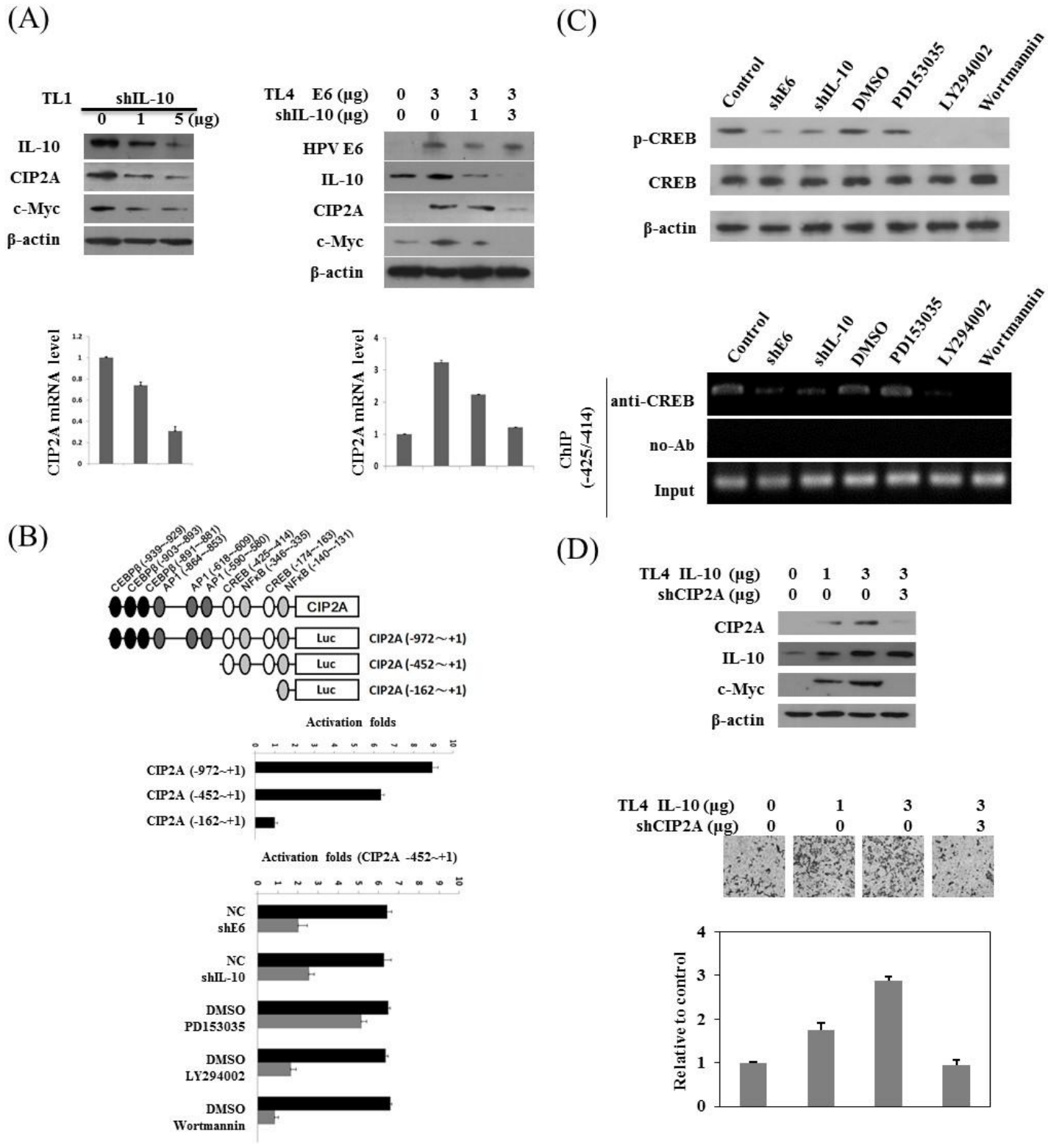

Figure 8. IL-10 upregulates CIP2A transcription by CREB phosphorylation via PI3K/AKT pathway in TL1 and E6-positive TL4 cells. (A) shRNA and cDNA plasmid of IL-10 were respectively transfected into TL1 and TL4 cells and various concentrations of IL-10 shRNA transfection in both cells were as indicated. Protein expression of HPV E6, IL-10, CIP2A, and c-Myc was determined by western blot and β-actin was used as a

protein loading control. The change of CIP2A mRNA expression levels was evaluated by real time RT-PCR in IL-10 knockdown TL1 cells and E6-overexpressed TL4 cells and then transfected with IL-10 shRNA. (B) Diagram summarized the positions of the putative binding sites of transcriptional factors on CIP2A promoter constructs (-972~+1) predicted by software analysis. Luciferase reporter assay was performed to evaluate the promoter activity of these three constructs including -972~+1, -452~+1, and -162~+1. TL1 cells were transfected with these three promoter constructs separately and β-gal was served as an internal control. The luciferase reporter activity of these three constructs was determined and the reporter activity of CIP2A (-452~+1) construct was served as control (activity = 1) for presentation. Luciferase reporter assay was performed to measure the promoter activity of CIP2A (-452~+1) construct in TL1 cells which were transfected with HPV E6 or IL-10 shRNA or treated with EGFR or PI3K inhibitors as indicated. TL1 cells were transfected with CIP2A (-452~+1) construct, TL1 cells transfected with CIP2A (-452~+1) construct were treated with E6 shRNA, EGFR (PD153035, 0.5μM) and PI3K inhibitors (LY294002, 30μM and wortmannin, 10μM) for 48 hr, and then to determine the reporter activity by luciferase reporter assay. β-gal was served as an internal control. (C) TL1 cells were transfected with 5μg HPV E6, IL-10 or NC shRNA; treated with EGFR (PD153035, 0.5μM) or PI3K inhibitors (LY294002, 30μM and wortmannin, 10μM). Protein expression of p-CREB, total CREB, and β-actin was measured by western blot. ChIP assay was performed to evaluate the DNA bonding ability of CREB on CIP2A promoter -478 to -346. Transfected or inhibitor-treated TL1 cells were fixed for ChIP assay. The products were amplified by PCR and the result was presented by gel-electrophoresis. (D) shRNA plasmid of CIP2A were respectively transfected into TL4 cells and various concentrations of IL-10 shRNA transfection in both cells were as indicated. Protein expression of IL-10, CIP2A, and c-Myc was determined by western blot and β-actin was used as a protein loading control. Matrigel invasion assay were used to evaluate the invasiveness after TL4 cells transfected with IL-10 cDNA and CIP2A shRNA plasmid as compared with their control cells. Experiments in this figure were repeated at least three times and similar results were obtained.

Table 1. Association of nickel levels with the risk of EGFR mutation occurrence in lung cancer patients with different tumor histology and gender.

Nickel levels	n	EGFR status		OR	95% CI	P [a.]
		Wild-type (%)	Mutation (%)			
No. of subjects	76	59	19			
Overall						
High	38	24 (63.2)	14 (36.8)	4.36	1.29-14.74	0.018 [b.]
Low	38	33 (86.8)	5 (13.2)	1	(Reference)	
Female						
High	21	9 (42.9)	12 (57.1)	12.70	2.16-74.56	0.005 [c.]
Low	17	15 (88.2)	2 (11.8)	1	(Reference)	
Male						
High	17	15 (88.2)	2 (11.8)	0.84	0.12-5.73	0.858 [c.]
Low	21	18 (85.7)	3 (14.3)	1	(Reference)	
ADC						
High	24	12 (50.0)	12 (50.0)	5.62	1.46-21.59	0.012 [d.]
Low	27	23 (85.2)	4 (14.8)	1	(Reference)	
SCC						
High	14	12 (85.7)	2 (14.3)	1.05	0.08-15.19	0.969 [d.]
Low	11	10 (90.9)	1 (9.1)	1	(Reference)	
Female ADC						
High	15	5 (33.3)	10 (66.7)	11.71	1.96-69.8	0.007
Low	15	13 (86.7)	2 (13.3)	1	(Reference)	
Male ADC						
High	9	7 (77.8)	2 (22.2)	1.40	0.17-11.83	0.755
Low	12	10 (83.3)	2 (16.7)	1	(Reference)	

ADC: adenocarcinoma; SCC: squamous cell carcinoma.

[a.] The P value was calculated by the multivariate logistic regression model.

[b.] OR adjusted for gender and tumor histology.

[c.] OR adjusted for tumor histology.

[d.] OR adjusted for gender.

Table 2. The correlation of miR-21 expression levels with nickel levels and EGFR mutations in lung cancer patients. .

Variables	n	MiR-21 levels		OR	95% CI	P
		Low (%)	High (%)			
No. of subjects	76	38	38			
Nickel levels						
High	38	14 (36.8)	24 (63.2)	2.73	1.07-6.96	0.035
Low	38	24 (63.2)	14 (36.8)	1	(Reference)	
EGFR status						
Mutation	19	8 (42.1)	11 (57.9)	1.19	0.40-3.53	0.759
Wild-type	59	30 (52.6)	27 (47.4)	1	(Reference)	
Nickel levels / EGFR status						
High / Mutation	14	6 (42.9)	8 (57.1)	1.78	0.47-6.76	0.399
High / Wild-type	24	8 (33.3)	16 (66.7)	4.61	1.44-14.76	0.010
Low / Mutation	5	2 (40.0)	3 (60.0)	3.34	0.46-24.06	0.232
Low / Wild-type	33	22 (66.7)	11 (33.3)	1	(Reference)	

The P value was calculated by the multivariate logistic regression model and adjusted for gender.

Table 3. Multivariate analysis of the influence of IL-10 and CIP2A on overall survival in lung adenocarcinoma patients.

Parameter	OS					
	Case no.	Median Survival, Month	5-year Survival, %	HR	95% CI	P
Stage						
I	32	79.3	57.4	1.000	Referent	0.003
II and III	66	19.2	18.3	2.498	1.373-4.546	
IL-10						
Low	49	34.2	36.8	1.000	Referent	0.005
High	49	17.2	23.8	2.083	1.241-3.495	
CIP2A						
Low	49	42.2	40.2	1.000	Referent	0.029
High	49	19.2	19.8	1.809	1.063-3.079	

Table 4. Multivariate analysis of the influence of IL-10 and CIP2A mRNA on overall survival in HPV E6 positive lung adenocarcinoma patients.

Parameter	OS					
	Case no.	Median Survival, Month	5-year Survival, %	HR	95% CI	P
E6 positive						
Stage						
I	16	83.8	56.3	1.000	Referent	0.044
II and III	29	22.8	23.1	2.449	1.026-5.850	
IL-10						
Low	22	55.4	41.7	1.000	Referent	0.009
High	23	16.6	25.4	3.096	1.333-7.193	
CIP2A						
Low	20	55.4	48.1	1.000	Referent	0.016
High	25	26.1	21.7	3.152	1.236-8.038	
E6 negative						
Stage						
I	16	79.3	60.9	1.000	Referent	0.025
II and III	37	17.8	13.8	2.762	1.138-6.701	
IL-10						
Low	27	20.4	33.4	1.000	Referent	0.159
High	26	17.5	19.2	1.618	0.829-3.158	
CIP2A						
Low	29	31.2	33.6	1.000	Referent	0.214
High	24	17.5	20.4	1.545	0.778-3.068	

Supplementary information

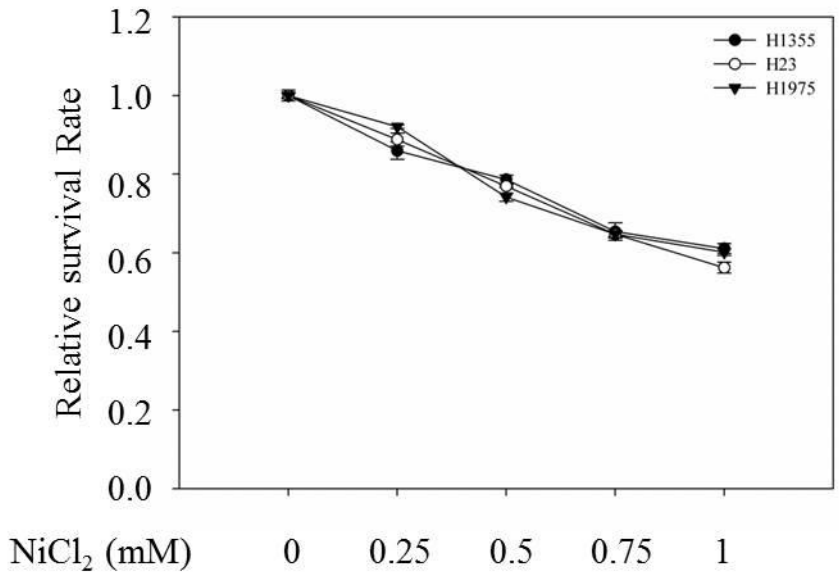

Supplementary Figure 1. The cytotoxicity of H1355, H23 and H1975 cells by nickel chloride treatment. These three cell types were treated with various concentrations of nickel chloride (0, 0.25, 0.5, 0.75 and 1 mM) for 24 h. The cytotoxicity of these three cell types caused by nickel chloride treatment was evaluated by MTT assay. The data represent three independent experiments.

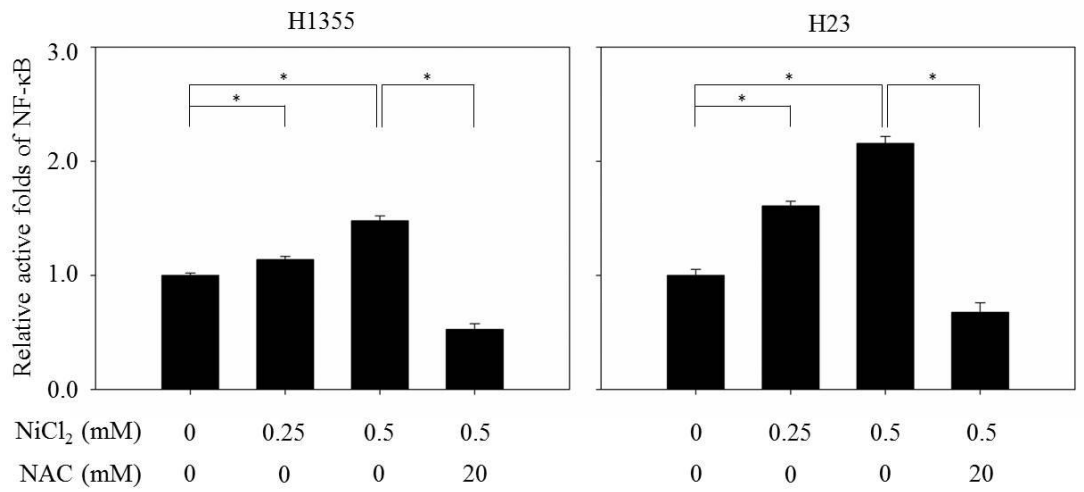

Supplementary Figure 2. NF-κB activation by nickel chloride is partially through ROS generation. H1355 and H23 cells were treated with nickel chloride for 20 h and/or co-treated with NAC for an additional 4 h. Luciferase reporter assay for NF-κB DNA binding activity was evaluated in both cell types with nickel chloride and/or combined with NAC treatment. The data represent three independent experiments. P value was calculated by student t test. * $P < 0.05$.

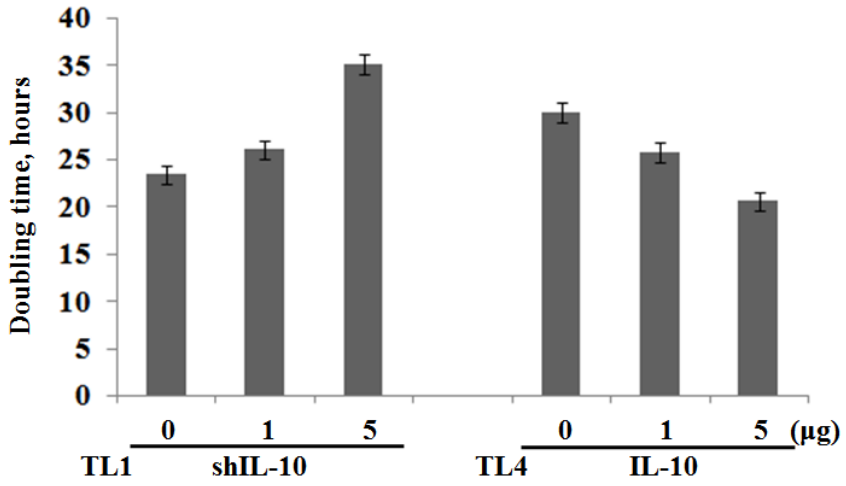

Supplementary Figure 3. Doubling time of IL-10-knockdown TL1 cells and IL-10-overexpressing TL4 cells and the error bars represent the S.D. of triplicate results.

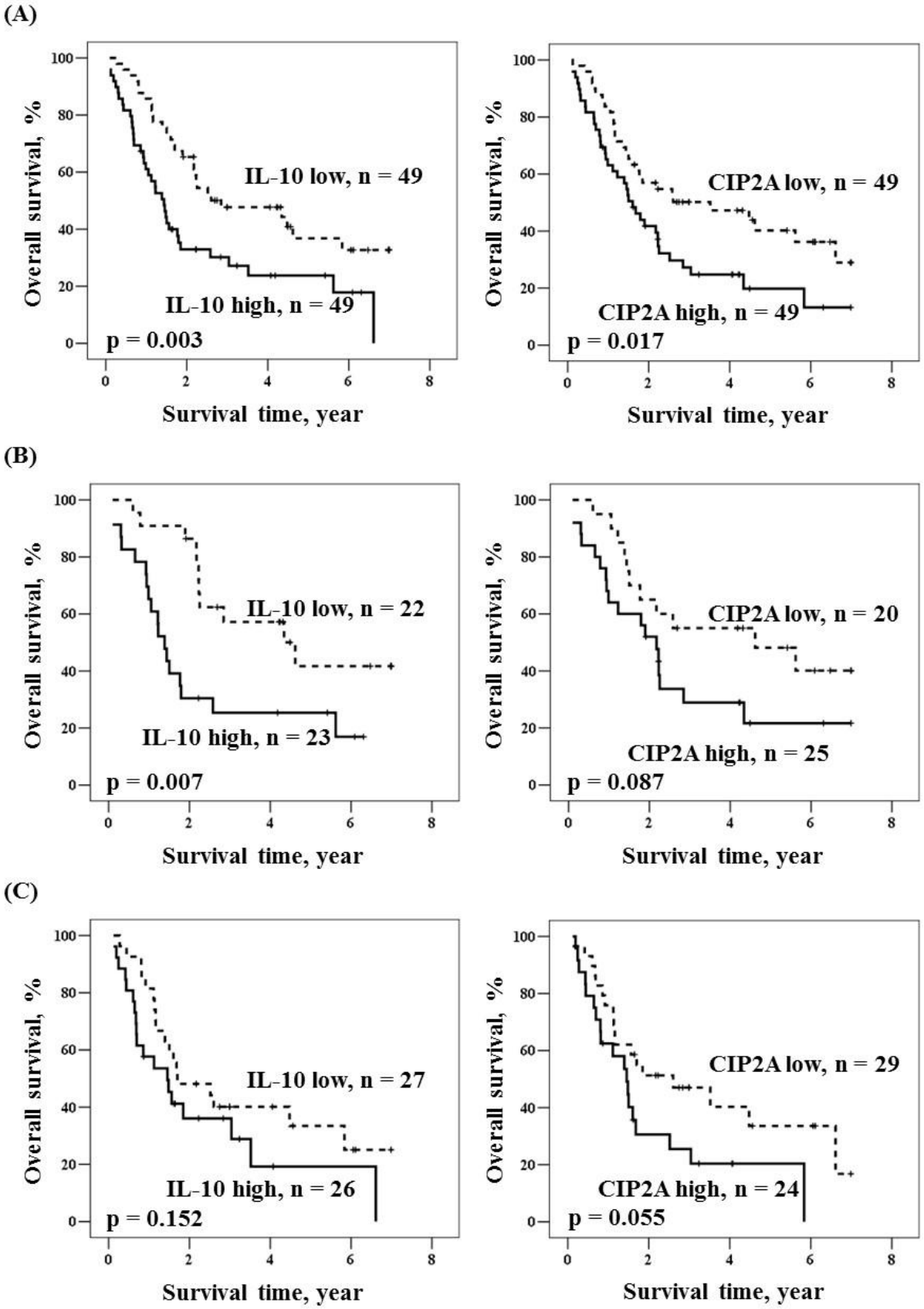

Supplementary Figure 4. Kaplan-Meier analysis was used to assess the influence of IL-10 and CIP2A on overall survival in (A) all study population, (B) patients with HPV 16/18 E6 positive tumor, and (C) patients with HPV 16/18 E6 negative tumor.

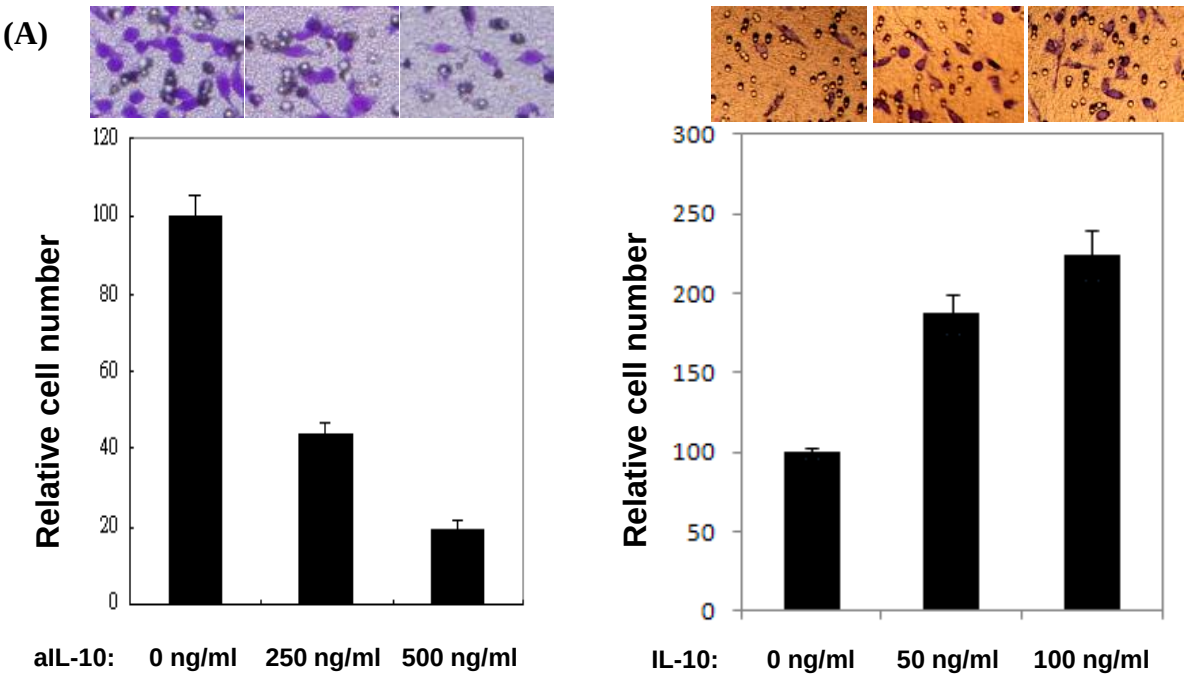

Supplementary Figure 5. Exogenous IL-10 regulates tumor migration capability of lung cancer cells. (A) The migration capability of TL1 cells were decreased after treated with IL-10 neutralize antibody (MAB2171, R&D Systems). (B) The migration capability of TL4 cells were increased by treating with IL-10 recombinant protein (CYT-500, Prospec). Experiments in this figure were repeated at least three times and similar results were obtained. aIL-10: IL-10 neutralized antibody.

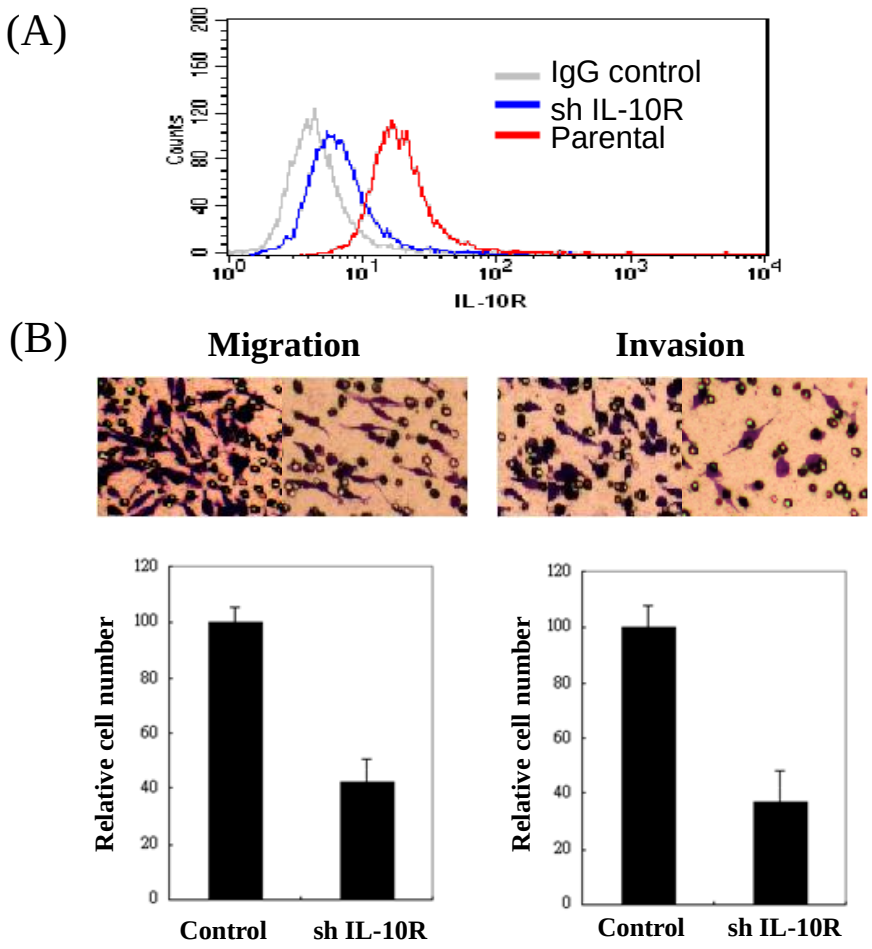

Supplementary Figure 6. The migration and invasion ability of TL1 cells was decreased in IL-10R knock down stable clone. (A) IL-10R expression of TL1 cells with stable IL-10R knock down by shRNA were determined by flow cytometry. (B) IL-10R-knockdown TL1 cells had lower migration and invasion capabilities than control cells.

Supplementary Table 1. Characteristics of 76 lung cancer patients.

Characteristics	Patient No.	Percentage (%)
No. of subjects	76	
Age (years)		
Mean ± SD	63.4 ± 9.7	
Range	40-82	
Age (years)		
> 63	38	50.0
≤ 63	38	50.0
Gender		
Male	38	50.0
Female	38	50.0
Tumor histology		
SCC	25	32.9
ADC	51	67.1
Tumor stage		
Ⅰ and Ⅱ	32	42.1
Ⅲ and Ⅳ	44	57.9
Tumor size (T)		
T1 and T2	56	73.7
T3 and T4	20	26.3
Nodal micrometastasis (N)		
N0	41	54.0
N1-N3	35	46.1

ADC: adenocarcinoma; SCC: Squamous cell carcinoma.

Supplementary Table 2. Univariate analysis of the influence of various clinical parameters, IL-10 mRNA and CIP2A mRNA levels on overall survival in lung adenocarcinoma patients.

Parameter	OS					
	Case no.	Median Survival, Month	5-year Survival, %	HR	95% CI	P
Age						
<65	45	26.8	36.2	1.000	Referent	
≥65	53	22.8	25.2	1.267	0.775-2.071	0.345
Gender						
Female	48	26.8	33.7	1.000	Referent	
Male	50	20.4	26.1	1.279	0.784-2.087	0.324
Smoking history						
Non-smoker	73	26.1	32.4	1.000	Referent	
Smoker	25	18.0	23.3	1.397	0.821-2.377	0.218
Stage						
I	32	79.3	57.4	1.000	Referent	
II and III	66	19.2	18.3	2.387	1.317-4.326	0.004
T classification						
1+2	78	31.0	35.9	1.000	Referent	
3+4	20	11.3	6.3	2.619	1.502-4.567	0.001
N classification						
0	36	79.3	54.5	1.000	Referent	
1+2	62	18.0	18.3	2.441	1.386-4.298	0.002
IL-10						
Low	49	34.2	36.8	1.000	Referent	
High	49	17.2	23.8	2.053	1.255-3.306	0.004
CIP2A						
Low	49	42.2	40.2	1.000	Referent	
High	49	19.2	19.8	1.806	1.104-2.955	0.019

Supplementary Table 3. The correlation of IL-10 mRNA levels with HPV E6 immunostaining and CIP2A mRNA levels in tumor tissues from lung adenocarcinoma patients.

	Case No.	IL-10 mRNA	P value
HPV E6			
Negative	53	64.7±24.5	0.032
Positive	45	168.1±40.5	
CIP2A mRNA			
Low	49	80.9±28.2	0.180
High	49	143.6±36.8	

Supplementary Table 4. Multivariate analysis of the influence of IL-10 and CIP2A mRNA on overall survival in HPV DNA positive lung adenocarcinoma patients.

Parameter	OS					
	Case no.	Median Survival, Month	5-year Survival, %	HR	95% CI	P
HPV DNA positive						
Stage						
I	22	83.8	52.4	1.000	Referent	0.031
II and III	38	21.5	20.1	2.223	1.075-4.599	
IL-10						
Low	31	34.2	35.7	1.000	Referent	0.002
High	29	17.2	24.1	3.043	1.482-6.251	
CIP2A						
Low	26	55.4	49.3	1.000	Referent	0.009
High	34	20.2	16.6	2.706	1.284-5.702	
HPV DNA negative						
Stage						
I	10	79.3	70.0	1.000	Referent	0.053
II and III	28	13.9	15.4	3.383	0.982-11.651	
IL-10						
Low	18	20.4	37.0	1.000	Referent	0.160
High	20	13.5	20.5	1.781	0.795-3.989	
CIP2A						
Low	23	20.4	30.7	1.000	Referent	0.615
High	15	13.3	30.5	1.241	0.535-2.880	

Supplementary Table 5. The association of miR-21 levels with RECK and SPRY2 mRNA expression in lung cancer patients.

		RECK levels			SPRY2 levels		
Variables	n	Low	High	P	Low	High	P
No. of subjects	76	38	38		38	38	
miR-21 levels							
High	38	24 (63.2)	14 (36.8)	0.022	24 (63.2)	14 (36.8)	0.022
Low	38	14 (36.8)	24 (63.2)		14 (36.8)	24 (63.2)	

RECK and SPRY2 mRNA levels in lung tumors were evaluated by real time PCR.

The P value was calculated by χ^2 test.

子計畫二

探討鎳調降 GST-M2 表現及其致癌腫瘤化之角色

中文摘要

背景：上皮-間質型態轉換(EMT)被認為是腫瘤轉移與肺纖維化的重要過程，鎳化合物被歸類為致癌物且能促使組織纖維化。我們過去研究發現氯化鎳會誘導人類支氣管上皮細胞進行EMT，然而，氯化鎳誘導 EMT 過程與癌化的機制目前仍不清楚，本研究主要目的為釐清其中機轉。

材料與方法：運用 Western blot 分析經氯化鎳處理後的細胞 EMT 標記表現量之變化，及以甲基化專一性聚合酶連鎖反應進行定量分析與亞硫酸鹽修飾 DNA 後定序檢測 E-cadherin 啟動子甲基化狀況。利用不同活性氧專一性偵測劑配合流式細胞儀分析鎳所產生的活性氧種類。氯化鎳處理的細胞以 Agilent SurePrint G3 Human V2 GE 8×60K 微陣列檢測 mRNA 與 HmiOA4.1 微陣列檢測 miRNA 表現量的變化，最後用 Gene ontology (GO)、MetaCore 與 Kyto Ecyclopedia Genes and Genomes (KEGG)軟體分析 miRNA 與 mRNA 表現差異的交互關係和相關途徑。

結果：微陣列結果顯示，經氯化鎳處理的細胞相較於控制組，其增加 1.74 倍的 miRNAs 有 18 個及減少 1.74 倍的 miRNAs 有 28 個；而增加 2 倍的 mRNAs 有 2131 個及減少 2 倍的 mRNAs 有 3039 個。TGF-β 抑制劑 (SB525334)可部分減少氯化鎳誘導的 miR-4417 表現，當 miR-4417 過度表現或以 shRNA 抑制 miR-4417 的標靶基因 TAB2 時，皆可提高 fibronectin 表現量。

結論：氯化鎳藉由增加 miR-4417 與抑制 miR-4417 標靶基因 TAB2 表現，進而誘導 fibronectin 表現，促使細胞進行上皮-間質型態之轉換。本研究提出氯化鎳在促進肺纖維化及腫瘤形成過程的細胞分子機制之影響。

關鍵字

氯化鎳、上皮-間質型態轉換、微 RNA、纖維化與癌化過程

英文摘要

Backgrounds: Epithelial-mesenchymal transition (EMT) has been considered an event in the pathogenesis of tumor metastasis and lung fibrosis. Nickel compounds are classified as carcinogens and have been shown to be associated with tissue fibrosis. Our previous study reported that nickel chloride ($NiCl_2$) induces EMT. However, the mechanisms of Ni-induced EMT process and carcinogenesis are still unclear. The aim of this study was to investigate the mechanisms of Ni-induced EMT and tumorigenesis.

Materials and Methods: NiCl2-induced EMT markers expressions were analyzed by Western blot. The quantitative real-time

methylation-specific PCR (QMSP) and bisulfite sequencing were used to examine the promoter methylation of E-cadherin. The types of reactive oxygen species (ROS) generation by NiCl2 were stained by specific detecting reagents and analyzed by flow cytometry. The mRNA and miRNA profiles in NiCl2-treated cells were established using Agilent SurePrint G3 Human V2 GE 8×60K and HmiOA4.1 microarrays, respectively. The differentially expressed miRNAs and mRNAs related miRNA-gene network have been analyzed by Gene ontology (GO), MetaCore, and Kyto Ecyclopedia Genes and Genomes (KEGG).

Results: Comparison to control group, the microarrays threshold identified 18 up-regulated and 28 down-regulated miRNAs with fold changes of ≥ 1.74 meanwhile 2431 up-regulated and 3039 down-regulated mRNAs with fold changes of ≥ 2 in expression. SB525334, a TGF-β inhibitor, partially inhibited the up-regulation of miR-4417 by $NiCl_2$. Overexpression of miR-4417 and silencing of the miR-4417-targeted gene TAB2 induced the expression of fibronectin. Moreover, oral administration of nickel promoted lung tumor growth in nude mice that had received BEAS-2B cells by intravenously injection.

Conclusion: $NiCl_2$ induces the expression of fibronectin via induction of miR-4417 and down-regulates the target gene of miR-4417, TAB2. These results shed new light on the contribution of $NiCl_2$ to fibrogenesis and carcinogenesis.

Keywords

Nickel chloride, epithelial-mesenchymal transition, miRNA, fibrosis and carcinogenesis

緒言

鎳（Nickel, Ni）是地球上豐富的元素之一，鎳金屬與鎳化合物無特殊的氣味與味道，被廣泛的運用於多種工業製程與商業應用，例如：錢幣、陶瓷上色、飾品、不鏽鋼、醫療器材、鎳鎘電池和鎳的精煉業等，另外，香菸與石油燃燒所產生的廢氣也包含鎳化合物，導致鎳汙染物被釋放到大氣層中，進入生態系統。美國毒性物質及疾病登記署(Agency for Toxic Substances and Disease Registry, ATSDR)指出，約有 10~20%的人口會對鎳引起過敏反應，常見於接觸鎳後對皮膚的影響。職業中吸入性暴露鎳化合物會影響工作者的健康，流行病學報導指出，鎳精煉廠工人產生慢性支氣管炎與肺功能下降，增加肺癌與鼻咽癌的發生率(Doll et al, 1977; Grimsrud et al, 2002)。除了職業性暴露鎳，也可能不知不覺中在生活環境接觸到鎳化合物，過去國衛院研究發現，台灣中部彰化地區的電鍍工廠密集度高，針對附近居民採集尿液進行分析，發現鄰近工廠的居民暴露鎳的

含量明顯地高於一般住宅區的民眾(Chang et al, 2006)。

西元1990年，國際癌症研究中心(Internation Agency for Research on Cancer, IARC) 將鎳化合物則是Group 1對人類致癌，而鎳金屬歸類為Group 2B對人類有致癌性(1990)。美國國家環境保護局(Environmental Protection Agency, EPA)與國家毒物計畫(National Toxicology Program, NTP)指出，鎳精煉廠的粉塵與次硫化鎳(nickel subsulfide, Ni_3S_2)皆為人類致癌物(1996)。非水溶性鎳化合物[包含：nickel sulfide (NiS)、 Ni_3S_2和nickel oxide (NiO)]與水溶性鎳化合物[包含：nickel sulfate ($NiSO_4$)、nickel acetate ($Ni(CH_3COO)_2$) 和 nickel chloride ($NiCl_2$)]皆會刺激動物呼吸道、引起化學性肺炎、肺癌以及不同程度的肺部細胞損傷(Zhao et al, 2009)。目前已發現幾種鎳誘導carcinogenesis的分子機轉，像是改變細胞的表觀遺傳(epigenetic)程序、破壞細胞中鐵的恆定(干擾iron-dependent酵素)、誘導細胞產生大量的活性氧物種(Reactive oxygen species, ROS)與活化低氧(hypoxia)訊息途徑等(Salnikow & Zhitkovich, 2008)。

上皮-間質型態轉換(Epithelial-Mesenchymal transition，EMT)是指細胞由極性不能移動的型態轉換成間質型態，這個細胞轉換過程是短暫且可逆的，EMT發展過程包含肌動蛋白細胞骨架重組、上皮細胞-細胞間和細胞-基質間的重建、細胞外型變成長條梭狀和缺乏基底-頂端極性(basal-apical polarity)、細胞具有可塑性、能動性、抗凋亡和似幹細胞的特性，其主要的分子特徵有細胞-細胞間的黏著蛋白/上皮型態標記E-cadherin表現下降，間質型態標記(包含：fibronectin、N-cadherin和vimentin)表現量增加。初始於胚胎發育與器官形成過程中發現EMT現象，然而，近年來發現EMT與癌症發展有關，腫瘤細胞經EMT後，而產生轉移的能力。

表觀遺傳是指有絲分裂與減數分裂過程中，DNA 序列不變，但基因表達型態產生遺傳變化，可維持細胞正常功能及參與癌症發展過程(Vaissiere et al, 2008)。表觀遺傳機制包括：DNA 甲基化、組蛋白的修飾作用和 microRNAs (miRNAs)，使細胞面對環境變化時可迅速反應。一些病理因素(例如：環境因子和老化)造成表觀遺傳異常修飾，而說明疾病與表觀遺傳的相關性(Fraga & Esteller, 2007; Skinner et al, 2010)。mRNAs 為基因表現的重要調節者，常因異常甲基化而在癌症失去調控基因的能力，比較乳腺細胞與乳癌細胞中 167 個 miRNAs 啟動子甲基化狀況，發現約有三分之一(55/167)的 miRNAs 啟動子異常甲基化，乳癌病患檢體 miRNAs 啟動子甲基話表示 DNA 甲基化可能與臨床特徵相關，包含 miR-31、miR-130a、let-7a-3/let-7b、miR-155、miR-137 與 miR-34b/miR-34c 表現量減少是由於啟動子高度甲基化(Vrba et al, 2013)。

本研究室先前實驗發現，鎳化合物誘導肺支氣管細胞進行上皮-間質型態轉換，上皮型態標記 E-cadherin 表現量下降與間質型態標記 Fibronectin 表現量增加，並發現氯化鎳透過活性氧物種(Reactive oxygen species , ROS)促

使 E-cadherin promoter 高度甲基化來抑制 E-cadherin 基因表現，然而，氯化鎳如何誘導間質標記 fibronectin 表現量增加則尚未釐清，因而進一步研究 miRNA 是否參與氯化鎳誘導的 EMT 作用中，目前仍未有相關的文獻探討，因此，我們將進一步運用 miRNA 與基因微陣列找尋其他調控 EMT 之分子機制。

材料與方法

1. 細胞株(cell lines)之來源：

BEAS-2B細胞株為人類正常之氣管上皮細胞 (normal human bronchial epithelial cell line)，經由 adenovirus 12-SV40 virus hybrid (Ad12SV40)轉染的永生細胞 (immortalized cells) (CRL-9609^{TM})；A549細胞株為人類肺腺癌細胞(CCL-185^{TM})，此兩株細胞皆購於American Type Culture Collection (ATCC)。

2. 聚合酶鏈鎖反應(polymerase chain reaction, PCR)

每管微量離心管中，有1 µl cDNA作為模板，再加入5 µl的10X PCR buffer、2 µl的10 mM dNTPs、2 µl的10 µM前置引子(forward primer)、2 µl的10 µM反置引子(reverse primer)及1 µl的Pro-Taq DNA polymerase (5單位/µl)，補二次蒸餾水至最終體積為50 µl。

3. 定量聚合酶連鎖反應 (real-time PCR)

每一管微量離心管中，有2 µl cDNA作為模板，再加入5 µl Smart Quant Green Master Mix with dUTP and ROX (ProTech, RT-GL-SQGR-V3)、0.5 µl 1 µM forward primer、0.5 µl 1 µM reverse primer (Guangzhou RiboBio Co., Ltd, Bulge-LoopTM miRNA qRT-PCR primer： has-miR-4417)和2 µl DEPC水。定量PCR的反應條件為95℃/10分鐘後，接著進行95℃/15 秒與60℃/1 min，共重複45 cycle。

最後計算分析方式根據機器紀錄每個cycle數所產生的螢光值而形成sigmoidal-shaped amplification plots，當螢光到達閾值(threshold)情況下所紀錄的cycle數稱為CT(threshold cycle)值，也就是剛達到可偵測到螢光的cycle數。標靶基因螢光到達閥值時，cycle數差異的計算公式為 ΔCT=CT(target gene)–CT(internal control)；以ratio = $2^{-\Delta C_T}$來表示此基因的相對表現量。

4. 西方墨點法(Western blot)

樣品進行電泳跑膠後，運用全濕式轉漬器 (Tank transfer system, Bio-Rad)將蛋白轉漬到 BioTrace^{TM} PVDF membrane上，接著BioTrace^{TM} PVDF membrane浸泡在含有5%脫脂奶粉的TTBS buffer (50 mM Tris、0.2% Tween 20和150 mM NaCl pH 7.5)中，置於室溫震盪作用1小時，進行阻斷(blocking)，最後再進行抗原蛋白質-抗原免疫反應。

5. 質體轉染作用(transfection)

5 µg質體DNA與250 µl Opti-MEM® I Reduced Serum Medium (Cat.No.31985-062, Invitrogen)混合均勻，另外，取10 µl Lipofectamine™ 2000試劑與250 µl Opti-MEM® I Reduced Serum Medium混合均勻並靜置室溫5分鐘，將Lipofectamine™ 2000溶液加到DNA溶液中，輕輕地混合均勻後靜置室溫20分鐘。去除細胞就培養液並加入5 ml Opti-MEM® I Reduced Serum Medium，滴入製備好的500 µl

Lipofectamine™ 2000/DNA 溶液於細胞中，細胞放回37℃培養箱中培養4~6小時後，去除培養液並加入新鮮的細胞培養液，再將細胞放回37℃培養箱中培養。

6. RNA干擾 (RNA interference, RNAi)

運用VSV-G (vesicular stomatitis virus glycoprotein) pseudotyped lentivirus system進行RNA干擾，RNAi載體選購於中研院RNAi核心設施，本研究使用的 shRNA 質體菌株有 shLuc (TRCN0000072246，target sequence：CAAATCACAGAATCGTCGTAT) 、shTAB2 #442 (TRCN0000378442，target sequence：CACTCAGCCCAATACGAAATA) 與 shTAB2 #452 (TRCN0000004452，target sequence：AGATTGACATTGACTGCTTAA)。

6-1 抽取 shRNA 質體

將帶有 shRNA 的菌種培養於 TB broth 複製放大，再使用 PureLinkTM HiPure Plasmid DNA Purification Kit (Invitrogen)抽取質體 DNA 備用。

6-2 製造含 shRNA 的 VSV-G pseudotyped lentivirus

種植 2.4×106 個 293T 細胞於 10 公分培養皿中，於 37℃培養箱中培養 16 小時，運用 jet-PEI® 轉染試劑將 5 μg shRNA 質體、0.5 μg pMD.G 與 4 μg pCMVΔR8.91 轉染到細胞中，置於 37℃培養箱中培養 6 小時後，更換成含 1% BSA 的細胞培養液 10 ml，24 小時之後收集培養液與更換新鮮的 1% BSA 培養液，收集來的培養液冰-80℃保存，經 24 小時再收集一次培養液並與先前培養液放在一起，培養液中含有細胞所釋放帶有 shRNA 的 VSV-G psudotyped Lentivirus，利用 0.22 μm filter 過濾收集到的培養液以去除受損細胞，接著將培養液分裝於微量離心管，存放於-80℃冰箱備用。注意要將所有碰過病毒的器材，以漂白水消毒後再丟棄。

6-3 病毒濃度測定

種植 5×103 個細胞/well 於 96 孔盤中，細胞放 37℃培養箱中培養 16 小時，接著稀釋病毒培養液，取病毒培養液 1、5、10、15、20、25 μl 分別加入 49、45、40、35、30、25 μl 新鮮的細胞培養液，使最終體積皆為 50 μl，再將稀釋後的病毒培養液加入細胞中，並在每個 well 加入 1 μl 的 0.8 μg/μl protamine sulfate 幫助病毒感染細胞，培養 24 小時之後，去除舊的培養液，每個 well 加入 100 μl 含 2 μg/ml puromycin 的新鮮培養液進行篩選，若有病毒感染的細胞則不會死亡，經過 48 小時後，進行 MTT assay，測細胞的存活率。取細胞存活率大約 60%的病毒濃度進行爾後的實驗。中研院 RNAi 核心設施指出，當慢病毒感染細胞後細胞存活率為 60％時，其感染相乘數(multiplicity of infection, MOI, virus/μl)約等於 1，此時含有 shRNA 的慢病毒對於細胞所引起的副作用最低。

6-4 慢病毒感染癌細胞之方法

種植 1×106 個 BEAS-2B 細胞於 6 公分培養皿中，培養 16 小時後，加入病毒

效價 MOI 約等於 1 的病毒量，並同時在每盤細胞中加入 0.8 μg/ml protamine sulfate 幫助病毒感染細胞。培養 24 小時後，換成含有 2 μg/ml puromycin 的新鮮培養液進行篩選，經 48 小時細胞進行繼代並收取部分細胞進行 RT-PCR 或 Western blot 進行確認 shRNA 抑制基因表現的效果，以利於進行爾後實驗。

實驗結果

延續上年度的計畫內容，我們進行後續研究，結果如下：

1. 氯化鎳對 A549 肺癌細胞 miR-4417 的標靶基因之影響

將不同濃度的氯化鎳處理 A549 細胞 48 小時，A549 細胞的 miR-4417 標靶基因 TAB2 mRNA 表現量減少不明顯(上年度期中研究結果)，因此，進一步以 Western blot 分析 A549 細胞 miR-4417 標靶基因 TAB2 蛋白表現量，結果顯示，氯化鎳抑制 TAB2 蛋白表現，以未加藥之細胞作為控制組(TAB2/β-actin 之 Ratio 值設定為 1)，0.25 與 0.5 mM 氯化鎳處理後，TAB2/β-actin 之 Ratio 值分別降為 0.76 與 0.62；而另一個 miR-4417 標靶基因 RAB6A 蛋白的變化幅度不明顯(Fig.1)。

2. miR-4417 抑制物對氯化鎳調控 miR-4417 標靶基因 TAB2 與 EMT 標記蛋白之影響

首先，將 miR-4417 抑制物(100 與 200 nM)轉染至 BEAS-2B 肺支氣管上皮細胞中並培養 24 小時，接著加入 0.25 mM 氯化鎳處理 48 小時，最後運用 real-time PCR 分析，結果顯示，氯化鎳誘導 BEAS-2B 細胞 miR-4417 表現量增加(P<0.05)，miR-4417 抑制物能明顯降低氯化鎳所誘導的 miR-4417 表現量(P<0.01)，而轉染 200 nM scramble miRNA 抑制物無法減少氯化鎳所誘導的 miR-4417 表現量(Fig. 2A)。

我們運用網路上的免費軟體 miRDB (http://mirdb.org/miRDB/) 分析 miR-4417 的 seed region 對於其標靶基因的互補程度，預測結果發現 miR-4417 seed region 分別有 8mer 與 NAP1L5 3'UTR 互補以及 7mer 與 TAB2 3'UTR 形成互補，因而推測 miR-4417 具有降解 NAP1L5 與 TAB2 mRNA 的能力。將 miR-4417 前驅物轉染至 BEAS-2B 細胞中培養 48 小時，進一步藉由 RT-PCR 分析，結果顯示，相較於載體控制組 (miR-vector，NAP1L5/β-actin 與 TAB2/β-actin 之 Ratio 值設定為 1)，過度表現 miR-4417 的 BEAS-2B 細胞 NAP1L5 與 TAB2 mRNA 表現量變少(NAP1L5/β-actin 之 Ratio 值為 0.61；TAB2/β-actin 之 Ratio 值為 0.55) (Fig.2B)。

由於氯化鎳誘導細胞發生 EMT 現象，且同時觀測到氯化鎳增加 miR-4417 的表現量，為了釐清 miR-4417 是否參與氯化鎳誘導的 EMT 現象，我們將 miR-4417 前驅物轉染於 A549 與 BEAS-2B 細胞中並培養 48 小時，運用 Western blot 分析過度表現 miR-4417 細胞的 EMT 標記蛋白表現量，結果顯

示，miR-4417 能促進 A549 與 BEAS-2B 細胞間質型標記蛋白 fibronectin 表現量增加，而上皮型標記蛋白 E-cadherin 表現量變化不明顯(Fig. 2C)。

將 miR-4417 抑制物或 scramble 抑制物轉染於 BEAS-2B 細胞中，接著加入 0.25 mM 氯化鎳處理 48 小時，結果發現，氯化鎳誘導 scramble 抑制物組別的 fibronectin 表現量增加，而 miR-4417 抑制物降低氯化鎳誘導的 fibronectin 表現(Fig. 2D)。另外，將 miR-4417 前驅物質體 miR-4417/pcDNA^{TM} 6.2-GW 與 miR-4417 抑制物或 scramble 抑制物共同轉染於 BEAS-2B 細胞中，以 Western blot 分析結果發現，miR-4417/pcDNA^{TM} 6.2-GW 質體與 scramble 抑制物共同轉染之細胞 fibronectin 表現量增加，而 miR-4417 抑制物降低 miR-4417/pcDNA^{TM} 6.2-GW 質體所誘導的 fibronectin 表現(Fig. 2E)。

3. 抑制細胞 TAB2 基因表現促進 fibronectin 表現量增加

從前面的實驗結果得知，細胞的 miR-4417 過度表現會抑制 TAB2 mRNA 表現，另外，氯化鎳誘導 EMT 的同時還促進 miR-4417 表現與抑制 TAB2，因此，進一步釐清 TAB2 是否與氯化鎳誘導的 EMT 現象具有相關性，運用 Lentivirus shRNA 系統抑制 BEAS-2B 細胞的 TAB2 基因表現，接著以 Western blot 進行分析，結果顯示，在 TAB2 表現量低的細胞中，其 fibronectin 表現量增加，而 E-cadherin 表現量並沒有隨著 TAB2 變少而發生改變(Fig. 3)。

4. 氯化鎳部份地透過 TGF-β 訊息路徑來增加 miR-4417 表現量

BEAS-2B 細胞經 0.5 mM 氯化鎳處理 48 小時之後，萃取細胞的 RNA 進行基因微陣列分析，相較於未處理氯化鎳的 BEAS-2B 細胞，基因表現量增加或減少 2 倍以上者共有 5170 個，經 KEGG (Kyoto Encyclopedia of Genes and Genomes) pathway 線上軟體 (http://www.genome.jp/kegg/pathway.html)分析氯化鎳可能影響之訊息路徑，其中的結果發現，氯化鎳改變 TGF-β 訊息路徑中多種基因表現量 (Supplementary Fig. 1)，因此，我們進一步研究 TGF-β 訊息路徑是否參與氯化鎳誘導 miR-4417 表現量增加其中之機轉。運用 TGF-β receptor 1 抑制劑 SB525334 阻斷 TGF-β 訊息路徑來進行實驗，將不同濃度 SB525334 (0、2.5、5 和 10 μM)與 0.5 mM 氯化鎳共同處理 A549 細胞 72 小時，於倒立顯微鏡下觀察細胞的形態並拍下影像，從圖片中我們發現，單純處理氯化鎳的細胞，其細胞形態相較於未加藥的細胞變得細長，細胞間的空隙變大，而 SB525334 與氯化鎳共同處理的細胞形態，則隨著 SB525334 的濃度逐漸變圓，細胞間距離較緊密(Fig. 4A)。

BEAS-2B 與 A549 細胞分別處理 0.5 與 1 mM 氯化鎳，同時加入 10 μM SB525334 共同處理 48 小時，萃取細胞的 RNA 進行 real-time PCR 分析，結

果顯示，氯化鎳促進 BEAS-2B 與 A549 細胞的 miR-4417 表現量增加，而 SB525334 與氯化鎳共同處理的情況下，miR-4417 表現量略微下降(未達顯著差異)，為了確認 SB525334 抑制 TGF-β 訊息路徑之藥效，我們將 BEAS-2B 與 A549 細胞加入 TGF-β (10 ng/ml)作為 positive control，結果發現，TGF-β 能促進 miR-4417 表現量增加，並達統計顯著差異($p<0.01$)，而 SB525334 可明顯抑制 TGF-β 所誘導的 miR-4417 表現量($p<0.05$) (Fig. 4B 和 4C)，上述的結果表示，氯化鎳可能部份地透過 TGF-β 路徑來促進 miR-4417 表現量增加。

5. SB525334 對氯化鎳調控的 miR-4417 標靶基因之影響

由於實驗發現氯化氯部份地透過 TGF-β 路徑來影響 miR-4417，因此，進一步探討氯化鎳是否經由 TGF-β 路徑調控 miR-4417 標靶基因的表現。我們將 BEAS-2B 與 A549 細胞暴露氯化鎳 72 小時後，以 Western blot 進行分析，結果顯示，氯化鎳抑制 miR-4417 的標靶基因 TAB2 與 ENOSF1 蛋白表現量減少，而 SB525334 與氯化鎳共同處理的情況下，SB525334 能些許提高 BEAS-2B 細胞的 ENOSF1 蛋白表現，對兩株細胞的 TAB2 蛋白表現量影響不明顯。將細胞加入 10 ng/ml TGF-β 作為對照組，結果發現，TGF-β 略為減少 TAB2 與 ENOSF1 蛋白表現，而 SB525334 可恢復 A549 細胞的 ENOSF1 蛋白表現量(Fig. 5A 和 5B)。

6. 氯化鎳對 Mitogen-Activated Protein Kinase (MAPK)與 Smad 途徑之影響

文獻指出，TGF-β 與細胞膜上的 TGFBR 結合後，可經由 Smad (Smad-dependent) 路徑或非 Smad (Smad-independent，例如：MAPK 途徑)來活化下游分子而影響細胞不同的生理反應(Ma et al, 2009)，在我們的研究中發現，氯化鎳具有活化 TGF-β 路徑的能力，因此，進一步分析氯化鎳是否影響 TGF-β 下游分子，BEAS-2B 細胞經氯化鎳處理 72 小時後，Smad 路徑方面的 Smad2 和 Smad3 表現量增加，Smad4 蛋白表現下降(Fig. 6A)；另外 MAPK 路徑中的 p-ERK 與 p-JNK 表現量下降，p-p38 表現量略微增加(Fig. 6B)。

討論

鎳化合物為致癌物，可促進人類肺癌細胞的侵襲能力(Xu et al, 2011)，本研究發現，氯化鎳造成 EMT 標記蛋白改變，包含抑制上皮型態標記 E-cadherin 表現與誘導間質型態標記 fibronectin 表現量增加。鎳刺激細胞產生大量的 ROS，爾後藉由 HIF-1α 途徑、轉錄因子 Snail 家族與 E-cadherin 啟動子高度甲基化來抑制 E-cadherin 表現，另外，抑制 ROS 或 HIF-1α 表現也可減緩氯化鎳刺激的 fibronectin 表現量，說明 ROS 可能在鎳誘導的癌化過程扮演重要的角色(Wu et al, 2012)。本計畫進一步研究氯化鎳誘導

間質標記 fibronectin 表現量增加之調控分子機轉，釐清氯化鎳是否透過表觀遺傳 miRNA 來影響 EMT 標記蛋白之變化，運用 miRNA 微陣列與基因微陣列分析經氯化鎳處理的 BEAS-2B 細胞，顯示氯化鎳增加 1.74 倍表現變化的 miRNAs 有 18 個與減少 1.74 倍表現變化的 miRNAs 有 28 個，另外，氯化鎳增加 2 倍表現變化的 mRNAs 有 2131 個與減少 2 倍表現變化的 mRNAs 有 3039 個，進一步以 DAVID (Huang da et al, 2009)分析基因微陣列結果，發現氯化鎳所影響的基因參與多條訊息途徑(附圖 1)，其中包含 TGF-β signaling pathway。TGF-β 為活化 EMT 反應之重要因子(Liu et al, 2015)，在氯化鎳與 TGF-β 抑制劑 SB525334 共同處理細胞的實驗結果顯示，氯化鎳會部份藉由 TGF-β 訊息路徑來誘導細胞產生 EMT 現象，說明氯化鎳還透過其他多條路徑調控 EMT 的發生。

本研究主要釐清氯化鎳透過表觀遺傳 miRNA 來誘導細胞發生 EMT 現象，實驗結果發現，氯化鎳透過提高細胞的 miR-4417 與抑制 TAB2 的表現，進而參與間質型態標記 Fibronectin 表現量增加之機轉。實驗證實，氯化鎳透過影響基因層面與基因表觀遺傳修飾來調控 EMT 反應，進而可能促進細胞變得有移動能力。在細胞發展癌化的過程中，氯化鎳誘導細胞發生 EMT 現象，可能促使轉型後的肺癌細胞即擁有能動性，因而提出肺細胞在癌化過程的新觀點。

表觀遺傳異常也可能減少抑癌基因表現，低氧狀態與暴露鎳會抑制 BEAS-2B 細胞的 histone demethylase JMJD1A 表現，進而增加整體 histone H3 的 lysine 9 甲基化並降低受體酪胺酸激酶(receptor tyrosine kinase/ERK)訊息的關鍵調節者 Sprouty homolog 2 (Spry2)基因表現(Chen et al, 2010)。越來越多的證據指出，基因功能缺陷會造成疾病與病態行為，尤其以癌症被廣泛地進行研究，其他包括自體免疫疾病、氣喘、第 2 型糖尿病與代謝疾病等，而導致基因表現異常的原因有 DNA 序列改變或是表觀遺傳程序脫軌。近幾年研究學者著重探討表觀遺傳調控基因表現活性，包含研究：DNA 甲基化、Histone 修飾與 miRNA，第一個調控表觀遺傳的藥物於西元 2004 年美國食品藥物管理局(U.S. Food and Drug Administration，FDA)宣佈正式上市，之後陸續核准更多種相關的新藥(Szyf, 2009)，透過藥物改變細胞表觀遺傳的訊息，發展疾病與癌症的治療策略。

miRNA 啟動子甲基化能調控 miRNA 表現量，miR-152 可結合在 DNMT1(DNA methyltransferase1) 的 3’UTR，硫化鎳轉型的 16HBE 細胞株透過 DNA 甲基化使 miR-152 表現量變少，進而提高 DNMT1 表現量，誘導 DNA 高度甲基化、增加 DNMT1 與 methyl-CpG-binding domain (MBD)蛋白 MeCP2 結合到 miR-152 啟動子上，表示 miR-152 與 DNMT1 為彼此負調

控因子，當抑制 16HBE 細胞 miR-152 表現時，增加細胞增生速度與群落形成(Ji et al, 2013)。三硫化鎳轉形的人類支氣管上皮細胞 miR-203 啟動子高度甲基化因而表現量很低，miR-203 透過負調控致癌基因 ABL1(參與細胞分化、細胞分裂、細胞黏附和壓力反應)而抑制腫瘤生成，表示腫瘤抑制 miRNA 的 DNA 甲基化有助於鎳誘導癌症發展(Zhang et al, 2013a)。因此，鎳透過多種不同表觀遺傳變異來抑制特定基因(例如：抑癌基因)的表現，進而誘導細胞走向癌化。

腫瘤細胞透過活化 EMT 路徑來進行去分化作用，細胞得以移行與侵襲，先前研究指出，多種癌症發展過程中，miR-200 家族表現量下降與調控 EMT 有關(Mongroo & Rustgi, 2010)，頭頸癌細胞 miR-138 表現低而改變細胞形態，像是細胞-細胞間的黏附、增加能動性與產生間質表型等 EMT 特徵，miR-138 經由不同路徑調控 EMT 相關基因 EZH2、ZEB2、RHOC 和 VIM(Liu et al, 2011)，然而，miRNAs 在鎳化合物誘導費支氣管上皮細胞進行 EMT 中所扮演的角色仍未完全釐清，在我們的 miRNAs 微陣列結果顯示，氯化鎳促使 18 個 miRNAs 增加與 28 個 miRNAs 減少，初步發現氯化鎳可能透過 miR-4417 調控 fibronectin，其他 miRNAs 是否參與氯化鎳誘導的 EMT 過程需有更多實驗證明。

先前本實驗室研究結果發現，氯化鎳透過 ROS 促進 HIF-1α 表現，另有文獻報導，鎳誘導的神經毒性包含細胞能量代謝異常，其主要特徵為抑制氧化磷酸化與增加細胞的糖解作用，低氧狀態下，HIF-1α 調控 miR-210 表現，miR-210 可藉由抑制 iron-sulfur cluster assembly protein (ISCU1/2) 與 iron-sulfur clusters (ISCs)來控制粒線體能量代謝，但是細胞中的鐵濃度不影響 miR-210 調控的 ISC-contaning 代謝酵素，小鼠腦神經瘤細胞暴露鎳後，HIF-1α 促進 miR-210 表現，隨後抑制 ISCU1/2 而變細胞能量代謝(He et al, 2014)，藉由釐清鎳對細胞分子機制產生之調控，將有助於了解鎳對人類健康之影響。

miR-200b 抑制 VEGF 表現與 miR-146a 抑制 fibronectin 表現，運用 miR-200b 與 miR-146a 抑制劑可增加 VEGF 和 fibronectin、傷口癒合、細胞移行與管狀生成(Feng et al, 2014)，肺支氣管發育不全的老鼠與病患中的 miR-206 表現量較控制組低，miR-206 過度表現可誘導細胞凋亡、減少細胞增生作用、抑制爬行與降低細胞貼附能力，fibronectin 為 miR-206 的標靶基因，miR-206 透過轉錄與轉譯層面調控 fibronectin 的表現，減少 miR-206 提高細胞 fibronectin 的量而調節生物功能，同時也在肺支氣管發育不全的老鼠與病患檢體發現 fibronectin 表現量增加(Zhang et al, 2013b)。miRNAs 與其標靶基因結合進而抑制標靶基因的表現或轉譯作用，本研究發現氯化鎳促進 miR-4417 表現量變多且

fibronectin 也增加，分析結果顯示，fibronectin mRNA 3'UTR 序列中並沒有 miR-4417 的結合位點，表示 miR-4417 為間接影響 fibronectin 表現，以 lentivirus 系統將 miR-4417 標靶基因 TAB2 進行靜默，實驗結果顯示，TAB2 表現量低的細胞其 fibronectin 表現量隨之增加，然而，TAB2 如何調控 fibronectin 仍尚待釐清。

EMT 是發育期間不可或缺的過程，但也參與纖維化與腫瘤轉移等病理機轉(Katsuno et al, 2013)，因此，EMT 被認為是腫瘤進展中重要的過程，TGF-β 訊息路徑為誘導細胞發生 EMT 的機轉之一，其他因子包括：TGF-β 相關的骨形成蛋白(bone morphogenic proteins, BMPs)亦可誘導 EMT，過去通常多以 TGF-β 來刺激各種上皮細胞產生 EMT 作為研究模式(Xu et al, 2009)，本研究發現氯化鎳同樣具有誘導 EMT 反應，同時在基因微陣列分析結果觀察到，氯化鎳能活化 TGF-β 訊息路徑，所以，推測 TGF-β 可能參與氯化鎳誘導 EMT 的路徑之一，在實驗結果顯示，氯化鎳確實部分藉由 TGF-β 路徑來誘導 EMT 的發生。TGF-β 具有促進間質型態標記 fibronectin mRNA 表現的能力(Varga et al, 1987)，我們的實驗結果顯示，氯化鎳促使 miR-4417 表現量變多，細胞過度表現 miR-4417 會增加 fibronectin 表現量而可能參與氯化鎳所誘導的 EMT 路徑，然而，TGF-β 抑制劑 SB525334 並無法抑制氯化鎳誘導的 miR-4417 表現量，表示 TGF-β 與氯化鎳雖然皆可誘導 EMT 發生，但可能是透過不同分子機制來調控 fibronectin，未來將可藉由釐清發病的生理機轉以發展癌症治療與診斷預後的新策略。

致謝

感謝提昇私校能量計畫，國科會 101-2632-B-040-001-MY3 計劃提供研究經

費

部分研究已發表於 *Molecular Cancer Research*;11(5);1-12. 2013 AACR (被 Editor 選為 High light issue)

miR-4417 的研究結果投稿於 *Archives of Toxicology*，current state：revision。

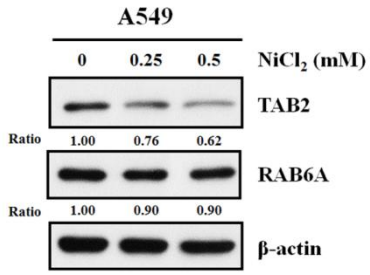

Figure 1. Analysis of miR-4417 target mRNAs by Western blot in A549 cells. A549 cells were treated with $NiCl_2$ (0, 0.25 and 0.5 mM) for 72 h and the protein levels were determined on Western blot. β-actin was used as the internal control. The relative ratios of TAB2/β-actin and RAB6A/β-actin are shown.

(A)

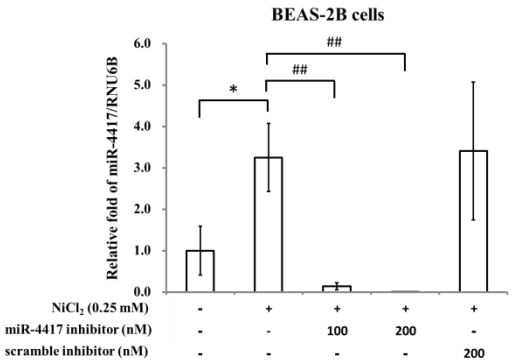

(B)

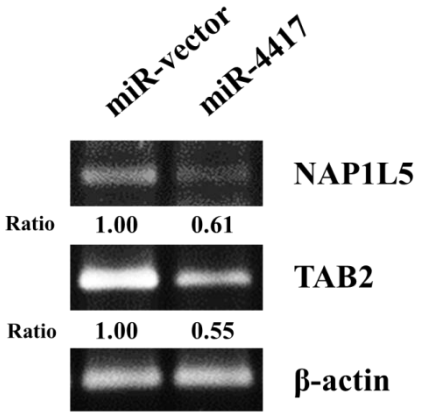

(C)

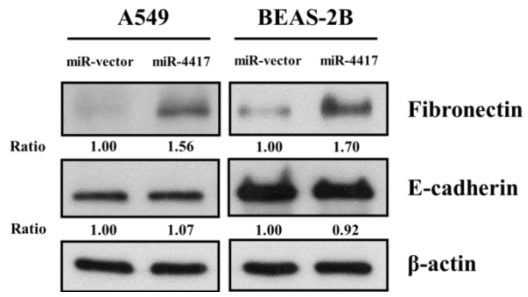

(D)

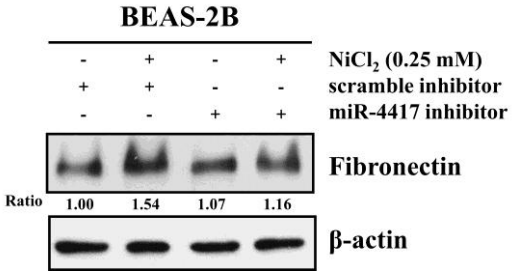

(E)

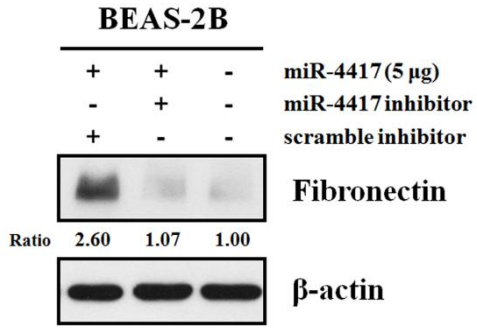

Figure 2. miR-4417 inhibitor abolishes the expression of $NiCl_2$-induced miR-4417 and fibronectin.

(A) BEAS-2B cells (1×10^6 cells/6 cm dish) were transfected with microOFF™ miR-4417 inhibitor (100 and 200 nM) or scrambled miRNA inhibitor (scramble inhibitor, 200 nM) following by exposed to NiCl2 (0 and 0.25 mM) for 48 h. Quantitative real-time PCR analysis was used to detect miR-4417 expression. All values have been normalized to the level of RNU6B and are the averages of three independent readings. *p<0.05; ##p<0.01 (B) The mRNA levels of

miR-4417-targeted genes in BEAS-2B cells, including NAP1L5 and TAB2, were determined on RT-PCR. β-actin was used as the internal control. The relative ratios of NAP1L5/β-actin and TAB2/β-actin are shown. (C) The protein levels of EMT markers (fibronectin and E-cadherin) were analyzed by Western blot. β-actin was used as the internal control. The relative ratios of Fibronectin/β-actin and E-cadherin/β-actin are shown. (D) BEAS-2B cells were transfected with microOFF^{TM} miR-4417 inhibitor (100 nM) or scrambled miRNA inhibitor (scramble inhibitor, 100 nM) following by exposed to NiCl2 (0 and 0.25 mM) for 48 h. (E) BEAS-2B cells were cotransfected with miR-4417/pcDNA^{TM} 6.2-GW (5μg) and miR-4417 inhibitor (100 nM) or scrambled miRNA inhibitor (scramble inhibitor, 100 nM). The protein levels of fibronectin were analyzed by Western blot. β-actin was used as the internal control. The relative ratios of Fibronectin/β-actin are shown.

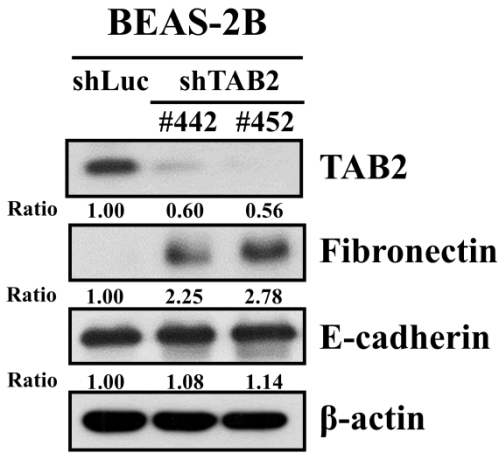

Figure 3. Silencing of TAB2 up-regulates fibronectin expression. BEAS-2B cells were infected with lentivirus carrying shTAB2 #442, #452 or vector control (shLuc). The protein levels were determined on Western blot. β-actin was used as the internal control. The relative ratios of TAB2/β-actin, Fibronectin/β-actin and E-cadherin/β-actin are shown.

(A)

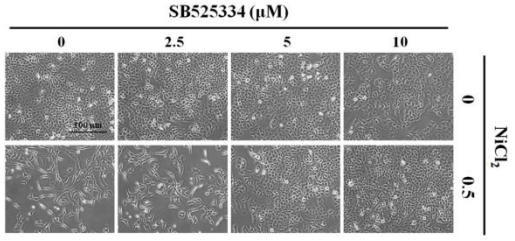

(B)

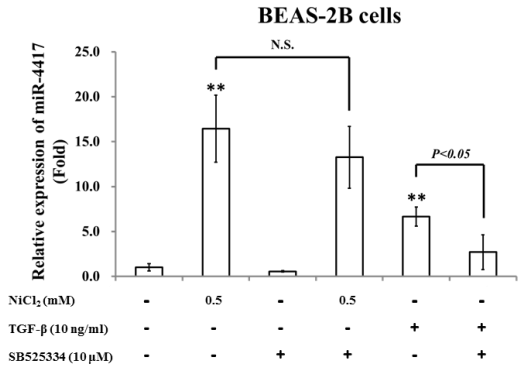

(C)

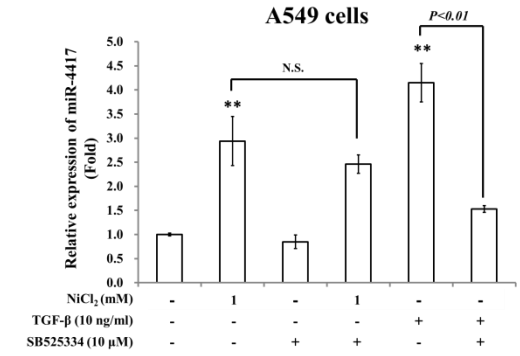

Figure 4. Ni-induced miR-4417

partially depends on TGF-β pathway. (A) A549 cells were incubated with $NiCl_2$ (0 and 0.5 mM) with or without TGF-β inhibitor (SB525334; 0, 2.5, 5 and 10 μM) for 72 hr and photographed at 100× magnification. The images are representative of 8 separate experiments. (B) BEAS-2B and (C) A549 cells were treated with $NiCl_2$ with or without SB525334 (TGF-β inhibitor) for 48 h and the miR-4417 were analyzed by qRT-PCR. TGF-β-treated cells were used as the positive control.*p<0.05, **p<0.01 (compared with untreated control); #p<0.05 (compared with 10 ng/ml TGF-β treatment) and N.S. (non-significance)

(A)

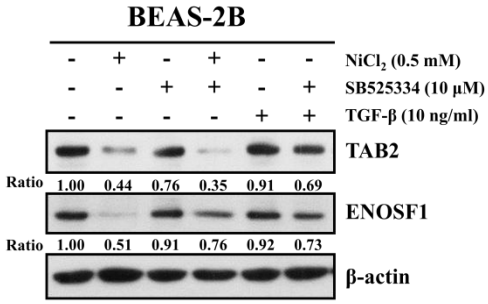

(B)

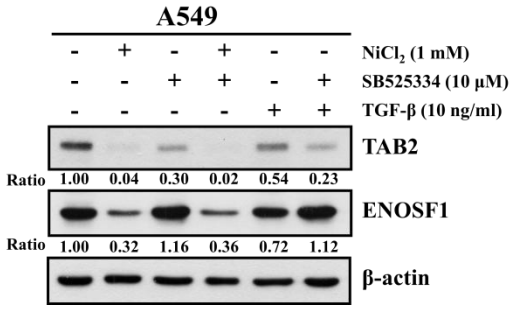

Figure 5. Effects of TGF-β inhibitor on miR-4417 target mRNAs in nickel-treated cells. (A) BEAS-2B (1x106 cells/6 cm dish) and (B) A549 (5x105 cells/6 cm dish) cells were treated with $NiCl_2$ (0.5 and 1 mM, respectively) or TGF-β (10 ng/ml) with or without SB525334 (10 μM) for 72 h and the protein levels were analyzed on Western blot. β-actin was used as the internal control. The relative ratios of TAB2/β-actin and ENOSF1/β-actin are shown.

(A)

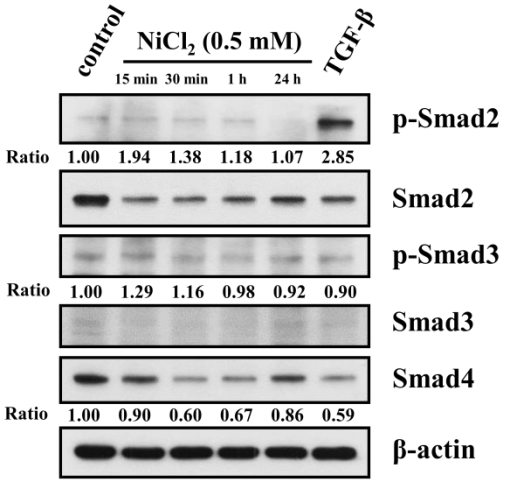

(B)

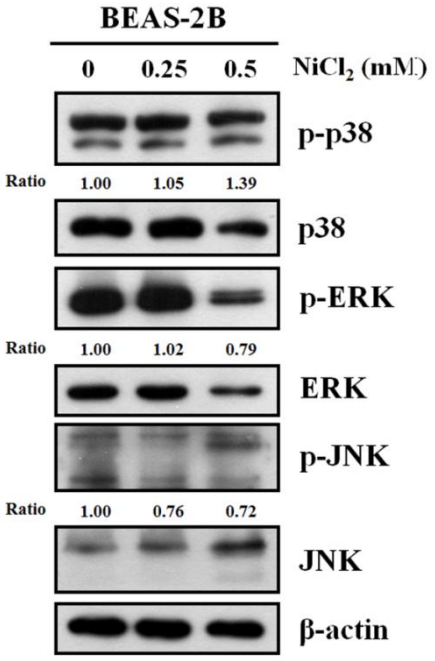

Figure 6. Effects of $NiCl_2$ treatment

on Smad-dependent and Smad-independent pathways in TGF-β signaling.

(A) BEAS-2B cells ($1x10^6$ cells/6 cm dish) were treated with $NiCl_2$ (0.5 mM) for 15 min, 30 min, 1 h and 24 h or TGF-β (10 ng/ml, positive control) for 30 min. The protein levels were analyzed on Western blot. β-actin was used as the internal control. The relative ratios of p-Smad2/Smad2, p-Smad3/Smad3 and Smad4/β-actin are shown. (B) BEAS-2B cells were treated with $NiCl_2$ (0, 0.25 and 0.5 mM) for 72 h and the protein levels were determined on Western blot. β-actin was used as the internal control. The relative ratios of p-p38/p38, p-ERK/ERK and p-JNK/JNK are shown.

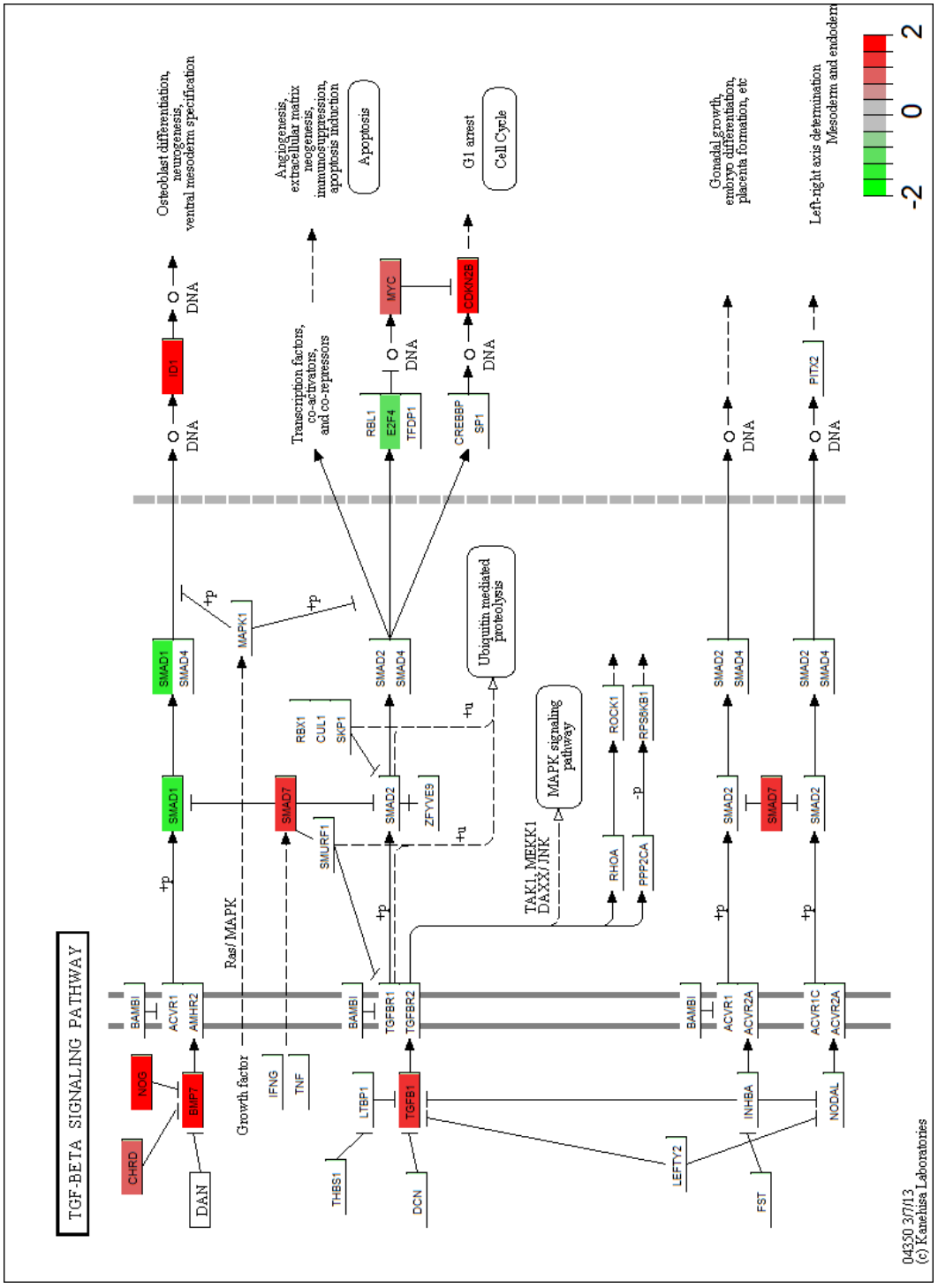

Supplementary figure 1. TGF-β signaling pathway . Up-regulated and down-regulated mRNAs are depicted in red and green, respectively, by Search&Color Pathway in KEGG.

References

(1990) Chromium, nickel and welding. *IARC monographs on the evaluation of carcinogenic risks to humans / World Health Organization, International Agency for Research on Cancer* **49:** 1-648

(1996) NTP Toxicology and Carcinogenesis Studies of Nickel Subsulfide (CAS No. 12035-72-2) in F344 Rats and B6C3F1 Mice (Inhalation Studies). *Natl Toxicol Program Tech Rep Ser* **453:** 1-365

Chang FH, Wang HJ, Wang SL, Wang YC, Hsieh DP, Chang LW, Ko YC (2006) Survey of urinary nickel in residents of areas with a high density of electroplating factories. *Chemosphere* **65:** 1723-1730

Chen H, Kluz T, Zhang R, Costa M (2010) Hypoxia and nickel inhibit histone demethylase JMJD1A and repress Spry2 expression in human bronchial epithelial BEAS-2B cells. *Carcinogenesis* **31:** 2136-2144

Doll R, Mathews JD, Morgan LG (1977) Cancers of the lung and nasal sinuses in nickel workers: a reassessment of the period of risk. *British journal of industrial medicine* **34:** 102-105

Feng B, Chen S, Zhang L, Cao Y, Chakrabarti S (2014) miRNA-146a and miRNA-200b Antagomirs Accelerate Wound Healing through the Regulation of VEGF and Fibronectin *Journal of Pharmacy and Pharmacology* **2:** 104-133

Fraga MF, Esteller M (2007) Epigenetics and aging: the targets and the marks. *Trends in genetics : TIG* **23:** 413-418

Grimsrud TK, Berge SR, Haldorsen T, Andersen A (2002) Exposure to different forms of nickel and risk of lung cancer. *American journal of epidemiology* **156:** 1123-1132

He M, Lu Y, Xu S, Mao L, Zhang L, Duan W, Liu C, Pi H, Zhang Y, Zhong M, Yu Z, Zhou Z (2014) MiRNA-210 modulates a nickel-induced cellular energy metabolism shift by repressing the iron-sulfur cluster assembly proteins ISCU1/2 in Neuro-2a cells. *Cell death & disease* **5:** e1090

Huang da W, Sherman BT, Lempicki RA (2009) Systematic and integrative analysis of large gene lists using DAVID bioinformatics resources. *Nature protocols* **4:** 44-57

Ji W, Yang L, Yuan J, Zhang M, Qi D, Duan X, Xuan A, Zhang W, Lu J, Zhuang Z, Zeng G (2013) MicroRNA-152 targets DNA methyltransferase 1 in NiS-transformed cells via a feedback mechanism. *Carcinogenesis* **34:** 446-453

Katsuno Y, Lamouille S, Derynck R (2013) TGF-beta signaling and epithelial-mesenchymal transition in cancer progression. *Current opinion in oncology* **25:** 76-84

Liu X, Wang C, Chen Z, Jin Y, Wang Y, Kolokythas A, Dai Y, Zhou X (2011) MicroRNA-138 suppresses

epithelial-mesenchymal transition in squamous cell carcinoma cell lines. *The Biochemical journal* **440:** 23-31

Liu X, Yun F, Shi L, Li ZH, Luo NR, Jia YF (2015) Roles of Signaling Pathways in the Epithelial-Mesenchymal Transition in Cancer. *Asian Pacific journal of cancer prevention : APJCP* **16:** 6201-6206

Ma FY, Sachchithananthan M, Flanc RS, Nikolic-Paterson DJ (2009) Mitogen activated protein kinases in renal fibrosis. *Front Biosci (Schol Ed)* **1:** 171-187

Mongroo PS, Rustgi AK (2010) The role of the miR-200 family in epithelial-mesenchymal transition. *Cancer biology & therapy* **10:** 219-222

Salnikow K, Zhitkovich A (2008) Genetic and epigenetic mechanisms in metal carcinogenesis and cocarcinogenesis: nickel, arsenic, and chromium. *Chemical research in toxicology* **21:** 28-44

Skinner MK, Manikkam M, Guerrero-Bosagna C (2010) Epigenetic transgenerational actions of environmental factors in disease etiology. *Trends in endocrinology and metabolism: TEM* **21:** 214-222

Szyf M (2009) Epigenetics, DNA methylation, and chromatin modifying drugs. *Annual review of pharmacology and toxicology* **49:** 243-263

Vaissiere T, Sawan C, Herceg Z (2008) Epigenetic interplay between histone modifications and DNA methylation in gene silencing. *Mutation research* **659:** 40-48

Varga J, Rosenbloom J, Jimenez SA (1987) Transforming growth factor beta (TGF beta) causes a persistent increase in steady-state amounts of type I and type III collagen and fibronectin mRNAs in normal human dermal fibroblasts. *The Biochemical journal* **247:** 597-604

Vrba L, Munoz-Rodriguez JL, Stampfer MR, Futscher BW (2013) miRNA gene promoters are frequent targets of aberrant DNA methylation in human breast cancer. *PloS one* **8:** e54398

Wu CH, Tang SC, Wang PH, Lee H, Ko JL (2012) Nickel-induced epithelial-mesenchymal transition by reactive oxygen species generation and E-cadherin promoter hypermethylation. *The Journal of biological chemistry* **287:** 25292-25302

Xu J, Lamouille S, Derynck R (2009) TGF-beta-induced epithelial to mesenchymal transition. *Cell research* **19:** 156-172

Xu Z, Ren T, Xiao C, Li H, Wu T (2011) Nickel promotes the invasive potential of human lung cancer cells via TLR4/MyD88 signaling. *Toxicology* **285:** 25-30

Zhang J, Zhou Y, Wu YJ, Li MJ, Wang RJ, Huang SQ, Gao RR, Ma L, Shi HJ (2013a) Hyper-methylated miR-203 dysregulates ABL1 and contributes to the nickel-induced tumorigenesis. *Toxicology letters* **223:**

42-51

Zhang X, Xu J, Wang J, Gortner L, Zhang S, Wei X, Song J, Zhang Y, Li Q, Feng Z (2013b) Reduction of microRNA-206 contributes to the development of bronchopulmonary dysplasia through up-regulation of fibronectin 1. *PloS one* **8:** e74750

Zhao J, Shi X, Castranova V, Ding M (2009) Occupational toxicology of nickel and nickel compounds. *J Environ Pathol Toxicol Oncol* **28:** 177-208

子計畫三

鎳誘發 Nrf2 表現在肺腫瘤化之角色

Abstract

Occupational exposure to nickel compounds has been associated with lung cancer. The correlation between high nickel levels and increased risk of lung cancer has been previously reported in a case-control study. This study assessed whether nickel exposure increased the occurrence of p53 mutations due to DNA repair inhibition by nickel. A total of 189 lung cancer patients were enrolled to determine nickel levels in tumor-adjacent normal lung tissues and p53 mutation status in lung tumors through atomic absorption spectrometry and direct sequencing, respectively. Nickel levels in p53 mutant patients were significantly higher than those in p53 wild-type patients. When patients were divided into high- and low-nickel subgroups by median nickel level, the high-nickel subgroup of patients had an odds ratio (OR) of 3.25 for p53 mutation risk relative to the low-nickel subgroup patients. The OR for p53 mutation risk of lifetime non-smokers, particularly females, in the high-nickel subgroup was greater than that in the low-nickel subgroup. To determine whether nickel affected DNA repair capacity, we conducted the host cell reactivation assay in A549 and H1975 lung cancer cells and showed that the DNA repair activity was reduced by nickel chloride in a dose-dependent manner. This was associated with elevated production of hydrogen peroxide-induced 8-oxo-deoxyguanosine. Therefore, increased risk of p53 mutation due to defective DNA repair caused by high nickel levels in lung tissues may be one mechanism by which nickel exposure contributes to lung cancer development, especially in lifetime female non-smokers. Nrf2 is a key transcription factor for genes coding for antioxidants, detoxification enzymes, and multiple drug resistance and it also confers resistance to anticancer drugs. We next hypothesized that mutant p53 could upregulate Nrf2 expression at the transcriptional level, thereby conferring cisplatin resistance in non-small cell lung cancer (NSCLC). Luciferase reporter assays and real-time PCR analysis indicated that the Nrf2 promoter activity and its mRNA levels were markedly suppressed by wild-type p53, but not by mutant p53. Chromatin immunoprecipitation (ChIP) further confirmed that wild-type p53 binds at the p53 putative binding site to block Sp1 binding to the Nrf2 promoter and consequently to suppress Nrf2 promoter activity. The MTT assay indicated that an increase in Nrf2 expression by mutant p53 is responsible for cisplatin resistance. Among the Nrf2 downstream genes, Bcl-2 and Bcl-xL contribute more strongly to Nrf2-mediated cisplatin resistance when compared with heme oxygenase 1 (HO-1). Cox regression analysis showed that patients with high-Nrf2, high-Bcl-2, high-Bcl-xL mRNA tumors were more commonly occurred unfavorable response to cisplatin-based chemotherapy than their counterparts. The prognostic significance of Nrf2 mRNA levels on OS and RFS was also observed in patients who have received cisplatin-based chemotherapy, particularly in p53-mutant patients. Collectively, mutant p53 may confer cisplatin resistance via upregulation of Nrf2 expression, and Nrf2 mRNA level may predict chemotherapeutic response and outcomes in NSCLC.

Introduction

Lung cancer is the leading cause of cancer death in Taiwanese women, and the second highest cause of cancer death in Taiwanese men, even though the majority of the population are non-smokers (96% women and 65% men) (Ministry of Health and Welfare, Taiwan, 2010). Despite advances in cancer prevention and early detection, the 5-year survival rate of lung cancer patients has remained below 15% over the past 3 decades (Siegel et al., 2012). Tobacco smoke is considered to be the predominant risk factor for lung cancer, but it cannot fully explain the etiology of lung cancer in Taiwan, especially in women. Therefore, environmental factors other than tobacco smoke might play a role in lung cancer development, especially in non-smoking Taiwanese women.

Nickel compounds are widely used in industrial processes (Kasprzak et al., 2003). Epidemiological studies have shown that chronic occupational exposure of workers to inhaled or ingested nickel compounds in the workplace increases the risk of respiratory cancers (Grimsrud et al., 2002; Kasprzak et al., 2003; Navarro Silvera and Rohan, 2007; De Matteis et al., 2012). The International Agency for Research on Cancer has classified nickel compounds as a Group 1 human carcinogen. Over the last 3 decades, industrialization and urbanization have seriously polluted agricultural soils in certain areas of Taiwan due to discharged wastewater in irrigation ditches (Chen et al., 2007; Lai et al., 2010). The release of nickel into the environment by manufacturing plants and high consumption of nickel-containing products or foods represents a potential risk for cancer development through non-occupational exposure routes (Ptashynski et al., 2002; Kasprzak et al., 2003; Hedouin et al., 2007; Luo et al., 2011). This speculation is supported by previous epidemiological studies. For example, high urinary nickel levels were associated with residential location being near a nickel refinery (Smith-Sivertsen et al., 1998). In central Taiwan, residents living in areas with a high density of electroplating factories were also shown to have higher urinary nickel levels compared with those living in low density areas (Chang et al., 2006). In addition, the concentration of nickel in residential areas was correlated with incidences of oral cancer in central Taiwan (Su et al., 2010; Yuan et al., 2011). Our previous case–control study also showed that nickel accumulation in lung tissues may be associated with increased lung cancer risk in central Taiwan (Kuo et al., 2006). Furthermore, a dose-relationship between soil nickel levels and lung cancer occurrence in Taiwan has been reported recently (Huang et al., 2013). Therefore, we hypothesized that nickel contamination from non-occupational exposure routes could contribute to lung cancer development, especially in Taiwanese non-smokers.

More than 50% of human cancers, including lung cancer, harbor p53 mutations that play a crucial role in tumorigenesis (Lavin and Gueven, 2006; Levine and Oren, 2009). Epidemiological studies have indicated that occupational exposure to nickel may be associated with p53 mutations in lung cancer, but this observation is confounded by cigarette smoking (Harty et al., 1996). One possible mechanism underlying nickel-induced carcinogenesis is nickel-induced reductions in DNA repair activity and subsequently increased susceptibility to DNA damaging agents (Hu et al., 2004). Thus, despite the classification of nickel compounds as weak

mutagens, nickel has the potential to exacerbate mutagenesis by promoting the occurrence of p53 mutation (Denkhaus and Salnikow, 2002; Oller, 2002). In this study, we hypothesized that nickel accumulation in lung tissues may contribute to lung carcinogenesis by increasing the risk of p53 mutation. We support this hypothesis by identifying a positive correlation between nickel levels in tumor-adjacent normal lung tissues and p53 mutation status of tumors from 189 lung cancer patients. In addition, the host cell reactivation assay was performed to verify whether the DNA repair activity could be suppressed by nickel chloride.

Lung cancer is the leading cause of cancer death around the world. Late diagnosis and low response to therapeutic drugs are viewed as the causes of poor patient outcomes (Jin et al, 2008). The five-year survival rate has remained at about 15% for the past three decades despite the development and use of several targeting drugs for lung cancer therapy (Molina et al, 2008). Therefore, mechanistic studies to uncover the possible pathway(s) involved in drug resistance are essential for improving the outcomes and life quality in patients with this disease.

Cisplatin-based chemotherapy is still considered the first-line therapeutic strategy for lung cancer (Santana-Davila et al, 2014; Tiseo et al, 2014). Cisplatin induces cancer cell death via induction of double strand DNA breaks caused by the generation of reactive oxygen species (ROS) (Itoh et al, 2011; Marullo et al, 2013). Gene expression of antioxidants that eliminate ROS is promoted by an NF-E2-related factor 2 (Nrf2), which binds to antioxidant response elements (ARE) of the promoters of these genes (Gorrini et al, 2013; Kansanen et al, 2013; Nguyen et al, 2009; Villeneuve et al, 2009; Zucker et al, 2014). Activation of Nrf2/ARE signaling has been demonstrated through mutations of Kelch-like ECH-associated protein 1 (Keap1) or Nrf2 to protect Nrf2 from degradation by Keap1 (Kim et al, 2010; Miura et al, 2014; Padmanabhan et al, 2006; Shibata et al, 2011; Singh et al, 2006; Yoo et al, 2012). The Keap1/Nrf2 mutations in NSCLC patients were ranged from 3.2% to 60% and this variation may be due to the number of study subjects and histologic subtypes. In fact, the Keap1/Nrf2 mutation was frequently reported to be uncommon in NSCLC patients including Taiwanese (< 3%) (Supplementary Table 1). High Nrf2 expression has been shown to promote resistance to different anticancer drugs in human cancers (Akhdar et al, 2009; Homma et al, 2009; Ji et al, 2013; Niture & Jaiswal, 2013; Wang et al, 2008). However, the underlying mechanism of an increase in Nrf2 expression is not fully understood although some mechanisms have been reported (23,24). For example, high Nrf2 expression driven by NF-κB signaling confers chemoresistance in human myeloid leukemia (Rushworth et al, 2012). Mutant k-ras confers chemoresistance by upregulating Nrf2 transcription through a TPA response element (Tao et al, 2014).

The cross-talk between Nrf2 and p53 plays a crucial role in cellular homeostasis. Positive or negative co-regulation at the post-translational level has been reported between Nrf2 and p53 (Rotblat et al, 2012). For example, binding of the p53 downstream p21 to Nrf2 inhibits Nrf2 degradation (Chen et al, 2009), whereas binding of the Nrf2 downstream NAD(P)H dehydrogenase quinone 1 (NQO1) to p53 prevents p53 degradation (Asher et al, 2002). However, Nrf2 promotes MDM2 expression for degradation of p53 protein

(You et al, 2011). P53 inhibits Nrf2 downstream expression of genes, such as NQO1 and heme oxygenase 1 (HO-1) by directly interacting with ARE-containing promoters (Faraonio et al, 2006). Therefore, we expected that the reciprocal regulation between Nrf2 and p53 may modulate cancer cell apoptosis induced by chemotherapeutic agents.

Our preliminary data from lung cancer patients showed that Nrf2 mRNA expression levels were higher in p53-mutant tumors than in p53-wild-type tumors. A software analysis revealed that putative binding sites for Sp1 and p53 could exist on the Nrf2 promoter (-1036/+1). We therefore hypothesized that mutant p53 might directly upregulate Nrf2 transcription to confer resistance of chemotherapeutic agents and consequently result in poor outcome in NSCLC patients.

Results

Part I: Nickel accumulation in lung tissues is associated with increased risk of p53 mutation in lung cancer patients

High nickel levels are more commonly found in males and smokers than in females and non-smokers

The median nickel level (0.47 μg/g dry weight of lung tissue) was used as a cutoff point to divide the study population into high-nickel and low-nickel subgroups. The high-nickel subgroup had 81 patients, and their nickel levels ranged from 0.49 to 85.11 μg/g dry weight of lung tissue. The low-nickel subgroup had 108 patients, and their nickel levels ranged from 0.20 to 0.47 μg/g dry weight of lung tissue. The unequal number of study subjects in the two subgroups is due to the inclusion in the low nickel subgroup of 27 study subjects whose nickel levels matched the median value. Excluding these 27 subjects from the analysis does not change the results that we report (data not shown). Male and smoker patients were more prevalent in the high-nickel subgroup than were female and non-smoker patients (48.5% of males were in the high nickel group vs. 30.5% of females, $P = 0.021$; 54.3% of smokers were in the high nickel group vs. 34.3% of non-smokers, $P = 0.006$; Table 1). In this study population, 81 smokers were male, and there were no female smoker patients. In addition, the nickel levels in male smokers were marginally higher than in male non-smokers, but the difference was not statistically significant ($P = 0.086$; Table 1). No difference in nickel levels was observed between male and female non-smokers ($P = 0.367$, Table 1). Furthermore, no association was observed between nickel levels and other clinical parameters, including age, tumor histology, tumor stage, tumor size (T), and nodal micro-metastasis (N) (Table 1). These results suggest that tobacco smoke might be more contributive to nickel accumulation in the lungs of male and smoker patients than in the lungs of female and non-smoker patients.

Nickel exposure may contribute to lung carcinogenesis in non-smokers by increasing the risk of p53 mutations

We examined whether high nickel levels in lung tissues could contribute to p53 mutation in lung cancer patients. The p53 mutation status was determined by direct-sequencing. The p53 mutation frequencies in males, smokers, and squamous cell carcinomas (SCC) were significantly higher than in females, non-smokers, and adenocarcinomas (ADC), respectively ($P = 0.031$ for gender; $P = 0.012$ for smoking status; $P = 0.004$ for tumor histology, Supporting Information Table SII). As shown in Figure 1, the average nickel level in the p53 mutant patients ($n = 76$) was significantly higher than in the p53 wild-type patients ($n = 113$) (6.02 ± 14.75 vs. 1.84 ± 4.79, $P < 0.001$). After adjusting for possible confounding factors including gender, smoking status, and tumor histology, the patients with high-nickel levels had an odds ratio (OR) 3.25 for the occurrence of p53 mutation relative to patients with low-nickel levels ($P < 0.001$, Table 2). A positive correlation between nickel levels and p53 mutation risk was observed in both ADC and SCC patients (OR, 3.36, 95% CI, 1.25–9.06, $P = 0.017$ for ADC; OR, 3.53, 95% CI, 1.51–8.27, $P = 0.004$ for SCC; Table 2). Among the non-smokers, those with high-nickel levels also had a higher frequency of p53 mutations than those with low-nickel levels (OR,

4.31, 95% CI, 1.82–10.25, P = 0.001; Table 2). However, only a marginal association between nickel levels and p53 mutations was observed in the smokers (OR, 2.59, 95% CI, 1.00–6.69, P = 0.05; Table 2). When the non-smoker patients were stratified by gender, the females had the highest OR among all the comparisons that we performed (9.35, 95% CI, 2.56–34.09, P = 0.001), but no association between nickel levels and p53 mutations was observed in the male non-smokers. This result could be due to a low number of male non-smokers that were available for this study (Table 2). Therefore, the gender difference in the association between nickel levels and p53 mutations in non-smokers should be further verified using a larger study population.

To confirm the accuracy of the nickel level measurement by AAS, we randomly selected 10 samples from each batch for analysis with inductively coupled plasma mass spectrometry (ICP-MS) by another laboratory. The data from the ICP-MS analysis were consistent with those of the AAS analysis (r = 0.98, P < 0.001, Supporting Information Fig. S1). Additionally, due to the AAS detection limit, the nickel concentrations of 70 of the 189 lung cancer subjects were less than three times the MDL (0.22 μg/L). Most of these patients were lifetime non-smokers (51.9%, 56 of 108 patients). To eliminate any false negatives in the AAS analysis, the nickel levels in 87 non-smoker lung tissues were further analyzed by IPC-MS (Agilent Technologies, Model 7700X), which had greater speed, precision, and sensitivity than AAS. The ICP-MS analysis showed that the average nickel level of these 87 samples was 0.94 ± 3.01 μg/g dry weight (0.04–24.27 μg/g dry weight). Among this subgroup (n = 87), the patients with high nickel levels had a marginally higher p53 mutation frequency than did those with low nickel levels (P = 0.052, Supporting Information Table SIII). Therefore, the ICP-MS results support the AAS data, indicating that non-smokers with high nickel levels had a higher risk of p53 mutation than those with low nickel levels (Table 2). Together, these results suggest that nickel accumulation in lung tissues might contribute to the p53 mutations that are found in lung cancer patients, especially in female non-smokers.

Nickel chloride inhibits DNA repair activity in lung cancer cells

We assessed whether nickel chloride could inhibit the DNA repair activity in lung cancer cells and subsequently lead to an increased risk of p53 mutation using the host cell reactivation assay. To determine the proper concentration of nickel chloride for the assay, the cytotoxicity of nickel chloride in A549 and H1975 cells was determined using the MTT assay. As shown in Figure 2A, the nickel chloride treatment (0–1.5 mM) produced a linear survival curve for each cell line. The concentration of nickel chloride that led to 35% cytotoxicity was used as the maximum concentration for the host cell reactivation assay (0.85 mM for A549 and 0.75 mM for H1975). The host cell reactivation assay showed that the DNA repair activity in both cell lines was decreased by nickel chloride in a dose-dependent manner (Figs. 2B and 2C). We then examined whether hydrogen peroxide-induced 8-oxo-dG production could be increased as a result of nickel-mediated DNA repair inhibition. In both A549 and H1975 cells, the level of 8-oxo-dG was significantly increased after co-treatment with nickel chloride and hydrogen peroxide compared with hydrogen peroxide treatment alone (Fig. 2D). The levels of 8-oxo-dG in A549 cells were also elevated by nickel chloride treatment alone, but this

was not observed in H1975 cells (Fig. 2D). These results suggest that nickel may inhibit DNA repair activity and consequently result in increased risk of occurrence of p53 mutations.

Nickel levels are associated with 8-oxo-dG levels in lung cancer patients

Nickel has been shown to induce oxidative DNA damage to produce 8-oxo-dG in lung tissues and cell lines (Tkeshelashvili et al., 1993; Kawanishi et al., 2002). Therefore, we hypothesized that high nickel levels might increase the risk of p53 mutation due to 8-oxo-dG production in lung tissues. Seventy-eight of the 189 tumor-adjacent normal lung tissues from lung cancer patients were available for 8-oxo-dG measurement by LC-MS/MS. As shown in Figure 3A, patients in the high-nickel subgroup had higher 8-oxo-dG levels on average than those in the low-nickel subgroup (11.2 ± 8.5 vs. 8.1 ± 3.6 8-oxo-dG/106 dG, $P = 0.032$). In the same group of samples that were analyzed for 8-oxo-dG, a similar observation was made regarding the association of nickel levels with p53 mutations. The average nickel level in the p53 mutant patients was higher than in the p53 wild-type patients (5.3 ± 11.6 vs. 2.2 ± 5.5 μg/g dry weight of lung tissue, $P = 0.022$, Fig. 3B). The 8-oxo-dG levels did not correlate with p53 mutation status in the study population (data not shown). However, the p53 mutation frequency in patients with high 8-oxo-dG plus high nickel levels was marginally higher than those with low 8-oxo-dG plus low nickel levels (data not shown). Therefore, we suggest that nickel levels were positively associated with the occurrence of p53 mutation in lung cancer patients, especially in female non-smokers. Moreover, nickel accumulation in lung tissues might induce 8-oxo-dG production and partially contribute to the p53 mutations.

Part II: Mutant p53 confers chemoresistance in non-small cell lung cancer by upregulating Nrf2

Nrf2 expression is suppressed by wild-type p53, but not by mutant p53 at the transcription level

Eight lung cancer cell lines were enrolled to test the hypothesis that Nrf2 expression is de-regulated at the transcription level by p53 status. The Nrf2/ARE downstream genes HO-1 and NQO1 expression were relatively lower in p53-wild-type cells than in p53-mutant cells (Figure 4A upper panel). Concomitantly, Nrf2 protein and its mRNA expression levels were significantly lower in p53-wild-type cells than in p53-mutant cells (Figure 4A). These results suggest that Nrf2 expression might be suppressed by wild-type p53, but not by mutant p53 at transcriptional level.

A software analyses predicted two p53 and four Sp1 putative binding sites located on the -1036/-1 Nrf2 promoter (http://www.genome.jp/tools/motif/). Three Nrf2 promoters (-1036/+1, -740/+1, and -229/+1) were constructed by PCR and deletion mutations for luciferase reporter assay (Figure 4B upper panel). These three Nrf2 promoters were respectively transfected into H1299, H1975, and CL3 cells. The reporter activity was significantly higher for the -1036/+1 Nrf2 promoter than for the other two Nrf2 promoters (-740/+1 and -229/+1) in these cells. These results revealed the possibility that p53 and Sp1 putative binding sites located near the transcriptional start site might play an important role in Nrf2 transcription in these three cell types.

The possibility that wild-type p53 could suppress Nrf2 promoter activity was explored using p53-null H1299 cells by transfection with wild-type p53 or different mutant p53 expression vectors including H179Y, L194R,

S240R, R249S, A276D, and E286Q. Western blotting showed that p53 expression was detected in H1299 cells transfected with wild-type or mutant p53 expression vectors, but was not observed in H1299 cells with an empty vector transfection (VC) (Figure 4C upper panel). Nrf2 expression was almost completely suppressed by wild-type p53 expression vector, but was unchanged by mutant p53 expression vector transfections in H1299 cells. The luciferase reporter assay indicated a marked decrease in Nrf2 promoter activity following wild-type p53 expression vector transfection, but showed unchanged or relatively increased Nrf2 promoter activity following transfection with mutant p53 expression vectors when compared with the activity in VC cells (Figure 4C lower panel). These results suggest that Nrf2 expression in lung cancer cells is suppressed by wild-type p53, but not by mutant p53 at the transcriptional level.

Nrf2 transcription is down-regulated by wild-type p53, but not by mutant p53 via decreased Sp1 binding to the Nrf2 promoter

We next examined the possibility that wild-type p53 could interact with Sp1 to suppress Nrf2 transcription. The p53-null H1299 cells were transfected with two doses of wild-type p53 or mutant p53 expression vectors (H179Y and L194R). The expression of p53 protein in H1299 cells with wild-type or mutant p53 expression vector transfection was revealed by western blotting, but Nrf2 expression was almost completely suppressed by a high dose of wild-type p53 transfection, but was nearly unchanged by mutant p53 expression vector transfections in H1299 cells (Figure 5A upper panel). The luciferase reporter assay and real-time PCR analysis revealed a dose-dependent decrease in Nrf2 promoter activity and its mRNA levels in response to wild-type p53 transfection in H1299 cells. However, Nrf2 promoter activity and its mRNA level were nearly unchanged in H1299 cells transfected with H179Y or L194R expression vector, whereas Nrf2 promoter activity was elevated by high transfection doses of L194R expression vector (Figure 5A middle panel). ChIP assay showed that wild-type p53 was indeed bound, but the binding of mutant p53 was not revealed on the p53 binding site of Nrf2 promoter. The binding of Sp1 to the Nrf2 promoter in H1299 cells with wild-type p53 transfection almost completely eliminated when compared with VC and H1299 cells transfected with mutant p53 expression vectors (Figure 5A lower panel). On the other hand, Nrf2 protein, Nrf2 promoter activity, and its mRNA expression were elevated by p53 knockdown in p53-wild-type H1975 and CL3 cells. The binding of p53 and Sp1 to the Nrf2 promoter was decreased and increased by p53 silencing in both cell types (Figure 5B). A ChIP analysis further indicated that the binding of p53 to the Nrf2 promoter was decreased by p53 silencing, but the binding of Sp1 to the Nrf2 promoter was increased in p53-knockdown H1975 and CL3 cells in a dose-dependent manner (Figure 5B lower panel). These results suggest that p53 may interfere Sp1 binding to the Nrf2 promoter to reduce its promoter activity.

We then constructed Nrf2 promoters mutated at the p53 or Sp1 binding site by site-directed mutagenesis to verify whether wild-type p53 could interact with Sp1 to suppress Sp1 binding to the Nrf2 promoter. The Nrf2 promoter activity was unchanged by transfection with an Nrf2 promoter mutated at the p53 binding site in H1299 VC cells and H1299 cells with mutant p53 expression vector transfections, but the promoter activity was significantly elevated in H1299 cells transfected with the Nrf2 wild-type promoter. However, the Nrf2

promoter activity was elevated by Nrf2 wild-type promoter transfection in mutant p53-tranfected H1299 cells, but this promoter activity was completely eliminated by transfection with an Nrf2 promoter mutated at the Sp1 binding site in H1299 cells subjected to different treatments (Figure 5C). On the other hand, the Nrf2 promoter activity was markedly increased by transfection with an Nrf2 promoter mutated at the p53 binding site, but the increase in the Nrf2 promoter activity in p53-knockdown H1975 and CL3 cells was nearly completely reversed by transfection with an Nrf2 promoter mutated in the Sp1 binding site (Figure 5D). These results clearly indicate that Nrf2 transcription in lung cancer cells is predominately down-regulated by wild-type p53 via decreased Sp1 binding to the Nrf2 promoter, but is not affected by mutant p53.

Nrf2-mediated Bcl-2, Bcl-xL, and HO-1 expression is dependent on p53 status and may confer cisplatin resistance

We investigated whether Nrf2 expression could determine cisplatin sensitivity in lung cancer cells that had different p53 status. Two types of p53-null cells (H1299 and H358) and three types of p53-wild-type cells (H1975, CL3, and TL4) were collected to evaluate the inhibitory concentration yielding 50% cell viability (IC50) for cisplatin using the MTT assay. Western blotting showed that Nrf2 expression was decreased by Nrf2 knockdown in H1299 and H358 cells, but was dose-dependently increased by Nrf2 overexpression in H1975, CL3, and TL4 cells (Figure 6A upper panel). Intriguingly, the IC50 value for cisplatin was concomitantly decreased by Nrf2-knockdown in H1299 and H358 cells, but was increased in Nrf2-overexpressing H1975, CL3, and TL4 cells (Figure 6A lower panel). However, the IC50 value for cisplatin was nearly unchanged by different mutant p53 expression vector transfections in H1299 cells when compared with VC cells; however, the IC50 value for cisplatin was almost completely rescued by Nrf2 knockdown in H1299 cells transfected with different mutant p53 expression vectors (Figure 7). These results clearly indicated that Nrf2 expression is dependent on p53 status and may confer cisplatin resistance in lung cancer cells.

Nrf2 upregulates Bcl-2 and Bcl-xL transcription and in turn confers drug resistance (Niture & Jaiswal, 2012; Niture & Jaiswal, 2013). HO-1 is a downstream gene of the Nrf2/ARE signaling that promotes tumor drug resistance (Berberat et al, 2005; Srisook et al, 2005; Tan et al, 2015). The possibility that wild-type p53-mediated Nrf2 reduction could promote cisplatin sensitivity was explored by transfecting wild-type p53 into H1299 cells. Western blotting indicated that Nrf2 expression was nearly completely eliminated by wild-type p53 transfection in H1299 cells when compared with VC cells (Figure 6B upper panel). As expected, the decrease in Nrf2 expression in wild-type p53-transfected H1299 cells was gradually increased by ectopic expression of Nrf2. As expected, p53-downstream p21 expression was increased by wild-type p53 overexpression in H1299 cells, but was decreased by wild-type p53 knockdown in H1975 cells. The expression of Bcl-2, Bcl-xL, and HO-1 was concomitantly elevated by ectopic expression of Nrf2 in wild-type p53-transfected H1299 cells. The IC50 value for cisplatin in H1299 cells was markedly decreased by wild-type p53 transfection, but the IC50 value was gradually increased by co-transfection with Nrf2 expression vector in H1299 cells (19.6 μM vs. 8.6 μM vs. 13.2 μM vs. 18.4 μM; Figure 6B left lower panel).

The increase in Nrf2, Bcl-2, Bcl-xL, and HO-1 expressions were observed in p53-knockdown H1975 cells, but the increases of these three molecules were reversed by Nrf2 silencing in p53-knockdown H1975 cells (Figure 6B, right upper panel). The IC50 value of p53-knockdown H1975 cells was increased to 16.2 μM when compared with H1975 cells with non-specific shRNA transfection (NC) (5.6 μM). However, the increase in the IC50 value in p53-knockdown H1975 cells was suppressed by Nrf-2 silencing in a dose-dependent manner (Figure 6B, right lower panel). Annexin-V/PI assay further indicated that the percentages of cell apoptosis in both cell types were elevated and reduced by p53 manipulation (Figure 8). These results suggest that Nrf2-mediated Bcl-2, Bcl-xL and HO-1 is dependent on p53 status and may confer cisplatin resistance via apoptotic machinery.

Bcl-2 and Bcl-xL are more involved than HO-1 in Nrf2-mediated cisplatin resistance

We next examined which genes regulated by Nrf2 were most involved in cisplatin resistance. High Nrf2 expressing H1299 cells were selected for transfection with shHO-1, shBcl-2, or shBcl-xL, and low Nrf2 expressing H1975 cells were transfected with the Nrf2 expression vector and then co-transfected with shHO-1, shBcl-2, or shBcl-xL. The MTT assay results showed that the IC50 value of H1299 and Nrf2-overexpressing H1975 cells was markedly decreased by shHO-1, shBcl-2, or shBcl-xL, when compared with H1299 NC cells and Nrf2-overexpressing H1975 cells (Figure 9). Interestingly, the IC50 value was lower for both cell types transfected with shBcl-2 or shBcl-xL than for both cell types transfected with shHO-1 (Figure 9). These results clearly indicated that Bcl-2 and Bcl-xL are more involved than HO-1 in Nrf2-mediated cisplatin resistance.

Nrf2 mRNA levels are associated with p53 status and related to tumor responses to cisplatin-based chemotherapy in NSCLC patients

We examined whether Nrf2 mRNA expression levels could be associated with p53 status in NSCLC patients. In total, 114 tumors from surgically resected NSCLC patients, who were determined not to have keap1 and Nrf2 mutation (n=109, Table 3), were evaluated for Nrf2 mRNA expression levels using real time RT-PCR. The median value of Nrf2 mRNA expression levels in lung tumors was used as a cutoff point to divide patients into high-Nrf2 and low-Nrf2 subgroups and the categories were further confirmed by a box plot analysis (Figure 10). The p53 mutation data were obtained from our previous reports (Chiou et al, 2014; Wu et al, 2008). Nrf2 mRNA expression was not associated with clinico-pathological parameters, including age, gender, smoking status, tumor histology, and stage. Interestingly, high-Nrf2 mRNA tumors were more commonly observed in p53-mutant patients than in p53-wild-type patients (70.8% vs. 43.5%, P =0.018; Table 4). High Bcl-2 and high Bcl-xL mRNA expression were more prevalently occurred in high-Nrf2 mRNA tumors than in low-Nrf2 mRNA tumors (59.3% vs. 40%, P = 0.044 for Bcl-2; 61.1% vs. 38.2%, P = 0.017; Table 4).

We next examined the possibility that Nrf2 mRNA expression levels could be associated with the tumor response to cisplatin-based chemotherapy. In total, 60 of the 109 patients were available for this retrospective

study, and data indicated that an unfavorable response to cisplatin-based chemotherapy was more likely in patients with high-Nrf2 mRNA tumors than with low-Nrf2 mRNA tumors (71.9% vs. 21.4%, P = 0.001; Table 5). Similar findings in an unfavorable response to cisplatin-based chemotherapy were more commonly observed in high-Bcl-2 or high-Bcl-xL mRNA tumors than their counterparts (62.5% vs. 32.1% for Bcl-2; 66.7% vs. 33.3%, P = 0.01; Table 5). We further showed that an unfavorable response to cisplatin-based chemotherapy was more common in p53-mutant patients who harbored high-Nrf2 mRNA tumors than low-Nrf2 tumors (70% vs. 15.8%, P = 0.004; Table 5). These results suggested that high-Nrf2 mRNA patients whose tumors harbored p53 mutations may more frequently show an unfavorable response to cisplatin-based chemotherapy when compared with patients whose tumors harbored wild-type p53. Bcl-2 and Bcl-xL expression may be partially contributive to Nrf2-mediated unfavorable response to cisplatin-based chemotherapy in NSCLC patients.

Nrf2 mRNA expression levels were associated with overall survival (OS) and relapse free survival (RFS) in NSCLC patients

We next examined the possibility that Nrf2 mRNA expression levels could be associated with OS and RFS in NSCLC patients. Cox regression analysis using all studied population (n = 109) indicated that high-Nrf2 mRNA patients exhibited worse OS and RFS than low-Nrf2 mRNA patients (hazard ratio, HR, 2.014, 95% CI, 1.03-3.87, P = 0.013 for OS; HR, 2.047, 95% CI, 1.17-4.069, P = 0.022 for RFS; Table 6). The five-year survival rate and median survival month for OS and RFS were lower and shorter in high-Nrf2 mRNA patients than in low-Nrf2 mRNA patients (OS: 12.3% vs. 36.8% for five-year survival rate, 22.3 months vs. 45.3 months; RFS: 3.9% vs. 14.8% for five-year survival rate, 13.4 months vs. 22.3 months). A prognostic significance of Nrf2 mRNA expression levels on OS and RFS was still observed in 60 patients who have received cisplatin-based chemotherapy (HR, 2.203, 95% CI, 1.11-4.36, P = 0.023 for OS; HR, 1.992, 95% CI, 1.10-3.93, P = 0.047; Table 6). However, a prognostic significance of p53 status on OS and RFS was not revealed in all studied cases or in the 60 patients who had received cisplatin-based chemotherapy. We also found worse RFS in p53-mutant patients who harbored high-Nrf2 tumors rather than low-Nrf2 mRNA tumors (HR, 2.269, 95% CI, 1.02-5.07, P = 0.046; Table 6), but a prognostic value for OS was not observed in the high-Nrf2 patients. The chemotherapeutic regimens for these sixty patients are listed in Table 7. These patients received cisplatin alone (8.3%) and/or combined with other chemotherapeutic agents including gemcitabine (73.3%), vp16 (8.3%), taxol (8.3%), and mitomycin C (1.7%). These results suggest that high Nrf2 mRNA expression levels may be useful for prediction of poorer OS and RFS in NSCLC patients. A prognostic significance of Nrf2 mRNA levels on OS and RFS was also observed in patients who had received cisplatin-based chemotherapy.

Discussion

In this study, nickel levels in tumor-adjacent normal lung tissues were positively correlated with the occurrence of p53 mutation in lung tumors from lung cancer patients. Moreover, the host cell reactivation assay revealed that nickel may inhibit DNA repair activity in lung cancer cells, supporting an association between the occurrence of p53 mutations in lung cancer and nickel-induced decreases in DNA repair activity.

The positive association between nickel levels and risk of p53 mutation was shown in both ADC and SCC patients (Table 2). This observation is consistent with a recent report showing that the incidence of squamous cell carcinoma and adenocarcinoma of the lung was positively correlated with soil nickel levels in Central Taiwan (Huang et al., 2013). Squamous cell carcinoma has a stronger correlation with cigarette smoking than does lung adenocarcinoma. The hotspot p53 mutations are predominately caused by the cigarette carcinogen benzo[a]pyrene 7,8-diol-epoxide (BPDE), and the mutation pattern is a G-to-T transversion (Denissenko et al., 1996). However, there was no p53 hotspot mutation in this study population (Supporting Information Fig. S2). We therefore proposed that environmental nickel exposure might partially contribute to p53 mutations in Taiwanese lung cancer patients, particularly in female non-smokers.

Although the mechanism of nickel-induced carcinogenesis is unknown (Denkhaus and Salnikow, 2002; Kasprzak et al., 2003; Arita and Costa, 2009), several possibilities have been proposed for the role of nickel in lung cancer, including nickel-induced reductions in nucleotide excision repair that enhances mutagenesis (Hartwig et al., 1994; Hu et al., 2004; Mehta et al., 2008). Nickel sulfide has been shown to induce promoter hypermethylation of the DNA repair gene O6-methylguanine DNA methyltransferase (MGMT) via alterations in histone H3 modification (Ji et al., 2008). An early report used a forward mutation assay and a sensitive reversion assay to show that nickel (II) can produce tandem double CC-to-TT mutations consistent with exposure to reactive oxygen species (ROS) (Tkeshelashvili et al., 1993). A reduction in mutation frequencies by the addition of oxygen radical scavengers also supports the hypothesis that ROS are involved in nickel (II)-mediated DNA damage and mutagenesis (Kawanishi et al., 2002). In addition, nickel (II)-induced mutagenesis can be enhanced by hydrogen peroxide (Tkeshelashvili et al., 1993). More recently, cell proliferation rate and distribution of G2/M phase cells in Beas-2B normal pulmonary epithelial cells and A549 lung cancer cells were shown to be markedly increased by nickel chloride via up-regulation of cyclin D1, cyclin E, and cyclin B1 expression (Ding et al., 2009). These studies suggest that nickel-induced carcinogenesis might be partially mediated through gene expression changes due to epigenetic and genetic defects.

Oxidative DNA damage plays a crucial role in mutation-driven human carcinogenesis. Nickel compounds, such as Ni3S2, have been shown to directly induce 8-oxo-dG formation in HeLa cervical cancer cells (Kawanishi et al., 2002). In rats, intratracheal instillation of nickel compounds, such as Ni3S2, NiO, and

NiSO4, significantly increased the 8-oxo-dG content of the lung by indirect oxidative DNA damage due to inflammation (Kawanishi et al., 2002). In this study, hydrogen peroxide-induced 8-oxo-dG production was elevated by nickel chloride in lung cancer cells (Fig. 2D). This was consistent with our findings in tumor-adjacent normal lung tissues demonstrating that patients with high nickel levels exhibited higher levels of 8-oxo-dG than patients with low nickel levels (Fig. 3A). In addition, the association between nickel levels and p53 mutations was strongest in female non-smokers but was absent in male non-smokers (Table 2). These results support the hypothesis that nickel-induced oxidative DNA damage contributes to p53 mutation-driven lung carcinogenesis.

Our findings suggest that nickel accumulation in the lungs may contribute to p53 mutation-driven lung carcinogenesis, especially in female lifetime non-smokers. We speculate one reason for this bias is that there are fewer risk factors involved in lung cancer development in female non-smokers than in male non-smokers. This might be due to the fact that Taiwanese female non-smokers are more frequently working in the home, whereas male non-smokers are more frequently employed as office workers or workers and are thus more likely to be exposed to pollutants in the workplace and from other environmental sources. We thus speculate that nickel exposure might play a more important role in lung cancer development in female non-smokers than in male non-smokers. However, this hypothesis should be verified in a larger study population of non-smokers. This finding may suggest a possible etiological factor of environmental nickel exposure for lung cancer development in lifetime non-smoking Taiwanese women.

We further provided evidence that suppression of Nrf2 transcription by wild-type p53, occurring via decreased Sp1 binding to the Nrf2 promoter, may confer cisplatin sensitivity, a favorable chemo-response, thereby leading to favorable outcomes in lung cancer patients. Moreover, a decrease in Nrf2 mRNA expression by wild-type p53 corresponded with its protein expression. These findings suggest that Nrf2 expression is predominately regulated by wild-type p53 at the transcription level. Conversely, Nrf2 mRNA and its protein expression levels in H1299 cells were markedly elevated by different mutant p53 expression vector transfections when compared with VC cells (Figure 1C). A previous report has indicated that Nrf2 expression is driven by the NF-κB signaling pathway in acute myeloid leukemia (Rushworth et al, 2012). Mutation of p53 gene prolongs NF-κB activation and promotes chronic inflammation and inflammation-associated colorectal cancer (Cooks et al, 2013). Therefore, mutant p53 not only confers drug resistance via upregulation of Nrf2 expression but it also may activate the NF-κB signaling pathway for additional enhancement of Nrf2 expression (Figure 1C).

The prevalence of “low” or “high” Nrf2 expression was not significantly revealed in p53-wild-type patients compared with p53-mutant patients. This conflicting may be due to wild-type p53 dysfunction by several mechanisms. For example, Nrf2 may promote MDM2 expression to increase p53 degradation. An early report indicated that MDM2 mRNA expression may be used to predict p53 transcriptional function and patients’ prognosis in NSCLC (Ko et al, 2000). We thus evaluated MDM2 mRNA expression in p53-wild-type patients

by real-time PCR in this study population and data showed that high Nrf2 mRNA expression was more commonly occurred in low-MDM2 mRNA tumors than in high-MDM2 tumors (Supplementary Table 3). Therefore, wild-type p53 dysfunction by different mechanisms may cause p53 wild-type patients with high Nrf2 mRNA tumors, and consequently resulting in the prevalence of “low” or “high” Nrf2 expression to be not significantly revealed in p53-wild-type patients..

ROS levels are tightly controlled by the Nrf2/Keap1 pathway (DeNicola et al, 2011). However, an increased in Nrf2 transcription, that were triggered by oncogenes such as mutations in K-ras^{G12D} and BrafV619V and overexpression of Myc^{ERT2}, promotes ROS detoxification and tumorigenesis (DeNicola et al, 2011). K-ras increases Nrf2 gene transcription through a TPA response element located on the Nrf2 promoter (Tao et al, 2014). In a mouse model of mutant K-ras^{G12D}-induced lung cancer, suppressing the Nrf2 pathway with the chemical inhibitor Brusatol enhanced the antitumor efficacy of cisplatin (Tao et al, 2014). These results strongly suggest that oncogenic K-ras promotes tumor malignancy as well as conferring cisplatin resistance in lung cancer through up-regulation of Nrf2 transcription. However, K-ras mutations were not detected in this study population (n = 114, data not shown). In the present study, mutant p53 upregulated Nrf2 transcription by blocking Sp1 binding to the Nrf2 promoter, thereby conferring cisplatin resistance. Consistent findings were also observed in wild-type p53 cells subjected to p53 silencing and in p53-null cells transfected with different mutant p53 expression vectors. We therefore suggest that mutant p53 may confer cisplatin resistance in lung cancer cells via upregulating Nrf2 transcription.

In summary, we provide evidence from the cell and human tissues that nickel exposure may be associated with an increase in p53 mutation risk in Taiwanese lung cancer via decreasing DNA repair capability. In addition, upregulation of Nrf2 transcription by mutant p53 may confer cisplatin resistance, an unfavorable response to cisplatin-based chemotherapy, and poor outcomes in NSCLC patients. Therefore, we suggest that Bcl-2 antagonists might be helpful in improving cisplatin sensitivity and outcomes in p53-mutant NSCLC patients who harbor high-Nrf2 mRNA tumors. We concluded that nickel exposure might play a role in the development of lung cancer in Taiwan and may partially contribute to chemoresistance and poor outcome in NSCLC patients who had high nickel exposure.

Materials and Methods

Part I: Nickel accumulation in lung tissues is associated with increased risk of p53 mutation in lung cancer patients

Study Subjects and Specimen Collection

Between 1993 and 2003, 189 patients with primary lung cancer received surgical therapy at Taichung Veterans General Hospital in Taichung, Taiwan. The lung tumors and adjacent normal lung tissues from these patients were examined by board-certified pathologists and the tumors were staged according to the World Health Organization (WHO) classification system. Informed consent was obtained from each patient, and demographic data including age, gender, and smoking history were collected through patient interviews and hospital chart reviews.

Determination of Nickel Levels in Tumor-Adjacent Normal Lung Tissues

The technique for measuring nickel levels in lung tissues from lung cancer patients has previously been described (Kuo et al., 2006). Briefly, nickel levels were measured by graphite furnace atomic absorption spectrometry (AAS) (Perkin Elmer, Model AA600) with Zeeman background correlation. All analytical glass and plasticware were of low-metal grade and were cleaned with diluted nitric acid before use. Initially, all frozen tissues were equilibrated for 0.5 hr at room temperature and then heated for 4.5 hr at 103–105℃. Subsequently, the dry tissue samples were digested with 2 mL of 65% nitric acid and 1 mL of 30% hydrogen peroxide. After cooling, the solutions were diluted to 5 mL with deionized water containing 0.2% nitric acid and stored at 4℃ until further analysis. For the analysis of nickel levels in lung tissues, the accuracy of the instrumental methods and the analytical procedure was checked against reference solutions (standard reference material (SRM) no. 1566; dogfish reference muscle-2 (DORM-2); and dogfish liver tissue-2 (DOLT-2)). The correlation coefficient for each standard curve was above 0.998. In addition, the mean recovery of nickel ranged from 84% to 117%, and the coefficient of variation (CV) for reproducibility was less than 10% for each standard curve. AAS measurements less than threefold of the method detection limit (MDL) (0.22 μg/L) were considered to be non-detection. The half value of MDL was used as the reference concentration for normalizing nickel level measurement. The nickel levels in lung tissue were expressed as micrograms per gram dry weight of lung tissue.

p53 mutation analysis by direct sequencing

For the p53 mutation analysis, target sequences were amplified by polymerase chain reaction (PCR) using the following primer pairs: E5S (5’-TGC CCT GAC TTT CAA CTC TG-3’) and E5AS (5’-GCT GCT CAC CAT CGC TAT C-3’) for p53 exon 5; E6S (5’-CTG ATT CCT CAC TGA TTG CT-3’) and E6AS (5’-AGT TGC AAA CCA GAC CTC-3’) for p53 exon 6; E7S (5’-CCT GTG TTA TCT CCT AGG TTG-3’) and E7AS (5´-GCA CAG CAG GCC AGG TGC A-3’) for p53 exon 7; and E8S (5’-GAC CTG ATT TCC TTA CTG C-3’) and E8AS (5’-TCT CCT CCA CCG CTT CTT GT-3’) for p53 exon 8. The PCR products were sequenced by an automated sequencing system (3100 Avant Genetic Analyzer, Applied Biosystems, Hitachi, Japan). All p53

mutations were confirmed by direct sequencing of both strands (Wu et al., 2008).

Analysis of 8-oxo-deoxyguanosine in tumor-adjacent normal lung tissues

Normal tissues were available from only 78 of the 189 patients, which were subject to 8-oxo-deoxyguanosine (8-oxo-dG) analysis using a liquid chromatography-mass spectrometry/mass spectrometry (LC-MS/MS) coupled with on-line solid-phase extraction (SPE) as described previously (Chao et al., 2008). Briefly, after automatic sample cleanup, the LC-MS/MS analysis was performed using a PE Series 200 HPLC system interfaced with a PE Sciex API 3000 triple quadrupole mass spectrometer with electrospray ion source (ESI). Detection was performed in the positive ion multiple reaction monitoring (MRM) mode for simultaneous quantitation of 8-oxo-dG and dG, and the transitions of the precursors to the product ions were as follows: 8-oxo-dG (m/z 284–168), 15N5−8-oxo-dG (m/z 289–173), dG (m/z 268–152), and 15N5-dG (m/z 273–157). With the use of isotopic internal standards and on-line SPE, this method exhibited a low limit of detection (LOD) of 1.8 fmol for 8-oxo-dG, which corresponded to 0.13 adducts/106 dG when using 20 µg of DNA per analysis.

Cell culture and cytotoxicity assay

A549 and H1975 lung adenocarcinoma cells were cultured in 96-well plates supplemented with DMEM or RPMI 1640 (HyClone, Logan, UT) containing 10% heat-inactivated fetal bovine serum, 100 units/mL penicillin, and 100 units/mL streptomycin. The cytotoxic effect of nickel chloride was assessed by the MTT assay after treating cells with varying concentrations of nickel chloride for 24 hr (Wu et al., 2010). The cell survival curves were used to calculate the concentration of nickel chloride that resulted in 65% cell survival in both cell lines. This concentration was then used for the host cell reactivation assay.

Host cell reactivation assay

A host cell reactivation assay was used to assess DNA repair capability based on a previously described protocol with modifications (Hu et al., 2004; Chiang and Tsou, 2009). Briefly, a standard protocol for TurboFect (Fermentas, Glen Burnie, MD) was used to co-transfect a hydrogen peroxide (20 mM)-treated pGL2-luciferase reporter plasmid (3 µg) and a pSV-β-galactosidase plasmid (3 µg) (for normalizing the transfection efficiency) into cells that were cultured in a 35-mm dish at a density of 3 × 105 cells/dish with or without nickel chloride pre-treatment. After transfection, the cells were incubated in fresh medium containing nickel chloride at the same concentrations as before for another 24 hr to allow time for repairing the hydrogen peroxide-induced plasmid DNA damage. Luciferase activity and β-galactosidase activity were determined using the Luciferase Assay System and the β-galactosidase Enzyme Assay System (Promega, Madison, WI), respectively. The luciferase activity was normalized to the β-galactosidase activity. An increase in luciferase activity is detected when hydrogen peroxide-modified pGL2 is repaired. The relative luciferase activity was used to represent the percentage of hydrogen peroxide-modified pGL2 that was recovered.

Part II: Mutant p53 confers chemoresistance in non-small cell lung cancer by upregulating Nrf2

Cell lines and culture conditions

H1299, H1355, H1650, H1975 and H358 cells were obtained from ATCC (Manassas, VA, USA) and were cultured as previously described (http://www.atcc.org). CL1-5 and CL3 cells were kindly provided by Dr. Pan-Chyr Yang (Department of Internal Medicine, National Taiwan University Hospital, Taiwan). TL4 cells were kindly provided by Dr. Ya-Wen Cheng (Graduate Institute of Cancer Biology and Drug Discovery, Taipei Medical University, Taipei, Taiwan). H1299 cells were grown in Dulbecco's modified Eagle's medium (Hyclone, Waltham, MA, USA) supplemented with 10% fetal bovine serum (Hyclone, Waltham, MA, USA). CL1-5, CL3, H1355, H1650, H1975, H358 and TL4 cells were grown in RPMI-1640 medium (Hyclone, Waltham, MA, USA) with 10% fetal bovine serum. All cell lines were grown at 37℃ in a 5% carbon dioxide atmosphere. These cells were cultured according to the suppliers' instructions and were stored used at passages 5 to 20. Once resuscitated, cell lines were routinely authenticated (once every 6 months; cells were last tested in December 2012) through cell morphology monitoring, growth curve analysis, species verification by isoenzymology and karyotyping, identity verification using short tandem repeat profiling analysis, and contamination checks.

Plasmid constructs and transfection assays

Nrf2 cDNA was cloned into pcDNA3.1 Zeo(+) (Invitrogen, Carlsbad, CA, USA) by PCR amplification with newly created XhoI and BamHI sites attached on the Nrf2 5'ends of forward and reverse primers, using H1299 cDNA as template. The Nrf2 promoter reporter plasmid was constructed by inserting 1036, 740, and 229 bps KpnI/HidIII fragments into a KpnI/HidIII-treated pGL3 vector (Promega, Madison, WI, USA). The primer sequences are listed in Table 8. The wild-type and mutant p53 constructs were kindly provided by Dr. Jiunn-Liang Ko (Institute of Medicine, Chung Shan Medical University, Taichung, Taiwan). The shRNA was purchased from National RNAi Core Facility, Academia Sinica, Taipei, Taiwan. Different concentrations of plasmids were transiently transfected into lung cancer cells (1 × 106 cells) using the Turbofect reagent (Fermentas, Waltham, MA, USA). After 48 h, cells were harvested and whole-cell extracts were used for subsequent experiments.

Real-time PCR analysis of mRNA expression levels

DNase I-treated total RNA (10 ng) was subjected to mRNA RT-PCR analysis with the Reverse Transcription Kit (Applied Biosystems, Foster City, CA), mRNA Assays (Applied Biosystems, Foster City, CA, USA), and a Real-Time Thermocycler 7500 (Applied Biosystems, Foster City, CA, USA). Glyceraldehyde 3-phosphate dehydrogenase (GAPDH) was used as the mRNA reference housekeeping gene. The primers used for real-time PCR analysis of mRNA expression are presented in Table 8.

Luciferase reporter assay

The luciferase reporter assay was conducted by transfecting appropriate numbers of cells with sufficient reporter plasmids, as determined from earlier studies (Wu et al, 2011).

ChIP assay

ChIP analysis was performed as described previously (Wu et al, 2011). The primer sequences are presented in Table 8.

3-(4,5-cimethylthiazol-2-yl)-2,5-diphenyl tetrazolium bromide (MTT) cytotoxicity assay

The cell lines were cultured in 96-well flat-bottomed microtiter plates supplemented with RPMI 1640 and DMEM containing 10% heat-inactivated fetal bovine serum, 100 units/mL penicillin, and 100 units/mL streptomycin in a humidified atmosphere containing 95% air and 5% CO2 at 37℃ in a humidified incubator. Before cisplatin treatment(0, 2, 4, 8, 16, 32 μM), the cells cultured in the exponential growth phase were pretreated with shRNAs, p53 and Nrf2 overexpression plasmid for 24 h. After 48 h incubation, the in vitro cytotoxic effects of these treatments were determined by MTT assay (at 570 nm).

Statistical Analysis

The patients were divided into high-nickel or low-nickel subgroups based on the median nickel level in the lung tissues (0.47 μg/g dry weight). Comparisons between the two subgroups with respect to age, gender, smoking status, tumor histology, tumor stage, tumor size (T), and nodal micrometastasis (N) were made using the x2 test for discrete variables. Subsequently, logistic regression analysis was used to adjust for significant covariates that were identified in the univariate analysis to evaluate potential differences in nickel levels according to p53 status. Continuous variables in the study are presented as the mean ± standard deviation (SD). Because of the positively skewed distribution of the nickel levels in tissues (skewness = 5.39 for nickel levels), non-parametric testing was applied to test the differences in nickel levels based on p53 status. There were 78 lung cancer tissues available for the analysis of 8-oxo-dG by LC-MS/MS. Students' t-test was used to analyze the differences in 8-oxo-dG production and in relative luciferase activity between the high- and low-nickel subgroups (skewness = 1.73 for 8-oxo-dG). All P values were calculated using two-tailed statistical tests and a value of <0.05 was considered statistically significant. SAS 9.1 for Windows (SAS, Cary, NC) was used for the analyses.

References

Arita A, Costa M. 2009. Epigenetics in metal carcinogenesis: Nickel, arsenic, chromium and cadmium. Metallomics 1:222-228.

Asher G, Lotem J, Kama R, Sachs L, Shaul Y 2002. NQO1 stabilizes p53 through a distinct pathway. Proceedings of the National Academy of Sciences of the United States of America 99: 3099-3104

Berberat PO, Dambrauskas Z, Gulbinas A, Giese T, Giese N, Kunzli B, Autschbach F, Meuer S, Buchler MW, Friess H 2005. Inhibition of heme oxygenase-1 increases responsiveness of pancreatic cancer cells to anticancer treatment. Clinical cancer research : an official journal of the American Association for Cancer Research 11: 3790-3798

Chang FH, Wang HJ, Wang SL, Wang YC, Hsieh DP, Chang LW, Ko YC. 2006. Survey of urinary nickel in residents of areas with a high density of electroplating factories. Chemosphere 65:1723-1730.

Chao MR, Yen CC, Hu CW. 2008. Prevention of artifactual oxidation in determination of cellular 8-oxo-7,8-dihydro-2'-deoxyguanosine by isotope-dilution LC-MS/MS with automated solid-phase extraction. Free Radic Biol Med 44:464-473.

Chen CW, Kao CM, Chen CF, Dong CD. 2007. Distribution and accumulation of heavy metals in the sediments of Kaohsiung Harbor, Taiwan. Chemosphere 66:1431-1440.

Chen W, Sun Z, Wang XJ, Jiang T, Huang Z, Fang D, Zhang DD 2009 Direct interaction between Nrf2 and p21(Cip1/WAF1) upregulates the Nrf2-mediated antioxidant response. Molecular cell 34: 663-673

Chiang HC, Tsou TC. 2009. Arsenite enhances the benzo(a)pyrene diol epoxide (BPDE)-induced mutagenesis with no marked effect on repair of BPDE-DNA adducts in human lung cells. Toxicol In Vitro 23:897-905.

De Matteis S, Consonni D, Lubin JH, Tucker M, Peters S, Vermeulen R, Kromhout H, Bertazzi PA, Caporaso NE, Pesatori AC, Wacholder S, Landi MT. 2012. Impact of occupational carcinogens on lung cancer risk in a general population. Int J Epidemiol 41:711-721.

Chiou YH, Wong RH, Chao MR, Chen CY, Liou SH, Lee H 2014. Nickel accumulation in lung tissues is associated with increased risk of p53 mutation in lung cancer patients. Environmental and molecular mutagenesis 55: 624-632

Cooks T, Pateras IS, Tarcic O, Solomon H, Schetter AJ, Wilder S, Lozano G, Pikarsky E, Forshew T, Rosenfeld N, Harpaz N, Itzkowitz S, Harris CC, Rotter V, Gorgoulis VG, Oren M 2013. Mutant p53 prolongs NF-kappaB activation and promotes chronic inflammation and inflammation-associated colorectal cancer. Cancer cell 23: 634-646

DeNicola GM, Karreth FA, Humpton TJ, Gopinathan A, Wei C, Frese K, Mangal D, Yu KH, Yeo CJ, Calhoun ES, Scrimieri F, Winter JM, Hruban RH, Iacobuzio-Donahue C, Kern SE, Blair IA, Tuveson DA 2011. Oncogene-induced Nrf2 transcription promotes ROS detoxification and tumorigenesis. Nature 475: 106-109

Denissenko MF, Pao A, Tang M, Pfeifer GP. 1996. Preferential formation of benzo(a)pyrene adducts at lung cancer mutational hotspots in P53. Science 274:430-432.

Denkhaus E, Salnikow K. 2002. Nickel essentiality, toxicity, and carcinogenicity. Crit Rev Oncol Hematol

42:35–56.

Ding J, He G, Gong W, Wen W, Sun W, Ning B, Huang S, Wu K, Huang C, Wu M, Xie W, Wang H. 2009. Effects of nickel on cyclin expression, cell cycle progression and cell proliferation in human pulmonary cells. Cancer Epidemiol Biomarkers Prev 18:1720-1729.

Faraonio R, Vergara P, Di Marzo D, Pierantoni MG, Napolitano M, Russo T, Cimino F 2006, p53 suppresses the Nrf2-dependent transcription of antioxidant response genes. The Journal of biological chemistry 281: 39776-39784

Gorrini C, Harris IS, Mak TW 2013, Modulation of oxidative stress as an anticancer strategy. Nature reviews Drug discovery 12: 931-947

Grimsrud TK, Berge SR, Haldorsen T, Andersen A. 2002. Exposure to different forms of nickel and risk of lung cancer. Am J Epidemiol 156:1123-1132.

Hartwig A, Mullenders LH, Schlepegrell R, Kasten U, Beyersmann D. 1994. Nickel(II) interferes with the incision step in nucleotide excision repair in mammalian cells. Cancer Res 54:4045-4051.

Harty LC, Guinee DG Jr, Travis WD, Bennett WP, Jett J, Colby TV, Tazelaar H, Trastek V, Pairolero P, Liotta LA, Harris CC, Caporaso NE. 1996. p53 mutations and occupational exposures in a surgical series of lung cancers. Cancer Epidemiol Biomarkers Prev 5:997–1003.

Hedouin L, Pringault O, Metian M, Bustamante P, Warnau M. 2007. Nickel bioaccumulation in bivalves from the New Caledonia lagoon: Seawater and food exposure. Chemosphere 66:1449–1457.

Homma S, Ishii Y, Morishima Y, Yamadori T, Matsuno Y, Haraguchi N, Kikuchi N, Satoh H, Sakamoto T, Hizawa N, Itoh K, Yamamoto M 2009, Nrf2 enhances cell proliferation and resistance to anticancer drugs in human lung cancer. Clinical cancer research : an official journal of the American Association for Cancer Research 15: 3423-3432

Hu W, Feng Z, Tang MS. 2004. Nickel (II) enhances benzo(a)pyrene diol epoxide-induced mutagenesis through inhibition of nucleotide excision repair in human cells: A possible mechanism for nickel (II)-induced carcinogenesis. Carcinogenesis 25:455-462.

Huang HH, Huang JY, Lung CC, Wu CL, Ho CC, Sun YH, Ko PC, Su SY, Chen SC, Liaw YP. 2013. Cell-type specificity of lung cancer associated with low-dose soil heavy metal contamination in Taiwan: An ecological study. BMC Public Health 13:330.

Itoh T, Terazawa R, Kojima K, Nakane K, Deguchi T, Ando M, Tsukamasa Y, Ito M, Nozawa Y 2011, Cisplatin induces production of reactive oxygen species via NADPH oxidase activation in human prostate cancer cells. Free radical research 45: 1033-1039

Ji L, Li H, Gao P, Shang G, Zhang DD, Zhang N, Jiang T 2013, Nrf2 pathway regulates multidrug-resistance-associated protein 1 in small cell lung cancer. PloS one 8: e63404

Ji W, Yang L, Yu L, Yuan J, Hu D, Zhang W, Yang J, Pang Y, Li W, Lu J, Fu J, Chen J, Lin Z, Chen W, Zhuang Z. 2008. Epigenetic silencing of O6-methylguanine DNA methyltransferase gene in NiS-transformed cells. Carcinogenesis 29:1267-1275.

Kasprzak KS, Sunderman FW Jr, Salnikow K. 2003. Nickel carcinogenesis. Mutat Res 533:67-97.

Jin J, Sklar GE, Min Sen Oh V, Chuen Li S 2008, Factors affecting therapeutic compliance: A review from the patient's perspective. Therapeutics and clinical risk management 4: 269-286

Kansanen E, Kuosmanen SM, Leinonen H, Levonen AL 2013, The Keap1-Nrf2 pathway: Mechanisms of activation and dysregulation in cancer. Redox biology 1: 45-49

Kawanishi S, Oikawa S, Inoue S, Nishino K. 2002. Distinct mechanisms of oxidative DNA damage induced by carcinogenic nickel subsulfide and nickel oxides. Environ Health Perspect 110 Suppl 5:789-791.

Kuo CY, Wong RH, Lin JY, Lai JC, Lee H. 2006. Accumulation of chromium and nickel metals in lung tumors from lung cancer patients in Taiwan. J Toxicol Environ Health A 69:1337-1344.

Lai HY, Hseu ZY, Chen TC, Chen BC, Guo HY, Chen ZS. 2010. Health risk-based assessment and management of heavy metals-contaminated soil sites in Taiwan. Int J Environ Res Public Health 7:3595-3614.

Lavin MF, Gueven N. 2006. The complexity of p53 stabilization and activation. Cell Death Differ 13:941-950.

Levine AJ, Oren M. 2009. The first 30 years of p53: Growing ever more complex. Nat Rev Cancer 9:749-758.

Luo J, Hendryx M, Ducatman A. 2011. Association between six environmental chemicals and lung cancer incidence in the United States. J Environ Public Health 2011:463701.

Marullo R, Werner E, Degtyareva N, Moore B, Altavilla G, Ramalingam SS, Doetsch PW 2013, Cisplatin induces a mitochondrial-ROS response that contributes to cytotoxicity depending on mitochondrial redox status and bioenergetic functions. PloS one 8: e81162

Mehta M, Chen LC, Gordon T, Rom W, Tang MS. 2008. Particulate matter inhibits DNA repair and enhances mutagenesis. Mutat Res 657:116-121.

Ministry of Health and Welfare, Taiwan, R.O.C. 2010. Adult smoking behavior survey, 2010.

Miura S, Shibazaki M, Kasai S, Yasuhira S, Watanabe A, Inoue T, Kageshita Y, Tsunoda K, Takahashi K, Akasaka T, Masuda T, Maesawa C 2014, A somatic mutation of the KEAP1 gene in malignant melanoma is involved in aberrant NRF2 activation and an increase in intrinsic drug resistance. The Journal of investigative dermatology 134: 553-556

Molina JR, Yang P, Cassivi SD, Schild SE, Adjei AA 2008, Non-small cell lung cancer: epidemiology, risk factors, treatment, and survivorship. Mayo Clinic proceedings 83: 584-594

Navarro Silvera SA, Rohan TE. 2007. Trace elements and cancer risk: A review of the epidemiologic evidence. Cancer Causes Control 18:7-27.

Nguyen T, Nioi P, Pickett CB 2009, The Nrf2-antioxidant response element signaling pathway and its activation by oxidative stress. The Journal of biological chemistry 284: 13291-13295

Niture SK, Jaiswal AK 2012, Nrf2 protein up-regulates antiapoptotic protein Bcl-2 and prevents cellular apoptosis. The Journal of biological chemistry 287: 9873-9886

Niture SK, Jaiswal AK 2013, Nrf2-induced antiapoptotic Bcl-xL protein enhances cell survival and drug resistance. Free radical biology & medicine 57: 119-131

Oller AR. 2002. Respiratory carcinogenicity assessment of soluble nickel compounds. Environ Health Perspect 110 Suppl 5:841-844.

Ptashynski MD, Pedlar RM, Evans RE, Baron CL, Klaverkamp JF. 2002. Toxicology of dietary nickel in lake whitefish (Coregonus clupeaformis). Aquat Toxicol 58:229-247.

Padmanabhan B, Tong KI, Ohta T, Nakamura Y, Scharlock M, Ohtsuji M, Kang MI, Kobayashi A, Yokoyama S, Yamamoto M 2006, Structural basis for defects of Keap1 activity provoked by its point mutations in lung cancer. Molecular cell 21: 689-700

Siegel R, Naishadham D, Jemal A. 2012. Cancer statistics, 2012. CA Cancer J Clin 62:10–29.

Rotblat B, Melino G, Knight RA 2012, NRF2 and p53: Januses in cancer? Oncotarget 3: 1272-1283

Rushworth SA, Zaitseva L, Murray MY, Shah NM, Bowles KM, MacEwan DJ 2012, The high Nrf2 expression in human acute myeloid leukemia is driven by NF-kappaB and underlies its chemo-resistance. Blood 120: 5188-5198

Santana-Davila R, Szabo A, Arce-Lara C, Williams CD, Kelley MJ, Whittle J 2014, Cisplatin versus carboplatin-based regimens for the treatment of patients with metastatic lung cancer. an analysis of Veterans Health Administration data. Journal of thoracic oncology : official publication of the International Association for the Study of Lung Cancer 9: 702-709

Shibata T, Kokubu A, Saito S, Narisawa-Saito M, Sasaki H, Aoyagi K, Yoshimatsu Y, Tachimori Y, Kushima R, Kiyono T, Yamamoto M 2011, NRF2 mutation confers malignant potential and resistance to chemoradiation therapy in advanced esophageal squamous cancer. Neoplasia 13: 864-873

Singh A, Misra V, Thimmulappa RK, Lee H, Ames S, Hoque MO, Herman JG, Baylin SB, Sidransky D, Gabrielson E, Brock MV, Biswal S 2006, Dysfunctional KEAP1-NRF2 interaction in non-small-cell lung cancer. PLoS medicine 3: e420

Smith-Sivertsen T, Tchachtchine V, Lund E, Bykov V, Thomassen Y, Norseth T. 1998. Urinary nickel excretion in populations living in the proximity of two russian nickel refineries: A Norwegian-Russian population-based study. Environ Health Perspect 106:503-511.

Srisook K, Kim C, Cha YN 2005, Molecular mechanisms involved in enhancing HO-1 expression: de-repression by heme and activation by Nrf2, the "one-two" punch. Antioxidants & redox signaling 7: 1674-1687

Su CC, Lin YY, Chang TK, Chiang CT, Chung JA, Hsu YY, Lian Ie B. 2010. Incidence of oral cancer in relation to nickel and arsenic concentrations in farm soils of patients' residential areas in Taiwan. BMC Public Health 10:67.

Tan Q, Wang H, Hu Y, Hu M, Li X, Aodeng Q, Ma Y, Wei C, Song L 2015, Src/STAT3-dependent HO-1 induction mediates chemoresistance of breast cancer cells to doxorubicin by promoting autophagy. Cancer science

Tao S, Wang S, Moghaddam SJ, Ooi A, Chapman E, Wong PK, Zhang DD 2014, Oncogenic KRAS confers chemoresistance by upregulating NRF2. Cancer research

Tiseo M, Ardizzoni A, Boni L 2014, First-Line Chemotherapy Treatment of Advanced Non-Small-Cell Lung Cancer: Does Cisplatin versus Carboplatin Make a Difference? Journal of thoracic oncology : official publication of the International Association for the Study of Lung Cancer 9: e82

Tkeshelashvili LK, Reid TM, McBride TJ, Loeb LA. 1993. Nickel induces a signature mutation for oxygen free radical damage. Cancer Res 53:4172-4174.

Villeneuve NF, Sun Z, Chen W, Zhang DD 2009, Nrf2 and p21 regulate the fine balance between life and death by controlling ROS levels. Cell cycle 8: 3255-3256

Wang XJ, Sun Z, Villeneuve NF, Zhang S, Zhao F, Li Y, Chen W, Yi X, Zheng W, Wondrak GT, Wong PK, Zhang DD 2008, Nrf2 enhances resistance of cancer cells to chemotherapeutic drugs, the dark side of Nrf2. Carcinogenesis 29: 1235-1243

Wu DW, Liu WS, Wang J, Chen CY, Cheng YW, Lee H 2011, Reduced p21(WAF1/CIP1) via alteration of p53-DDX3 pathway is associated with poor relapse-free survival in early-stage human papillomavirus-associated lung cancer. Clinical cancer research : an official journal of the American Association for Cancer Research 17: 1895-1905

Wu HH, Wu JY, Cheng YW, Chen CY, Lee MC, Goan YG, Lee H. 2010. cIAP2 upregulated by E6 oncoprotein via epidermal growth factor receptor/phosphatidylinositol 3-kinase/AKT pathway confers resistance to cisplatin in human papillomavirus 16/18-infected lung cancer. Clin Cancer Res 16:5200-5210.

Wu JY, Wang J, Lai JC, Cheng YW, Yeh KT, Wu TC, Chen CY, Lee H. 2008. Association of O6-methylguanine-DNA methyltransferase (MGMT) promoter methylation with p53 mutation occurrence in non-small cell lung cancer with different histology, gender, and smoking status. Ann Surg Oncol 15:3272-3277.

Yoo NJ, Kim HR, Kim YR, An CH, Lee SH 2012, Somatic mutations of the KEAP1 gene in common solid cancers. Histopathology 60: 943-952

You A, Nam CW, Wakabayashi N, Yamamoto M, Kensler TW, Kwak MK 2011, Transcription factor Nrf2 maintains the basal expression of Mdm2: An implication of the regulation of p53 signaling by Nrf2. Archives of biochemistry and biophysics 507: 356-364

Yuan TH, Lian Ie B, Tsai KY, Chang TK, Chiang CT, Su CC, Hwang YH. 2011. Possible association between nickel and chromium and oral cancer: A case-control study in central Taiwan. Sci Total Environ 409:1046–1052.

Akhdar H, Loyer P, Rauch C, Corlu A, Guillouzo A, Morel F 2009, Involvement of Nrf2 activation in resistance to 5-fluorouracil in human colon cancer HT-29 cells. European journal of cancer 45: 2219-2227

Zucker SN, Fink EE, Bagati A, Mannava S, Bianchi-Smiraglia A, Bogner PN, Wawrzyniak JA, Foley C, Leonova KI, Grimm MJ, Moparthy K, Ionov Y, Wang J, Liu S, Sexton S, Kandel ES, Bakin AV, Zhang Y, Kaminski N, Segal BH, Nikiforov MA 2014, Nrf2 amplifies oxidative stress via induction of Klf9. Molecular cell 53: 916-928

Tables

Table 1. Relationships of Nickel Levels With Clinico-Pathological Parameter in Lung Cancer Patients

Characteristic	Case no.	Nickel levels*		*P***
		Low (%)	High (%)	
	189	108 (57.1)	81 (42.9)	
Age				
≦66	94	52 (55.3)	42 (44.7)	0.614
＞66	95	56 (58.9)	39 (41.1)	
Gender				
Female	130	67 (51.5)	63 (48.5)	0.021
Male	59	41 (69.5)	18 (30.3)	
Smoking status				
Nonsmoking	81	37 (45.7)	44 (54.3)	0.006
Smoking	108	71 (65.7)	37 (34.3)	
Gender smoke				
Female non-smokers	59	41 (69.5)	18 (30.5)	0.367
Male smokers	81	37 (45.7)	44 (54.3)	0.089
Male non-smokers	49	30 (61.2)	19 (38.8)	
Tumor type				
SCC	100	54 (54.0)	46 (46.0)	0.355
ADC	89	54 (60.7)	35 (39.3)	
Stage				
I and II	101	56 (55.4)	45 (44.6)	0.614
II	88	52 (59.1)	36 (40.9)	
Tumor size (T)				
T1 and T2	141	79 (56.0)	62 (44.0)	0.596
T3 and T4	48	29 (60.4)	19 (39.6)	
Nodal micro-metastasis (N)				
N0	87	50 (57.5)	37 (42.5)	0.933
N1, N2 and N3	102	58 (56.9)	44 (43.1)	

*The average level of nickel in lung cancer patients was 3.52 ± 10.23 μg/g dry weight. The patients were divided into high-nickel or low-nickel subgroups based on the median nickel level in the lung tissues (0.47 μg/g dry weight); the range for low-nickel subgroup is 0.2–0.47 μg/g dry weight and high-nickel subgroup is 0.49–85.11 μg/g dry weight.

**The P value was calculated by x2 test. ADC: adenocarcinoma; SCC: squamous cell carcinoma.

Table 2. Association of Nickel Levels With p53 Mutation Risk in Lung Cancer Patients With Different Tumor Histology, Smoking Status and Genders

Variables	Case no	p53 status				OR	95CI	p^a
		Wild-type (%)		Mutation (%)				
Nickel levels								
All patients								
High	81	35	(43.2)	46	(56.8)	3.25[b]	1.72–6.11	<0.001
Low	108	78	(72.1)	30	(27.8)	1.00	reference	
ADC								
High	35	20	(57.1)	15	(42.9)	3.36[c]	1.25–9.06	0.017
Low	54	43	(79.6)	11	(20.4)	1.00	reference	
SCC								
High	46	15	(32.6)	31	(67.4)	3.53[c]	1.51–8.27	0.004
Low	54	35	(64.8)	19	(35.2)	1.00	reference	
Non-smokers								
High	37	17	(45.9)	20	(54.1)	4.31[d]	1.82–10.25	0.001
Low	71	56	(78.9)	15	(21.1)	1.00	reference	
Smokers								
High	44	18	(40.9)	26	(59.1)	2.59[d]	1.00–6.69	0.050
Low	37	22	(59.5)	15	(40.5)	1.00	reference	
Female non-smokers								
High	18	7	(38.9)	11	(61.1)	9.35[e]	2.56–34.09	0.001
Low	41	35	(85.4)	6	(14.6)	1.00	reference	
Male non-smokers								
High	19	10	(52.6)	9	(47.4)	2.10[e]	0.63–7.03	0.228
Low	30	21	(70.0)	9	(30.0)	1.00	reference	

[a]The P value was calculated by the multivariate logistic regression model.

[b]OR was adjusted for gender, smoking status, and tumor histology.

[c]OR was adjusted for gender and smoking status.

[d]OR was adjusted for gender and tumor histology.

[e]OR was adjusted for tumor histology.

Table 3. The mutation rates of Nrf2 and Keap1 in NSCLC patients.

	Case number	Mutation number	Mutation rate
Nrf2	114	3	2.6%
Keap1	114	2	1.8%

Table 3. The mutation rates of Nrf2 and Keap1 in NSCLC patients.

	Case number	Mutation number	Mutation rate
Nrf2	114	3	2.6%
Keap1	114	2	1.8%

Table 4. Relationships between Nrf2 mRNA expression and clinical-pathological parameters NSCLC patients.

Characteristic	Case no.	Nrf2 mRNA		*P*
		Low (%)	High (%)	
	109	55 (50.5)	54 (49.5)	
Age				
≦66	56	28 (50.0)	28 (50.0)	0.708
＞66	53	27 (50.9)	26 (49.1)	
Gender				
Female	37	21 (56.8)	16 (36.8)	0.346
Male	72	34 (47.2)	38 (52.8)	
Smoking status				
Nonsmoking	61	35 (57.4)	26 (49.0)	0.103
Smoking	48	20 (41.7)	28 (58.3)	
Tumor type				
AD	67	37 (55.2)	30 (44.8)	0.209
SQ	42	18 (42.9)	24 (57.1)	
Stage				
I	38	20 (52.6)	18 (47.4)	0.423
II	19	7 (36.8)	12 (63.2)	
III	52	28 (53.8)	24 (46.2)	
p53 mutation				
No	85	48 (56.5)	37 (43.5)	0.018
Yes	24	7 (29.2)	17 (70.8)	
Bcl-2				
Low	55	33 (60.0)	22 (40.0)	0.044
High	54	22 (40.7)	32 (59.3)	
Bcl-xL				
Low	55	34 (61.8)	21 (38.2)	0.017
High	54	21 (38.9)	33 (61.1)	

Table 5. Association between Nrf2, Bcl-2 and Bcl-xL mRNA in lung tumors and tumor response to cisplatin-based chemotherapy in NSCLC patients with tumor recurrence and/or metastasis after surgical resection.

Characteristic		Tumor Response		*P*
		Unfavorable (%)	Favorable (%)	
		29 (48.3)	31 (51.7)	
Nrf2				
Low	27	6 (22.2)	21 (77.8)	0.001
High	33	23 (69.7)	10 (30.3)	
Bcl-2				
Low	28	9 (32.1)	19 (67.9)	0.019
High	32	20 (62.5)	12 (37.5)	
Bcl-xL				
Low	33	11 (33.3)	22 (66.7)	0.010
High	27	18 (66.7)	9 (33.3)	
p53/Nrf2				
WT/Low	19	3 (15.8)	16 (84.2)	0.004
Mutation/High	10	7 (70.0)	3 (30.0)	

Table 6. Cox regression analysis for Nrf2 mRNA, p53 status, and combining Nrf2 mRNA with p53 status on OS and RFS in NSCLC patients.

	OS						RFS					
	Case no.	5- year survival (%)	Median survival (month)	HR	95% CI	P	Case no.	5- year survival (%)	Median survival (month)	HR	95% CI	P
	109						98					
Nrf2 mRNA												
Low	55	36.8	45.3	1			47	14.8	22.3	1		
High	54	12.3	22.3	2.014	1.03-3.87	0.013	51	3.9	13.4	2.047	1.17-4.069	0.022
p53 status												
Wild type	85	22.7	25.4	1			78	10.3	12.6	1		
Mutation	24	30.8	33.9	0.785	0.42-1.31	0.351	20	15.0	21.2	0.842	0.39-1.21	0.521
Nrf2 mRNA (chemo)												
Low	28	37.4	46.0	1			27	11.1	21.0	1		
High	32	5.4	21.0	2.203	1.11-4.36	0.023	29	0.0	16.9	1.992	1.10-3.93	0.047
p53 status (chemo)												
Wild type	42	21.6	20.7	1			40	10.8	17.2	1		
Mutation	18	26.1	35.3	0.644	0.32-1.28	0.208	16	6.3	28.5	0.706	0.36-1.40	0.319
p53/Nrf2												
WT/Low	48	41.1	32.7	1			35	25.7	14.1	1		
Mutation/High	17	32.7	22.4	1.758	0.82-3.79	0.151	12	0.0	12.9	2.269	1.02-5.07	0.046

HR: adjusted by stage.

Chemo: the prognostic value of Nrf2 mRNA, p53 status, and combining Nrf2 mRNA with p53 status in patients who received cisplatin-based chemotherapy.

Table 7. Chemotherapeutic agents used in this study population.

Chemotherapeutic agents	Patient number (%)
Cisplatin	5 (8.3)
Cisplatin+ gemzar	44 (73.3)
Cisplatin+ vp16	5 (8.3)
Cisplatin+ taxol	5 (8.3)
Cisplatin+ mitomycin C	1 (1.7)

Patients were collected from 1996 to 2003

Table 8. List of primer sequences used in the present study.

Target gene	Sequence
Real-time PCR	
GAPDH Forward	5’-GGAGCCAAAAGGGTCATCATC-3’
GAPDH Reverse	5’-GATGGCATGGACTGTGGTCAT-3’
Nrf2 Forward	5’-GTGAAGGCGCTATTTGGCG-3’
Nrf2 Reverse	5’-GGTCCATAGTGACGGTCAGGT-3’
Bcl-2 Forward	5’-CTGTGGATGACTGAGTACC-3’
Bcl-2 Reverse	5’-CAGCCAGGAGAAATCAAAC-3’
Bcl-xL Forward	5’- GCTGGGACACTTTTGTGGAT-3’
Bcl-xL Reverse	5’- TGTCTGGTCACTTCCGACTG-3’
Nrf2 promoter reporter plasmid	
-1036 Forward	5’-GGTACCTCGTTGATTCCACAGCATTT-3’
-740e Reverse	5’-GGTACCCTGCCGGAGCTGTCCACATCTC-3’
-229 Forward	5’-GGTACCGAAGGAAGGGCCCGGACTCTTG-3’
Reverse	5’-AAGCTTGAGCTGTGGACCGTGTGTTGGG-3’
Mutated p53 binding site Forward	5’- CCCTGATTTGGAGTTGCAGAACTTTTCTCTGCTTTTATCTCACTTTACCG-3’
Mutated p53 binding site Reverse	5’-CGGTAAAGTGAGATAAAAGCAGAGAAAAGTTCTGCAACTCCAAATCAGGG-3’
Mutated Sp1 binding site Forward	5’- GGCGCCAGCCGGGGTTGTGTGGGCTAAAGATTTGGA-3’
Mutated Sp1 binding site Reverse	5’-TCCAAATCTTTAGCCCACACAACCCCGGCTGGCGCC-3’
ChIP primer	
Forward	5′-GAATGGAGACACGTGGGAGT-3′
Reverse	5′-CCTTGCCCTGCTTTTATCTCA-3′
Nrf2 expression vector plasmid	
Forward	5’-CTCGAGATGATGGACTTGGAGCTGCCGCC-3’
Reverse	5’-GGATCCCTAGTTTTTCTTAACATCTGGCT-3’
RNAi target	
Shp53	5’- CACCATCCACTACAACTACAT-3’
shNrf2	5’- CCGGCATTTCACTAAACACAA-3’

Figure

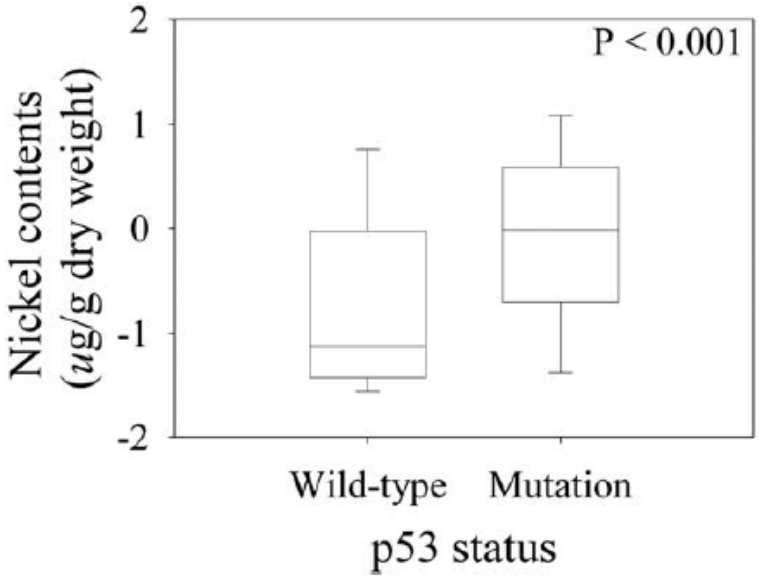

Figure 1. Association of nickel levels with p53 mutations in lung cancer patients. The average nickel level in p53 wild-type patients (n = 113) was 1.83 ± 4.79 µg/g dry weight of lung tissue, with a range of 0.02–27.38 µg/g dry weight. The average nickel level in p53 mutant patients (n = 76) was 6.02 ± 14.75 µg/g dry weight, with a range of 0.02–85.11 µg/g dry weight. The P value was calculated using the Wilcoxon rank sum test, and the data are presented on a log scale.

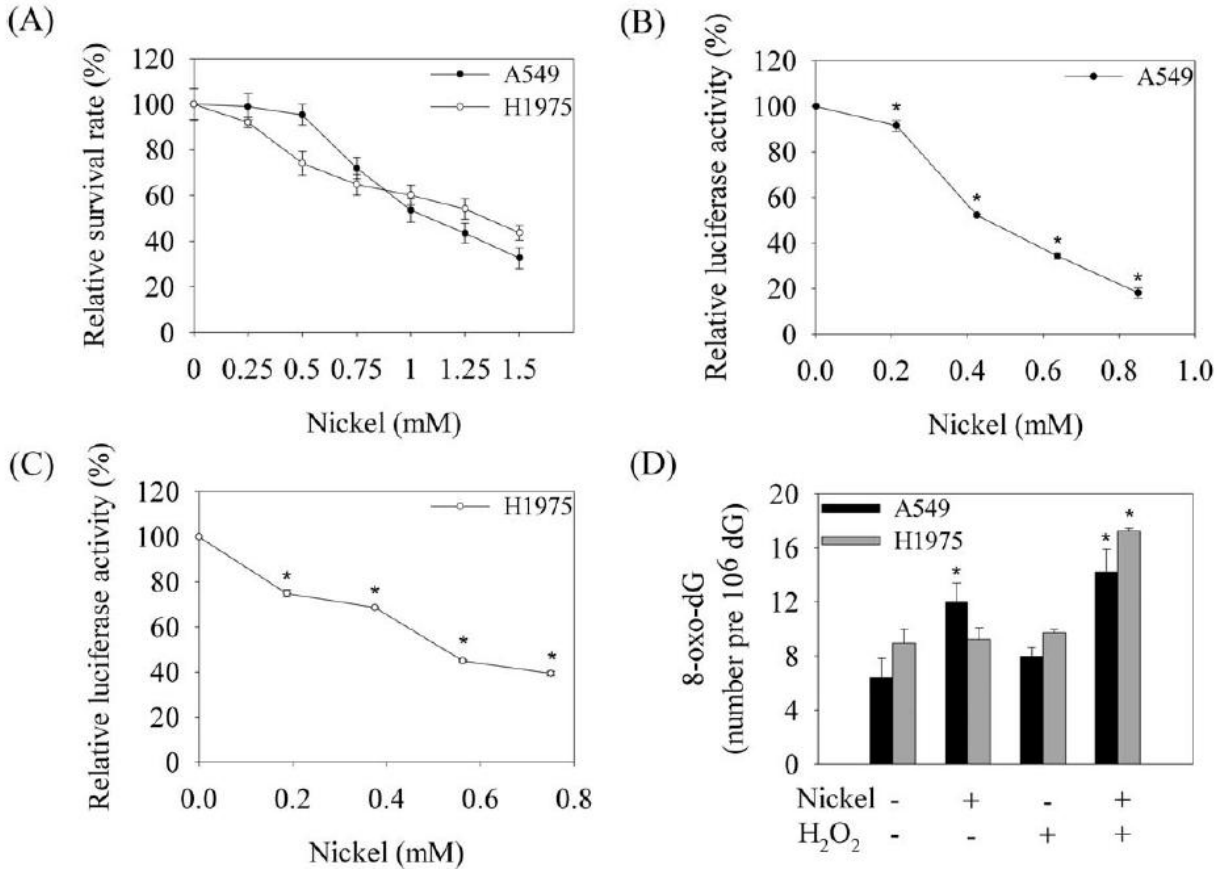

Figure 2. Effects of nickel chloride on cell proliferation, DNA repair activity, and hydrogen peroxide-induced 8-oxo-dG production in A549 and H1975 lung cancer cells. Nickel chloride cytotoxicity and DNA repair activity were evaluated by the MTT assay and the host cell reactivation assay, respectively, as described in the text. (A) The cell lines were treated with various concentrations of nickel chloride (0, 0.25, 0.5, 0.75, 1, 1.25, and 1.5 mM) for 24 hr and incubated at 37℃ for the MTT assay. The cell survival curves were used to calculate the concentration of nickel chloride that inhibited cell growth by 35% (A549: 0.85 mM; H1975: 0.75 mM). The same concentration of nickel chloride was then used for the host cell reactivation assay. The pGL2 vector was pre-treated with 20 mM hydrogen peroxide and then transfected into A549 and H1975 cells that have been pre-treated with various concentrations of nickel chloride for 24 hr (B and C). After pGL2 transfection, the cells were incubated for an additional 24 hr. The percentage recovery of hydrogen peroxide-treated pGL2 was represented by the relative luciferase activity, which was normalized to the β-galactosidase activity. (D) A549 and H1975 cells were treated with nickel chloride (0.85 mM for A549, 0.75 mM for H1975) and 1 μM hydrogen peroxide for 24 hr. The genomic DNA was extracted for 8-oxo-dG measurement by LC/MS-MS. P-values were calculated using a Students' t-test. The data are presented as the mean ± SD from three independent experiments.

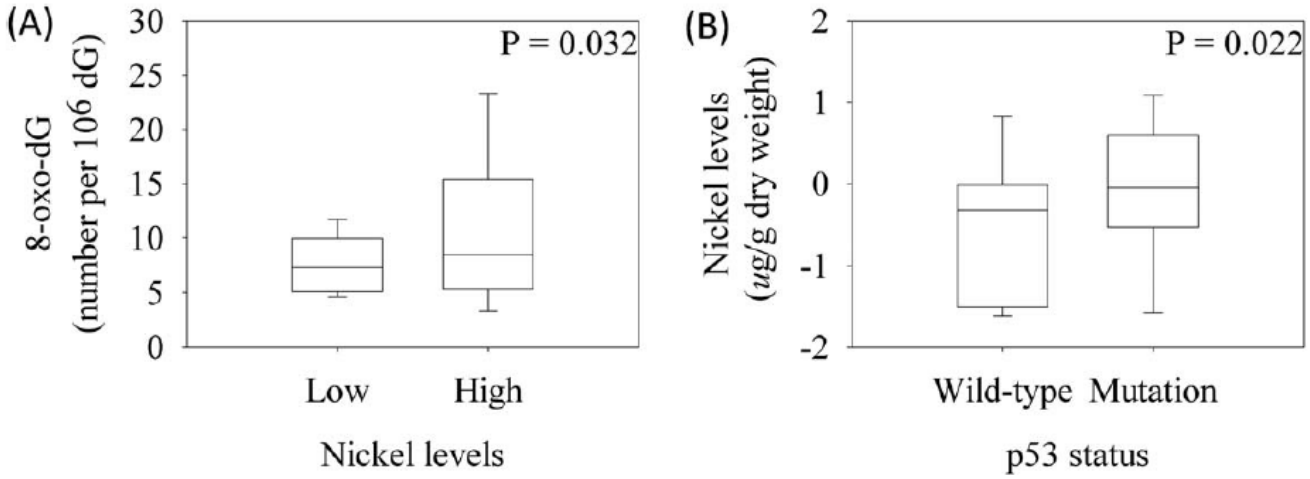

Figure 3. Association of nickel levels with 8-oxo-dG levels and with p53 mutations in lung cancer patients. (A) The average level of 8-oxo-dG in lung cancer patients (n = 78) was 9.5 ± 6.0 8-oxo-dG/106 dG, ranging from 2.4 to 32.1 8-oxo-dG/106 dG. The average level of 8-oxo-dG in patients with low-nickel levels was 8.1 ± 3.6 8-oxo-dG/106 dG, ranging from 3.8 to 21.2 8-oxo-dG/106 dG. The average level of 8-oxo-dG in patients with high-nickel levels was 11.2 ± 8.5 8-oxo-dG/106 dG, ranging from 2.4 to 32.1 8-oxo-dG/106 dG. The P value was determined using a Students' t-test. (B) The average nickel level in p53 wild-type patients was 2.21 ± 5.52 µg/g dry weight of lung tissue, ranging from 0.02 to 26.8 µg/g dry weight. The average nickel level in p53 mutant patients was 5.33 ± 11.64 µg/g dry weight, ranging from 0.02 to 56.48 µg/g dry weight. The P value was calculated using the Wilcoxon rank sum test and the data are presented on a log scale.

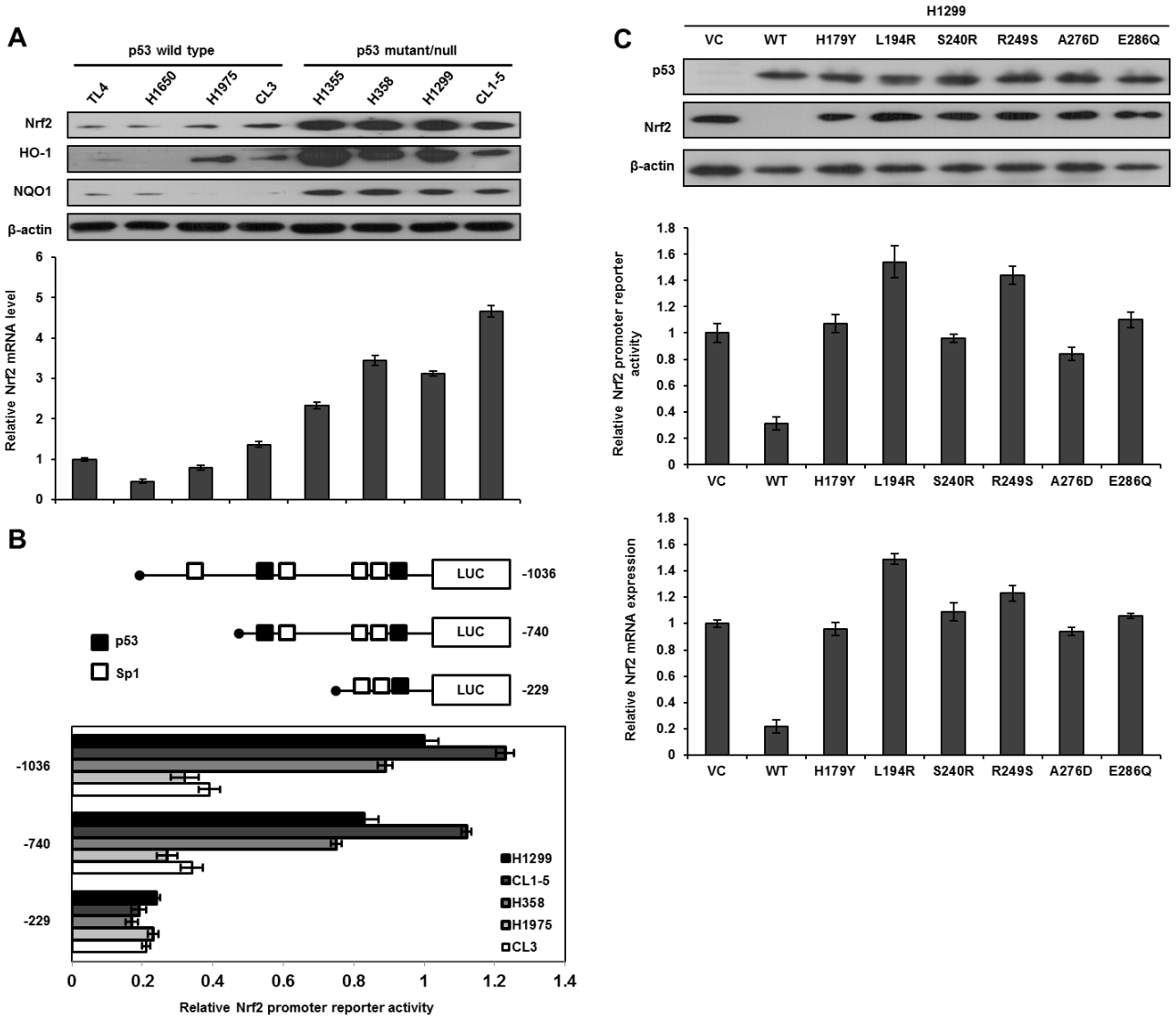

Figure 4. Nrf2 transcription is suppressed by wild-type p53. (A) Western blotting analysis for Nrf2, HO-1, and NQO1 expression in various lung cancer cell lines, β-Actin was used as a loading control. Real-time PCR analysis was performed to determine Nrf2 mRNA expression; GAPDH was served as an internal control. Nrf2 mRNA expression in TL4 cells (mRNA level = 1) was used as a reference to evaluate Nrf2 mRNA levels in other lung cancer cells. (B) Diagram summarizing the positions of the p53 and Sp1 putative binding sites on Nrf2 promoter constructs (–1036~+1) predicted by software analysis (*http://www.atcc.org*). An luciferase reporter assay was performed to evaluate the reporter activity of these three promoter fragments, including –1036/+1, –740/+1, and –229/+1. H1299, CL1-5, H358, H1975, and CL3 cells were separately transfected with these three promoters (5μg) for the luciferase reporter assay; β-gal was served as an internal control. The reporter activity of the Nrf2 (–1036/+1) promoter in H1299 cells served as a reference (activity = 1). (C) Number of p53 wild-type/mutants plasmid and Nrf2 promoters plasmid (-740/+1) were co-transfected into H1299 cells, the cells lysates were separated by SDS-PAGE for the evaluation p53 expression by a specific antibody using western blotting. Luciferase reporter assay was performed to evaluate the reporter activity of Nrf2 promoter. Real-time PCR analysis was performed to determine Nrf2 mRNA expression.

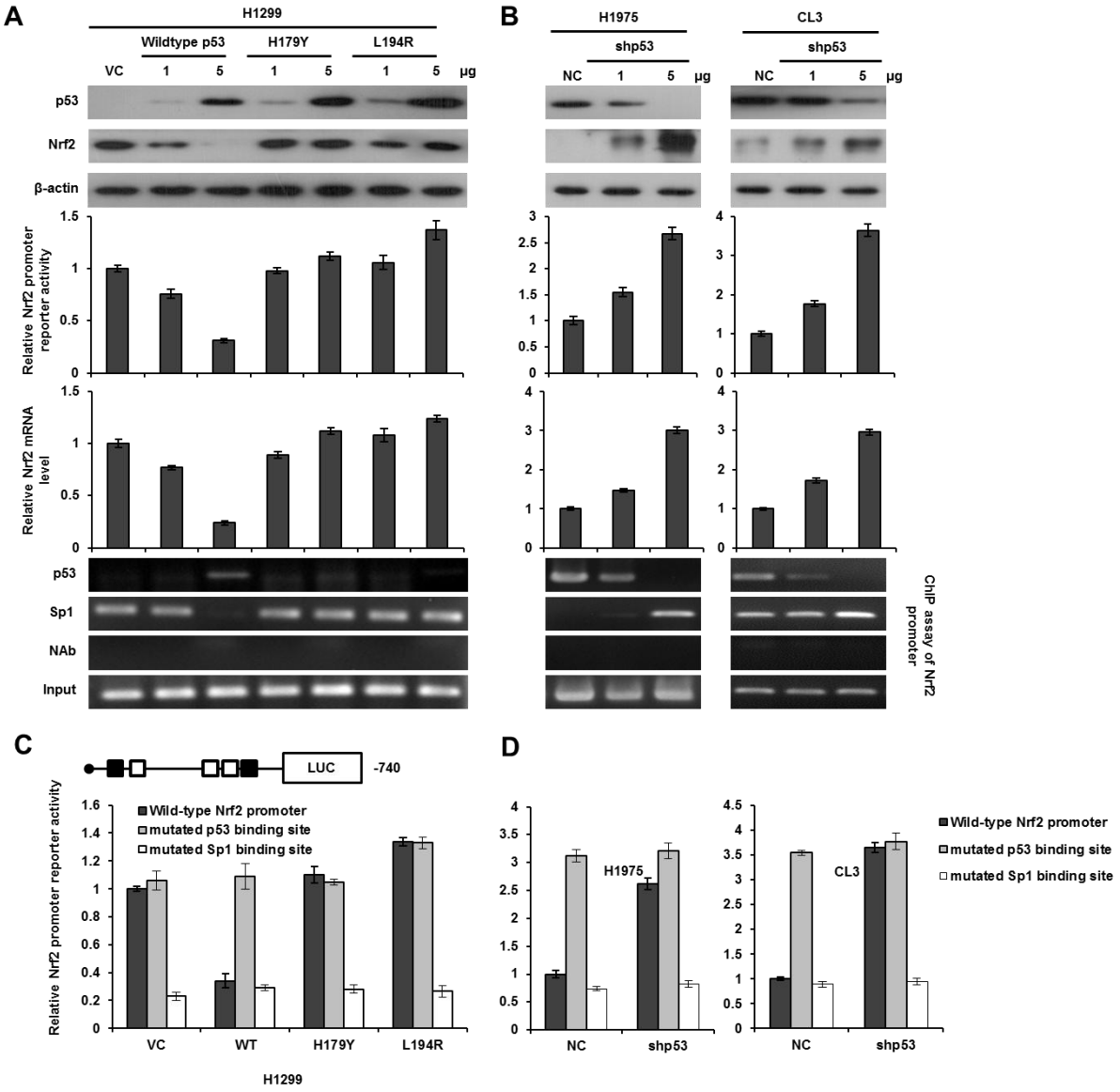

Figure 5. Nrf2 transcription is down-regulated by wild-type p53 via decreased Sp1 binding to Nrf2 promoter. (A) The reporter activity of the Nrf2 (–740/+1) promoter in H1299 cells, which were transfected with p53 wild-type/mutants plasmid. The cells lysates were separated by SDS-PAGE for the evaluation p53 and Nrf2 expression by specific antibodies using western blotting. An luciferase reporter assay was performed to evaluate the reporter activity of Nrf2 promoter. A ChIP assay was performed to evaluate the binding ability of p53 and Sp1 to the putative binding site of the Nrf2 promoter region. The products were amplified by PCR and the as gel electrophoresis results are presented. (B) The reporter activity of the Nrf2 (–740/+1) promoter in H1975 and CL3 cells, which were transfected with shp53 plasmid. The cells lysates were separated by SDS-PAGE for the evaluation p53 and Nrf2 expression by specific antibodies using western blotting. Luciferase reporter assay was performed to evaluate the reporter activity of Nrf2 promoter. A ChIP assay was performed to evaluate the binding ability of p53 and Sp1 to the putative binding site of the Nrf2 promoter region. The products were amplified by PCR and the as gel electrophoresis results are presented. (C) The reporter activity of the wild-type-, p53 binding site mutated-, and Sp1 binding site mutated-Nrf2 (–740/+1) promoter in H1299, which were transfected with p53 wild-type/mutants plasmid. An luciferase reporter assay was performed to evaluate the reporter activity of Nrf2 promoter. (D) The reporter activity of the wild-type-, p53 binding site mutated-, and Sp1 binding site mutated-Nrf2 (–740/+1) promoter in H1975 and CL3 cells, which were transfected with shp53 plasmid. An luciferase reporter assay was performed to evaluate the reporter activity of Nrf2 promoter.

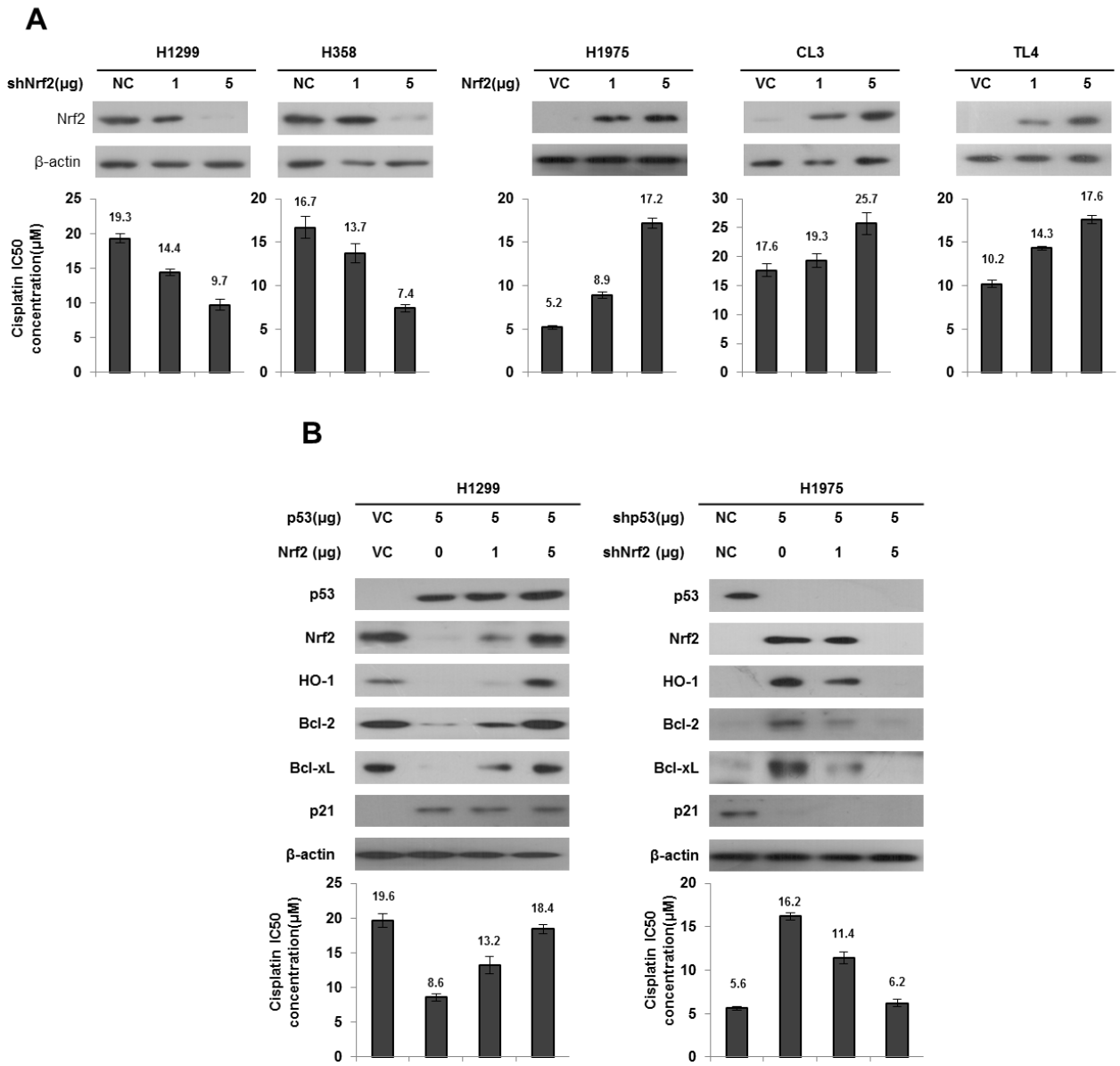

Figure 6. Nrf2 expression is responsible for cisplatin sensitivity in lung cancer cells. (A) shNrf2 plasmids were transfected into high Nrf2-expressing (H1299 and H358) cell lines compared with both cell types transfected with a non-specific shRNA (NC), Nrf2 expression plasmids were transfected into low Nrf2-expressing (H1975 and CL3) cell lines compared with both cell types transfected with an empty vector (VC). After 24h, the indicated cells were incubated with or without cisplatin (0, 2, 4, 8, 16, 32 μM) for 48 h for MTT assay. The cell lysates were separated by SDS-PAGE for the evaluation Nrf2 expression by specific antibodies using western blotting. The MTT assay was used to determine the 50% inhibition concentration (IC50) of cisplatin. (B) H1299 cells were transfected with p53 and/or Nrf2 plasmid. H1975 cells were transfected with shp53 and/or shNrf2 plasmid. After 24h, the indicated cells were incubated with or without cisplatin for 48 h for MTT assay. The cell lysates were separated by SDS-PAGE for the evaluation p53, Nrf2, HO-1, Bcl-2 and Bcl-xL expression by specific antibodies using western blotting. The MTT assay was used to determine the IC50 of cisplatin.

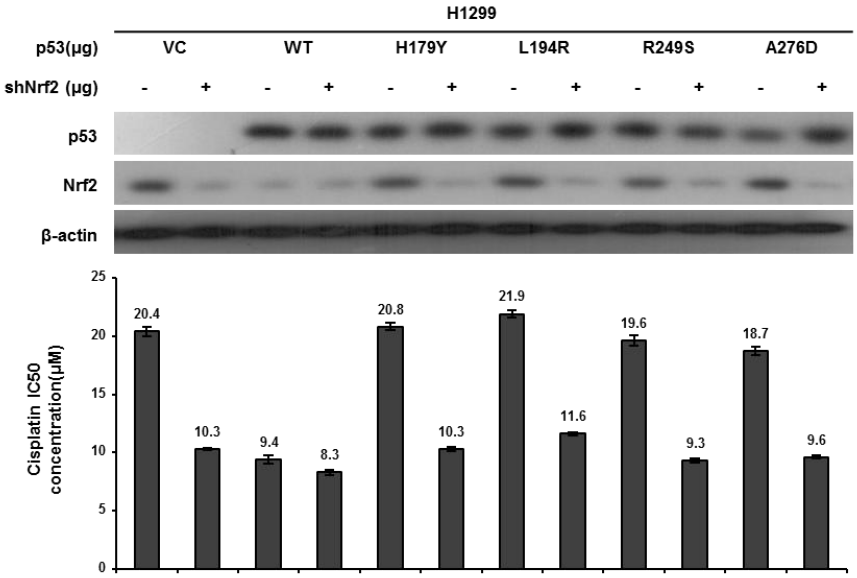

Figure 7. The H1299 cells were transfected with wild-type p53, mutant p53 and/or shNrf2 plasmid. After 24 h, the cells were treated with or without cisplatin for an additional 48 h for MTT assay. The cell lysates were separated by SDS-PAGE for the evaluation of p53, Nrf2, expression by specific antibodies using western blotting. The MTT assay was used to determine the IC50 of cisplatin.

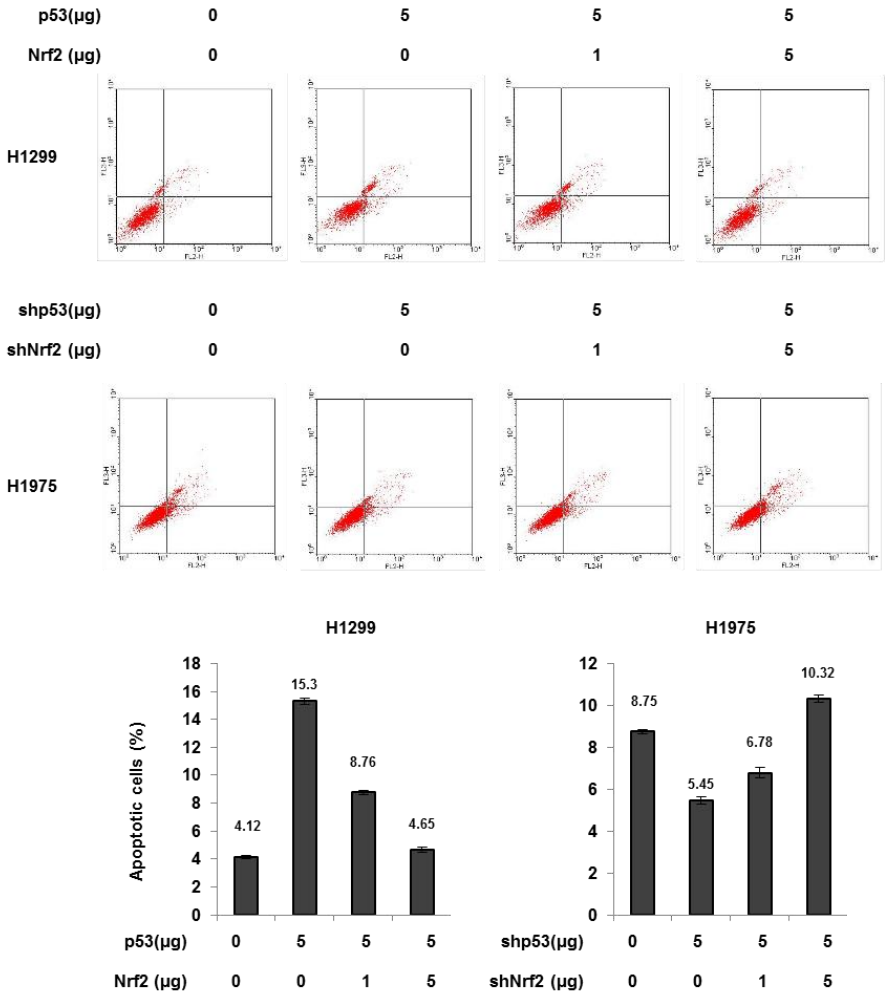

Figure 8. Flow cytometric analysis of apoptosis with annexin V/PI staining. H1299 cells were transfected with p53 and/or Nrf2 plasmid. H1975 cells were transfected with shp53 and/or shNrf2 plasmid. The cells were then subjected to annexin V and PI staining, followed by a flow cytometry. Percentage of apoptotic cells including with the Annexin V+/PI− population (early apoptosis) plus Annexin V+/PI+ (late apoptosis/secondary necrosis) was summarized by a flow cytometric analysis. Data are expressed as means±s.d., n=3.

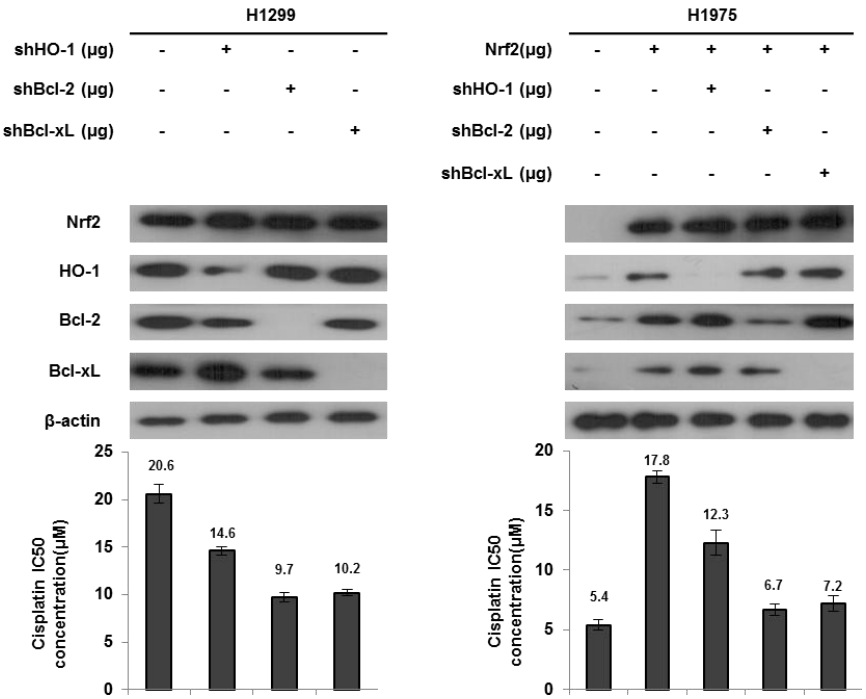

Figure 9. Bcl-2 and Bcl-xL are more involved than HO-1 on Nrf2-mediated cisplatin resistance. H1299 cells were transfected with shHO-1, shBcl-2 or shBcl-xL plasmid. H1975 cells were transfected with Nrf2, shHO-1, shBcl-2 or shBcl-xL plasmid. After 24h, the indicated cells were incubated with or without cisplatin for 48 h for MTT assay. The cell lysates were separated by SDS-PAGE for the evaluation Nrf2, HO-1, Bcl-2 and Bcl-xL expression by specific antibodies using western blotting. The MTT assay was used to determine the IC50 of cisplatin.

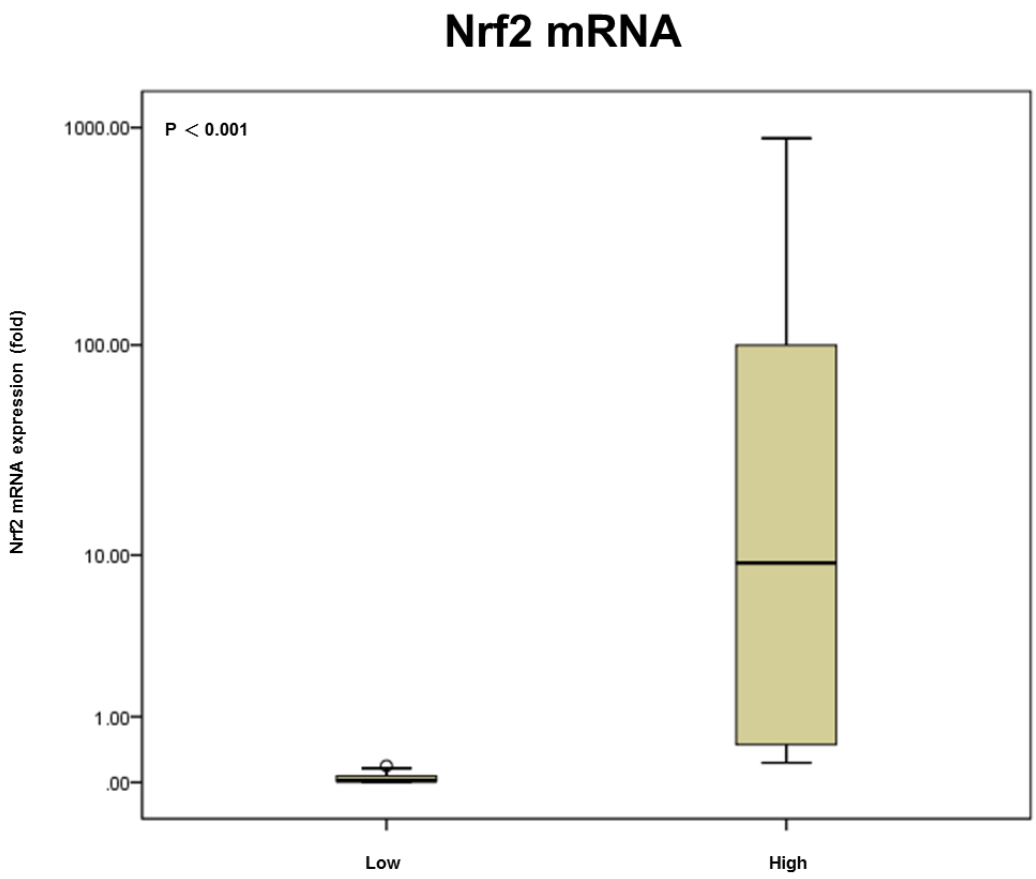

Figure 10. The Box plot analysis for Nrf2 mRNA expression levels between low and high subgroups in lung cancer patients. The charts show the expression of relative quantification values.

子計畫四

鎳引起肺慢性發炎和腫瘤生成過程中肺 C 纖維過度敏感之重要性

中英文摘要**:**

鎳(Ni^{2+})在人類生活中為常見的接觸性過敏原之一，在前人的研究中顯示，鎳會引發肺 C 纖維的過度敏感進而導致神經性的發炎反應，並誘導 TLR-4、AKT、pp70S6K 及 pS6 表現量增加；並活化肺癌細胞內和轉移有關的細胞激素(如: IL-6、IL-8、MCP-1 及 Rantes)。因此，本年度將進一步探討鎳與物質 P 暴露的時間是否會調控細胞的免疫功能。

首先我們將 RAW264.7 細胞株以不同濃度的氯化鎳($NiCl_2$: 100、50 或 25 μM)培養 1.5 或 24 小時，再以 LPS (0.1 μg/ml)處理 24 小時來誘發 RAW264.7 細胞產生炎症反應，之後再以各項實驗進行分析。由實驗結果發現，RAW264.7 細胞以氯化鎳及物質 P 處理 1.5 小時後，對 LPS 所誘導的炎症反應並無顯著的影響；但以氯化鎳處理 RAW264.7 細胞 24 小時後，發現氯化鎳會顯著增加由 LPS 誘導之 RAW264.7 細胞之死亡率，且會抑制炎症反應，如: 降低 IL-6 與 TNF-α的分泌及 iNOS、pSTAT1、COX-2 的表現；同時我們也發現氯化鎳會抑制細胞表面抗原 CD14、CD68、CD80、CD86 與 MHC II 的表現量。綜合上述的實驗結果，初步證實，長時間的暴露在氯化鎳下會損害巨噬細胞在 LPS 刺激下的基本功能，是藉由調控細胞表面抗原之表現。

Nickel chloride represents one of the most common contact allergens in humans. In previous studies shows that the nickel can cause hypersensitivity of pulmonary C-fiber leading to neurological inflammation and induce the expression of TLR-4, AKT, pp70S6K and pS6; and activation the metastasis-related cytokines (eg: IL-6, IL-8, MCP-1 and Rantes) in lung cancer cells. Therefore, we will further explore the immune function of substance P and nickel in RAW264.7 cells.

The aim of this study was to evaluate the effect of nickel chloride and on the expression of functionally distinct surface antigens in murine RAW 264.7 macrophages. The expression of the surface antigens CD14, CD68, MHC class II, CD80, and CD86 were analyzed by flow cytometry. The bacterial endotoxin lipopolysaccharide (LPS) was used as a positive control to induce antigen expression. Cells were stimulated with $NiCl_2$ (100, 50 and 25 μM) for 1.5 h or 24 h in the presence or absence of LPS (0.1 μg/ml) for the 24 h. The results showed that nickel chloride (100, 50 and 25 uM) treated with 24 h or 48 h, the cell viability decreased and released a large amount of LDH.

Our results findings, LPS up-regulated MHC class II molecules as well as costimulatory surface antigens (CD14, CD68, CD80, CD86) and induced proinflammatory cytokines released (IL-6 and TNFα) in RAW264.7 macrophages. However, treatment with $NiCl_2$ (100 and 50 uM) of 48h inhibited the LPS-induced expression of all surface antigens and cytokines, while in cells stimulated only by $NiCl_2$ (25 uM) was up-regulated only on CD14/CD68 and CD80.

These results show that nickel chloride is able to down-regulation of surface antigen expression, but a long exposure time may impair essential functions of macrophages stimulated by LPS.

前言:

人類長期暴露於鎳化合物中對人體健康有負面影響，會導致肺纖維化、心血管疾病，以及腎臟疾病。於 1990 年，International Agency for Research on Cancer(IARC) 將鎳化合物分類為人類的致癌物(IARC, 1990)。研究指出鎳化合物會引發多種腫瘤的產生，如肺臟和腎臟的腫瘤(Kasprzak *et al*., 1990; Kasprzak *et al*., 1994)，在腫瘤的形成過程中，鎳還扮演著 initiator 及 promoter 的角色 (Eker＆Sanner, 1983)。另外，鎳也可引起基因毒性及 DNA base 的氧化性傷害 (Kasprzak, 1995)。

由各種臨床研究顯示發炎反應發生時，發炎細胞激素(inflammatory cytokines)及趨化因子所形成複雜的 network，在肺部發炎反應發生時扮演著傳遞、放大及維持的重要角色。這中間還包括了刺激產生抗發炎細胞激素(anti-inflammatory cytokines)與前發炎組織激素之間的相互抗衡，來調節整個發炎反應的過程。IL-1β 可以刺激許多的趨化因子產生，如細胞激素 (IL-8)(Orringer et al., 1993), (MCP-1)(Suter et al., 1992), 及巨噬細胞發炎反應蛋白-1α 單核球趨化蛋白-1(MIP-1α)(Siler al., 1989)。巨噬細胞所特有的 CD11b、CD14 與 CD68 等細胞表面抗原，當其有增加的現象，則顯示有發炎反應的發生。當 APC 呈獻 antigen 給 T 細胞藉以產生免疫反應時，因為 TCR 與 antigen 的 binding affinity 沒有像 BCR 那麼的高，所以需要很多其他 co-stimulatory molecules 的幫忙來完成 two signals stimulation，其中就以 CD28 和 B7 (CD80、CD86)的作用最為重要。抗原呈現細胞(APC)但表面具有豐富的抗原遞呈分子(MHC-Ⅰ和 MHC-Ⅱ)、共刺激因子(CD80/B7-1、CD86/B7-2、CD40、CD40L 等)和粘附因子(ICAM-1、ICAM-2、ICAM-3、LFA-1、LFA-3 等)。

先前的研究指出，在吸入LPS 於肺中，由LPS 刺激的分子機制會開始啟動發炎的細胞激素及化學趨化因子及附著因子等造成中性移到血管內皮細胞及肺上皮細胞產生移入肺泡內(Pittet et al., 2001)。發炎前之細胞激素，如tumor necrosis factor-α (TNF-α),interleukin-1β (IL-1β) 及 interleukin-6(IL-6) ，會在肺部發炎發生之前大量的表現(Giri etal., 1993)。 這許早期反應出來的細胞激素，如TNF-αand IL-1β，可以刺激核內轉錄因子 NF-κB進入核中開啟一系列發炎開始前一系列的細胞激素產生。 在一系列的研究中發現呼吸道的上皮細胞可因NF-kB 的持續作用使得一些化學趨化因子，如IL-8、KC、MIP-2、MCP-1大量的表現,，使得肺部發炎因而加重(Yaoo et al., 2013)。 這些因子會使得大量有關發炎的白血球，如中性白血球，大量進入肺部的空間中，媒介白血球入侵組織之三步驟當組織受到傷害產生發炎反應時，血流中的白血球會被吸引並遷移至發炎組織，以對抗外來物質或是過敏原。本研究針對金銀花的萃取物在鎳誘發肺部的上細胞及巨噬細胞產生發炎反應時, 對發炎相關的細胞激素(TNF-α, IL-1β, IL-6, 及IL-8)的抑制作用，並且對發炎反應中最重要的核轉錄因子(NF-κB)的轉錄上是否有影響進行免疫學上的評估。有學著指出免疫細胞會被吸引到發炎的地置，是因為細胞和發炎位置間有細胞激素與細胞激素受體（receptor）互相吸引的作用力存在(Oppenheim et al., 1991)。而目前仍然不太清楚癌細胞為什麼會轉移到特定的目標器官，有較多的假說及證據支持把發炎機轉的『細胞激素（cytokines）與細胞激素受體（cytokine receptors）交互作用』用在解釋轉移機轉，即癌細胞會運用許多種細胞激素來告訴它要轉移到何處(Kakinuma et al., 2006)。因此，目標器官上間質細胞所表現的激素或相對應受體，應能調控癌細胞的轉移速率。

在過去的研究中，JAK-STAT pathway主要被探討腫瘤與癌症的產生，但JAK-STAT pathway的活化也參與調控炎症反應，JAK-STAT pathway由三個部分組成包括受體(receptor; gp130)、JAK (janus kinases)以及STAT(signal transducers and activators of transcription) (Aaronson et al., 2002)。JAK與STAT是許多細胞因子受體的組成部分，可以調節細胞生長、細胞存活、細胞分化以及對病原體的對抗。AK與STAT是許多細胞因子受體的組成部分，可以調節細胞生長、細胞存活、細胞分化以及對病原體的對抗。JAK kinase (janus kinases)是一個酪胺酸家族，包含四個主要成員JAK 1、JAK2、JAK 3及Tyk2。外來生長分

化訊息，如: 細胞激素IL-6與細胞表面的接受器結合後，會活化在接受器上的JAK kinase而進行磷酸化，磷酸化的JAK kinase會繼續磷酸化下游的STAT，活化的STAT能進入細胞核並與一些目標基因的特異性增強子（Enhancer）進行結合，因此調節基因序列的轉錄作用。JAK-STAT pathway可經由IL-6與gp130結合而誘導活化，異常活化的IL-6信號表現可能造成自身免疫性疾病、炎症反應或癌症的產生，如前列腺癌、多發性骨髓瘤(Yao et al., 2013)。2007年Kim 與Lee 也指出了STAT1可經兩種方式調控細胞死亡，1.)transcription-dependent 的機制中STAT1可經由與GAS或ISRE的結合而促使caspases、death receptors與ligands, iNOS, 活化cell-cycle arrest相關的基因如 p21waf1與抑制Bcl-xL,來誘發apoptosis；2.)transcription-independent的機制中STAT1可經由與p53或TRADD的結合，或導致STAT1的acetylation (Ace)而促使經NF-κB 訊息路徑的antiapoptotic。2012年Avalle等人也指出，STAT1與STAT3的平衡決定了腫瘤(tumor)的形成與否，若STAT1被活化則可直接導致cell cycle arrest與促使cancer cells走向apoptosis，同時也指出了STAT1可刺激適應性免疫反應(adequate immune response)來增加毒殺形T細胞(cytotoxic T cell ; CTL) 的活化來對抗腫瘤；在STAT3的活化則可藉由刺激IL-10的分泌來誘使免疫細胞產生tolerance，或著刺激腫瘤細胞(tumor cell)增生(proliferation)而存活下來，同時可也可藉由其他的間接調控誘使激癌細胞腫瘤的血管新生作用(angiogenesis)與轉移(metastatization)增加。

二、材料與方法

RAW264.7 與 MHS 細胞株培養

RAW264.7 與 MHS 細胞， cells 維持在含有 5%胎牛血清、2mM *L*-glutamate、100μM 非必須胺基酸及抗生素(100units/ml of penicillin, 100g/ml streptomycin and 0.25μg/ml of fungizone)的 DMEM 培養基，培養於 37℃、5% CO2/95% air 培養箱。每四天以胰蛋白酶消化繼代，培養在 75 平方公分細胞培養皿。

細胞存活分析(MTT assay) 與細胞毒性 LDH 分析

- **MTT assay**

將1 X 10^5的細胞培養於12孔的培養盤。分別先處理或不處理氯化鎳或添加Substance P，1.5或24小時後，再添加LPS (0.1 μg/ml)並於37℃含5% CO_2之培養箱中培養24小時後，先以顯微鏡觀察其細胞形態後，收集上清液；之後在每一個well中加入10 μl Cell Counting Kit-8 試劑，再放回37℃且含有5% CO2的恆溫培養箱中，培養至其變色(約為2~3小時)。 最後以ELISA Reader 測其在450~595 nm 波長下之吸光值(OD 450和630)。

- **LDH 分析**

當細胞膜受損或破裂時，位於細胞質的 LDH (Lactate Dehydrase) 便可逃逸出到細胞外，藉由加入呈色受質就可以定量被毒害的細胞。將上述樣本的上清液收集，出 100 μl 加入 100 μl 之 LDH 試劑 (Sigma. St.Louis, MO)提供之呈色受質，反應後以 ELISA Reader 測其在 492 nm 波長。來分析處理或不處理氯化鎳及添加 Substance P 在 LPS 的處理下對細胞是否有細胞毒性。

- **以 flow cytometry 分析細胞表面抗原**

將1 X 10^5的RAW264.7細胞培養於12孔的培養盤。分別先處理或不處理氯化鎳或添加Substance P，1.5或24小時後，再添加LPS (0.1 μg/ml)並於37℃含5% CO_2之培養箱中培養24小時後，將細胞分別收集到1.5 ml的離心管中，離心去除上清液，以含2%FBS及0.05%NaN3的PBS (FACS buffer)清洗離心兩

次後，吸掉上清液。將2 X 10^5的RAW264.7細胞分別以添加50ul的 antimouse MCH class II (clone M5/114.15.2), anti-mouse CD14 (clone rmC5-3), antimouse CD68 (clone 3/23), , anti-mouse CD80 (clone 16- 10A1), and anti-mouse CD86 (clone GL1)，**置於4℃反應30分鐘，加2ml的**FACS buffer清洗離心兩次後，每個樣本分析10000個細胞，利用 FACSCalibur 與CellQuest software (Becton Dickinson, San Jose, CA, USA)來分析。

- **西方墨點法**

將各種處理過的細胞培養後，收集細胞，PBS 沖洗後，以 3,000 rpm 離心 5 分鐘，取沈澱細胞，PBS 沖洗離心後，移除上清液加入 cell lysis reagent (10 mM Tris-HCl pH 7.5, 10 mM KCl, 5 mM $MgCl_2$)，用 1 mL 針筒吸放 20 次，於 4℃、18000 × *g* 離心 20 分鐘後取上清液。取部分上清液以 Bradford 蛋白質分析試劑套組 (Amresco, Inc., USA) 定量蛋白質之濃度，其餘則加入等體積之 sample buffer (100 mM DTT, 2 % SDS, 50 mM Tris, 10 % glycerol, 0.1 % Bromophenol blue) 將細胞懸浮混勻，並於乾浴鍋以 95℃ 加熱 5 分鐘，之後立即置於冰上，儲存於-20℃備用。製備好之細胞萃取液，每孔加入等量之蛋白質含量並以 10% SDS-PAGE 進行垂直式電泳分離。電泳結束後將膠片取下以半乾式轉漬器 (Bio-Rad) 將膠片上之蛋白質轉印至 PVDF 膜。接著將轉印好的 PVDF 膜以 5%脫脂奶之 PBST (1X PBS 含 0.1% Tween 20) 浸漬 1-2 小時，減少非專一性的鍵結，再加入一級抗體 (包含 COX2、iNOS、cytochrome *c*、caspase -1、-3、8、9、MAPK pathway、NF-κB、AP-1、p53、JAK/STAT.等) 於 4℃ 反應 24 小時，以 PBST 洗去未鍵結的一級抗體 (3 次，10 分鐘/次)，再以 HRP-conjugated goat anti-mouse/rabbit antibody 反應 50-60 分鐘，以相同的方式 wash NC-paper，最後加入 Western Blot Chemiluminescence Reagent Plus 反應後，於 LAS-1000 plus system 影像分析並定量之。

檢測細胞上清液 IL-6、IL-8 的表現量

細胞培養液取，測 IL-6、IL-8、MCP-1 與 Rantes 含量，採用一般商業測試套組(ELISA kit)測得 (BioSource International, Inc., USA)。將 cytokines 的 capture Ab 以 coating buffer 稀釋 250 倍後，取 100 µl 加入 96 孔盤，於 4℃靜置一夜。去除多餘的 capture Ab，並以 wash buffer (1X PBS+0.05％ Tween-20) 清洗 3 次(250 µl/well)，再加入套組中所附的 assay diluent reagent 於室溫反應 1 小時，接著以 wash buffer 清洗 3 次，再於盤中指定之位置加入待測的上述收集的細胞培養液，檢體及各 cytokines 的標準稀釋品 (100 µl/well)，於室溫反應 2 小時，接著以 wash buffer 清洗 3 次，然後加入 100 µl/well 的 Detection Ab (250 倍稀釋)，於室溫反應 1 小時，接著以 wash buffer 清洗 5 次，再加入 100 µl/well 的 Avidin-HRP 於室溫反應 15 分鐘，接著以 wash buffer 清洗 7 次，最後在加入 100 µl/well 的 substrate solution (1X TMB) 於室溫作用 5-10 分鐘，再加入 50 µl stop solution (2N H_2SO_4)去終止反應。以全波長酵素分析儀以 450 nm 去測量其 OD 值，並以標準品來推算帶測檢體之濃度。

三、結果

氯化鎳對RAW264.7細胞生長及毒性分析

結果發現， RAW264.7細胞以氯化鎳(100、50或25 µM)先處理1.5小時後，再添加LPS (0.1 µg/ml)並培養24小時後，結果會導致細胞存活率下降約20~30%(圖1.)，且會誘導大量的LDH釋放約增加1.5倍，但在24小時後卻發現細胞存活率回升與LDH釋放量下降(圖2.)。而在添加物質P的實驗中我們發現，物

質P可提升細胞的存活率與暴露時間長短無關，但無法回復氯化鎳所導致的細胞死亡率(圖1.與2.)。RAW264.7細胞以氯化鎳(100、50或25 μM)先處理24小時後，再添加LPS (0.1 μg/ml)並培養24小時後，結果會導致細胞存活率下降約70~30%(圖1.)，且會誘導大量的LDH釋放約增加1.5倍相較於不添加LPS的Mock組(圖2.)。

分析RAW264.7細胞以氯化鎳處理不同時間下對LPS 誘導發炎反應的影響

結果發現， RAW264.7細胞以氯化鎳(100、50或25 μM)先處理1.5與24小時後，結果發現氯化鎳無法影響LPS所誘導的IL-6(圖3.)與TNFα(圖4.)的分泌。

RAW264.7細胞以氯化鎳(100、50或25 μM)先處理24小時後，再添加LPS (0.1 μg/ml)並培養24小時後，結果發現氯化鎳會顯著抑制LPS所誘導的IL-6(圖3.)與TNFα(圖4.)的分泌。添加物質P的實驗中我們發現，不管有無LPS的處理皆無法調控IL-6(圖3.)與TNFα(圖4.)的分泌。

分析RAW264.7細胞的表面抗原以氯化鎳處理不同時間下對LPS的影響

結果發現， LPS處理下會誘導RAW264.7細胞的表面抗原CD14 、CD68、CD80、CD86與MHC II表現量增加。RAW264.7細胞以氯化鎳(100、50或25 μM)先處理24與48小時後，結果發現以100與50 μM氯化鎳處理的實驗組會抑制細胞表面抗原$CD14^+/CD68^+$(圖5.)、CD80(圖6.)、CD86(圖7.)與MHC II (圖8.)表現量，且48小時的實驗組抑制$CD14^+/CD68^+$高達1.79倍(圖5.)。以25μM氯化鎳處理的實驗組在24與48小時皆會誘導$CD14^+/CD68^+$ (圖5.)與CD80的表現量(圖6.)。在添加物質P的實驗中我們發現，物質P會增加$CD14^+/CD68^+$(圖5.)、CD80(圖6.)與CD86(圖7.)的表現量，但在處理LPS後則會抑制此表面抗原的表現。RAW264.7細胞以氯化鎳(100、50或25 μM)先處理1.5或24小時後，再添加LPS (0.1 μg/ml)並培養24小時後，氯化鎳皆會抑制細胞表面抗原$CD14^+/CD68^+$(圖5.)、CD80(圖6.)、CD86(圖7.)與MHC II (圖8.)表現量，處理24小時後再添LPS (0.1 μg/ml)的實驗組下降得更為顯著。

分析氯化鎳與物質P對RAW264.7與MHS細胞細相關蛋白表現情形

我們發現RAW264.7與MHS細胞在以氯化鎳(100、50或25 μM)先處理1.5與24小時後，結果發現氯化鎳會抑制iNOS、pSTAT1、COX-2的表現(圖9.與10.)。添加物質P的實驗中我們發現，不管有無LPS的處理皆不會顯著的抑制iNOS、pSTAT1、COX-2的表現(圖9.與10.)。

四、討論

本研究發現了短期(24小時)的暴露於氯化鎳會促使細胞死亡,但當細胞暴露於長時間(24小時)的氯化鎳時便會下降細胞的存活率。而當氯化鎳與LPS同時存在時，則會加劇細胞的死亡。此現象可能與氯化鎳會抑制巨噬細胞的活性有關，其機制可能藉由抑制發炎相關細胞激素IL-6與TNFα的分泌、iNOS、pSTAT1、COX-2的表現及細胞表面抗原$CD14^+/CD68^+$(圖5.)、CD80(圖6.)、CD86(圖7.)與MHC II (圖8.)表現量有關。

參考文獻

1. Avalle L, Pensa S, Regis G, Novelli F, Poli V.(2012). STAT1 and STAT3 in tumorigenesis: A matter

of balance. JAKSTAT, 1(2), 65-72.
2. Yao X, Huang J, Zhong H, Shen N, Faggioni R, Fung M, Yao Y. (2013).Targeting interleukin-6 in inflammatory autoimmune diseases and cancers. Pharmacol Ther. 27, doi: 10.1016/j.pharmthera.2013.09.004.
3. Kim HS and Lee MS.(2007).STAT1 as a key modulator of cell death.Cell Signal, 19(3),454-65.
4. NOZAWA H, WATANABE T, NAGAPA H. Phosphorylation of ribosomal p70 S6 kinase and rapamycin sensitivity in human colorectal cancer. Cancer Lett, 2007, 251(1):105-113.
5. VAZQUEZ-MARTIN A, OLIVERAS-FERRAROS C, COLOMER R, et al. Low-scale phosphoproteome analyses identify the mTOR effector p70 S6 kinase 1 as a specific biomarker of the dual-HER1/HER2 tyrosine kinase inhibitor lapatinib (Tykerb) in human breast carcinoma cells. Ann Oncol, 2008, 19(6):1097-1109.
6. PATEL RA, AHMAD I, SHEEHAN CE, et al. Expression of phosphorylated mTOR (p-mTOR) correlates with advanced stage in diffuse large-B-cell lymphomas . Blood (ASH Annual Meeting Abstracts), 2007, 110:1573.
7. Ho, W.Z., Kaufman, D., Uvaydova, M., Douglas, S.D., 1996. Substance P augments interleukin-10 and tumor necrosis factor-alpha release by human cord blood monocytes and macrophages. J. Neuroimmunol. 71, 73– 80.
8. Kincy-Cain, T., Bost, K.L., 1997. Substance P-induced IL-12 production by murine macrophages. J. Immunol. 158, 2334– 2339.
9. Laurenzi, M.A., Persson, M.A., Dalsgaard, C.J., Haegerstrand, A., 1990. The neuropeptide substance P stimulates production of interleukin 1 in human blood monocytes: activated cells are preferentially influenced by the neuropeptide. Scand. J. Immunol. 31, 529– 533.
10. Lieb, K., Fiebich, B.L., Berger, M., Bauer, J., Schulze-Osthoff, K., 1997. The neuropeptide substance P activates transcription factor NFkappa B and kappa B-dependent gene expression in human astrocytoma cells. J. Immunol. 159, 4952–4958.
11. Lotz, M., Vaughan, J.H., Carson, D.A., 1988. Effect of neuropeptides on production of inflammatory cytokines by human monocytes. Science 241, 1218– 1221.
12. Marriott, I., Mason, M.J., Elhofy, A., Bost, K.L., 2000. Substance P activates NF-kappaB independent of elevations in intracellular calcium in murine macrophages and dendritic cells. J. Neuroimmunol. 102, 163–171.
13. O'Connor, T. M., O'Connell, J., O'Brien, D. I., Goode, T., Bredin, C. P., Shanahan, F., 2004. The role of substance P in inflammatory disease. J. Cell. Physiol. 201, 167–180.
14. Schaffer, M., Beiter, T., Becker, H. D., Hunt, T. K., 1998. Neuropeptides: mediators of inflammation and tissue repair? Arch. Surg. 133, 1107–1116.
15. Pittet JF, Griffiths MJD, Geiser T, Kaminski N, Dalton SL, Huang XZ. TGF-b1 is a critical mediator of acute lung injury. J Clin Invest 2001; 107(12):1537–1544
16. Giri SN, Hyde DM, Hollinger MA. Effect of antibody to transforming growth factor beta on bleomycin induced accumulation of lung collagen in mice. Thorax 1993; 48(10):959–966
17. Suter PM, Suter S, Girardin E, Roux-Lombard P, Grau GE, Dayer JM. High bronchoalveolar levels of tumor necrosis factor and its inhibitors, interkeukin-1,interferon, and elastase, in patients with respiratory distress syndrome after trauma,shock, or sepsis. Am Rev Respir Dis. 1992;145(5):1016–22.
18. Siler TM, Swierkosz JE, Hyers TM, Fowler AA, Webster RO. Immunoreactive interleukin-1 in

bronchoalveolar lavage fluid of high-risk patients and patients with the adult respiratory distress syndrome. Exp Lung Res. 1989;15(6):881–94.

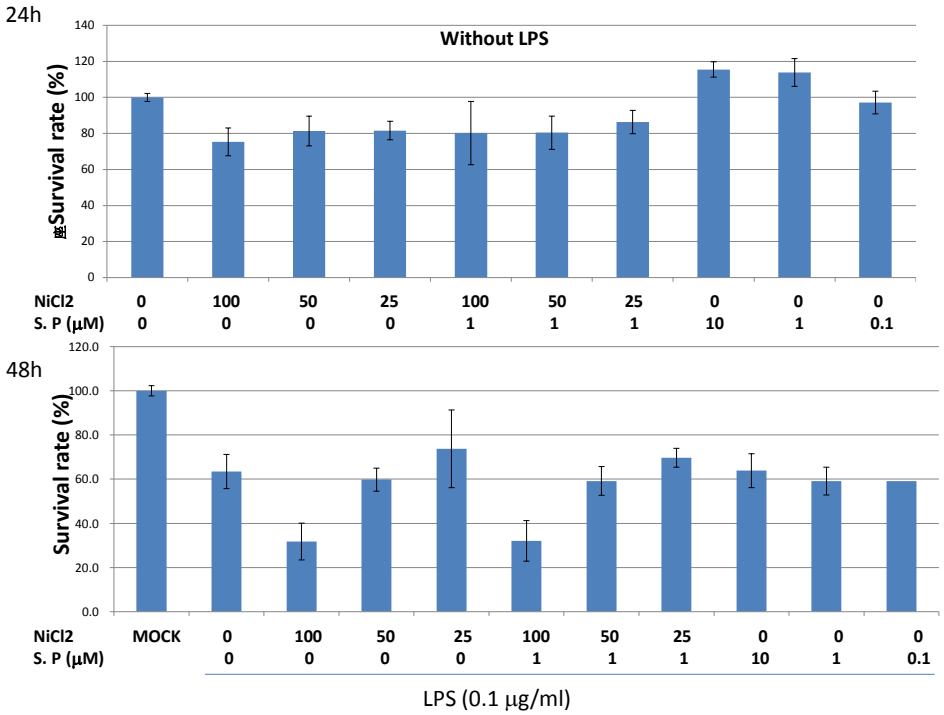

Fig. 1. Effect of $NiCl_2$ on the cell viability of RAW264.7 cells.

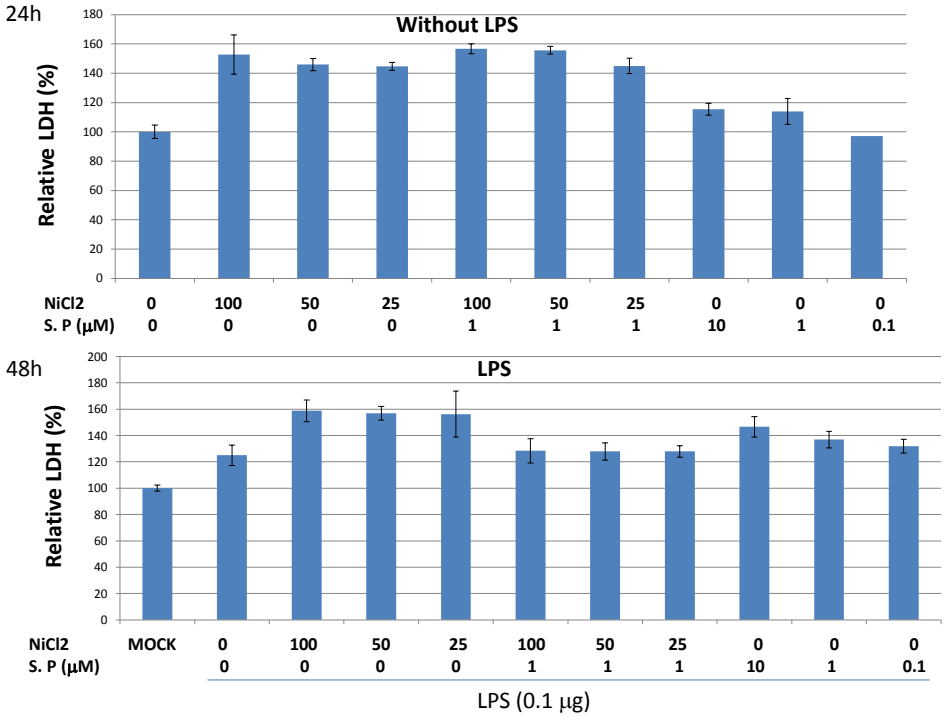

Fig. 2. Effect of $NiCl_2$ on the cytotoxicity of RAW264.7 cells.

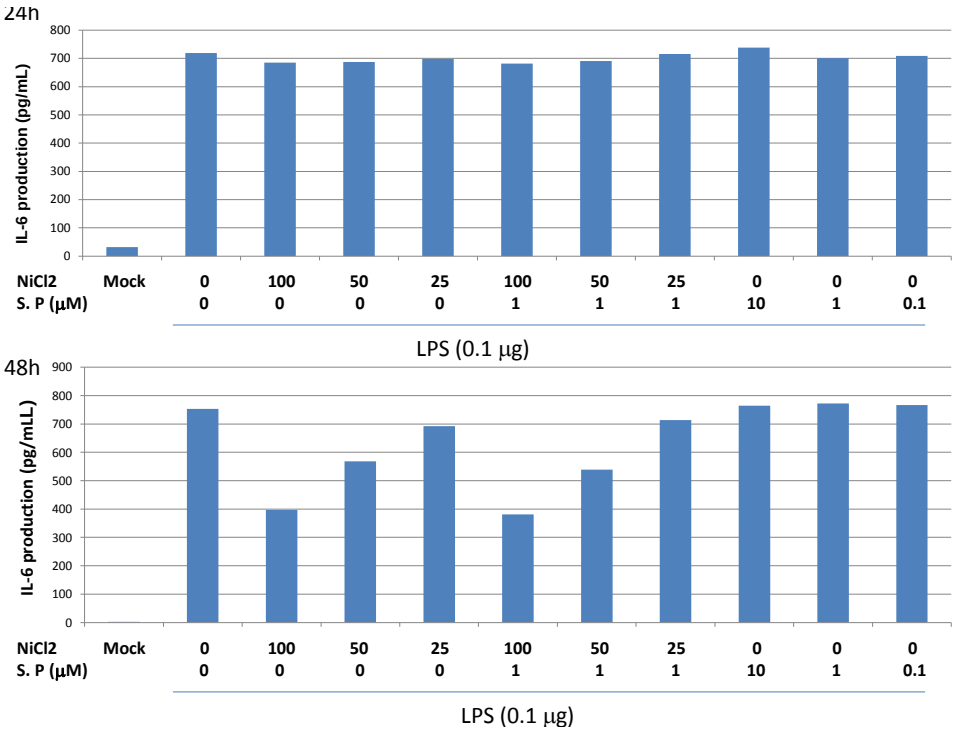

Fig.3. Effect of $NiCl_2$ on the secretion of IL-6 in RAW26.47 cells.

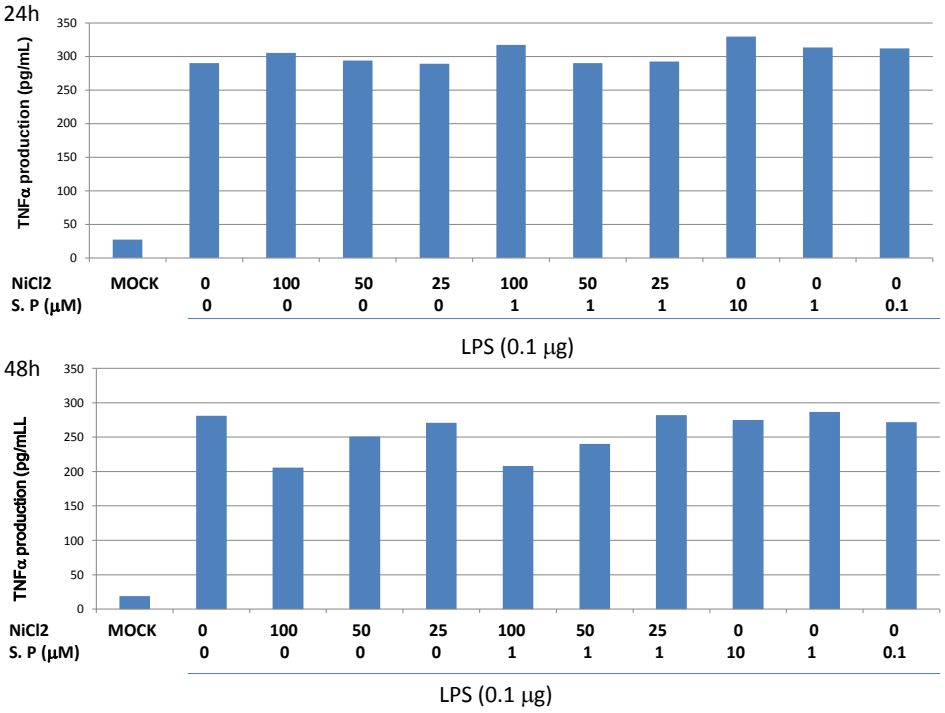

Fig.4. Effect of $NiCl_2$ on the secretion of TNFα in RAW26.47 cells.

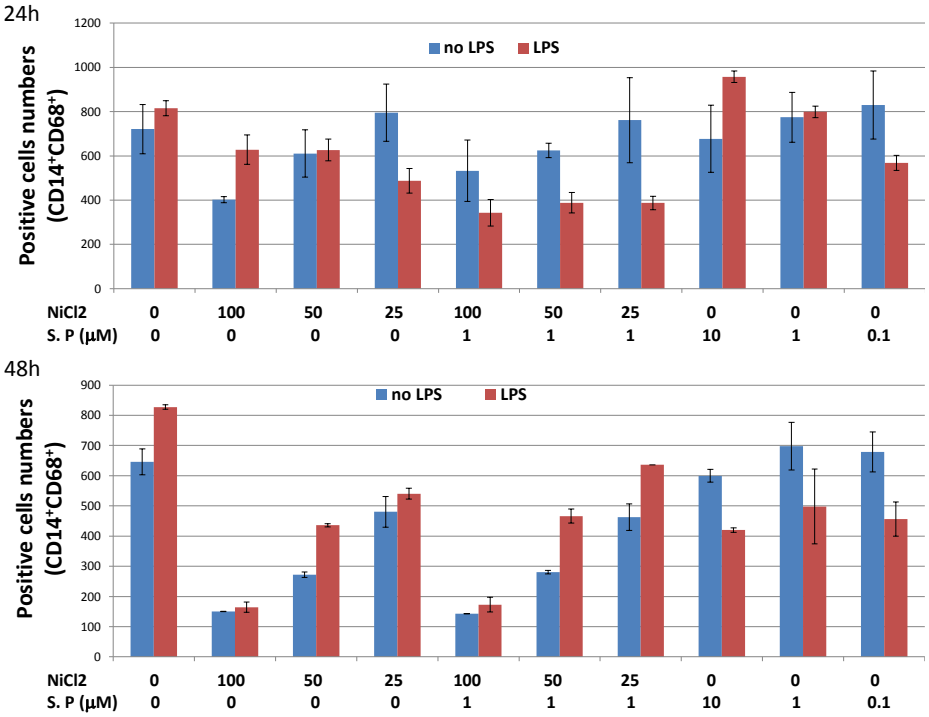

Fig.5. Effect of LPS on the expression of surface antigens (CD14$^+$/CD68$^+$) in RAW26.47 cells..

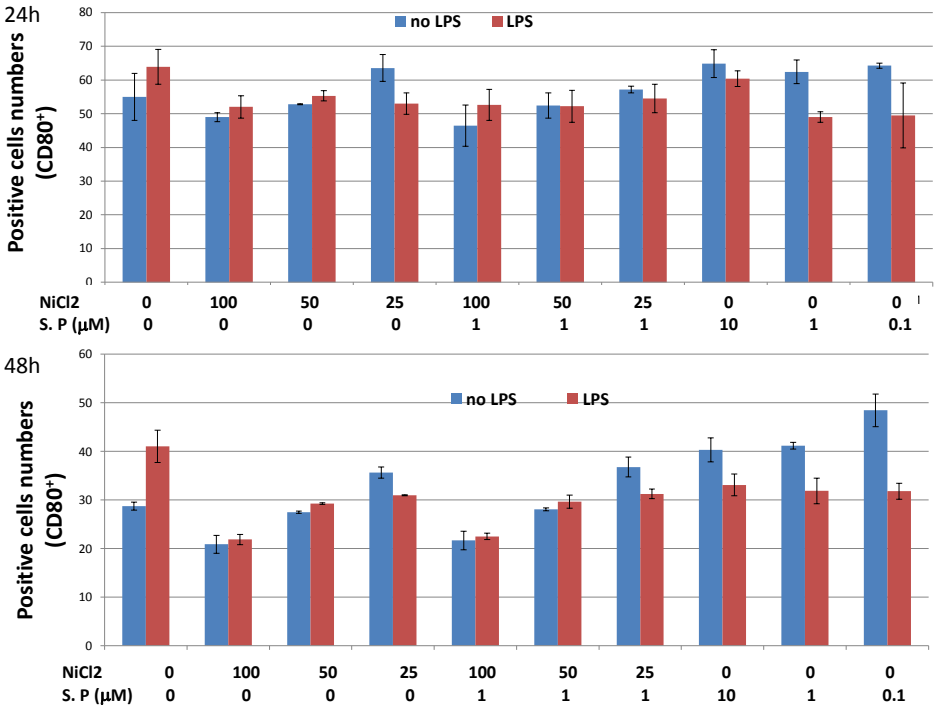

Fig.6. Effect of LPS on the expression of surface antigens (CD80) in RAW26.47 cells..

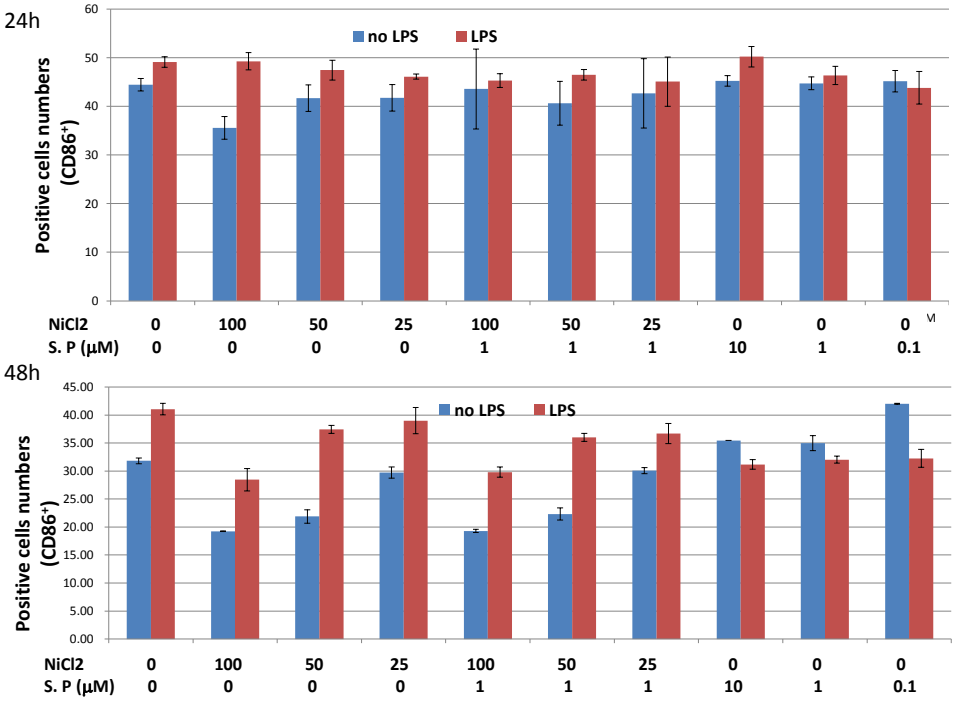

Fig.7. Effect of LPS on the expression of surface antigens (CD86**) in RAW26.47 cells..**

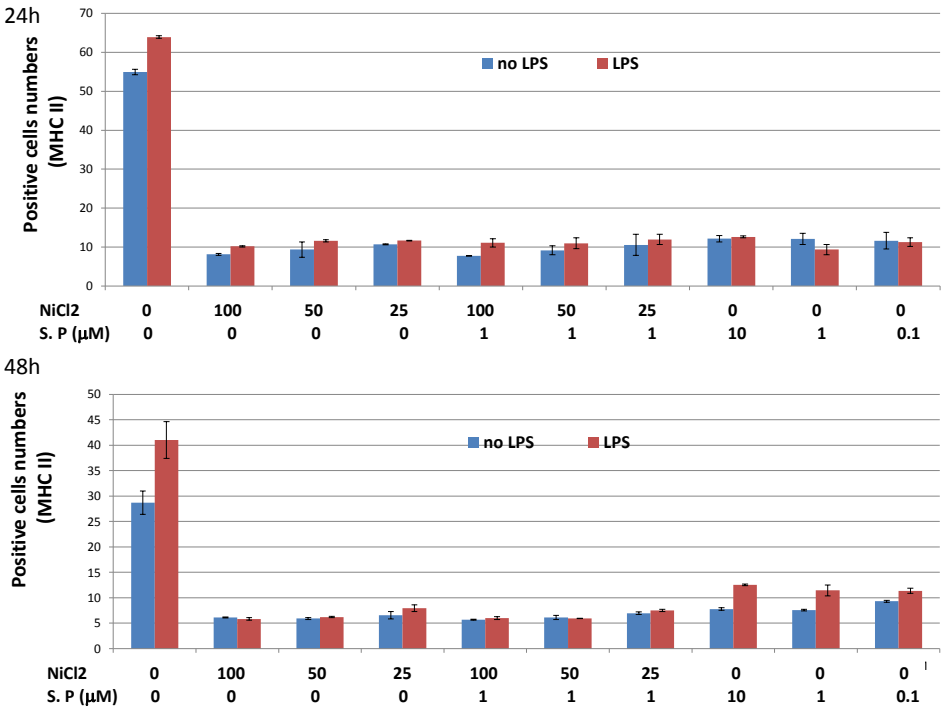

Fig.8. Effect of LPS on the expression of surface antigens (MHC II**) in murine macrophages.**

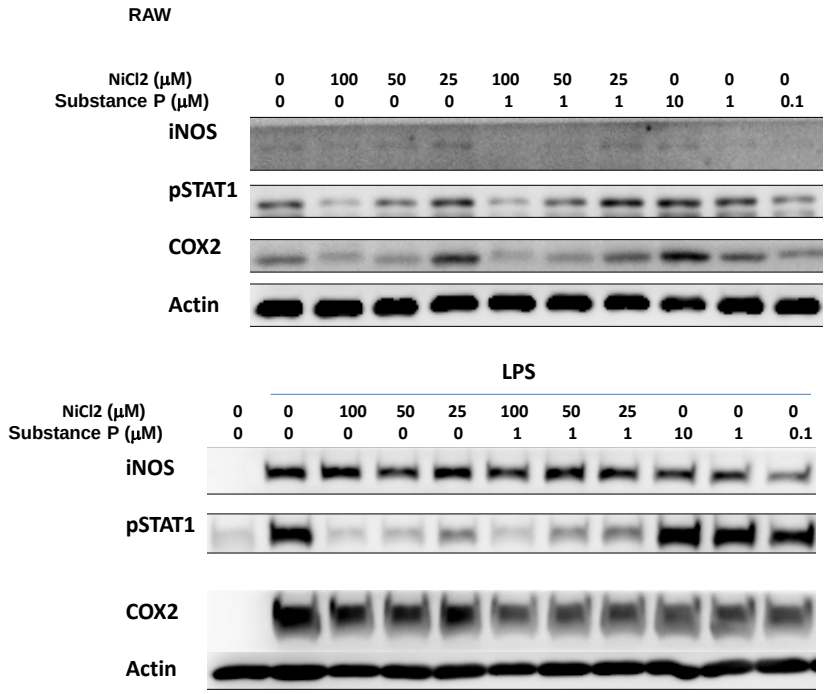

Fig. 9. Effects of $NiCl_2$ on iNOS、pSTAT1、COX-2 protein expression in RAW26.47 cells..

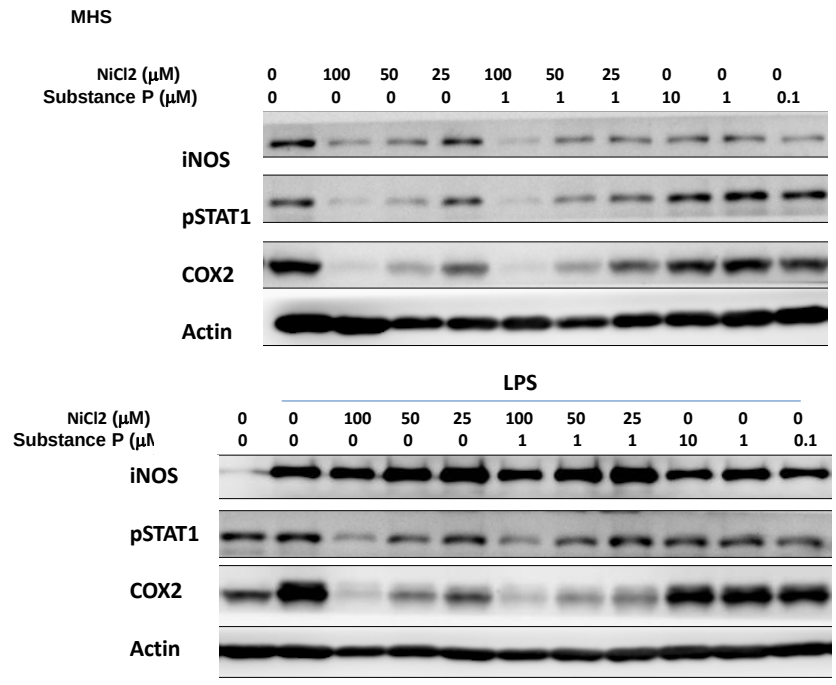

Fig. 10. Effects of $NiCl_2$ on iNOS、pSTAT1、COX-2 protein expression in MHS cells..

子計畫五

植化素之篩選及研究：抑制鎳經由 TLR4 誘發人類肺癌細胞侵犯及腫瘤化

Abstract

Nickel (Ni) is a pollutant commonly found in atmosphere. Studies showed that Ni-exposure promotes the invasive potential of human lung cancer cells through TLR4 signaling. The aims of this study were to investigate whether phytochemicals suppress the promoting effect of Nickel and the possible mechanisms. In the first year study we determined the effects of several phytochemicals, quercetin, curcumin, chrysin, apigenin, luteolin and two sesquiterpene aryl esters, on the invasion and migration in A549 and NCI-H1975 (H1975) cells exposed to $NiCl_2$. We found that all tested compound suppressed Ni-induced invasion, migration and the upregulation of inflammatory cytokines, especially quercetin and chrysin. In the second year study, we determined the possible mechanisms by which quercetin and chrysin exerted their effects. The results showed that Ni-exposure significantly increased the mRNA and protein expression of TLR4 and Myd88, the phosphorylation of IκB kinase (IKK) and IκB, the translocation of p65 and the MMP-9 expression and activation. Similar to TLR4 and IKKβ inhibitors, quercetin and chrysin suppressed all the effects of Ni in A549 cells. However, the dose effects of quercetin and chrysin were not significant in all parameters. In the third year study, we determined the effects of quercetin given by IP injection on the metastasis ability of A549 cells (treated with or without Ni) in nude mice. The results showed that quercetin administration (IP, 10 mg/kg, 3 times/week) decreased lung weights, the levels of TNF-α and IL-10 in the plasma and lung, lipid peroxidation and DNA damage in lymphocyte in two study models. These results support our in vitro findings, that is, quercetin suppresses the metastasis ability of lung cancer cells.

一、前言

鎳與台灣地區肺癌的罹患及發展可能有密切關連（Kuo et al., 2006），鎳誘發細胞惡性化發展的機制可能有許多，其中包括鎳對細胞 TLR4/NF-κB 路徑的促進作用而增加轉移的機會（Xu et al., 2011）。根據研究，許多植化素（phytochemicals）可能具有防範癌症發展的功效，其機制可能與調節細胞信號路徑有關(Bhaskar et al., 2011；Bae et al., 2011；Lee et al., 2007 ；Kao et al., 2011)。本計畫的假說是食物中的植化素可能透過對 TLR4/NF-κB 信號路徑的抑制作用抑制鎳誘發的肺癌細胞轉移，因此本計畫第一年的研究比較多種 phytochemicals 對鎳誘發的肺癌細胞激素分泌、細胞生長、侵犯性、移動性的影響，找出對鎳傷害具抑制作用的植化素進行接下來機制研究。因此在第二年的研究，我們探討 quercetin 及 chrysin 對 TLR4/NF-κB 信號路徑及 MMP 酵素的調節作用，我們並以 TLR4 抑制劑 CLI-095 及 IKK 抑制劑 SC-514 作為 positive control 來評估 quercetin 及 chrysin 的效果。第三年我們則以異體移植的動物模式，探討 quercetin 體內抑制轉移的可能性。

二、研究方法

1 第一年:利用人類肺癌細胞株 NCI-H1975 (H1975)，及 A549 細胞篩選出抑制鎳($NiCl_2$)誘發的細胞移動及侵犯性最佳之分子，並研究其對發炎因子及 ROS 生成的調節情形。細胞先以 5 μM phytochemicals (quercetin, curcumin, chrysin, apigenin, luteolin (Q, Cur, Chy, Api, Lut) 及兩種蜜球菌分離出之 sesquiterpene aryl esters (SA, SR)預培養 4 小時，之後經鎳暴露 12-24 h 後進行各項分析。

2 第二年:

以 quercetin，chrysin 與蜜球菌萃出物(2 or 5 μM)與 A549 細胞或 H1975 預培養 4 小時後，再以鎳(1 mM)培養一段時間。之後檢測 TLR4、Myd88 蛋白質及 mRNA 表現、以及 IKKβ 磷酸化 NF-κB 位移至細胞核內及 MMP-9 蛋白質及活性表現情形。我們並以 TLR4 抑制劑 CLI-095 及 IKK 抑制劑 SC-514 作為 positive control 來評估 quercetin 及 chrysin 的效果。

3. 第三年

我們移植鎳處理過或未處理的肺癌細胞到裸鼠體內，探討 quercetin(以腹腔注射給予)體內抑制肺癌細胞生長及轉移的效果。

研究分兩部分:

1.裸鼠入動物房適應 1 週後，隨機分為 3 組，經腹腔注射 (IP)給予 quercetin (10 mg/kg, 3 times/week，直至實驗結束)或 vehicle，1 週後，經尾靜脈注射 (IV)A549 細胞/Ni-treated A549 細胞 (細胞數 1 x 10^6 cells/100 μL)，每週 1 次，連續 3 週，實驗共為期 4 個月，其組別與各試劑給予情形如下：

1. C3: A549 cells only.
2. CN3: Ni-treated A549 cells only.
3. CN3Q: Ni-treated A549 cells + quercetin (IP, 10 mg/kg, 3 times/week, 25 μL 99.9% alcohol+175 μL normal-saline).

＊CN3 組及 CN3Q 組之 A549 細胞在注射前先以鎳培養 12 小時。

2.裸鼠入動物房適應 1 週後，隨機分為 2 組，經腹腔注射 (IP)給予 quercetin (10 mg/kg, 3 times/week，直至實驗結束)或 vehicle1 週後，經尾靜脈注射 (IV) A549 細胞 (細胞數 1 x 10^6 cells/100 μL)，每週給予 1 次，共給予 4 週，實驗共為期 7 週，其組別與各試劑給予情形如下：

1. C4: A549 cells only.
2. Q4: A549 cells + quercetin (IP, 10 mg/kg, 3 times/ week, 25 μL 99.9% alcohol+175 μL normal-saline).

＊本實驗所用 A549 細胞未經鎳處理。

三、結果討論

1. 第一年

我們的研究顯示 1 mM 鎳顯著誘發 H1975 及 A549 細胞移動及侵犯性(Fig1, 2)，但對細胞生長沒有顯著影響(Fig3)，另外鎳顯著增加細胞激素 TNF-α, IL-1β, IL-6 及 IL-10 的分泌(Fig4)以及 ROS 的生成量(Fig5)。而所有測試的植化素均在 5μM 濃度下均具顯著的抑制鎳的這些促進作用，與其他研究相比我們所使用的濃度較低，此濃度下對正常細胞一般不具毒性（Hayashi et al., 2012）。以細胞移動及侵犯性來看，整體而言 quercetin 的抑制效果最佳，其次為 chrysin 及 CH205R。我們所測試的 phytochemicals 抑制細胞移動與轉移的機制在兩株細胞中可能均與抑制細胞激素分泌有關，因為許多研究顯示促發炎激素 TNF-α, IL-1β, IL-6 會增加細胞的轉移侵犯性(Wang K, Karin M, 2015)，另外，本整體計畫之一子計畫發現肺癌細胞中 HPV E6 能透過 PI3K/AKT 訊號路徑增加 IL-10 的表現，進而透過 CIP2A 促進細胞侵襲和異種移植腫瘤的形成(Chiou et al., 2015) ，而與抑制細胞移動及侵犯性相似的，quercetin 抑制細胞激素分泌的效果可能是最好或與其他 phytochemicals 相當。第二個可能調節的機制是降低 ROS 的表現。另外對於 A549 細胞而言，phytochemicals 對細胞的生長抑制作用可能也有部分貢獻。

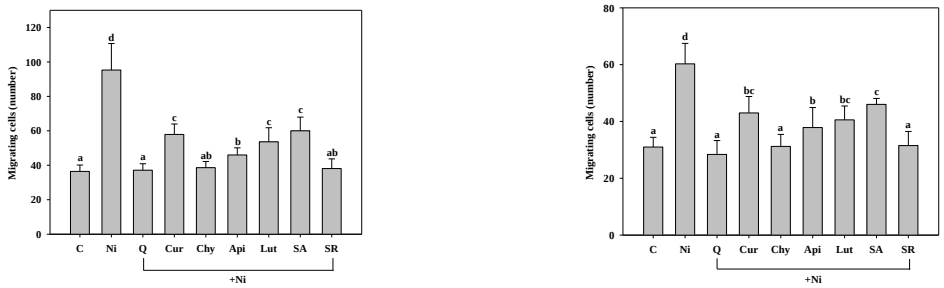

Fig. 1 Effects of phytochemicals on migration of nickel (Ni)-exposed H1975 (A) and A549 (B) cells. quercetin, curcumin, chrysin, apigenin, luteolin: Q, Cur, Chy, Api, Lut; two sesquiterpene aryl esters, SA and SR. Values (means ± SD, n=3) not sharing a common letter are significantly different (P<0.05).

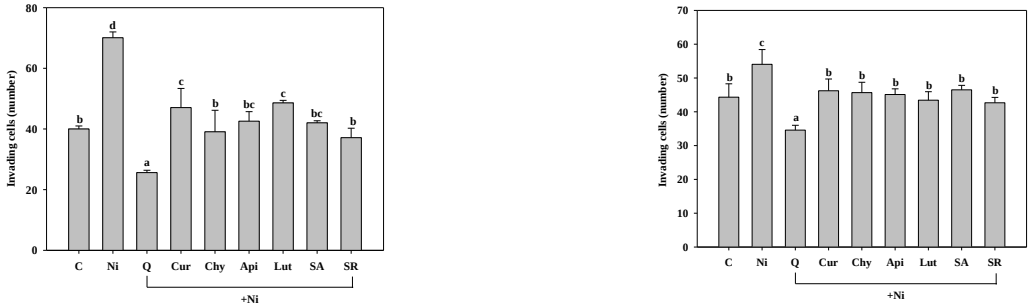

Fig. 2 Effects of phytochemicals on invasion of nickel (Ni)-exposed H1975 (A) and A549 (B) cells. The cells were pre-incubated with 5 μM phytochemicals (quercetin, curcumin, chrysin, apigenin, luteolin (Q, Cur, Chy, Api, Lut) and two sesquiterpene aryl esters (SA, SR)) for 4 h before Ni exposure for 12 h. Values (means ± SD, n=3) not sharing a common letter are significantly ifferent (P<0.05).

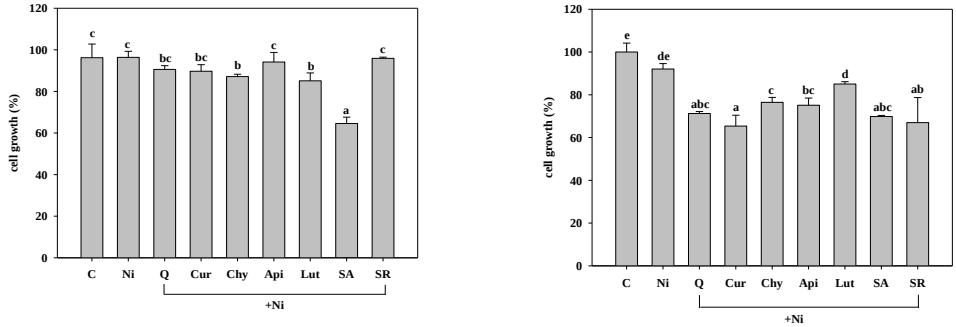

Fig. 3. Effects of phytochemicals on the growth of nickel (Ni)-exposed H1975 (A) and A549 (B) cells. The cells were pre-incubated with 5 μM phytochemicals (quercetin, curcumin, chrysin, apigenin, luteolin (Q, Cur, Chy, Api, Lut) and two sesquiterpene aryl esters (SA, SR)) for 4 h before nickel exposure for 12 h. Values (means ± SD, n=3) not sharing a common letter are significantly different (P<0.05)

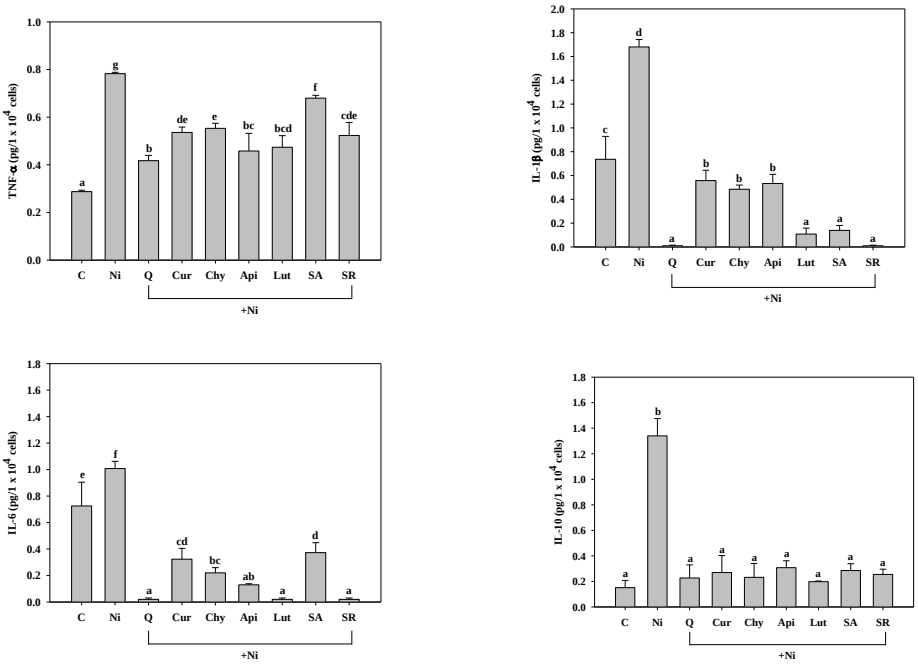

Fig. 4. The secretion of TNF-α (A), IL-1β (B), IL-6 (C) and IL-10 (D) in A549 cells. The cells were pre-incubated with 5 μM phytochemicals (quercetin, curcumin, chrysin, apigenin, luteolin (Q, Cur, Chy, Api, Lut) and two sesquiterpene aryl esters (SA, SR)) for 4 h before Ni exposure for 12 h. Values (means ± SD, n=3) not sharing a common letter are significantly different (P<0.05)

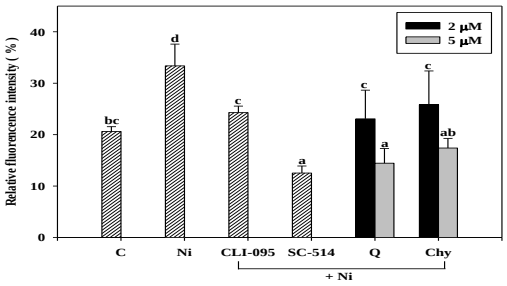

Fig.5 Effect of quercetin (Q), chrysin (Chy), CLI-095 and SC-514 on the production of ROS induced by nickel chloride (Ni) in the A549 cells.

第二年

與 Xu 等(2011）的研究結果一致的，本年度的研究顯示 1 mM 鎳亦顯著誘發 A549 細胞 TLR4 蛋白質及 mRNA 的表現約 30% (Fig. 6)，quercetin 及 chrysin 顯著的抑制鎳的促進作用，5 μM quercetin 及 chrysin 降低鎳誘發的 TLR4 蛋白質表現效果較 CLI-095 好（$p<0.05$）。對鎳促進 M yd88 蛋白質及 mRNA 表現的影響，與前面相似的，quercetin 及 chrysin 顯著的抑制鎳的促進作用(Fig. 7)，且二者的效果較 CLI-095 好。鎳暴露顯著的增加 IKK 及 IκB-α的磷酸化(Fig. 8, 9)，並顯著的增加 p65 轉移至細胞核內(Fig. 10)。quercetin 及 chrysin 均能抑制鎳所促進的 IKK 及 IκB-α磷酸化的作用，以及細胞內 p65 量的增加且對此項目的影響其效果較 TLR4 及 IKK 抑制劑佳($p<0.05$)。最後我們的結果顯示鎳暴露顯著的增加 MMP-9 活性及蛋白質表現量，而 quercetin 及 chrysin 亦具顯著的抑制作用(Fig. 11)。我們的研究顯示 quercetin 及 chrysin 可能藉由抑制 TLR4 及 Myd88 的表現以及 IKK 磷酸化及 NF-κB 轉移至細胞核，而減少 MMP9 的活化，進而降低肺癌細胞的轉移及侵犯性。此二植化素為何能調節這些相關訊號分子的表現目前機制尚不明確，有可能是透過對 ROS 的影響或直接對細胞訊號分子產生調節，另外有研究顯示 quercetin

可能透過有機陰離子運送 polypeptides 進入細胞並快速堆積在細胞核，並影響許多基因的轉錄(transcript)，受其調節的 transcripts 包括了調節，細胞週期、貼附、代謝、免疫相關分子及轉錄作用相關基因((Notas et al., 2012)。

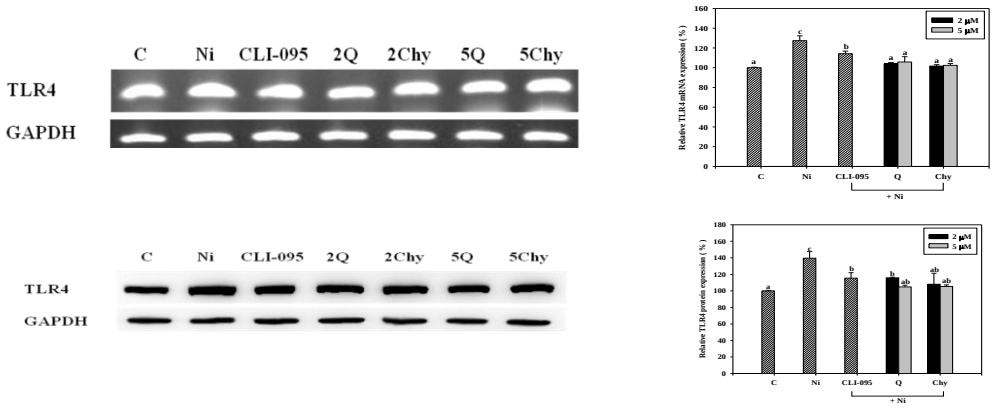

Fig.6. Effect of quercetin (Q), chrysin (Chy) and CLI-095 on the TLR4 mRNA (A) and protein (B) expression induced by nickel chloride (Ni) in the A549 cells.

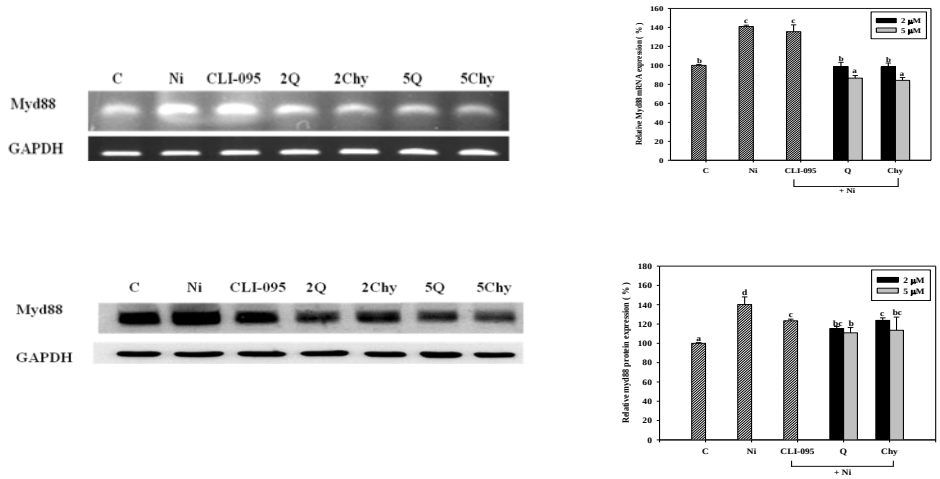

Fig.7. Effect of quercetin (Q), chrysin (Chy) and CLI-095 on the Myd88 mRNA (A) and protein (B) expression induced by nickel chloride (Ni) in the A549 cells.

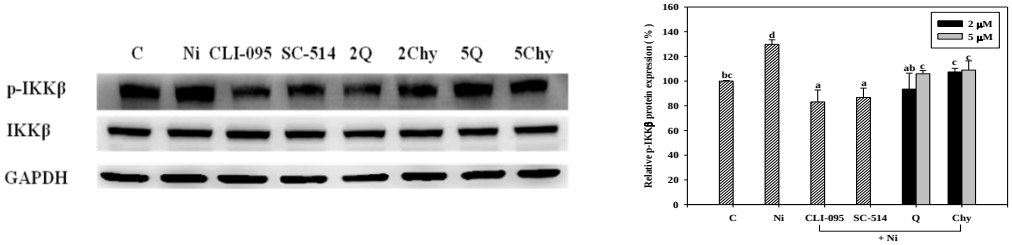

Fig.8. Effect of quercetin (Q), chrysin (Chy), CLI-095 and SC-514 on the p-IKKβ protein expression induced by nickel chloride (Ni) in the A549 cells. The values (mean ± SD, n=3) not sharing a common letter are significantly different (p<0.05).

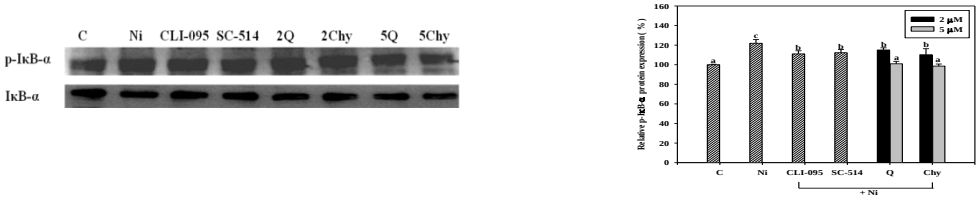

Fig.9. Effect of quercetin (Q), chrysin (Chy), CLI-095 and SC-514 on the p-IκB-α/IκB-α protein expression induced by nickel chloride (Ni) in the A549 cells. The values (mean ± SD, n=3) not sharing a common letter are significantly different (p<0.05).

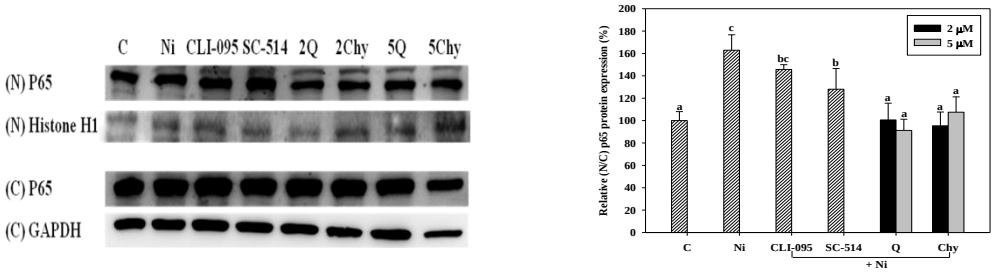

Fig.10. Effect of quercetin (Q), chrysin (Chy), CLI-095 and SC-514 on the p65 nuclear (N) protein expression induced by nickel chloride (Ni) in the A549 cells. The values (mean ± SD, n=3) not sharing a common letter are significantly different (p<0.05).

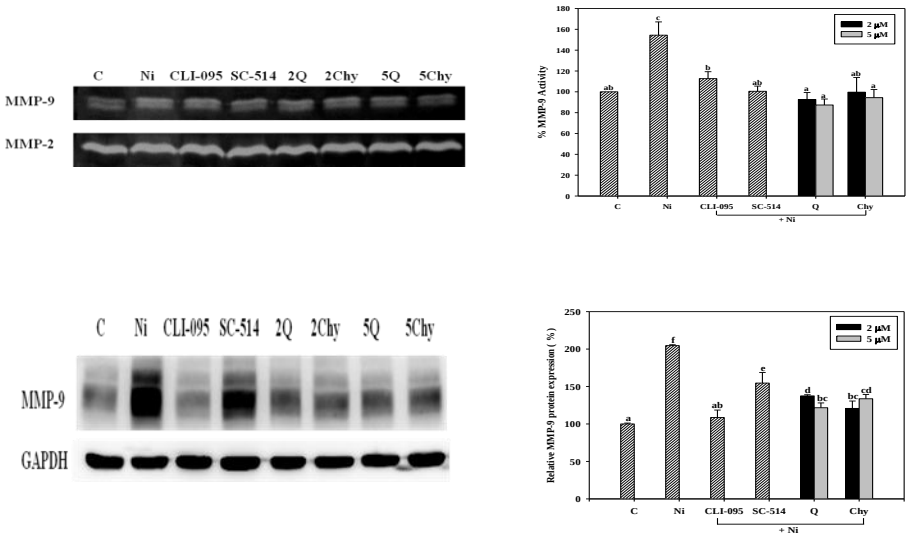

Fig.11. Effect of quercetin (Q), chrysin (Chy), CLI-095 and SC-514 on the MMP-9 activity (A), mRNA (B) and protein (C) expression induced by nickel chloride (Ni) in the A549 cells. The values (mean ± SD, n=3) not sharing a common letter are significantly different (p<0.05).

第三年

在體外研究，包括我們自己的研究，發現鎳可能促進癌細胞的移動及轉移 ，然而在此體內的第一部分

研究，結果卻顯示，肺癌細胞 A549 預先以鎳培養鎳 12 小時，再自尾靜脈注入裸鼠體內 (共 3 次，CN3 組)，並不如預期的降低裸鼠體重或是增加肺部腫瘤重量(CN3 組與 C3 組比)(Fig 12, 13)，初步推測這結果可能與鎳的細胞毒性有關，因為我們初步的研究發現，鎳與細胞預培養 12 小時雖未顯著降低細胞存活率，卻會降低其後續增生速度 (data not shown)。反之沒有預先鎳培養的 A549 增生較快，使得 C 組的體重明顯降低。而 quercetin 經腹腔注射雖有降低肺重量的趨勢但不顯著 (CN3Q 組與 CN3 組相比)。我們分析肺臟及血漿中 TNF-α及 IL-10 的含量，CN3 組裸鼠血漿中的細胞激素 TNF-α含量有顯著的增加，quercetin 的補充會降低此一現象，此結果與體外觀察到的現象一致(Fig 14)，但肺臟中 TNF-α含量則與血漿相反，推測可能因為在肺臟腫瘤組織取樣時 (腫瘤不均勻分布於肺臟)，混雜正常的肺臟組織，而導致 CN3 組中 TNF-α含量較低，而肺臟及血漿中 IL-10 的含量結果一致，CN3 顯著增加其含量(Fig 15)， 給予 quercetin 組中 IL-10 的含量則是顯著較低。另外我們也發現，CN3 組裸鼠白血球細胞 DNA 的傷害及 TBARs 較另外兩組嚴重(Fig 16)，顯示此組動物體內可能有較高的氧化壓力，而補充 quercetin 則具能降低氧化壓力，quercetin 的此一體內抗氧化能力可能是直接或間接的，我們實驗室先前的研究顯示，腹腔注射 quercetin 可以增加體內抗氧化酵素的表現 (Wu et al., 2015)。由於我們想確認沒有鎳的影響下，quercetin 體內抑制癌細胞轉移的情形，因此我們接著直接以未經鎳處理的 A549 細胞經尾靜脈注射 (注射 4 次)至裸鼠體內，並觀察 quercetin 對癌細胞在肺部生長及其他參數的影響，結果和體外觀察到的現象一致的，由腹腔注射給予 quercetin，會顯著降低肺部重量，亦即抑制 A549 細胞轉移侵犯至肺部(Fig 17)，同時也抑制住腫瘤生長所造成的 TNF-α (Fig 18)及 IL-10 (Fig 19)激素的分泌及氧化壓力增加的現象(Fig 20) 。以上了個動物研究除了證實 quercetin 可以抑制 A549 細胞體內的轉移，研究結果也顯示其機制胞含對 IL-10 產生的抑制作用，IL-10 被認為是一個與腫瘤增生及血管新生相關的重要指標 (Bermudez-Morales et al., 2008; Ren et al., 2009) ，另外研究也顯示 IL-10 的表現增加，會促進細胞侵襲和異種移植腫瘤的形成 (Chiou et al., 2015) 。

(Part 1)

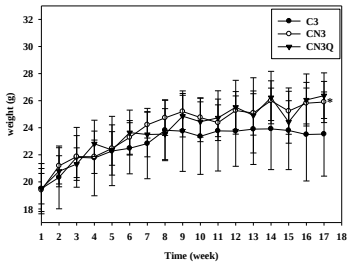

Fig.12. The lung weight of nude mice bearing Ni-treated A549 cells. The nude mice in C3 group were injected with A549 cells (1 x10^6/100 μL) by IV, while those in CN3 and CN3Q groups were injected with Ni-treated A549 cells. The mice in CN3Q were given quercetin (10 mg/kg; 3 times/week) by IP, while the others were given the vehicle only. There were no significant different among goups.

Fig.13. The lung weight of nude mice bearing Ni-treated A549 cells. The nude mice in C3 group were injected with A549 cells (1 x10^6/100 μL) by IV, while those in CN3 and CN3Q groups were injected with Ni-treated A549 cells. The mice in CN3Q were given quercetin (10 mg/kg; 3 times/week) by IP, while the others were given the vehicle only. There were no significant different among groups.

Fig.14. The level of TNF-αin plasma (A) and in lung (B) of nude mice. The nude mice in C3 group were injected with A549 cells (1 x 10^6/100 μL) by IV, while those in CN3 and CN3Q groups were injected with Ni-treated A549 cells. The mice in CN3Q were given quercetin (10 mg/kg; 3 times/week) by IP, while the others were given the vehicle only. * denotes there was a significant difference from C3 groups (p<0.05). # denotes there was a significant difference from CN3 groups (p<0.05).

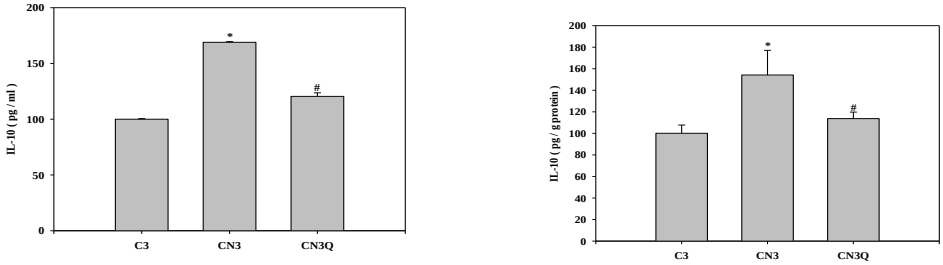

Fig.15. The level of IL-10 in plasma (A) and in lung (B) of nude mice. The nude mice in C3 group were injected with A549 cells (1 x 10^6/100 μL) by IV, while those in CN3 and CN3Q groups were injected with Ni-treated A549 cells. The mice in CN3Q were given quercetin (10 mg/kg; 3 times/week) by IP, while the others were given the vehicle only. * denotes there was a significant difference from C3 groups (p<0.05). # denotes there was a significant difference from CN3 groups (p<0.05).

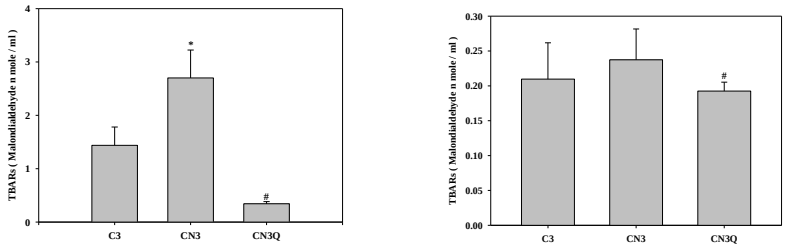

Fig.16. The level of TBARs in plasma (A) and in lung (B) of nude mice. The nude mice in C3 group were injected with A549 cells (1 x 10^6/100 μL) by IV, while those in CN3 and CN3Q groups were injected with Ni-treated A549 cells. The mice in CN3Q were given quercetin (10 mg/kg; 3 times/week) by IP, while the others were given the vehicle only. * denotes there was a significant difference from C3 groups (p<0.05). # denotes there was a significant difference from CN3 groups (p<0.05).

(part 2)

(A) (B)

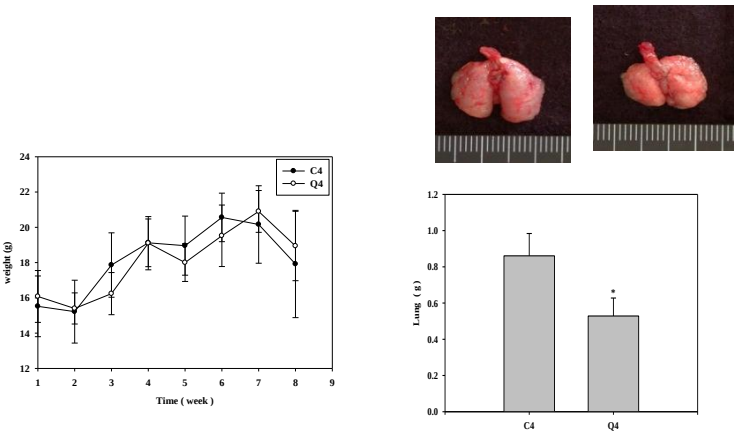

Fig.17. The effect of quercetin on the body weights (A) and lung weights (B) of nude mice. The nude mice were injected with A549 cells (1 x 10^6/100 μL) by IV. The mice in Q4 group were given quercetin (10 mg/kg; 3 times/week) by IP. * denotes there was a significant difference from C3 groups (p<0.05).

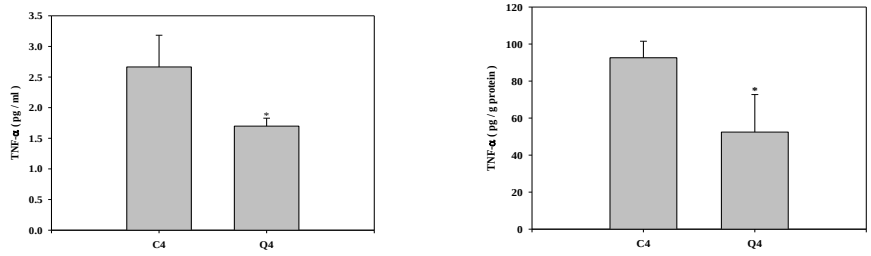

Fig.18. The level of TNF-α in plasma (A) and in lung (B) of nude mice. The nude mice were injected with A549 cells (1 x 10^6/100 μL) by IV. The mice in Q4 group were given quercetin (10 mg/kg; 3 times/week) by IP. * denotes there was a significant difference from C3 groups (p<0.05).

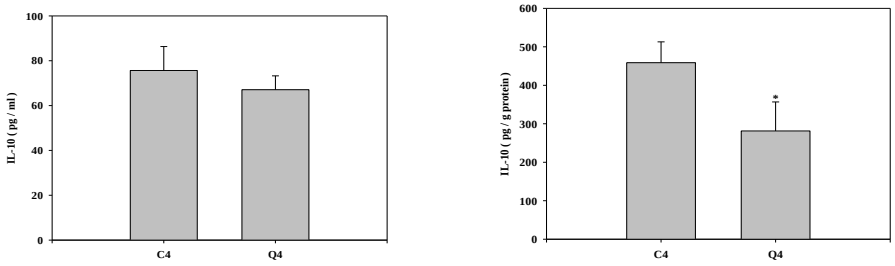

Fig.19. The level of IL-10 in plasma (A) and in lung (B) of nude mice. The nude mice were injected with A549 cells (1 x 10^6/100 μL) by IV. The mice in Q4 group were given quercetin (10 mg/kg; 3 times/week) by IP. * denotes there was a significant difference from C3 groups (p<0.05).

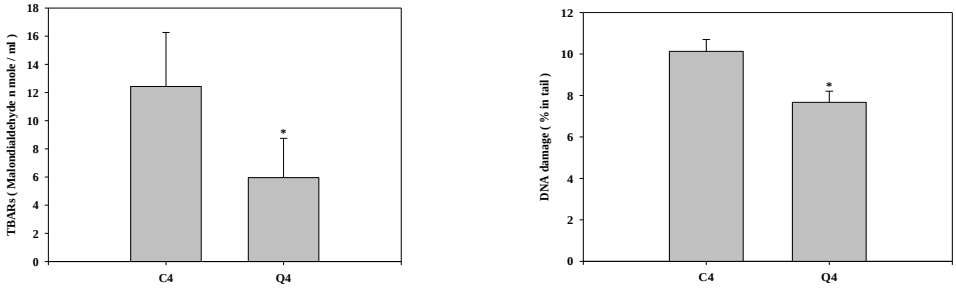

Fig.20. The level of TBARs in plasma (A) and in lung (B) of nude mice. The nude mice were injected with A549 cells (1 x 10^6/100 μL) by IV. The mice in Q4 group were given quercetin (10 mg/kg; 3 times/week) by IP. * denotes there was a significant difference from C3 groups (p<0.05).

References

Bae Y, Lee S, Kim SH. Chrysin suppresses mast cell-mediated allergic inflammation: involvement of calcium, caspase-1 and nuclear factor-κB. Toxicol Appl Pharmacol. 2011, 254:56-64.

Bermudez-Morales VH, Gutierrez LX, Alcocer-Gonzalez JM, Burguete A, Madrid-Marina V. Correlation between IL-10 gene expression and HPV infection in cervical cancer: a mechanism for immune response escape. Cancer Invest. 2008, 26(10):1037-43.

Bhaskar S, Shalini V, Helen A. Quercetin regulates oxidized LDL induced inflammatory changes in human PBMCs by modulating the TLR-NF-κB signaling pathway. Immunobiology. 2011, 216:367-73.

Chang CN. Quercetin and chrysin inhibit nickel-induced cell migration by regulating TLR4/ NF-κB signaling pathway in A549 cells. 2014, Master thesis, Shung shan Medical university.

Chiou YH, Liou SH, Wong RH, Chen CY, Lee H. Nickel may contribute to EGFR mutation and synergistically promotes tumor invasion in EGFR-mutated lung cancer via nickel-induced microRNA-21 expression. Toxicol Lett. 2015,;237:46-54.

Hayashi Y, Matsushima M, Nakamura T, Shibasaki M, Hashimoto N, Imaizumi K, Shimokata K, Hasegawa Y, Kawabe T. Quercetin protects against pulmonary oxidant stress via heme oxygenase-1 induction in lung epithelial cells. Biochem Biophys Res Commun. 2012, 417:169-74.

Kao TK, Ou YC, Lin SY, Pan HC, Song PJ, Raung SL, Lai CY, Liao SL, Lu HC, Chen CJ. Luteolin inhibits

cytokine expression in endotoxin/cytokine-stimulated microglia. J Nutr Biochem. 2011, 22:612-24.

Kuo, C.Y., Wong, R.H., Lin, J.Y., Lai, J.C. & Lee, H. Accumulation of chromium and nickel metals in lung tumors from lung cancer patients in Taiwan. *Journal of toxicology and environmental health. Part A* 69, 1337-1344 (2006).

Lee JH, Zhou HY, Cho SY, Kim YS, Lee YS, Jeong CS. Anti-inflammatory mechanisms of apigenin: inhibition of cyclooxygenase-2 expression, adhesion of monocytes to human umbilical vein endothelial cells, and expression of cellular adhesion molecules. Arch Pharm Res. 2007, 30:1318-27.

Notas G, Nifli AP, Kampa M, Pelekanou V, Alexaki VI, Theodoropoulos P, Vercauteren J, Castanas E. Quercetin accumulates in nuclear structures and triggers specific gene expression in epithelial cells. J Nutr Biochem. 2012, 23(6):656-66.

Ren T, Xu L, Jiao S, Wang Y, Cai Y, Liang Y, Zhou Y, Zhou H, Wen Z.. TLR9 signaling promotes tumor progression of human lung cancer cell in vivo. Pathol Oncol Res. 2009, 15(4):623-30.

Wang K, Karin M. Tumor-Elicited Inflammation and Colorectal Cancer. Adv Cancer Res. 2015, 128:173-96.

Wu TC, Huang SY, Chan ST, Liao JW, Yeh SL. Combination of β-carotene and quercetin against benzo[a]pyrene-induced pro-inflammatory reaction accompanied by the regulation of antioxidant enzyme activity and NF-κB translocation in Mongolian gerbils.Eur J Nutr. 2015, 54:397-406.

Xu Z, Ren T, Xiao C, Li H, Wu T. Nickel promotes the invasive potential of human lung cancer cells via TLR4/MyD88 signaling. Toxicology. 2011, 285:25-30.

(二)計畫執行迄今之成果(請具體明列成果項目，如：論文/專利/重大突破/或其他…)

1. 計畫執行至今有相當好的學術成果除了參加國內外學術研討會報導成果外，目前已有 6 篇論文發表在 SCI 期刊上，1 篇修改中， 另有 4 篇投稿中。另外還出版了 5 本碩博士論文(如下列)。

本計畫 SCI 論文及學位論文發表情況

SCI 論文

(1). Chiou YH, Liou SH, Wong RH, Chen CY, Lee H. Nickel may contribute to EGFR mutation and synergistically promotes tumor invasion in EGFR-mutated lung cancer via nickel-induced microRNA-21 expression. Toxicology Letters 2015(237):46-54.

(2). Tung MC, Lin PL, He TY, Lee MC, Yeh SD, Chen CY, Lee H.Mutant p53 confers chemoresistance in non-small cell lung cancer by upregulating Nrf2. Oncotarget 2015(6):41692-41705.

(3). Chou YH, Wong RH, Chao MR, Chen CY, Liou SH, Lee H.Nickel accumulation in lung tissues is associated with increased risk of p53 mutation in lung cancer patients. Environ and Mol Mutagen 2014(55):624-632.

4. Sung WW, Wang YC, Lin PL, Cheng YW, Chen CY, Wu TC, Lee H.IL-10 Promotes Tumor Aggressiveness via Upregulation of CIP2A Transcription in Lung. Adenocarcinoma Clinical Cancer Research 2013(19):4092-4103.

5. Lin HW, Chen YC, Liu CW, Yang DJ, Chen SY, Chang TJ, and Chang YY. Regulation of virus-induced inflammatory response by Dunaliella salina alga extract in macrophages. Food and Chemical Toxicology 2014(71):159-165.

6. Tang SC, Wu CH, Lai CH, Sung WW, Yang WJ, Tang LC, Hsu CP and Ko JL. Glutathione S-transferase mu2 suppresses cancer cell metastasis in non-small cell lung cancer. American Association for Cancer Research 2013(5):518-29. (同時被 Editor 選為 High light issue)

7. Upregulation of microRNA-4417 and Its Target Genes Contributes to Nickel Chloride-promoted Lung Epithelial Cell Fibrogenesis and Tumorigenesis. Archives of Toxicology, current state：revision

學位論文

1.宋文瑋/IL-10 和 FasL 在非小細胞肺癌患者之腫瘤進展和臨床預後之角色/中山醫學大學/醫學研究所/民國 100 年/博士論文。

2. 探討氯化鎳透過活性氧誘導上皮-間質型態轉換與細胞自噬之表觀遺傳機制；中山醫學大學/醫學研究所/102/博士 研究生：吳芝嫻

3.邱育瑚/鎳暴露與台灣肺癌之 p53 與 EGFR 基因突變的相關性研究/中山醫學大學/醫學研究所/民國 103 年/博士論文

4.張致寧/Quercetin 及 chrysin 透過調節 TLR4/NF-κB 信號路徑抑制鎳促進 A549 細胞之轉移/中山醫學大學/營養所/民國 103 年/碩士論文

5.余佩璇/蜜環菌萃出的 sesquiterpene aryl ester 抑制鎳誘發 A549 及 H1975 細胞侵犯及轉移經由向下調節 TLR4/NF-κB/中山醫學大學/營養所/民國 103 年/碩士論文

2. 最主要的突破在於對肺癌與空氣汙染物鎳的相關性，及肺癌轉移、發展有更清楚的認識，可提供未來公共衛生的防制參考。另外對植化素的保護作用的研究

3. 本計畫共有 5 名博士生 11 名碩士生參與，對學生研究能力的訓練有非常大的助益。

(三)請說明計畫執行迄今經費運用狀況(含大型設備之購置狀況)及學校配合款支用情形。

本計畫之經費包括業務費、出國差旅費均按規定運用，學校亦按規定提供 20%之配合款，由於有學校貴儀中心的配合運作，本計畫並沒有購買大型儀器。經費運用情形如已繳交至科技部之報表，末頁附表一。

(四)經費使用表：支用金額請統計至該年度計畫截止日

年　度	第一年			第二年			第三年		
項　目	科技部補助		學校配合款使用情形	科技部補助		學校配合款使用情形	科技部補助		學校配合款使用情形
	核定金額	使用金額		核定金額	使用金額		核定金額	使用金額	
金　額	5000000	5000000	1375000	5000000	5000000	1375000	5000000	5000000	1374490

說　明：學校均按規定提撥 20%配合款，並要求 PI 優先使用，唯第三年由於略有報帳上的疏失，因此配合款使用短少 510 元，使用達成率 99%。

二、團隊研究能力：總計畫與各子計畫之間的分工架構、整合性及工作協調為何？(請提出具體作法說明)。

本計畫之核心議題及分工架構如下:

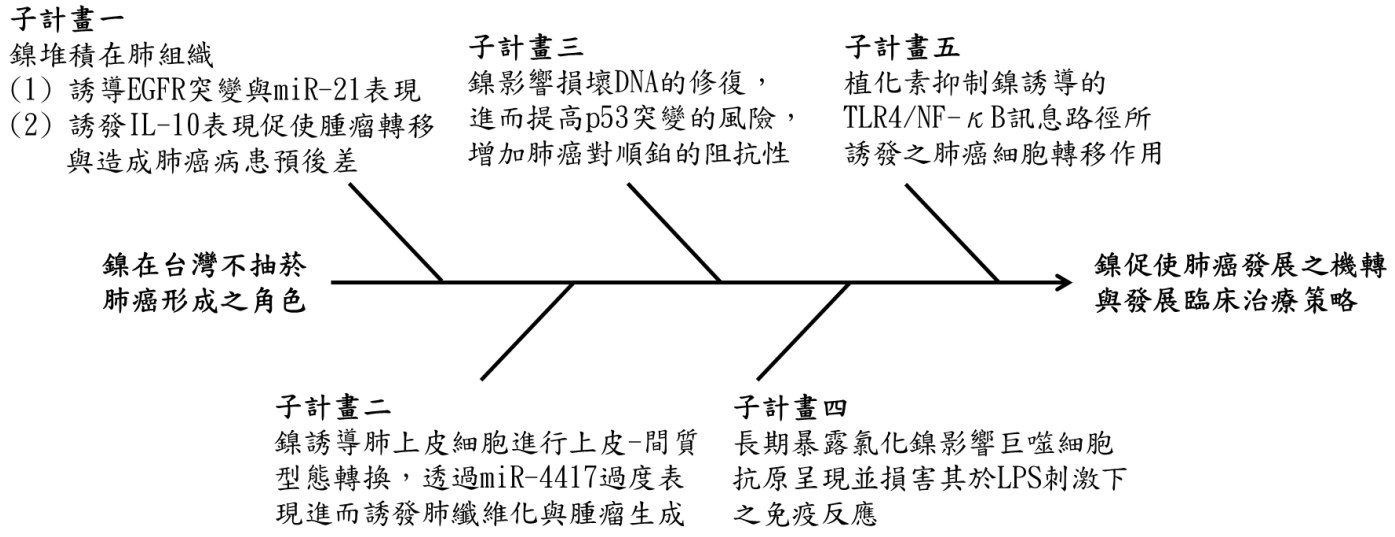

本整合型計畫是一個透過基礎研究團隊與附設醫院醫療團隊結合基礎與臨床之研究，團隊成員在研究成果及技術上互相討論支援，例如分子技術及動物研究技術的支援等，有助各子計畫的研究進展。吳子卿教授及王耀震醫師結合基礎研究室分析研究臨床肺癌病患檢體，探討未抽菸的病人中，鎳累積的情形及可能之致病機制及可能的預後，相關結果有部分已發表。而柯俊良教授及張元衍教授則分別藉由細胞或動物研究探討鎳暴露增加細胞轉移的分子機制，發現誘發 GST 啟動子 CpG 島上過度甲基化而使 GST-M2 及 E-cadherin 喪失、增加 miR-4471 與抑制其標靶基因 TAB2 表現、及對發炎反應的調控是重要的分子機制。另外我們的子計畫五中，葉姝蘭教授研究近年非常受矚目的保健素材植化素抑制鎳誘發的肺癌細胞轉移的能力及機轉，篩檢出數種具有保健潛力的分子。

近年來台灣空氣品質日趨惡化，懸浮微粒($PM_{2.5}$)濃度飆高，$PM_{2.5}$ 已被證實對肺部健康有相當不良的影響，本校公衛研究團隊發現 $PM_{2.5}$ 其中金屬離子鎳的含量最高，因此，本研究成果研不僅奠定本校在癌症研究上的研究能量，並且將有助於後續更深入探討台灣空氣汙染 $PM_{2.5}$ 所誘導的支氣管炎、氣喘與肺癌等發展，並有效提供預防與治療策略。

三、學校方面：

(一)學校提供之具體配套措施(如：配合款；相關行政、空間、設備等之支援及協助；獎勵等)，請提出已配合之措施辦法或具體資料證明。

學校提供 20% 配合款，優先作為耗材費用，另方面本校貴儀中心(提供實驗所需之儀器，包含：高速離心機、流式細胞儀、定量 PCR、數位化影像處理系統、冷光螢光數位影像分析系統等)，及動物中心配合提供了相當好的設備、協助及管理，有助學生學習及研究進行。另外對於論文的發表，校方亦提供獎勵金。

(二)學校對本計畫是否訂有考核機制？如有請列出，及考核結果為何？

1. 學校在計畫申請之初，即由研發處評核計畫內容，並訂定補助順位，本計畫為第一順位補助計畫。
2. 提醒催繳期中報告，並依報告繳交否，決定是否繼續補助。

(三)本計畫執行至今對於學校推展或提升研發環境有何具體成效？

癌症研究原本就是本校的特色研究項目之一，因此設有癌症研究中心，本研究成果研不僅增加本校在癌症研究上的研究能量，證實鎳汙染對肺癌的影響，並且將有助於後續更深入探討台灣空氣汙染 $PM_{2.5}$ 所誘導的支氣管炎、氣喘與肺癌等發展，並有效提供預防與治療策略。

成果報告自評表

請就研究內容與原計畫相符程度、達成預期目標情況、研究成果之學術或應用價值（簡要敘述成果所代表之意義、價值、影響或進一步發展之可能性）、是否適合在學術期刊發表或申請專利、主要發現（簡要敘述成果是否有嚴重損及公共利益之發現）或其他有關價值等，作一綜合評估。

1. 請就研究內容與原計畫相符程度、達成預期目標情況作一綜合評估

Ｖ達成目標

□ 未達成目標（請說明，以 100 字為限）

□ 實驗失敗

□ 因故實驗中斷

□ 其他原因

說明：

2. 研究成果在學術期刊發表或申請專利等情形：

論文：Ｖ已發表?篇 Ｖ未發表之文稿 3 篇 Ｖ撰寫中 1 篇

專利：□已獲得 □申請中 □無

技轉：□已技轉 □洽談中 □無

其他：（以 100 字為限）

3. 請依學術成就、技術創新、社會影響等方面，評估研究成果之學術或應用價值（簡要敘述成果所代表之意義、價值、影響或進一步發展之可能性），如已有嚴重損及公共利益之發現，請簡述可能損及之相關程度（以 500 字為限）

肺癌近年來一直是國人十大癌症死因中的首要原因，其不易在罹患初期察覺，而病患晚期的5年存活率偏低，另外，近年來國人罹患率增加，患者年齡下降，顯示這個疾病的成因及防範是一個相當需要加緊研究的議題。本校的肺癌研究團隊及其他研究人員發現病毒及空氣汙染物中的鎳可能是肺癌的重要成因之一，例如肺部健康的重要殺手-空氣細懸浮微粒(以下簡稱PM2.5)即含有大量鎳。，

我們在鎳誘發的肺癌細胞病變及轉移機制的重大發現包括:
(1)在未抽菸的病人中，鎳累積在肺組織與EGFR的突變、miR21表現及較差的預後較差是有相關性的。此外，在肺腺癌HPV-16/18 E6呈陽性的腫瘤當中，IL-10調控CIP2A表現增加與增加癌細胞的侵犯相關。(2) 長期的鎳暴露誘發GST啟動子CpG 島上過度甲基化而使GST-M2及E-cadherin喪失，進而促進細胞擴散，氯化鎳藉由增加miR-4471與抑制其標靶基因TAB2表現，進而誘發細胞的纖維化。(3) 鎳藉由損壞DNA修復，而增加p53突變的風險，特別在未抽菸的女性當中。 (4) 活性氧及肺C纖維在氯化鎳引起的肺慢性發炎上扮演相當重要的角色，阻斷ROS產生或破壞肺C纖維功能，能抑制鎳在動物所引起的較大呼吸暫停反應與肺發炎現象，鎳會向下調控巨噬細胞表現抗原的表現，長時間暴露在氯化鎳下亦會損害巨噬細胞在LPS刺激下的基本功能。這些利用臨床檢體或體內外研究或體內外研究對於鎳於肺癌相關性確認，有助於制定公共衛生防範策略，而對於鎳促進癌分子轉移機制的闡明，有助於吾人在未來治療策略的研究。另外我們的一個子計畫發現數種植化素能夠抑制鎳誘發肺癌細胞侵犯轉移的情形，特別是槲皮酮及白楊素。在異腫瘤移植裸鼠中，槲皮酮亦能顯著的抑制肺癌細胞的轉移。顯示適當的飲食或補充劑可能有助於抑制肺癌細胞轉移，若能進一步於臨床研究證實，將提供國人可行之防範策略。

除臨床實用性，這些研究成果也都有相當好的學術價值，如前述已有良好的發表，其中柯俊良老師發表於 Molecular Cancer Research;11(5);1–12. 2013AACR 的研究，被 Editor 選為當期 High light issue。

科技部

補助專題研究計畫經費收支明細報告表

主持人： 吳子卿　　執行機關：中山醫學大學醫學系

計畫編號： NSC 101-2632-B-040-001-MY3

計畫名稱： 鎳在台灣不抽菸肺癌形成之角色,-鎳在台灣不抽菸肺癌之角色

執行期限： 101/08/01~104/07/31

製表日期：105/02/04

金額單位：新臺幣元

補助項目	核定金額	收付數					備註
		實收金額 (A)	支出憑證起訖號碼		實付金額 (B)	結餘金額 (C=A-B)	
			起號	訖號			
業務費	13,921,000	13,921,000	001	630	14,301,740	-380740	一、研究人力費：4,678,575元。二、耗材、物品及雜項費用：9,623,165元。國外差旅費流入至業務費398,000元(依科技部103年08月18日科部綜字第1030060809號函辦理)。
國外差旅費	528,000	528,000	631	632	130,000	398,000	國外差旅費流出至業務費398,000元(依科技部103年08月18日科部綜字第1030060809號函辦理)。
管理費	2,051,000	2,051,000	633	635	2,051,000	0	
合計	16,500,000	16,500,000	校務基金 0		16,482,740	17,260	學校配合款三年實支金額4,124,490元。

＊執行機構如報經本部同意轉撥研究計畫部分經費至共同主持人任職之機構執行，依本部補助專題研究計畫經費處理原則第七點規定，計畫主持人應於收支報告表簽章，以瞭解該計畫全部經費支用情形。

＊執行率：99 %，原因：無

＊國外差旅費繳回新臺幣0 元，執行情形說明：無

參展論文摘要

Quercetin enhances the vorinostat-induced apoptosis in H1299 cells through uprequlation of p300 protein expression

Shu-Ting Chan, Shu-Lan Yeh
Department of Nutritional Science, Chung Shan Medical University, Taichung, Taiwan.

Our previous study showed that quercetin enhances the growth-arrest effect of TSA, a histone deacetylase inhibitor, in H1299 cells (p53 null mutant) through a p53-independet pathway. However, the mechanisms are unclear. In the present study, we investigated the enhancing effect of quercetin on the apoptosis in H1299 cells exposed to vorinostat, a FDA proved histone deacetylase inhibitor for cancer treatment. We also investigated the role of the acetylation of histone H3 and H4 in the enhancing effect of quercetin. H1299 cells were incubated with vorinostat (200 ng/mL equal to 757 nM) alone or in combination with quercetin (5 μM) for the various times. Then, cell growth, apoptosis, the expression of DR-5, p300 and acetyl-histones as well as the activities of caspase10/3 were determined. We found that quercetin significantly increased the growth arrest and apoptosis in H1299 cells exposed to vorinostat at 72 h by about 40%. Vorinostat in combination with quercetin also significantly increased the protein expression of DR-5 and caspase-10/3 activities in H1299 cells compared with the group treated with vorinostat alone. In addition, vorinostat in combination with quercetin rather than vorinostat alone significantly increased the expression of p300 (a histone acetyltransferase). Transfection of *p300* siRNA significantly diminished the increase of histones H3/H4 acetylation, DR5 protein expression, caspase-10/3 activity and apoptosis induced by quercetin in H1299 cells exposed to vorinostat. In conclusion**,** these data indicates that the upregulation of p300 expression, which in turn increases histone acetylation, plays an important role in the enhancing effect of quercetin on vorinostat-induced apoptosis in H1299 cells.

Key word: quercetin, vorinostat, p300, H1299

本次研討會”12th Asian Congress of Nutrition” 在日本橫濱舉辦，大會的研討主題是 Nutrition and Food for longevity: for the well-being of all.

1.大會一共安排了 40 場 symposium

主題包括

New Insights in Vitamin Metabolism and Function
Basic and Clinical Aspects of Amino Acid Sciences
Asian Herbal and Medicinal Food for the Prevention of Lifestyle-related Diseases
The Cutting Edge of Mineral Nutrition: Physiological and Molecular Perspectives
Challenges of Scaling Up Nutrition Intervention to Achieve the Development Goal
Selection of Dietary Assessment Method in Accordance with the Purpose
Research and Development of Functional Foods: Study Cases of Food Science and Technology

2.**還有**13**場的**Educational lecture

主題包括對抗老化、青春期肺胖的影響、進康促進的分子機制、營養標準、慢性營養不良問題、營養與基因體學問題等相當精彩豐富

3.另外大會還安排參觀學校午餐計畫、安養中心的照護供參等，讓與會人士獲益良多

科技部補助計畫衍生研發成果推廣資料表

日期:2015/10/28

科技部補助計畫	計畫名稱: 鎳在台灣不抽菸肺癌之角色
	計畫主持人: 吳子卿
	計畫編號: 101-2632-B-040-001-MY3　　學門領域: 藥理及毒理

無研發成果推廣資料

101年度專題研究計畫研究成果彙整表

計畫主持人：吳子卿	計畫編號：101-2632-B-040-001-MY3
計畫名稱：鎳在台灣不抽菸肺癌之角色	

成果項目			量化			單位	備註（質化說明：如數個計畫共同成果、成果列為該期刊之封面故事...等）
			實際已達成數（被接受或已發表）	預期總達成數（含實際已達成數）	本計畫實際貢獻百分比		
國內	論文著作	期刊論文	0	0	100%	篇	
		研究報告/技術報告	0	0	100%		
		研討會論文	5	5	100%		
		專書	0	0	100%	章/本	
	專利	申請中件數	0	0	100%	件	
		已獲得件數	0	0	100%		
	技術移轉	件數	0	0	100%	件	
		權利金	0	0	100%	千元	
	參與計畫人力（本國籍）	碩士生	11	11	100%	人次	
		博士生	5	5	100%		
		博士後研究員	1	1	100%		
		專任助理	2	2	100%		
國外	論文著作	期刊論文	6	9	70%	篇	一篇論文刊登於Molecular cacner Research, 2013, 11(5):1-12被列為high light issue.
		研究報告/技術報告	0	0	100%		
		研討會論文	3	3	100%		
		專書	0	0	100%	章/本	
	專利	申請中件數	0	0	100%	件	
		已獲得件數	0	0	100%		
	技術移轉	件數	0	0	100%	件	
		權利金	0	0	100%	千元	
	參與計畫人力（外國籍）	碩士生	0	0	100%	人次	
		博士生	0	0	100%		
		博士後研究員	0	0	100%		
		專任助理	0	0	100%		
其他成果（無法以量化表達之		本群體計畫目前已發表論文篇數為6,尚有多篇在撰寫中,研究成果豐碩,相信對台灣肺癌機制的瞭解,治療方式的開發多有助益					

成果如辦理學術活動、獲得獎項、重要國際合作、研究成果國際影響力及其他協助產業技術發展之具體效益事項等，請以文字敘述填列。)	這些研究成果也有相當好的學術價值，如前述已有良好的發表，其中柯俊良老師發表於Molecular Cancer Research;11(5);1－12. 2013的研究，被選為當期High light issue。

	成果項目	量化	名稱或內容性質簡述
科教處計畫加填項目	測驗工具(含質性與量性)	0	
	課程/模組	0	
	電腦及網路系統或工具	0	
	教材	0	
	舉辦之活動/競賽	0	
	研討會/工作坊	0	
	電子報、網站	0	
	計畫成果推廣之參與（閱聽）人數	0	

科技部補助專題研究計畫成果報告自評表

請就研究內容與原計畫相符程度、達成預期目標情況、研究成果之學術或應用價值（簡要敘述成果所代表之意義、價值、影響或進一步發展之可能性）、是否適合在學術期刊發表或申請專利、主要發現或其他有關價值等，作一綜合評估。

1. 請就研究內容與原計畫相符程度、達成預期目標情況作一綜合評估
   ■達成目標
   □未達成目標（請說明，以100字為限）
   　□實驗失敗
   　□因故實驗中斷
   　□其他原因
   說明：

2. 研究成果在學術期刊發表或申請專利等情形：
   論文：■已發表 □未發表之文稿 □撰寫中 □無
   專利：□已獲得 □申請中 ■無
   技轉：□已技轉 □洽談中 ■無
   其他：（以100字為限）
   目前已發表之論文總數為6篇 另有5篇在撰寫或投稿中

3. 請依學術成就、技術創新、社會影響等方面，評估研究成果之學術或應用價值（簡要敘述成果所代表之意義、價值、影響或進一步發展之可能性）（以500字為限）
   本研究確認了相當多的鎳誘發細胞惡性化或轉移的機制，有助於制定公共衛生防範策略，而對於分子轉移機制的闡明，有助於在未來治療策略的研究。另外我們的研究發現數種植化素能夠抑制鎳誘發肺癌細胞侵犯轉移的情形。顯示適當的飲食或補充劑可能有助於抑制肺癌細胞轉移，若能進一步於臨床研究證實，將提供國人可行之防範策略。這些研究成果也有相當好的學術價值，如前述已有良好的發表，其中柯俊良老師發表於Molecular Cancer Research;11(5);1－12. 2013的研究，被選為當期High light issue。